SAINT PETERSBURG STATE UNIVERSITY

As a manuscript

Pavel Mikhailovich Docshin

Notch-Dependent Mechanisms of Functional Regulation of Cardiac Mesenchymal Cells in Acute Infarction and Malformations

1.5.22. Cell biology

Dissertation for the degree of Candidate
Biological Sciences

Translation from Russian

Academic Supervisor:
Doctor of Biological Sciences,
Malashicheva Anna Borisovna

St. Petersburg – 2024

INTRODUCTION

Relevance of the study

Cardiovascular diseases rank first among the causes of disability and mortality worldwide [1, 2]. According to the latest estimates by the World Health Organization, approximately 17.9 million people died from cardiovascular diseases in 2019 [3]. Most cases are associated with heart muscle diseases, characterized by loss and replacement of myocardial cellular composition and irreversible changes in the organ's structure and function. The modern classification of myocardial diseases distinguishes between coronary and non-coronary diseases, based on the causes of their development. The former includes diseases related to coronary artery damage, while the latter encompasses other heart muscle diseases, including congenital and acquired defects [4].

The most prevalent birth defects are congenital heart defects (CHD), affecting about 8 in 1,000 newborns globally. Among CHDs, tetralogy of Fallot (TF) is the most common, a complex cyanotic condition occurring in approximately 1 in 3,000 live births [5]. TF has a specific morphological phenotype in the form of four heart malformations, namely: ventricular septal defect (VSD), right ventricular hypertrophy (RV), narrowing of the right outflow (pulmonary stenosis), and dextroposition of the aorta to the right side above the VSD (primary aorta). Surgical interventions now enable correction of pulmonary stenosis and closure of the VSD, allowing oxygenated blood to flow solely through the left ventricle [6]. However, the etiology of the TF remains unclear due to the complexity of the pathogenesis, and the search for potential candidate genes associated with the phenotype of the disease is actively continuing at the present time [7].

Among coronary myocardial diseases, progressive heart failure following an acute infarction is predominant. This condition results from the narrowing of coronary arteries supplying the myocardium, leading to cardiomyocyte death at the injury site [8]. The post-infarction myocardium gradually transforms into fibrous tissue, as meaningful regeneration is unattainable [9]. Disease progression involves pathological remodeling and dilation of the heart chambers, precipitating critical heart failure [10].

Current treatments for coronary artery disease aim to halt disease progression and prevent heart failure. For example, myocardial revascularization, bypass surgery, etc., serve to improve blood supply to the heart after myocardial infarction. In addition, pharmacological approaches that slow down or stop the pathological remodeling of the heart, such as angiotensin-converting enzyme inhibitors, β-blockers, etc., are actively used. However, the mortality rate among patients with heart failure is still excessively high, suggesting that conventional treatments are still ineffective [11]. In addition, these approaches are

more aimed at relieving painful symptoms, rather than ensuring complete and functional myocardial recovery [12].

The search for mechanisms enabling endogenous heart muscle recovery is pivotal for developing novel therapeutic approaches that can supersede replacement therapies. In pursuit of effective heart regeneration methods, researchers have shifted focus to cell therapy. The initial foray into this field involved 'first generation' stem cell transplantation, comprising a non-selective suspension of unfractionated mononuclear stem cells from bone marrow. This step allowed for a prospective view of these operations. However, researchers were only able to partially regenerate the heart muscle due to difficulties with directed cell differentiation [13].

The discovery in 2003 of the heart's endogenous regenerative potential revolutionized the scientific understanding of this organ's capabilities and spurred interest in the use of resident heart stem cells for myocardial regeneration [14]. This heralded the 'second generation' of cell therapy. Contrary to prior beliefs that the human heart is definitively differentiated, it was found that areas of proliferative cellular activity can occur in the heart, especially in the peri-infarct zone [15]. The discovery of cardiac stem cells has stimulated the development of new approaches in myocardial cell therapy, but the ability of these cells to directly form cardiomyocytes is still controversial [16].

The turnover of cardiomyocytes in a healthy myocardium is approximately 0.5-2% per year, and these numbers increase slightly when the heart is affected. The mechanism for the renewal of cardiomyocytes is primarily due to the re-entry of the contractile cells themselves into the cell cycle, rather than through the differentiation of mesenchymal cells of the heart [17]. Mesenchymal stem cells (including cardiac stem cells) may be involved in regenerative processes in the myocardium by releasing paracrine factors that provide myocardial protection, neovascularization, remodeling, and differentiation in the heart [18].

There is evidence that the mechanisms of myocardial functional recovery are contained in paracrine intercellular signaling, and their activation can occur during the period of early response to injury. In this regard, the study of the mechanisms of early activation of regenerative processes in post-infarction tissue is an urgent issue. Although the existence of resident cardiac progenitor cells has been questioned [19]. It is clear that myocardial regeneration is possible, but the mechanisms remain unknown.

One of the proposed molecular mechanisms implicated in the regenerative response of the myocardium is the Notch signaling pathway. Several studies on vertebrates have demonstrated that modulation of Notch signaling may facilitate functional cardiac recovery by reducing fibrosis following injury [20, 21]. In addition, the relationship between hypoxia and cardiomyocyte proliferation in adult mammals was revealed, which led to significant myocardial regeneration in the conditions of systemic

hypoxemia [22]. The potential link between the Notch signaling pathway and hypoxia in cardiac muscle repair mechanisms remains unclear.

Thus, the functional restoration of the myocardium after a heart attack remains an urgent problem of modern regenerative biomedicine. The search for an effective therapeutic strategy is still ongoing, and many studies are aimed at exploring the possibilities of cell therapy of myocardial therapy. However, the cellular mechanisms of post-infarction cardiac repair remain elusive. This study aimed to analyze early transcriptional events in cardiac tissue after myocardial infarction and the study of a cell population isolated from post-infarction myocardial tissue of rats. Cyanotic congenital heart disease in the form of tetralogy of Fallot remains one of the most common and serious defects in cardiac development. To date, the mechanisms underlying the formation of tetralogy of Fallot, at the cellular and molecular levels, remain unclear.

Aims and objectives of the study

The aim of this study was to study the Notch-dependent mechanisms of functional regulation of cardiac mesenchymal cells in the context of hypoxic effects on the myocardium in acute infarction and congenital heart defects.

Tasks:

1. To analyze early transcriptional events occurring in rat postinfarction tissue 24 hours after induction of myocardial infarction.
2. To assess the expression of components of the Notch signaling pathway and early remodeling genes in post-infarction and healthy rat myocardial tissues at early time points – 8 and 24 hours after acute infarction.
3. To assess the expression of components of the Notch signaling pathway and early remodeling genes in mesenchymal cells derived from post-infarction and intact rat myocardial tissues.
4. To compare the expression of components of the Notch signaling pathway in human heart mesenchymal cells obtained from patients with tetralogy of Fallot and in cells from patients with ventricular septal defect.
5. To assess the ability to migrate, proliferate, and differentiate postinfarction and healthy rat heart mesenchymal cells, as well as the proliferation and differentiation of human heart mesenchymal cells obtained from patients with tetralogy of Fallot and ventricular septal defect.
6. To analyze the activation of the Notch signaling pathway under conditions of hypoxia *in vitro* in rat and human heart mesenchymal cells.

7. To assess the interaction of components of the Notch signaling pathway and early remodeling genes in rat and human heart mesenchymal cells by exogenous activation of *BMP2* and Notch signaling.

Scientific novelty of the work

For the first time, the early transcriptional profile of activated rat cardiac mesenchymal cells in response to acute hypoxic stress was characterized, and the molecular mechanisms of regulation of rat and human cardiac mesenchymal cells in the form of deregulation of embryonic signaling pathways, such as the Notch and Bmp signaling pathways, were established.

Theoretical and practical significance of the work

The study revealed significant changes in the transcription profile of early post-infarction myocardial tissues, including the reactivation of embryonic signaling pathways, which provides valuable theoretical information about the cellular mechanisms underlying post-infarction cardiac remodeling. Moreover, activation of key components of the Notch and Bmp signaling pathways in postinfarction tissues indicates their crucial role in early myocardial remodeling, suggesting the presence of potential targets for therapeutic interventions.

The discovery of resident populations of activated cardiac mesenchymal cells in the heart after myocardial infarction, and the ability to isolate and cultivate them *in vitro*, is of practical significance. These cells show an increased capacity for proliferation, migration, and differentiation compared to populations of intact cells, indicating their potential for regenerative therapy. In addition, the presented gene expression profiles as post-infarction mesenchymal cells and cells from tetralogy of Fallot patients provide valuable information about specific dysregulation of several genes, paving the way for more targeted diagnostic and therapeutic approaches.

Key Scientific Findings

1. Research has demonstrated [23] that acute hypoxic stress triggers the reactivation of embryonic signaling pathways, specifically Notch and Bmp, in the cardiac mesenchymal cells following myocardial infarction. This underscores the significance of hypoxia in cellular activation and highlights potential targets for enhancing the regenerative capacity

of the myocardium. In this work, I conducted all experimental aspects, including data analysis and manuscript preparation for publication (pp. 50–65). Except for work on the induction of myocardial infarction in rats, conducted at the Centre for Experimental Pharmacology of the SPCPU with the participation of Andrey Aleksandrovich Karpov.

2. The study revealed [24] that myocardial infarction leads to the activation of cardiac mesenchymal cells, as evidenced by their increased proliferative capacity, enhanced migratory ability, and heightened expression of differentiation markers in response to induction, compared to cells from healthy myocardial tissue. I was responsible for the entire experimental process, data analysis, and manuscript preparation for publication (pp. 66–74).
3. This work demonstrated [25] the interaction between the Notch signaling pathway and Bmp2 in regulating markers of endothelial-mesenchymal transition, revealing tissue-specific effects in cardiac mesenchymal cells and human umbilical vein endothelial cells. This underscores the critical role of this interaction in the formation of heart fibrosis. In this study, I undertook all experimental work, data analysis, and manuscript preparation for publication (pp. 112–125).
4. The investigation identified [26] deregulated Notch pathway activity in cardiac mesenchymal cells from patients with Tetralogy of Fallot, compared to controls, suggesting a potential role for the Notch signaling pathway in the disease's pathogenesis and its importance for the functional state of these cells. In this study, I conducted *in vitro* research and participated in data analysis (pp. 92–107). Except for work related to the collection of material from patients with cardiac malformations, with the participation of Ivan Aleksandrovich Kozyrev.
5. Research shows [27] that cardiac mesenchymal cells of patients with ventricular septal defects and Tetralogy of Fallot exhibit differences in the expression of surface markers CD90 and PDGFRB, indicating the pathology's impact on their phenotype. I was involved in conducting *in vitro* studies (pp. 91).
6. The review [28] highlights the ambiguous results of treating heart failure with stem cells, noting their safety but limited efficacy in improving cardiac function, thus emphasizing the need for the development of next-generation cell therapy. In this work, I was responsible for the preparation and formatting of the publication text (pp. 29–34).
7. The review demonstrates [29] that while the direct differentiation of resident cardiac mesenchymal cells into cardiomyocytes is debated, their use to enhance heart function after myocardial infarction highlights the potential of these cells and induced pluripotent stem

cell therapies in regenerative medicine, emphasizing the importance of further research into their mechanisms and therapeutic roles. In this work, I handled the preparation and formatting of the publication text (pp. 28–29).

Theses for Defense

1. The transcriptional profile of post-infarction myocardial tissues changes significantly 24 hours after lesion and leads to the reactivation of embryonic signaling pathways such as Notch and Bmp (*Runx2/Bmp2*), which may indicate their key role in early myocardial remodeling processes after infarction.
2. Myocardial infarction leads to the activation of resident populations of cardiac mesenchymal cells, which can be isolated from the post-infarction zone and cultured with temporary preservation of their properties in the form of improved ability to proliferate, migrate, and differentiate *in vitro.* In addition, cardiac mesenchymal cells from patients with tetralogy of Fallot had a greater tendency to proliferate and differentiate than cells from patients with an isolated ventricular septal defect.
3. The transcriptional profile of post-infarction cardiac mesenchymal cells differs from that of healthy cells, and gene expression characteristic of ischemic tissue is partially preserved, including the expression of the components of the Notch signaling pathway (*Jag1, Hes1*) and *Bmp2/Runx2* in post-infarction cells. In addition, significant deregulation of the Notch signaling pathway has also been identified in cardiac mesenchymal cells from patients with tetralogy of Fallot.
4. *In vitro* hypoxic stress has a stimulating effect on the activation of components of the Notch signaling pathway and *Bmp2/Runx2* early remodeling genes in healthy cardiac mesenchymal cells from rat and human.
5. Exogenous activation of *NOTCH1* leads to a dose-dependent increase in the expression of the components of the Notch and *RUNX2* signaling pathways in healthy cardiac mesenchymal cells from rat and human and does not affect *BMP2* expression.
6. The expression levels of the components of the Notch signaling pathway affect the expression of proliferative and differentiation processes in the human cardiac mesenchymal cells, and the dose-dependent activation of Notch enhances the ability to differentiate in the cardiogenic direction.
7. Alternating activation of *NOTCH1* and *BMP2* affects the expression of endothelial-mesenchymal transition marker genes and the synthesis of alpha-actin and promotes the activation of human

cardiac mesenchymal cells.

Publication and approbation of the work

Based on the materials of the dissertation, 20 works have been published: seven scientific articles in journals indexed by the RSCI, WoS and/or Scopus systems, and 13 publications in the proceedings of international and all-Russian conferences.

The main provisions and scientific results of the dissertation were presented in reports at scientific conferences:

1. III National Congress on Regenerative Medicine, November 15–18, 2017, Moscow, Russia.
2. XVIII Winter Youth School on Biophysics and Molecular Biology, March 11–16, 2017, St. Petersburg, Russia.
3. Cell Biology: Problems and Prospects, October 2–6, 2017, St. Petersburg, Russia.
4. XI Annual Scientific Conference of Young Scientists and Specialists, Almazov National Medical Research Centre, 27–28 April 2017, St. Petersburg, Russia.
5. The Frontiers in Cardiovascular Biology, April 20-22, 2018, Vienna, Austria.
6. All-Russian Youth Medical Conference with International Participation "Almazov Readings – 2018", May 16–18, 2018, St. Petersburg, Russia.
7. All-Russian Conference with International Participation "StemCellBio-2018: Fundamental Science as the Basis of Cell Technologies", November 15–17, 2018, St. Petersburg, Russia.
8. Almazov Youth Medical Forum, 16–18 May 2018, St. Petersburg, Russia.
9. The Notch Meeting XI, 6–10 October 2019, Athens, Greece.
10. I All-Russian Congress with International Participation "Physiology and Tissue Engineering of Heart and Blood Vessels: From Cell Biology to Prosthetics", November 04–07, 2019, Kemerovo, Russia.
11. IV National Congress on Regenerative Medicine, November 20–23, 2019, Moscow, Russia.
12. Conference "Actual Problems of Developmental Biology", October 12–14, 2021, Moscow, Russia.
13. Forum of Young Cardiologists "From Prevention to High-Tech Care for Cardiovascular Diseases", May 13–14, 2022, Moscow, Russia.

The dissertation was recommended for defense for the scientific degree of Candidate of Biological Sciences based on the results of the presentation of the main results and their discussion at the seminar of the Institute of Cytology of the Russian Academy of Sciences, 01/24/2024.

List of articles published in journals indexed by RSCI, WoS and/or Scopus:

1. **Docshin, P. M.**, Karpov, A. A., Eyvazova, S. D., Puzanov, M. V., Kostareva, A. A., Galagudza, M. M., & Malashicheva, A. B. (2018). Activation of Cardiac Stem Cells in Myocardial Infarction. Cell and Tissue Biology, 12(3), 175–182. https://doi.org/10.1134/S1990519X18030045 // **Докшин, П. М.,** Карпов, А. А., Эйвазова, Ш. Д., Пузанов, М. В., Костарева, А. А., Галагудза, М. М., & Малашичева, А. Б. (2018). Активация Стволовых Клеток Сердца при Инфаркте Миокарда. Цитология, 60(2), 81–88. https://doi.org/10.31116/tsitol.2018.02.02

2. Козырев И.А., Головкин А.С., Игнатьева Е.С., **Докшин П.М.,** Грехов Е.В., Гордеев М.Л., Первунина Т.М., Костарева А.А., Малашичева А.Б. (2019). Фенотипическая характеристика мезенхимных клеток сердца, полученных от пациентов с тетрадой Фалло и дефектом межжелудочковой перегородки. Трансляционная Медицина, 6(5), 16–23. https://doi.org/10.18705/2311-4495-2019-6-5-16-23

3. Ivan Kozyrev, **Pavel Dokshin**, Aleksandra Kostina, Artem Kiselev, Elena Ignatieva, Alexey Golovkin, Tatiana Pervunina, Evgeny Grekhov, Mikhail Gordeev, Anna Kostareva & Anna Malashicheva (2020). Dysregulation of Notch signaling in cardiac mesenchymal cells of patients with tetralogy of Fallot. Pediatric Research, 88, 38–47. https://doi.org/10.1038/s41390-020-0760-6

4. **Docshin P.M.,** Bairqdar A., Malashicheva A.B. Current status, challenges and perspectives of mesenchymal stem cell-based therapy for cardiac regeneration. *Complex Issues of Cardiovascular Diseases*. 2021;10(3):72-78. (In Russ.) https://doi.org/10.17802/2306-1278-2021-10-3-72-78

5. **Dokshin P.M.,** Malashicheva A.B. Heart stem cells: hope or myth? *Russian Journal of Cardiology*. 2021;26(10):4749. (In Russ.) https://doi.org/10.15829/1560-4071-2021-4749

6. **Docshin, P.M**.; Karpov, A.A.; Mametov, M.V.; Ivkin, D.Y.; Kostareva, A.A.; Malashicheva, A.B. Mechanisms of Regenerative Potential Activation in Cardiac Mesenchymal Cells. Biomedicines 2022, 10, 1283. https://doi.org/10.3390/biomedicines10061283

7. **Docshin P**, Bairqdar A, Malashicheva A. Interplay between BMP2 and Notch signaling in endothelial-mesenchymal transition: implications for cardiac fibrosis. Stem Cell Investig 2023;10:18. https://doi.org/10.21037/sci-2023-019

Abstracts:

1. **Docshin, P.,** Malashicheva, A., & Karpov, A. (2017). The effect of hypoxia on the potential of cardiac stem cells in myocardial regeneration (In Russ.). Genes & Cells, XII (3), 86. III National Congress on Regenerative Medicine, November 15–18, 2017, Moscow, Russia.

2. **Docshin P.M.,** Malashicheva A.B. (2017). The role of hypoxia in the induction of reparative properties of cardiac stem cells (In Russ.). XVIII Winter Youth School on Biophysics and Molecular Biology, March 11–16, 2017, St. Petersburg, Russia.

3. **Docshin P.M.,** Malashicheva A.B. (2017). Activation of the reparative properties of cardiac stem cells during acute myocardial infarction (In Russ.). Cell biology: problems and prospects, October 2–6, 2017, St. Petersburg, Russia.

4. **Docshin P.M.** (2017). The role of hypoxia in the induction of reparative properties of cardiac stem cells (In Russ.). XI annual scientific conference of young scientists and specialists, Almazov National Medical Research Centre, April 27-28, 2017, St. Petersburg, Russia.

5. **Dokshin, P.**, Karpov, A., Eyvazova, S., & Malashicheva, A. (2018). Hypoxia activates stem cells in myocardial tissue. Cardiovascular Research, 114(suppl_1), S66–S71. https://doi.org/10.1093/cvr/cvy060 The Frontiers in Cardiovascular Biology, April 20-22, 2018, Vienna, Austria.

6. **Docshin P.M.** (2018). Activation of the Notch signaling pathway in the peri-infarct zone of the myocardium during acute infarction (In Russ.). All-Russian youth medical conference with international participation “Almazov Readings – 2018”, May 16–18, 2018, St. Petersburg, Russia.

7. **Docshin, P.,** & Malashicheva, A. (2018). Assessment of the level of activation of mesenchymal cells of the heart under the influence of hypoxia *in vitro* (In Russ.). Collection of Materials of the All-Russian Conference with International Participation “StemCellBio-2018: Fundamental science as the basis of cellular technologies”, November 15–17, 2018, St. Petersburg, Russia.

8. **Docshin P.M.** (2018). Activation of cardiac mesenchymal stem cells under the influence of hypoxia (In Russ.). Almazov Youth Medical Forum, May 16–18, 2018, St. Petersburg, Russia.

9. **Dokshin, P.**, Karpov, A., Malashicheva, A. (2019). Notch-Dependent Mechanisms of Regenerative Potential Activation in Cardiac Mesenchymal Cells. The Notch Meeting XI, October 6-10, 2019, Athens, Greece.

10. **Dokshin, P.M.,** Karpov, A.A., Malashicheva, A.B. (2019). Notch-dependent mechanisms of activation of the regenerative potential of cardiac mesenchymal cells (In Russ.) https://www.doi.org/10.17802/2306-1278 I All-Russian Congress with international participation "Physiology and tissue engineering of the heart and blood vessels: from cell biology to prosthetics", November 04-07, 2019, Kemerovo, Russia.

11. **Dokshin, P. M**., Karpov, A. A., & Malashicheva, A. B. (2019). Activation of the Notch signaling pathway and early remodeling genes in cardiac mesenchymal cells under acute hypoxic stress (In Russ.). Genes & Cells, 78. IV National Congress on Regenerative Medicine, November 20–23, 2019, Moscow, Russia.

12. **Dokshin P.M.,** Malashicheva A.B. (2021). Search for molecular targets involved in the regenerative response during myocardial infarction in cardiac mesenchymal cells using transcriptomic analysis (In Russ.). Current problems in developmental biology, October 12–14, 2021, Moscow, Russia.

13. **Dokshin P.M.,** Panferov E.V., Malashicheva A.B. (2022). Interaction of Notch and Bmp signaling pathways in cardiac regenerative processes (In Russ.). Forum of young cardiologists "From prevention to high-tech care for cardiovascular diseases", May 13–14, 2022, Moscow, Russia.

1 LITERATURE REVIEW

1.1 Heart Development

During vertebrate embryogenesis, the heart emerges as the first functional organ. It forms from precursor cells in the process of early gastrulation. These heart precursor cells originate during the stage of the primary streak, located behind Hensen's node. They occupy two small areas, one on each side of the epiblast, extending to half the length of the streak. After migrating through the primitive streak, they differentiate into two groups of lateral plate mesodermal cells [30]. The specification of the cardiac field begins during this migration. It is marked by the appearance of cardiogenic mesoderm, which constructs the dual-layered wall of the primary heart tube. This structure comprises an inner endocardial layer with endothelial cells and an outer myocardial layer. These layers are separated by an extracellular matrix [31]. Subsequently, the formation of the first structure known as the atrioventricular canal cushion occurs. This crucial structure regulates blood flow between the atrium and ventricle. It also gives rise to the tricuspid and mitral valves, as well as part of the atrioventricular septum. It is at this stage that the first rhythmic heart contractions commence.

Researchers distinguish between primary and secondary heart fields, each contributing to specific regions of the developing organ [32]. Precursor cells of the primary heart field form the primary heart tube, which primarily gives rise to the left and right ventricles of the heart. However, the cells forming this tube have limited proliferative ability, mainly contributing to the formation of a significant part of the left ventricle [30]. In contrast, the precursor cells of the secondary heart field located at the posterior end of the heart tube develop into the two atria (**Figure 1**). At the anterior end, these cells form the right ventricle and the outflow tract, comprising the arterial cone and arterial trunk [31]. During the subsequent looping process, the heart acquires a four-chambered structure, with the atria shifting to a position anterior to the ventricles.

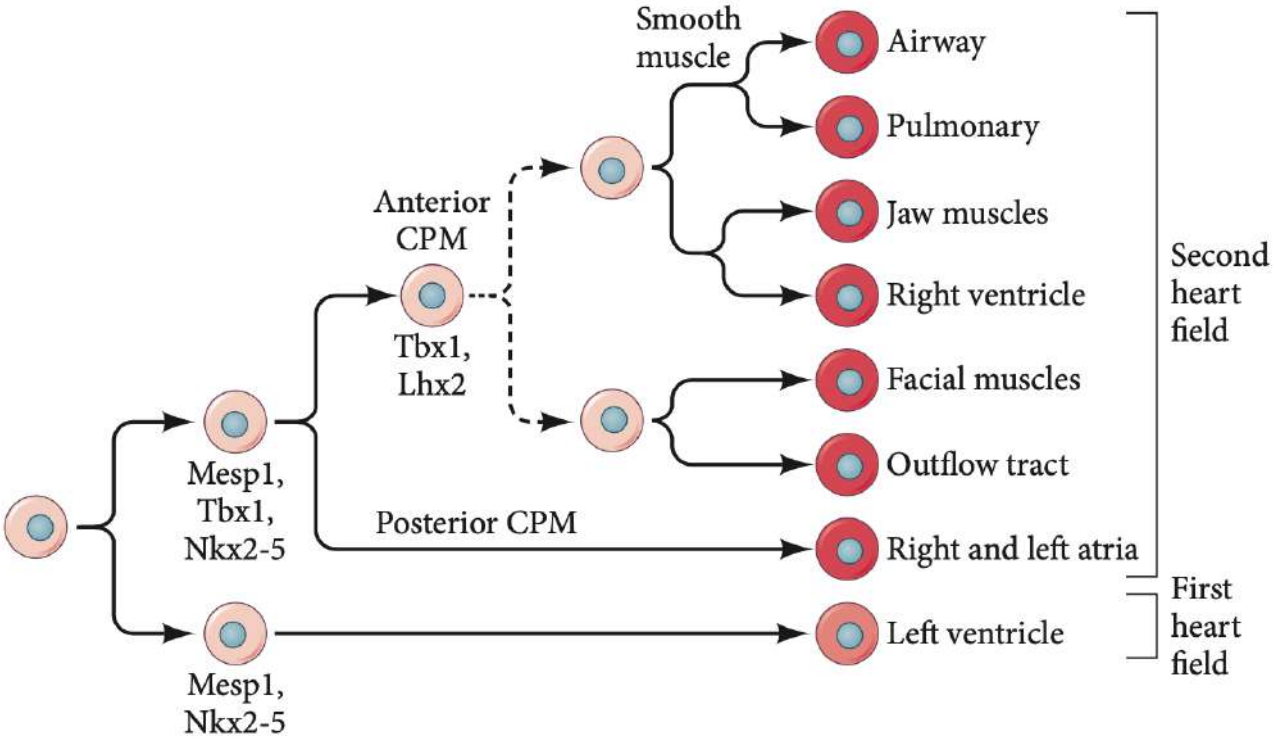

Figure 1. Hypothetical Diagram of Heart Precursor Cell Development Originating from Primary and Secondary Heart Fields. The dashed line indicates that precise data on the division of precursor cells for the lungs, their vessels, facial muscles, and the heart have not yet been obtained. Some transcription factors associated with these precursor cells are listed below them [30].

Despite their specific designation as heart precursor cells, these cells demonstrate remarkable plasticity. They possess the unique ability to substitute for one another during the differentiation process. This adaptability allows them to form various types of heart cells. Moreover, within the secondary heart field's precursor cells, a subset is also involved in developing facial muscles, pulmonary arteries and veins, and the pulmonary mesenchyme [30]. Numerous embryonic signaling pathways play a critical role in the specification of cardiac mesoderm and the overall organ development. These pathways are essential for the proper formation of cardiac structures. Among these, the Notch signaling pathway stands out as a significant contributor to these processes.

1.2 Notch Signaling Pathway

In human development, several evolutionarily conserved signaling pathways are involved, including Notch, Wingless, Hedgehog, Transforming Growth Factor β, and others. This is a classical group of molecular mechanisms that can function either individually or in coordination with each other [33]. The Notch signaling pathway is a significant contributor to morphogenesis and organ formation. It is responsible for numerous developmental processes, including the maintenance of stem cell populations and tissue homeostasis in the postnatal period. Notch signaling plays a central role in cell fate determination, thereby participating in the differentiation of various cell types such as epithelial, neuronal, endothelial, and cells of the blood, bone, and muscles. Any deviations in Notch intercellular signaling can lead to various human developmental anomalies or tumor formation [34]. Therefore, regulating the intensity and duration of the Notch signal is an imperative condition for actively studying this cellular regulation mechanism.

This key regulator of cell fate has been identified in many organisms, starting with the simply structured nematode C. elegans, through a gene orthologous to Notch. This suggests that Notch signaling is a highly conserved process. The Notch signaling pathway comprises receptor proteins, ligands for these proteins, target genes, and a transcriptional complex. In mammals, there are only four types of transmembrane Notch receptors (Notch-1, 2, 3, 4). Each receptor consists of three domains: intracellular, transmembrane, and extracellular. Additionally, five types of transmembrane ligands are identified: three varieties of Delta-like proteins (Dll-1, 2, 4) and two types of Jagged proteins (Jagged-1, 2) [35].

The mechanism of the canonical Notch signaling pathway operates as follows: The DSL ligand (Delta, Serrate, and Lag2) binds to the Notch receptor located on the surface of an adjacent cell. This interaction triggers a two-step proteolytic cleavage process of the Notch transmembrane receptor domain. Through the initiation of the ADAM/TACE metalloproteinase, the intracellular domain of Notch (NICD) is released into the cytoplasm. The NICD then penetrates the cell nucleus, where it binds with a transcription factor from the CSL family (CBF1/RBPJK in mammals, Su(H) in flies, and LAG-1 in worms) to form a transcriptional complex. This complex also includes proteins from the ICN and Mastermind family (MAM/Lag-3), with MAM/Lag-3 acting as a co-activator of the process. Subsequently, they activate target genes using an additional co-activator, p300, and mediate transcription activation on the chromatin template with the help of ICN [36] (**Figure 2**).

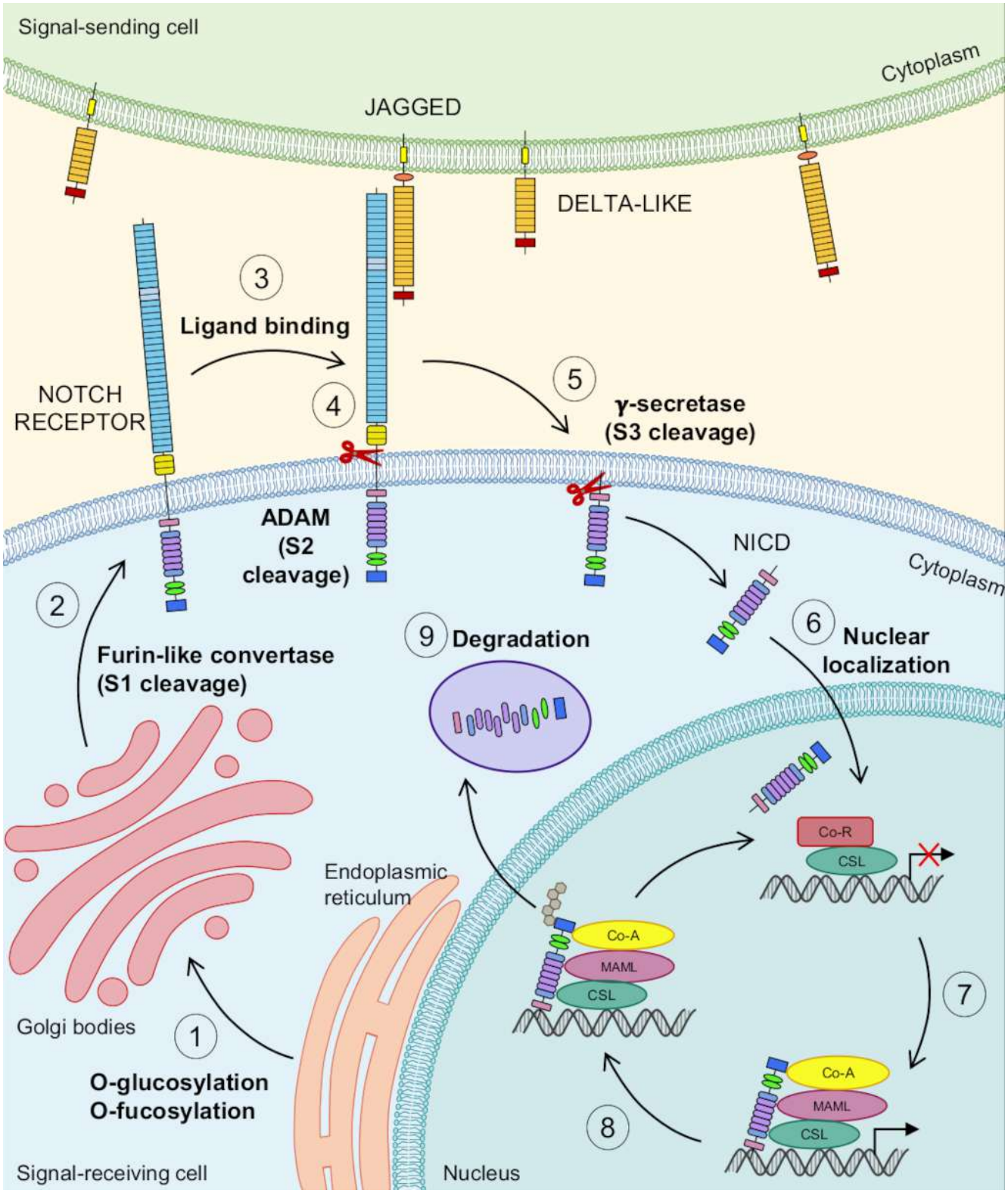

Figure 2. Canonical Notch Signaling Pathway. 1) Post-translation, the Notch receptor is modified through glycosylation and fucosylation in the endoplasmic reticulum. 2) In the Golgi complex, the receptor undergoes further modifications, including cleavage at the S1 position by furin-like convertase. 3) Notch receptor ligands capable of activating it are of two types: JAGGED and DELTA-LIKE. 4) Notch activation occurs when a ligand from one cell binds to the receptor of another cell, leading to receptor cleavage by a protease from the family of proteins containing a disintegrin and metalloproteinase domain (ADAM10 or ADAM17) at the S2 position. 5) The γ-secretase protein complex performs subsequent cleavage at S3 (valine 1744 in human and mouse Notch1), releasing the

Notch intracellular domain (NICD) into the cytoplasm. 6) NICD translocates to the nucleus. 7) In the nucleus, NICD binds to the DNA-binding transcription factor CBF1, suppressor of hairless, Lag-1 (CSL). Following this binding, NICD displaces corepressors and recruits transcription coactivators, such as Mastermind/Lag-3 (MAML). This process enables the regulation of downstream Notch target genes. 8) NICD undergoes ubiquitination by the suppressor/enhancer of ubiquitin ligase E3 Lin-12 (SEL-10), targeting it for degradation. 9) NICD is cleaved by the proteasome [37].

The most well-known target genes of the Notch pathway are members of the "Hairy and enhancer-of-split" (*HES*) and "Hairy and enhancer-of-split-related" (*HEY, HESR, HRT,* or *CHF*) gene families. Many of these repressor genes suppress genes necessary for cell differentiation. One of the most extensively studied functions of Notch signaling is lateral inhibition, which prevents surrounding cells from adopting the same fate [38].

Lateral inhibition is a process of symmetry disruption in which a population of identical cells differentiates into various cell types through alternating patterns. This process involves local competition among neighboring cells, all of which simultaneously strive to differentiate into the same cell type while preventing their "neighbors" from selecting the same fate. Within each small group of cells, one cell prevails, suppressing its immediate "neighbors" through the Notch signaling pathway [39]. There are three primary models of lateral inhibition: classical lateral inhibition, pattern formation through cis-inhibition, and patterning via filopodia (**Figure 3**).

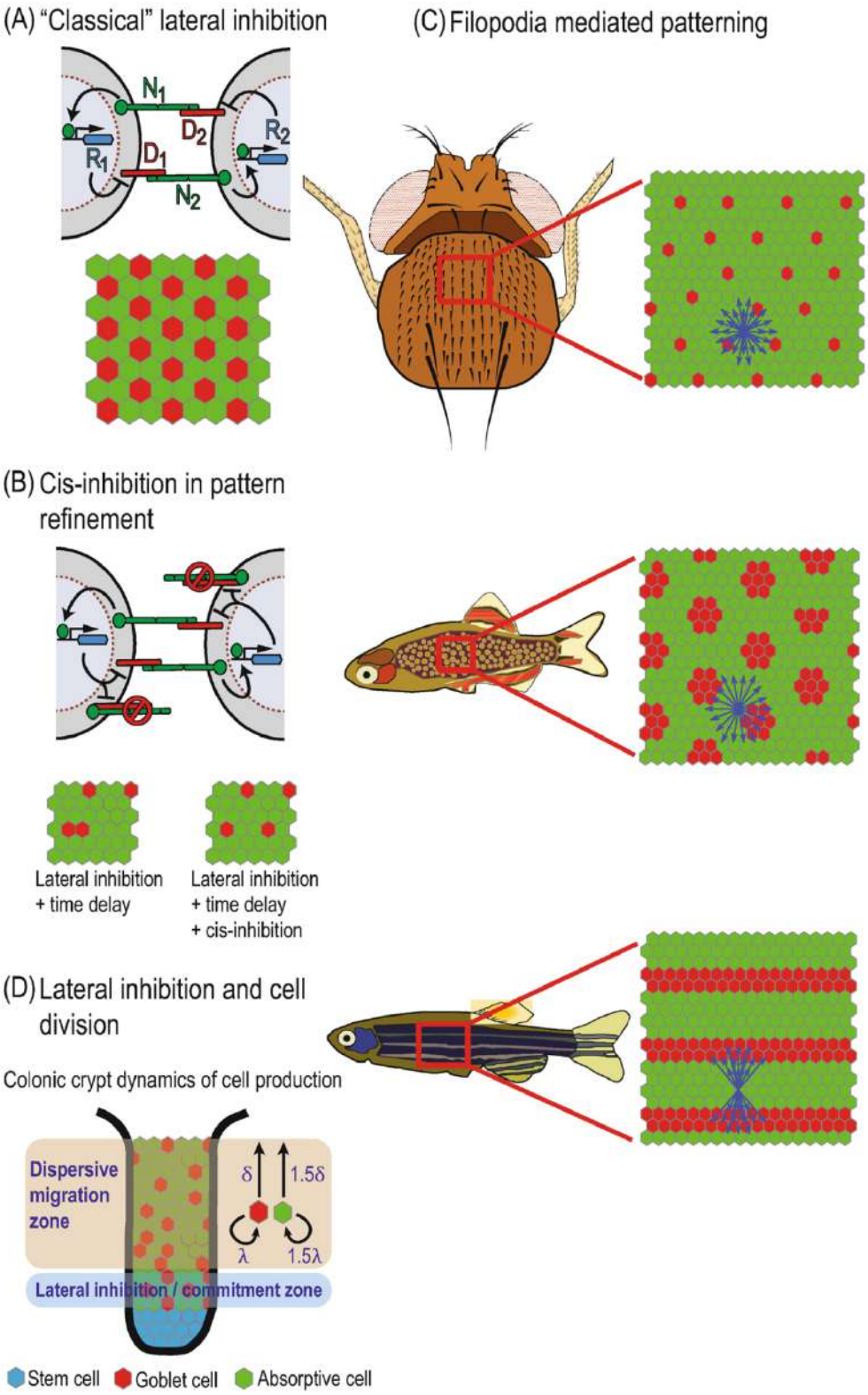

Figure 3. Models of Lateral Inhibition. a) 'Classical' lateral inhibition. At the top is a schematic representation of molecular interactions in lateral inhibition between two cells. In this scheme, NOTCH signaling in each cell is activated by interactions between NOTCH receptors (N1 and N2) and NOTCH ligands (D1 and D2). A repressor (R1 and R2) in each cell activates NOTCH signaling, which suppresses the expression or activity of DELTA in that cell. At the bottom is the result, a typical hexagonal lattice pattern of cells. b) Pattern formation via cis inhibition. At the top is a schematic representation of a lateral inhibition model incorporating cis inhibition between receptors and ligands. In the cis-inhibition model,

a ligand on one cell binds to a receptor on the same cell, leading to the formation of an inactive complex. These cell-autonomous interactions reduce the number of free ligands and receptors on the cell surface. At the bottom, cis inhibition decreases the likelihood of events where two adjacent cells choose the same fate (red cells). c) Patterning mediated by filopodia. Diagrams of models that consider NOTCH signaling over greater distances through filopodia. d) Lateral inhibition and cell division. A schematic model describing the dynamics of differentiation in the crypts of the colon. Stem cells at the bottom of the crypt (blue) differentiate into goblet cells (red, high delta) and enterocytes (green, low delta), which migrate towards the top of the crypt (lumen). Stem cells divide at the base of the crypt (stem cell layer), leading to upward cell movement. Lateral inhibition occurs in the layer adjacent to the stem cell layer (lateral inhibition zone or commitment zone). At this level, cell fate decisions are determined by the process of lateral inhibition, as described in (a). After differentiation, cells migrate from the commitment zone to the dispersal migration zone. In this zone, goblet cells divide at a slower rate (λ) and migrate slower (δ) compared to enterocytes (1.5λ and 1.5δ) [39].

In the hematopoietic system, Notch signaling significantly influences the functions of hematopoiesis. For example, during the intrauterine period, Notch1 is responsible for inducing definitive hematopoiesis in the endothelial cells of the dorsal aorta. In the postnatal period, it plays a minor role in maintaining hematopoietic stem cells in the bone marrow. Additionally, Notch acts as a key regulator in the early development of T-cells in the thymus [40].

In the differentiation of endothelial cells, the Notch signaling pathway plays a role, but it does so in conjunction with another important regulatory element - Bone Morphogenetic Protein (BMP). A direct synergistic interaction occurs between them, as seen, for example, in the activation of transcription of *HESR* and *HERP2* in endothelial cells. Furthermore, the variable synergism and antagonism between BMP and Notch signaling pathways are responsible for the migration of endothelial cells [41].

Disruptions in the regulation of Notch signaling lead to various lung diseases, including lung cancer. It is known that the Notch signaling pathway plays a vital role in coordinating events during lung development. These events include the selection of terminal differentiation of epithelial cells in the respiratory tract and the development of pulmonary vessels [42].

Notch signaling also plays a role in the differentiation and morphogenesis of the central nervous system. A direct impact of Notch is observed during the segregation of epidermal and neuronal cell lines during differentiation. This process involves the inactivation of Notch signaling, leading to the development of a neurogenic phenotype in neuronal precursor cells. Thus, the Notch pathway can maintain a population of precursor cells by inhibiting their premature differentiation. Nevertheless, it has been established that the Notch pathway in the central nervous system can regulate the diversification of the precursor cell pool and neuronal maturation [43, 44].

Kidneys are human organs responsible for filtering and maintaining chemical balance in the body. They are involved in the excretion of metabolites and regulate the level of electrolytes in the blood and its pH. The main structural and functional unit of the kidney is the nephron, the development of which

is controlled by the Notch signaling pathway during embryogenesis. The Notch signaling pathway plays a significant role in both undifferentiated and mature nephron cells. It is important to note that in embryonic development this signaling pathway is critical for cell differentiation and secondary bud formation [45].

Several stages in skeletal formation involve the Notch signaling pathway, which acts as a critical regulator. This includes the development of segmentation of the dorsal part of the mesoderm into somites, the formation and differentiation of prechondrogenic cells in the sclerotome, which is essential for the proper development of the axial skeleton. Subsequently, it has been established that the Notch pathway regulates somitogenesis, chondrogenesis, osteoblastogenesis, and osteoclastogenesis. This regulation ultimately affects the formation of the entire skeleton. Dysregulation of this signaling pathway during embryogenesis leads to irreversible changes in the skeleton, resulting in congenital developmental defects [46].

The basal layer of the skin's epidermis consists of proliferating precursor cells, which are responsible for forming differentiated cell layers to provide a barrier between the internal and external environments. The epidermis is maintained throughout life through the proliferation and differentiation of stem cells. This process is facilitated by the highly conserved Notch signaling pathway, which plays a significant role in cell differentiation during both embryogenesis and the postnatal period [47].

The Notch signaling pathway plays a role in the development of hair follicles, but its involvement is limited to the postnatal period. It is responsible for regulating the formation of the hair bulb and the outer root sheath, as well as in the differentiation of stem cells or their precursors by stimulating or inhibiting towards the epidermal direction. The Notch pathway regulates cell differentiation, ensuring the proper development of each layer of the hair shaft and the inner root sheath [48].

Lateral inhibition of surrounding cells, a fundamental function of the Notch signaling pathway, is utilized in the development of sensory regions of the inner ear. This process involves the formation of a mosaic structure composed of sensitive hair cells and non-sensory supporting cells. Two Notch ligands (Dll-1 and Jagged2) are believed to act synergistically during the cell diversification stage in mammals. Notably, Notch signaling has an inductive rather than inhibitory character in determining the prosensory region. This stage precedes the cellular diversification of sensitive hair cells and supporting cells, with Jagged1 playing a key role as one of the essential ligands in this process [49].

Cancer stem cells are specific subpopulations of cancer cells that exhibit pronounced stem cell properties and have been identified in a wide range of human oncological diseases. They are characterized by the ability for self-renewal and can be heterogeneous. One common trait shared between cancer stem cells and normal stem cells is their significant reliance on certain signaling pathways. The main signaling pathways in stem cells are Wnt, Notch, and Hedgehog. These pathways

are also responsible for regulating the self-renewal and survival of cancer cells [50].

1.3 The Notch Signaling Pathway in Heart Development

The specification of cardiac mesoderm is largely dependent on the Notch signaling pathway. Signal transmission, mediated by Notch receptors, ligands, and target genes, regulates the processes of defining the left-right axis and, consequently, the correct twisting of the heart tube [51]. In the atrioventricular canal (AVC), there is expression of Bone Morphogenetic Protein 2 (*BMP2*) and the transcription factor T-box 2 (*TBX2*). Notably, a BMP2 deficiency leads to defects in the AVC, in contrast to TBX2, where suppression results in the initiation of channel-specific myocardial gene expression in the AVC. In this process, Notch target genes *HEY1* and *HEY2* are directly involved. Their actions lead to restricting the expression of *BMP2* and *TBX2* in the AVC. Research on the role of the Notch signaling pathway in the developing heart of mice has shown that the expression of *Hey2* and *Hey1* occurs in the myocardium of the atrial and ventricular chambers. However, their expression is completely absent in the atrioventricular canal, an important feature for proper myocardial differentiation. [52]. When these genes are deactivated, severe heart defects occur, including myocardial thinning and complete absence of arterial differentiation. This, in turn, leads to the embryonic lethality. It was found that the expression of the *Bmp2* ligand was observed from the AVC to the atrial myocardium in *Hey1*-deactivated genes. In contrast, in the 'wild type,' *Bmp2* expression was confined to the AVC myocardium. An experiment involving the overexpression of a constitutively active intracellular domain of Notch1 in mice induced the activation of *Hey1* and *Hey2* expression and suppressed *Bmp2* expression in the AVC myocardium. This resulted in trabeculae formation and the differentiation of AVC myocardium into ventricular myocardium. Thus, the expression of Hey genes in the atrial and ventricular myocardium creates a boundary between the AVC and the myocardial chambers. [53].

Tissue interactions between the myocardium and endocardium in the areas of the AVC and the outflow tract led to the epithelial-mesenchymal transition (EMT) of endocardial cells. At this stage, the expression of *NOTCH1-2,4* receptors, *JAGGED1* and *DLL4* ligands, and *HEY1* and *HEY2* target genes in the endocardium of the AVC occurs. Thus, the Notch signaling pathway can regulate the initial events of EMT, as well as contribute to the acquisition of mesenchymal morphology of cells through the targeted expression of various target genes [54] (**Figure 4**).

The vascular endothelial growth factor VEGF is also one of the key regulators of epithelial-mesenchymal transition (EMT) in the AVC. Induced forced expression of *VEGF165* in the myocardial cells of the AVC, prior to the development of the cardiac cushion, leads to excessive proliferation of endocardial cells. This results in a reduction in EMT and a delay in the fusion of the cardiac cushion

[55]. Based on this, VEGF acts as a negative regulator of epithelial-mesenchymal transition (EMT) and contributes to the formation of the endocardial phenotype.

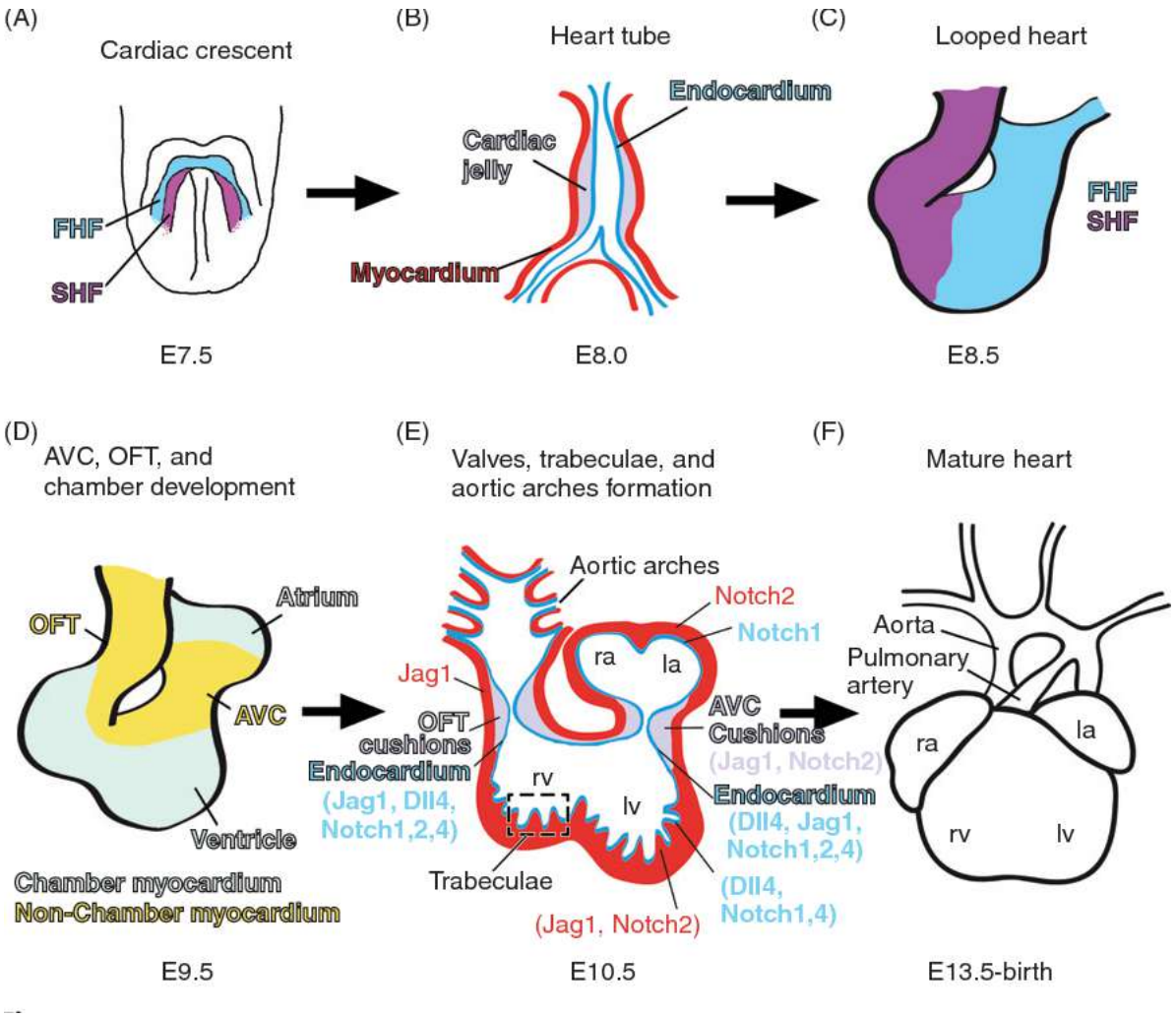

Figure 4. Stages of Heart Formation and Expression of Notch Signaling Pathway Components in Mouse Embryogenesis. (A) At stage E7.5, the mouse heart is represented by the cardiac crescent, formed by two populations – the primary and secondary heart fields, which have fused along the midline of the embryo. (B) During E8.0, the heart transforms into an endothelial tube (endocardium, blue), surrounded by a layer of myocardial cells (red). Between the endocardium and myocardium lies the extracellular matrix – cardiac jelly (gray). (C) At E8.5, the heart elongates and begins to twist to the right, forming a complex structure with four chambers. (D) The formation of the atrioventricular canal occurs at stage E9.5 and is crucial for separating the two chambers of the developing atria and ventricles. (E) The formation of valve primordia occurs between E9.5 and E10.5, along with the development of the ventricular chamber, beginning with the formation of trabeculae in the developing left and right ventricles. Tissue expression of Notch ligands and receptors is color-coded: endocardium – blue; myocardium - red, endocardial cushions - gray. (F) The cardiac outflow tract is remodeled between stages E10.5 to E13.5, forming the aorta and pulmonary arteries. Developmental stages are indicated in embryonic days. In all panels, the heart is viewed from the ventral side, with anterior upwards [56].

Maintaining a balance between proliferation and differentiation of cardiomyocytes is crucial in forming the ventricular chambers during heart development and in the homeostasis of cardiac function

in the postnatal period. During heart embryogenesis, this developmental stage occurs as the process of heart tube twisting is completed, resulting in the formation of trabeculae as highly organized layers of cardiomyocytes. Subsequently, they form muscular ridges lined with endocardial cells, arising from the interaction of primitive myocardium and endocardium. The formation of these structures is an early hallmark of ventricular differentiation. Gradually, the trabeculae give rise to parts of the papillary muscles, the interventricular septum, and the heart's conduction system. The Notch signaling pathway is directly involved in these processes, playing a pivotal role in the formation of ventricular trabeculae and chamber development. For instance, EphrinB2 serves as a direct target of Notch in the endocardium, and the activities of BMP10 and Neuregulin-1 (NRG1) also depend on Notch, which further promotes the proliferation and differentiation of ventricular myocardium [57, 58].

Heart development is closely linked with the processes of blood vessel formation, which originate from populations of angioblasts – mesodermal precursors of endothelial cells. These cells are among the first to differentiate and form primitive blood vessels or the primary vascular plexus [59]. Following vasculogenesis, the processes of angiogenesis begin, in which genetically embedded mechanisms also participate. It is known that during embryonic development, even before the onset of blood flow, endothelial cells acquire their specific markers and follow a predetermined path. The Notch signaling pathway plays a direct role in this process. For example, *Notch1-2, 4* receptors are expressed in murine endothelial cells. While the expression of *Notch1* and *Notch2* receptors is constitutive and necessary for normal development, the inactivation of *Notch4* does not affect vascular development. Moreover, hyperexpression of *Notch4* can lead to functional disturbances [60]. In addition to receptors, endothelial cells express specific Notch ligands, such as *Dll4* and *Jagged1*. The latter, for example, is expressed in the endothelium of mice. Its suppression leads to irreversible changes characterized by defects in angiogenesis, although this disruption does not affect larger vessels [61].

In studies aimed at elucidating the role of Notch in arteriovenous differentiation during the formation of embryonic blood vessels in *Danio Rerio* (zebrafish), it has been established that *NOTCH3* expression occurs only in the endotheliocytes of the dorsal aorta and is not observed in the cells of the posterior cardinal vein [62]. This specific functioning is linked to preventing endothelial cells from transitioning into venous differentiation. In embryos with deactivated Notch signaling pathways, the expression of the transmembrane protein ephrinB2, specific to cells with arterial differentiation, did not occur in cells. Instead, the expression of venous markers began within the dorsal aorta. Furthermore, disruption of Notch signaling during the embryogenesis of the vascular system led to numerous morphological defects, such as remodeling of major trunk vessels. Thus, the Notch signaling pathway exerts a strong influence on the arteriovenous differentiation of blood vessels.

1.4 Congenital Heart Defects

Tetralogy of Fallot (TF) is a severe cyanotic congenital heart defect (CHD) characterized by subpulmonary stenosis and predominant right-to-left shunting through a ventricular septal defect (VSD), resulting in circulation of deoxygenated blood through the systemic arteries. Modern surgical techniques make it possible to correct right ventricular outflow obstruction and close the ventricular septal defect, ensuring effective circulation of oxygenated blood through the left ventricle [63]. Patients with TF often present with a variety of cardiac abnormalities, such as hypertrophy and degeneration of cardiomyocytes, as well as various types of fibrosis of varying severity. These conditions are thought to be a consequence of increased right ventricular pressure and hypoxia [64].

The exact causes of the development of TF remain poorly understood, and definitive candidate genes directly associated with the formation of the disease have not been identified. About 20% of TF cases are associated with specific syndromes or chromosomal abnormalities [65], with 15% of TF patients having a deletion of chromosome 22q11.2, primarily associated with changes in the *TBX1* gene [66]. Most cases of TF, approximately 80%, are not syndromic and do not have a clear Mendelian pattern of inheritance [67]. This has led to the assumption of a polygenic basis for TF, which has prompted genome-wide studies to elucidate the genetic factors contributing to the development of TF and other congenital disorders [63].

Whole exome sequencing has identified novel candidate genes for the development of congenital heart disease, reflecting the complex nature of heart formation due to several transcription factors and signaling molecules critical for heart formation, such as *GATA4, NKX2.5, FOXC2, TBX5* and *TBX1* are involved in the pathogenesis of TF [68]. It is assumed that an imbalance in the interactions of these transcription factors important for cardiogenesis is critical in the occurrence of nonsyndromic TF.

Alterations in the *NOTCH1, NOTCH2*, and *JAG1* genes, which are part of the Notch signaling pathway, are associated with TF, although mutations in these genes are more often associated with other congenital heart defects [69, 70]. These studies support the important role of Notch genes in the development of tetralogy of Fallot. For example, copy number variations of the *NOTCH1* and *JAG1* genes have been identified in patients with this condition [71]. In addition, analysis of right ventricular tissue from these patients revealed a significant decrease in the activity of genes associated with the Wnt and Notch pathways [72]. Whole-exome studies have also shown [73, 74] that the *NOTCH1* gene locus is of increased interest in the context of non-syndromic tetralogy of Fallot: rare deleterious variants were found in 7% of patients, which may predispose to the development of this disease. Therefore, Notch signaling is an integral part of cardiac development, and its dysregulation may contribute to the pathogenesis of congenital heart defects.

1.5 Cardiac Homeostasis and Regeneration

The ability of the heart to regenerate is the subject of active debate in the scientific community. Whether the human heart could regenerate remains an open question. Existing ideas have been repeatedly challenged and criticized [75, 76]. Research by Pavel Pavlovich Rumyantsev on frog and mouse models was the first to show the presence of hyperplasia of cardiac cells, which were described in his monograph [77]. These results marked the beginning of a broader study of possible regenerative mechanisms of the heart of mammals, including humans.

Current consensus suggests that the human heart has a limited ability to regenerate. Studies show that the formation of new cardiomyocytes occurs in adults, although at a moderate rate, around 0.5–1% per year, according to various estimates [78, 79]. However, more pronounced regenerative activity was observed in mice in the natal period of life, whose hearts had a significant ability to regenerate [80, 81]. This is confirmed by the active proliferation of cardiomyocytes during the first week of life after injury [29].

Subsequently, regenerative processes in mice shift to typical adult patterns of wound healing, which leads to the formation of fibrous tissue at sites of injury [82]. A remarkable case of functional cardiac regeneration was reported in an infant who experienced myocardial recovery after severe ischemia caused by coronary artery occlusion, suggesting the presence of some regenerative mechanism [83].

Current research is primarily focused on the rate of cardiomyocytes turnover in both healthy and damaged hearts of adult animals. For example, studies have shown varying levels of cell cycle activity in ventricular cardiomyocytes in adult rats, ranging from 0 to 3.15% [84]. These differences may be due to different methodologies used to assess cell cycle activity, such as the incorporation of bromodeoxyuridine-labeled thymidine or tritium, indicating higher turnover rates due to extended S phases. In contrast, cytological methods may demonstrate lower proliferation rates.

Accurate identification of cardiomyocytes and their nuclei has been a methodological challenge. The traditional use of confocal microscopy and immunofluorescence to detect cytoplasmic markers such as troponin T has been considered accurate for identifying cardiomyocyte nuclei in tissue sections [85]. However, the limited z-axis resolution of confocal microscopy, especially for cells smaller than 0.5 micrometers, affected the accurate identification of specific cell nuclei. Modern techniques such as fluorescence-activated cell sorting (FACS) now allow the separation of mononucleated and binucleated cardiomyocytes [86]. Which is a significant achievement considering that cardiomyocytes make up about 30% of the total number of cardiac cells, as shown by single cell sequencing technologies and other methods [87].

Stem cell therapy and related cell products are emerging as a promising approach for the prevention and treatment of heart failure [88-90]. Advances in this area could change the way heart muscle is repaired. There is growing interest in resident stem cells in adult tissues, including those found in bone marrow, adipose tissue, and muscle, which are known to harbor stem cell populations [91, 92]. Determining whether the heart has its own regenerative potential for myocardial repair remains a key question in cardiac regenerative medicine.

1.6 Cardiac Mesenchymal Cells

1.6.1 Discovery of Cardiac Stem Cells

The adult human myocardium is a complex structure consisting of a variety of cells, including not only cardiomyocytes. Endothelial cells predominate, forming a network of coronary and lymphatic vessels, as well as lining the endocardium. In addition, the myocardium contains fibroblasts, pericytes, elements of the nervous system and immune cells [93].

The reorientation of researchers to the study of cardiac stem cells (CMCs), discovered about twenty years ago [94], became a significant step in the development of "second generation" cell therapy. The discovery of CMCs prompted the scientific community to reconsider the strategy for conducting clinical trials, shifting the emphasis from the use of exogenous stem cells to the use of resident cells of the organ itself. Adult cardiac stem cells were identified and isolated using similar criteria used for hematopoietic stem cells, including the presence of c-Kit and Sca-1 proteins on the surface, but the absence of hematopoietic lineage markers. However, the ability of these cells to differentiate into cardiomyocytes remains a matter of debate, although their potential to proliferate and become endothelial cells is beyond doubt [95].

Research from the laboratory of Pierre Anversa, which made an important discovery in the field of studying CMCs, was subject to revision due to doubts about the reliability of its data. In 2003, they published an article in which they described c-Kit$^+$ CMCs cells that have the c-Kit tyrosine kinase receptor and do not express hematopoietic markers [14]. Then, in their subsequent works, they described the properties of CMCs, such as the ability to form clones and self-renewal, as well as the presence of multipotency [96].

The human heart contains diverse cell populations that presumably have stemness potential [97]. However, their proportion in the heart is very small - from 0.005 to 2.0% of all cells, which makes them difficult to study in living organisms. It was found that transplantation of these cells has a positive effect on cardiac repair due to their paracrine and angiogenic effects, rather than the ability to divide and

differentiate CSCs into cardiomyocytes [98]. However, the discovery of these cells has given rise to new areas of research related to their extracellular vesicles, such as exosomes, which secrete CSCs and participate in the formation of the cardiac secretome [28]. It has been suggested that it is possible to enhance the natural mechanisms of cardiac repair by activating the internal regenerative potential or using exogenous cell therapy [99].

The myocardium contains diverse populations of cardiac mesenchymal cells that have been described and classified [100]. They have high proliferative activity and the ability to exhibit different phenotypes depending on cultivation conditions (**Figure 5**).

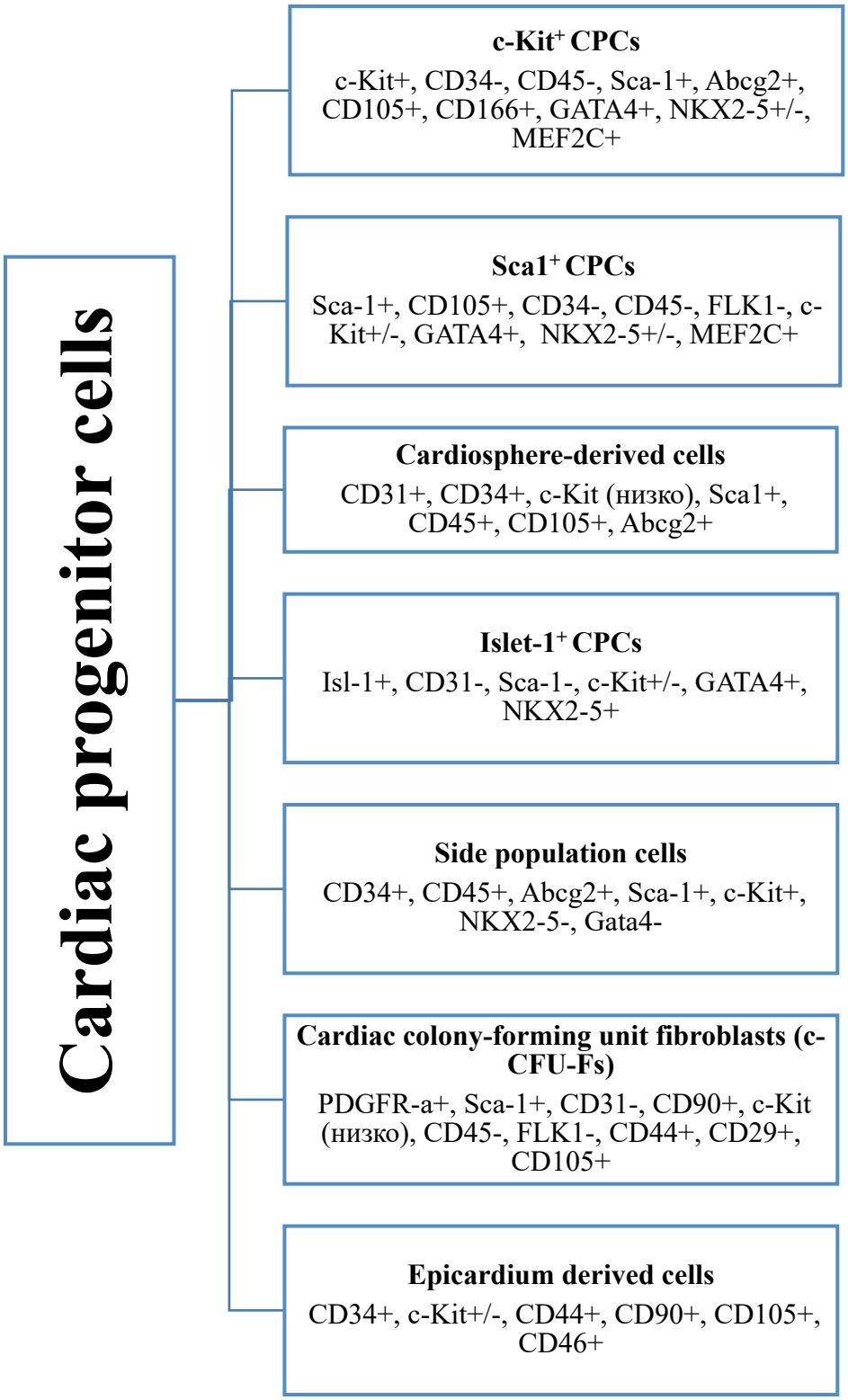

Figure 5. General Characteristics of Phenotypes of Resident Cardiac Progenitor Cells [100].

1.6.2 c-Kit$^+$ Cell Population

The presence of c-Kit expression found in cardiac cells has led to the consideration of this population of cells as cardiac progenitor cells. However, it was later found that such expression was also present in neonatal cardiomyocytes, mature dedifferentiated cardiomyocytes, and in epicardial and endothelial cells of the coronary arteries [101]. One study on adult mice showed [102], that the presence of a heterozygous c-Kit$^{W/Wv}$ mutation contributed to enhanced cardiac regeneration processes after cardiac stress in the form of re-entry of adult cardiomyocytes into the cell cycle and activation of proliferation in them. Without the presence of the mutation, only cardiomyocyte hypertrophy occurred in wild-type mice. This confirms the importance of c-Kit expression for the regulation of cellular state, especially in terminal differentiation, making c-Kit not a marker of a specific cell type, but a marker of cell state [28].

The heterogeneous population of c-Kit$^+$ cells in the adult heart and their origin are poorly understood, but there is experimental evidence suggesting a connection between embryonic and adult populations [101]. Mouse embryonic stem cells, when differentiated *in vitro*, yielded immature mesodermal cells expressing c-Kit and the cardiac transcription factor *Nkx2-5*, which could differentiate into cardiomyocytes and smooth muscle cells. But adult c-Kit$^+$ cells did not have such capabilities and could not differentiate into cardiomyocytes, even when transplanted into a healthy or ischemic heart [28]. According to studies [14, 103], c-Kit$^+$ cells, which have some potential for differentiation into cardiomyocytes, are very rare in the adult heart, and their selection helps to increase the population of self-renewing cells with multipotent properties.

c-Kit$^+$ cells have demonstrated myogenesis and angiogenesis capabilities upon transplantation in several preclinical studies [104-106]. This prompted clinical trials that confirmed safety and preliminary clinical efficacy. Results from the phase 2 CONCERT-HF trial (NCT02501811), a multicenter study involving 125 patients using mesenchymal and c-Kit$^+$ cells as a new type of potential regenerative therapy for heart failure, showed improved clinical outcomes for patients. These results also support the future potential of such treatment [107].

1.6.3 Cardiac Fibroblast Colony-Forming Units

In 2011, a population of cells in the adult heart was discovered that resembled mesenchymal stem cells in their properties. They expressed platelet-derived growth factor receptor alpha (*PDGFRα*) and *Sca-1*, and had stem cell properties, including the active ability to form cell clones [108]. These cells

were named cardiac fibroblast colony-forming units (cF-CFUs), having some similarities to fibroblast colony-forming units from bone marrow.

PDGFRα plays an important role in cardiogenesis, expressed in early mesoderm, including cardiac mesenchyme. Knockout of the *PDGFRα* gene led to disturbances in the development of the outflow tract, coronary arteries, septum, and cardiac chambers in mouse embryos, which confirmed the importance of PDGFRα for early cardiogenesis [101]. Predominantly, the expression of *PDGFRα* was noted in the proepicardium and epicardium itself, as well as in interstitial fibroblasts, which are formed from the epicardium via epithelial-mesenchymal transition [108]. In PDGFRα knockout mice, epithelial-mesenchymal transition was impaired in the epicardium and the number of cardiac stromal fibroblasts was reduced. However, this did not affect the development of smooth muscle cells, also derived from the epicardium. The role of PDGFRα signaling in cF-CFUs is not fully understood, although PDGFRα is known to be required for epithelial-mesenchymal transition and stromal fibroblast formation during development, which may indicate its importance in maintaining the stemness phenotype [109].

Epicardial stem cells expressing *PDGFRα* and occupying the interstitial and perivascular space have been identified in adult mouse and human hearts. Some of them corresponded to cF-CFUs, such as PDGFRα^{+}/SCA1^{+}/PECAM1^{-} (CD31), which gave rise to clonal colonies of mesenchymal cells *in vitro*. They had markers CD29, CD44, CD90 and CD105, characteristic of bone marrow mesenchymal stem cells [108]. In addition, the expression of cardiac-specific markers *HAND1, MEF2C, GATA4* and *TBX5*, found in populations of cardiac stem cells and cF-CFUs, also indicates their belonging to resident cardiac cells [110]. The possibility of long-term cultivation of cF-CFUs demonstrates their active ability for self-renewal, as well as multipotency when co-cultivated with embryonic stem cells to obtain teratomas and when transplanted into an ischemic heart [110].

1.6.4 Isl-1^{+} Cell Population

The *Isl-1* gene is actively expressed in mesodermal precursors found in both the primary and secondary cardiac fields. With the development and differentiation of these cells into different cardiac lineages as they migrate towards the cardiac region, the level of *Isl-1* expression decreases significantly [111]. However, the process of heart tube formation can be completely disrupted because of knockout of the *Isl-1* gene in progenitor cells, which then lose the ability to grow, migrate and survive. Recent studies have confirmed that cells expressing *Isl-1* have the potential to differentiate into cardiomyocytes and smooth muscle cells in vitro [112]. Tracking the Isl-1^{+} cell lineage from embryonic period showed their contribution, albeit small, to the cardiomyocyte population in the heart of newborn mice.

In adult mouse hearts, Isl-1-expressing cells are rare and primarily localized to the sinoatrial node, prompting debate regarding their role as stem cells in adult cardiac repair. Their rarity, coupled with observations suggesting a limited role in regenerative processes after cardiac injury, makes this question even more uncertain. A significant presence of Isl-1^+ cells was not observed in areas adjacent to damaged areas of cardiac tissue, although a slight increase in their numbers was noted after ischemia-reperfusion injury.

It has been shown that mouse and human embryonic stem and progenitor cells expressing *Isl-1* can differentiate into cardiomyocytes, smooth muscle and endothelial cells *in vitro* [101]. Such embryonic cells that express *Isl-1* have been used in clinical studies. For example, Isl-1^+/$CD15^+$ progenitor cells have been integrated into a fibrin matrix for subsequent transplantation into the epicardium of patients suffering from severe left ventricular dysfunction. This study was carried out as part of the first phase of the ESCORT trial (NCT02057900), which was completed in 2018 and showed both the safety of this procedure in the short and medium term, and the technical feasibility of its implementation in obtaining progenitor cells from human embryonic stem cells for clinical application [113].

1.6.5 Sca-1^+ Cell Population and Cardiospheres-derived cells

Among the resident cardiac progenitor cells, Sca-1^+ cells and cardiospheres-derived cells (CDCs), which could form clones, are also, distinguished. However, their exact origin remains unknown. Sca-1^+ cells in the heart constitute a heterogeneous population that includes c-Kit^+ progenitor cells, microvascular endothelial cells, PDGFRα^+ cardiac fibroblasts, stem cells, and other cells of the interstitial and perivascular space. A hallmark of Sca-1^+ cells is the expression of cardiac-specific transcription factors such as *TEF1, MEF2C* and *GATA4*, in the absence of *NKX2-5* expression [101]. It was shown that cardiac fractions of Sca-1^+ cells are able to differentiate into cardiomyocytes *in vitro* under the influence of 5-azacytidine, and also improve cardiac function when transplanted into mice with myocardial infarction [114]. In experiments, it was found that two weeks after transplantation, about 18% of cardiomyocytes in the infarct area were of donor origin, and most of them were formed as a result of the fusion of donor cells with resident cardiomyocytes [115].

Cardiosphere-derived cells are low-adhesive cells that originate in the developing heart and form heterogeneous clusters *in vitro*. These clusters create a niche for the proliferation of c-Kit^+ cardiac progenitor cells [116]. The origin of CDCs is not fully understood, but they are cardiac cells not associated with cardiomyocytes [117]. CDCs can differentiate into cardiomyocytes when co-cultured with cardiomyocytes from newborn rats [114]. Their transplantation into the myocardium of mice, rats

or pigs that have suffered a heart attack improves cardiac function [118]. In the CADUCEUS trial, in which patients with myocardial infarction were administered autologous CDCs through the coronary artery, no side effects were found after six months [119]. Patients treated with CDCs showed decreased scar tissue formation, increased viable cardiac tissue, and improved cardiac function, prompting further clinical trials [119]. However, the next phase of the ALLSTAR trial, completed in 2019, did not confirm the same positive results as the first phase, showing only the safety of administering allogeneic CDCs to patients with left ventricular dysfunction after myocardial infarction, but not finding scar reduction compared with placebo at six months [120].

1.7 The Role of the Notch Signaling Pathway in Regulating the Properties of Cardiac Mesenchymal Cells

Currently, the epicardium is believed to play an increasingly significant role in myocardial homeostasis and repair, potentially serving as a niche for populations of cardiac mesenchymal cells (CMCs). Electron and immunofluorescent microscopy studies have identified approximately 10 different types of cells, including CMCs, in the epicardium during the postnatal period. In one study, a group of scientists activated regenerative processes in the myocardium by controlling the cell cycle of mesenchymal cells within the epicardial microenvironment [121]. Jamie L. Russell and colleagues developed a unique model that provides a functional characterization of Notch pathway activation using a transgenic Notch reporter (TNR). Through TNR, they were able to identify and isolate a specific population of resident cells, termed Notch-activated epicardium-derived cells (EPDCs). Genomic expression analysis revealed their kinship with multipotent stromal cells, confirming their heterogeneity and suggesting a greater potential for differentiation. In other studies, the role of mesenchymal stem cells in heart regeneration has been repeatedly demonstrated, further emphasizing the significance of these cells in cardiac repair and regeneration [122]. This further confirms that multipotent stromal cells (MSCs) constitute a pool of cells capable of cardiac repair. However, epicardium-derived cells (EPDCs) exhibit certain phenotypic differences from general MSCs, such as the expression of epicardial lineage markers and direct localization in the epicardium, as well as the expression and regulation of muscle transcriptome levels. In one study, EPDCs were found to respond to injury by forming fibrotic tissue. Like most tissue-derived MSCs, EPDCs also secrete trophic factors for growth and differentiation, but uniquely include thymosin-β4, PDGF-α, TGF-β3, 2, BMP-1, 4, hepatoma-derived growth factor, interleukins-18, 25, and macrophage colony-stimulating factor [121].

In some vertebrate species, complete regeneration of damaged myocardium is possible through the remaining cardiomyocytes. Long Zhao and colleagues were able to establish that heart regeneration

in the zebrafish (*Danio rerio*) is dependent on the Notch signaling pathway [123]. Adult individuals, unlike mammals, retain the ability to regenerate their hearts after damage by utilizing partially dedifferentiated cardiomyocytes that have not been affected by the injury. This capacity for cardiomyocyte proliferation is also observed in mice, but only during the neonatal stage of their development. Notably, by the 7th day of embryonic development, there is a decrease in endogenous regenerative potential, and cardiomyocytes exit the cell cycle under the regulatory influence of Meis1 [124]. A group of researchers managed to pinpoint the location of actively proliferating cells during the regeneration process. Following the amputation of the ventricular apex in *Danio rerio*, they identified the expression of three Notch receptors in the endocardium and epicardium, but not in the myocardium. It was clarified that ligands to TGFβ and hedgehog participate in the regenerative signaling pathway. Additionally, it was established that suppressing the Notch signaling pathway weakens heart regeneration and induces scar formation at the amputation site. However, the same result occurs with hyperactivation of Notch signaling. A contrasting outcome is observed in mice, where hyperactivation of the Notch pathway in the epicardium leads cells to adopt a fibroblast phenotype. Thus, the activity of the Notch signaling pathway is necessary for maintaining the regenerative capacity in *Danio rerio* and stimulates the proliferation of immature cardiomyocytes in mammals. At the same time, it induces cell cycle arrest in mature cardiomyocytes. This finding highlights the nuanced role of Notch signaling in cardiac regeneration, varying significantly across different species and stages of cardiac cell development [123].

One reason for the cessation of the cell cycle in mature cardiomyocytes and the overall transformation of the heart into a post-mitotic organ may be the reactive oxygen species (ROS) of mitochondrial origin, which serve as a source of oxidative stress in postnatal cardiomyocytes [22]. Considering that the intrauterine period in mammals occurs under hypoxic conditions, the potential for heart regeneration remains active, while in the postnatal period, there is a delay in the cell cycle of cardiomyocytes due to oxidative DNA damage caused by the induction of mitochondrial reactive oxygen species (ROS). Consequently, researchers have hypothesized that systemic hypoxia can suppress aerobic respiration and reduce oxidative DNA damage, thereby triggering cardiomyocyte proliferation in adult mammals. Yuji Nakada and colleagues applied the effect of severe systemic hypoxemia in adult mice, which led to the inhibition of oxidative metabolism, reduction of ROS and oxidative DNA damage, and initiation of cardiomyocyte mitosis reactivation. Following myocardial infarction induction and one week of hypoxemia in vivo, there was activation of regenerative processes in the mouse heart with a decrease in fibrosis and an improvement in left ventricular systolic function [22]. It is crucial to note that the exposure to chronic severe hypoxemia, induced by gradually decreasing the oxygen inhaled, contributed to the reactivation of the cell cycle in mature cardiomyocytes. This, in turn, led to significant

functional recovery following a myocardial infarction. Thus, it has been established that the endogenous regenerative properties of the mammalian heart in the postnatal period can be activated through systemic hypoxemia. This is because exogenous oxygen causes mitochondrial-dependent oxidative DNA damage, which plays a role in regulating the cell cycle of both newborn and adult mammalian cardiomyocytes.

1.8 Interaction of BMP2 and the Notch Signaling Pathway in the Context of Endothelial-Mesenchymal Transition

The endothelial-mesenchymal transition (EndoMT) is one of the key events occurring in the heart, both during its development and in pathology. During this process, endothelial cells undergo a series of changes, including the loss of tight intercellular contacts, an increase in migratory activity, and enhanced secretion of extracellular matrix proteins. As a result, they acquire a phenotype characteristic of "mesenchymal nature" cells [125]. For instance, during normal physiological development, such cellular transformation is essential for the proper formation of heart valves in the developing heart [126]. Conversely, the reactivation of endothelial-to-mesenchymal transition (EndoMT) processes is characteristic of the development of various cardiovascular pathologies, such as atherosclerosis and myocardial fibrosis [127, 128].

Cardiac fibrosis develops because of heart failure, for instance, following a myocardial infarction, and is characterized by excessive collagen deposition, leading to remodeling of the organ [129, 130]. Numerous signaling pathways participate in endothelial-to-mesenchymal transition (EndoMT) and actively modulate the process, with the Notch signaling pathway being of paramount importance. Notch functions as a critical regulator of EndoMT during myocardial fibrosis, stimulating the expression of transcription factors such as *Snai*, *Slug*, and *Zeb1* [128, 131, 132]. Previously, we noted that the factor BMP2, from the TGF-β superfamily, is involved in the early myocardial remodeling processes in the cardiac mesenchymal cells (CMC) [23]. Activation of BMP2 in cardiac mesenchymal cells was accompanied by increased expression of components of the Notch signaling pathway, indicating the reactivation of embryonic signaling pathways in myocardial fibrosis. The signaling cascade induced by TGF-β is the most important regulatory pathway in the initiation and development of endothelial-mesenchymal transition (EndoMT) [133]. It remains unclear whether the Notch and BMP2 signaling pathways interact with each other in the processes of endothelial-mesenchymal transition (EndoMT).

Thus, the Notch signaling pathway may be a key mechanism responding to hypoxia and participating in the processes of activation of cardiac mesenchymal cells and early myocardial remodeling. Considering this, studying the relationship between hypoxia and the Notch signaling

pathway is extremely important for identifying molecular targets involved in the pathogenesis of diseases.

2 MATERIALS AND METHODS

Research was conducted at the Laboratory of Molecular Cardiology and Genetics of the Research Institute of Molecular Biology and Genetics at the Almazov National Medical Research Centre (Saint Petersburg, Russia). Surgical operations on animals were carried out at the Center for Experimental Pharmacology of the Saint Petersburg State Chemical Pharmaceutical University (Saint Petersburg, Russia).

2.1 Laboratory Animals

The animal research protocol was approved by the Bioethics Committee of the Saint Petersburg State Chemical Pharmaceutical University (protocol code 'Rats-MI-SC-2018', approval date: January 10, 2018). The experiment utilized male Wistar rats (Pushchino, Russia) of the same age with body weights ranging from 200 to 250 grams. Throughout the experiment, the animals were housed in individual plastic cages with free access to food and water according to a standard diet. All work with animals was conducted in accordance with the 'Guide for the Care and Use of Laboratory Animals' [134].

2.2 Induction of Myocardial Infarction

Male Wistar rats (n = 16) were anesthetized with chloral hydrate (2 mg/kg, intraperitoneally), intubated, and connected to a ventilator (SAR-830P; CWE, Inc., Ardmore, PA) that supplied room air with respiratory volume 2 ml/100 g and respiratory rate 60 breaths per minute. Body temperature was maintained at 37.0 ± 0.5°C using a thermoregulated heating pad (TCAT-2LV controller; Physitemp Instruments Inc., Clifton, NJ). Electrocardiography made it possible to monitor heart rate and arrhythmias. After thoracotomy through the fourth intercostal space, the heart was visualized. The pericardium was then removed bluntly using anatomical forceps. At the border of the left atrial appendage, the left coronary artery was discovered, under which a ligature (Prolene 6/0, Ethicon, Germany) was placed at the edge of the appendage [135]. Myocardial ischemia was determined by visual changes in the anterior wall of the heart and ST segment elevation on the ECG.

2.3 Patients

The protocol for work with human material was approved by the ethics committee of the Almazov National Medical Research Centre (ethical approval dated 26.12.2014) and adhered to the principles of

the Helsinki Declaration (as amended in 2013) [136]. Informed consent was obtained from each patient (or his or her representative).

Myocardial tissue samples were collected during surgical interventions performed at the Almazov National Medical Research Centre. Fragments of the right ventricle (n = 42) and right atrium (n = 14) were collected during the correction of Tetralogy of Fallot and ventricular septal defect, respectively. The average age of the patients at the time of surgery was 120–150 days from birth. Pronounced cyanosis (saturation ≤ 85%) was only characteristic for 14 (33%) patients with Tetralogy of Fallot syndrome.

2.4 Cell Cultures

In this study, primary cell cultures were used, specifically:

- Rat cardiac mesenchymal cells (CMCr);
- Human cardiac mesenchymal cells (CMCh);
- Human umbilical vein endothelial cells (HUVECs).

Additionally, permanent cell line was used:

- Human embryonic kidney 293-T cells.

2.4.1 Rat Cardiac Mesenchymal Cells

2.4.1.1 Isolation of Rat Cardiac Mesenchymal Cells from Myocardial Tissue

The induction of myocardial infarction was carried out through permanent ligation of the left coronary artery, resulting in damage to a portion of the myocardium in the left ventricle of the heart. Tissue samples were collected at 8- and 24-hours post-infarction. Rat cardiac mesenchymal cells (CMCr) were obtained from the post-infarction zone (including the peri-infarct area) of the myocardium, which was visually slightly separated by a whitish hue and located beneath the ligature. The post-infarction tissues were mechanically minced and enzymatically digested using type 2 collagenase solution (2 mg/ml, Worthington) for 90 minutes in an incubator (37°C, 5% CO_2, 99% humidity); healthy rat myocardium, from rats subjected to a sham operation, served as a negative control.

The cells were centrifuged for 5 minutes at 300 g, resuspended in the medium (twice), seeded on a flask with a filter and incubated at 37°C, 5% CO_2, 99% humidity. The medium for CMCr consisted of 70% DMEM/F_{12} (Invitrogen, USA), 20% endothelial cell growth medium (Cell Applications Inc., USA), 10% fetal serum (HyClone, USA), 100 μM MEM NEAA (Gibco, USA), a mixture of penicillin and streptomycin (10,000 units/ml) (Gibco, USA), and 2 mM L-glutamine (Gibco, USA). The medium was

changed to fresh one every day for three days. On the third day, the remaining tissue was removed and cultured until a monolayer was formed (~1 week). There were no living cardiomyocytes in the culture, and the cells were homogeneous. The study used rat heart mesenchymal cells of passages 2–3, isolated from the myocardium 8 and 24 hours after surgery.

2.4.1.2.Immunophenotyping of Rat Cardiac Mesenchymal Cells

The CMCr phenotype was determined using flow cytometry on CytoFlex (Beckman Coulter, USA). Cells were resuspended in Fetal Bovine Serum (FBS) (100 µl) with 1% bovine serum albumin (Sigma-Aldrich, USA), incubated for 30 minutes in the dark at room temperature with antibodies according to the manufacturer's instructions. The antibody panel included: CD31 (CD31 Polyclonal Antibody, FITC Conjugated, cat. #bs-0468R-FITC, Bioss Antibodies, USA), CD34 (CD34 Polyclonal Antibody, FITC Conjugated, cat. #bs-0646R-FITC, Bioss Antibodies, USA), CD45 (PE Mouse Anti-Rat CD45, cat. #554878, BD Pharmingen™, USA), CD90 (PE Mouse Anti-Rat CD90/Mouse CD90.1, cat. #551401, BD Pharmingen™, USA), CD166 (CD166 Polyclonal Antibody, ALEXA FLUOR® 488 Conjugated, cat. #bs-1251R-A488, Bioss Antibodies, USA). Controls included unstained cells and isotypes: Rabbit IgG Isotype Control, PE Conjugated (cat. #bs-0295P-PE, Bioss Antibodies, USA), Rabbit IgG Isotype Control, FITC Conjugated (cat. #bs-0295P-FITC, Bioss Antibodies, USA). Debris was excluded based on the FSC threshold. Fluorescence was analyzed using both single and dual parameter plots. Each sample contained no less than 10,000 events. Data was processed in CytExpert 2.1 (Beckman Coulter, USA).

2.4.2 Human Cardiac Mesenchymal Cells

2.4.2.1 Isolation of Human Cardiac Mesenchymal Cells

CMCh were obtained from myocardial tissue taken after operations to correct Tetralogy of Fallot or ventricular septal defect at the Almazov National Medical Research Centre. The myocardial tissue was washed in PBS, minced, and incubated with collagenase-2 (2 mg/ml) for 100 minutes at 37ºC [137]. The suspension was centrifuged twice for 5 minutes at 300g and resuspended in a medium (70% DMEM/F_{12} (Invitrogen, USA), 20% endothelial cell growth medium (Cell Applications Inc., USA), 10% fetal bovine serum (HyClone, USA), 100 µM MEM NEAA (Gibco, USA), penicillin and streptomycin mixture (10,000 units/ml) (Gibco, USA), and 2 mM L-glutamine (Gibco, USA)) and

seeded onto a flask. The medium was changed daily for 3 days. After reaching a confluent state, the cells were passaged. CMCh of 2-3 passages were used in the experiments.

2.4.2.2 Immunophenotyping of Human Cardiac Mesenchymal Cells

Immunophenotyping of CMCh was performed using flow cytometry with the CytoFlex instrument from Beckman Coulter, USA. For this, cells were resuspended in a volume of 100 µl of PBS buffer solution with the addition of 1% fetal bovine serum from Sigma-Aldrich (St. Louis, Missouri, USA) and incubated with a set of specific antibodies for 20 minutes at room temperature in the absence of light. The following panel of antibodies was used: PE-labeled anti-CD31 (Beckman Coulter, USA, IM2409), APC-labeled anti-CD34 (Beckman Coulter, USA, IM2472U), PE-labeled anti-CD90 (Beckman Coulter, USA, IM1840U), PE-labeled CD146 (Beckman Coulter, USA, A07483) and CD166 (Beckman Coulter, USA, A22361), as well as APC-labeled anti-PDGFR-β (BD Pharmingen, USA, FAB1263A). Cells without staining were used as a control. To exclude debris, thresholds were set for direct (FSC) and side (SSC) light scatter, with settings on a logarithmic scale of amplification. During the analysis, 10 thousand events were considered. Processing and analysis of the obtained data were performed in the Kaluza 2.0 program from Beckman Coulter.

2.4.3 Differentiation of Cardiac Mesenchymal Cells in Cardiogenic, Adipogenic, and Osteogenic Directions

CMCs were differentiated in three directions: cardiogenic, osteogenic, and adipogenic. Cells were seeded at a concentration of 104 cells per square centimeter in wells using 12-well plates. A day after seeding, the culture medium was changed to a specialized differentiation medium. Which included 97% DMEM/F_{12} medium (Invitrogen, USA), 2% horse serum (Invitrogen, USA), MEM-NEAA amino acid solution (Gibco, USA) at a concentration of 100 µM, 1% insulin-transferrin-selenium mixture (Invitrogen, USA), and a mixture of antibiotics penicillin and streptomycin (Gibco, USA) at a dosage of 10,000 units/ml.

For cardiogenic differentiation, 5 µM 5-azacytidine (Sigma-Aldrich, USA) was used, which was added to the medium a day after seeding and refreshed daily for three days [138]. On the sixth day, ascorbic acid (10^{-4}M) (Sigma-Aldrich, USA) and TGF-β1 (1 ng/ml) (Peprotech, USA) were added to the medium, which were then added every two days (ascorbic acid), and TGF-β1 twice a week respectively, with medium renewal every 2–3 days for 24 days [139]. The phenotype of cells, similar to cardiomyocytes, was confirmed by immunocytochemical staining with antibodies to α-actinin and

analyzed on a fluorescent microscope Axio Observer (Carl Zeiss, Germany).

Osteogenic differentiation began the next day after seeding with the replacement of the medium to a differentiation one, containing ascorbic acid (50 μM), dexamethasone (1 μM), and beta-glycerophosphate (10 mM) from Sigma, USA, with a twice-weekly medium renewal for 21 days. Qualitative analysis of differentiation was carried out using the NBT/BCIP substrate (Roche, Switzerland) to detect alkaline phosphatase. For this, the culture medium was taken, washed twice with PBS solution, and incubated with NBT/BCIP for 10 min until staining appeared. The results were recorded using a microscope AxioObserver.D1 (Carl Zeiss, Germany).

Adipogenic differentiation was carried out in a medium with the addition of 3-isobutyl-1-methylxanthine (0.5 mM), dexamethasone (1 μM), insulin (1 μM), indomethacin (0.2 mM), and rosiglitazone (0.5 mM) from Sigma, USA, with a twice-weekly medium change for 14 days. Differentiated cells were stained with the OilRed dye (Sigma, USA). For this, the culture medium was taken and washed with PBS solution. Then, the cell monolayer was fixed with a 4% solution of paraformaldehyde (PFA) for 30 minutes at room temperature with subsequent washing with PBS. After that, the OilRed dye was added and incubated for 30 min. Cells were washed twice with water and a small amount of water was left to prevent cell drying. The analysis of the staining results was carried out using an inverted microscope Axiovert (Zeiss, Germany).

2.4.4 Analysis of Proliferative Activity of Cardiac Mesenchymal Cells

The proliferative activity of the cardiac mesenchymal cells (CMCs) was evaluated using two methods – manual and automatic. In the first approach, the growth curve method was utilized. Cells were seeded at a density of 10^3 cells per cm^2. Every two days, cell counting was performed in a Goryaev chamber.

The second method involved real-time proliferation rate registration using the xCELLigence RTCA DP system. Impedance was used as an indicator, recorded by the xCELLigence system, to assess the proliferative capacity of the cells [140]. The system measures the electrical impedance of cells using microelectrodes located at the bottom of the E-Plate wells. This allows you to evaluate the cellular index, which reflects quantitative information about the biological status of cells, including their number and viability. Samples were prepared as a cell suspension (100 μl) containing 5,000 cells and seeded into wells in duplicate. The cell index value in each well was automatically recorded in real time for 72 hours using the xCELLigence system. Data were analyzed in RTCA Software (version 1.0.0.1304).

2.4.5 Analysis of Rat Cardiac Mesenchymal Cell Migration Rate

The method for assessing the migratory activity of CMCs was carried out using the “scratch” test: after the formation of a monolayer of cells, the culture medium was replaced with a medium without the addition of serum containing hydroxyurea (10 mM) to inhibit cell proliferation, and the growth factor PDGF-BB was also added (10 ng/ml) [141]. An artificial scratch was created in the layer of cells at the bottom of the dish, and subsequent analysis recorded the number of cells that migrated to the damaged area after 12, 24 and 36 hours.

2.4.6 Induction of Hypoxia *in vitro*

To induce hypoxia *in vitro*, healthy CMCs obtained from sham-operated rats were used. Cells were seeded onto Petri dishes (5 cm) and cultured in CMC medium. The next day, the cells were transferred to an incubator with controlled oxygen levels. CMCs were incubated at 1% or 5% O_2 (37°C, 5% CO_2, 99% humidity) for 8 or 24 hours. Control CMCs were incubated at 20% O_2 (37°C, 5% CO_2, 99% humidity).

CMCs were incubated in Heracell 150 (Thermo Scientific, USA) at 1.0% or 5.0% O_2, 5.0% CO_2, and 94% or 90% N_2, respectively, for 6–72 hours. Control CMCs were incubated at 21% O_2, 5.0% CO_2 and 74% N_2. Cells were analyzed immediately after incubation to avoid the influence of normoxia.

2.4.7 Immunocytochemical Staining of Cardiac Mesenchymal Cells

Cells on coverslips after cardiogenic differentiation were fixed in Petri dishes (10 cm) with 4% paraformaldehyde for 12 minutes on ice. Slides with cells were washed in PBS, treated with 0.5% Triton X-100 in PBS for 3 min, incubated in 1% Bovine Serum Albumin (BSA) in PBS for 40 min, and the area around the glass was delimited with a hydrophobic marker. Primary antibodies to α-actinin 1:200 (Invitrogen, USA) in BSA were applied to the slides and incubated in a humid chamber for 1 hour at room temperature. Then the slides were washed in PBS and incubated with secondary antibodies conjugated to Alexa Fluor 488, 1:10000 in the dark for 40 min at room temperature. After washing in PBS, the nuclei were stained with DAPI (Invitrogen, USA) 1:10000 with PBS for 5 s and slides with cells were mounted on slides with Fluoromount (Sigma, USA). The preparations were analyzed on an Observer.D1 fluorescent microscope (Carl Zeiss, Germany).

2.4.8. Human Umbilical Vein Endothelial Cells

Endothelial cells were obtained from human umbilical vein (HUVECs) by enzymatic tissue dissociation [142]. The vein was filled with a 0.1% solution of collagenase II (Worthington Biochemical Corporation, USA) and placed in an incubator for 10 min at 37°C in a PBS solution [143]. The cell suspension with collagenase solution was centrifuged for 5 min at 300 g. The supernatant was collected, and the cell pellet was resuspended and transferred to Petri dishes coated with 0.2% gelatin (Sigma-Aldrich, USA). HUVECs were cultured in ECM medium (ScienCell, Canada) at 37°C and 5% CO_2.

2.4.9. Co-cultivation of Human Umbilical Vein Endothelial Cells and Cardiac Mesenchymal Cells Cultures

HUVECs and CMCh cell cultures were co-seeded together in two different combinations: first seeding CMCh followed by HUVECs, and vice versa. The second cell culture was seeded 24 hours after the first. The cells were cultured in 12-well plates (for isolating total RNA, 75,000 cells per well) and 6-well plates (for α-SMA staining, 25,000 cells per well), coated with 0.2% gelatin in a special ECM medium for endothelial cell cultivation (ScienCell, Canada).

2.5. Plasmids

To construct lentiviral vectors, we used the pLVTHM plasmid provided by Professor D. Trono (École Polytechnique Fédérale de Lausanne, Switzerland). Based on it, a construct was made with the Notch1 intracellular domain gene (NICD) [132, 144, 145].

2.5.1 Production of Lentiviral Particles

To obtain lentiviral particles, we used a protocol developed in the laboratory of Professor D. Trono (École Polytechnique Fédérale de Lausanne, Switzerland) and adapted in the Tomilin's laboratory [144]. Lentiviral particles were produced using HEK293-T cells [144]. HEK293-T was cultured in medium containing DMEM (Gibco), 10% FBS (Gibco) and 1% penicillin-streptomycin (Invitrogen) in an incubator (37°C, 5% CO_2, 99% humidity). The efficiency of transgene expression with the NICD-carrying virus was confirmed using real-time PCR with primers to the Notch1 target gene - *HEY1*.

2.5.2 Transduction of Human Umbilical Vein Endothelial Cell and Cardiac Mesenchymal Cell Cultures with Lentiviral Vectors Carrying BMP2 and NICD

Lentiviral transduction was performed during cell seeding by adding 25 µl of viral concentrate, either with NICD or with BMP2. In the case of double transduction, the NICD vector was added 18 hours after cell seeding and initial transduction with the lentivirus carrying BMP2.

2.6 Gene Expression Analysis

Real-time PCR was used to analyze gene expression. RNA from cells was isolated using ExtractRNA (Evrogen, Russia) and treated with DNase I (Thermo Fisher Scientific, USA). The concentration and purity of RNA were determined using a Nanodrop 7500 spectrophotometer (Wilmington, USA). The quality of RNA was checked using electrophoresis with a current of 80 mA on BioRad chambers (USA) in a 1% agarose gel. Reverse transcription was done with MMLV RT (Evrogen, Russia). Real-time PCR was performed with gene-specific primers on a LightCycler 480 (Roche, Switzerland). For real-time PCR, a 5-fold mixture of qPCR mix-HS SYBR with SYBR Green I (Evrogen, Russia) was used. cDNA (50 ng), primers (10 µM each) were added to the mixture, and the volume was adjusted to 25 µl with sterile water. The primer sequences used for CMCs are shown in **Table No.1**.

Gene Symbol	Forward Primer (5'-3')	Reverse Primer (5'-3')
Bmp2	CTGCCATGGGGAATGTCCTT	TGCACTATGGCATGGTTGGT
Ccnd1	CTTACTTCAAGTGCGTGCAGAG	TTCATCTTAGAGGCCACGAACA
Dll1	TAACCCCGATGGAGGCTACA	GCACCGTTAGAACAAGGGGA
Dll4	GCAGCTGTAAGGACCATGAGA	TTCACAGTGCTGGCCATAGT
Fabp4	TGGGCGTGGAATTCGATGAA	CACATGTACCAGGACCCCAC
Gapdh	CCAGTATGACTCTACCCACG	CATTTGATGTTAGCGGGATCTC
Hes1	ACCAAAGACAGCCTCTGAGC	TTGGAATGCCGGGAGCTATC
Hes7	CATCAACCGCAGCCTAGAAGAG	CACGGCGAACTCCAGTATCTCT
Hey1	CCTGGCTATGGACTATCGGAG	AGGCATCGAGTCCTTCAATGAT
Hif-1a	GGCGAGAACGAGAAGAAAAATAGG	AGATGGGAGCTCACGTTGTG
Jag1	CGCCCAATGCTACAATCGTG	TCTTGCCCTCGTAGTCCTCA
Myc	CAGCTCGCCCAAATCCTGTA	TGATGGGGATGACCCTGACT

Notch1	CAATGAGTGTGACTCACGGC	GCACAAGGTTCTGGCAGTTG
Notch2	CCGTGGGGCTGAAGAATCTC	CTTTCTTTGGCTGGGGTCCT
Notch3	GCCTAGTCCAGTGCACTGGCTACTG	GGGAACAGATATGGGGTGTGG
Runx2	TCCCTCCGAGACCCTAAGAAA	GCTGCTCCCTTCTGAACCTAC
Tnnt2	CAGGCTCTTCATGCCCAACT	GCTCGTTCAGGTCCTTCTCC
Vegf-a	GCAGCGACAAGGCAGACTAT	TGGCACGATTTAAGAGGGGA
Vim	TGCCAACCGGAACAACGAT	ACTGCACCTGTCTCCGGTA

Table No.1. List of primers used to assess gene expression in CMCr using polymerase chain reaction in real time.

The primer sequences used for CMCh are shown in **Table No.2**.

Gene Symbol	**Forward Primer (5'-3')**	**Reverse Primer (5'-3')**
ACTA2	GTTACTACTGCTGAGCGTGAG	CAGGCAACTCGTAACTCTTC
ACTN1	GCAACGACCCCCAGAAGAAGA	GTTGTAACCCATGGAGATCAGGC
BMP2	GCCAAGCCGAGCCAACAC	CCCACTCGTTTCTGGTAGTTCTTC
DLL4	AGGCCTGTTTTGTGACCAAG	CTCCAGCTCACAGTCCACAC
GAPDH	CAAGGTCATCCATGACAACTTTG	GTCCACCACCCTGTTGCTGTAG
HES1	AGCACAGAAAGTCATCAAAG	AGGTGCTTCACTGTCATTTC
HEY1	TGGATCACCTGAAAATGCTG	CGAAATCCCAAACTCCGATA
HEY2	AGCAGGGCCGGAGACCTAGAT	GCCCCACGCCCTGTTTCTTTGA
HPRT	TGACACTGGCAAAACAATGCA	GGTCCTTTTCACCAGCAAGCT
JAG1	TGCCAAGTGCCAGGAAGT	GCCCCATCTGGTATCACACT
MEF2C	CCAACTTCGAGATGCCAGTCT	GTCGATGTGTTACACCAGGAG
NKX2.5	CCAAGGACCCTAGAGCCGAA	ATAGGCGGGGTAGGCGTTAT
NOTCH1	GTCAACGCCGTAGATGACC	TTGTTAGCCCCGTTCTTCAG
NOTCH2	ATGGTGGCAGAACTGATCAAC	TTGGCAAAATGGTCTAACAGG
NOTCH3	GGAGCCAATAAGGACATGCAGGAT	GGCAAAGTGGTCCAACAGCAG
NOTCH4	GTTGTGACAGGGTTGGGACT	CAGCCCAGTGGGTATCTCTG
RUNX2	GAGTGGACGAGGCAAGAGTT	GGGTTCCCGAGGTCCATCTA
*SNAI*1	CTCTTTCCTCGTCAGGAAGC	GGCTGCTGGAAGGTAAACTC
SNAI2	TCCAGACCCTGGTTGCTTCA	GAATGGGTCTGCAGATGAGCC

TWIST1	TGAAGATGCTTCAGGCAACAGGG	CGCAACTTCTGTTAGGCACTCTCG

Table No.2. List of primers used to assess gene expression in CMCh using polymerase chain reaction in real time.

The RT-PCR was performed on the LightCycler480 system (Roche Diagnostics, Indianapolis, USA) using specific forward and reverse primers for target genes. The quantitative PCR was carried out over 45 cycles. Data analysis was performed using the $2^{-\Delta\Delta Ct}$ method; relative gene expression was normalized to the GAPDH gene. Gene expression data were analyzed using GraphPad Prism 9.4.1 (458) (GraphPad Software, San Diego, California, USA). Values were expressed in median and interquartile range. Groups were compared using the Mann-Whitney non-parametric unpaired test. A P-value of ≤ 0.05 was considered significant.

2.7 RNA Sequencing Library Preparation

In this study, we used left ventricular myocardial tissues from rats subjected to myocardial infarction and from sham-operated rats (healthy controls). Additionally, rat cardiac mesenchymal cells (CMCr), isolated from both the post-infarct and healthy hearts, were utilized. Total RNA was extracted from the post-infarct tissues and CMCr ($n = 3$ each) following the manufacturer's protocol by Eurogene, Russia. The quality and quantity of the extracted RNA were assessed using a NanoDrop 1000 spectrophotometer (Thermo Fisher Scientific) and an Agilent 2100 bioanalyzer (Agilent Technologies). To create libraries, 1 μg of total RNA was used with the TruSeq RNA Sample Preparation Kit (Illumina), according to the protocol for samples with low nucleic acid content (LS) as provided in the manufacturer's instructions.

2.8 Differential Gene Expression Analysis

The raw RNASeq reads were aligned using STAR 2.7 against the Rnor_6.0 reference genome (GCA_000001895.4) and its transcript annotations (Ensembl 97), as described [146]. The differential expression analysis was conducted using the DESeq2 Bioconductor package [147]. Genes with a p-value of 0.05 or less were designated as differentially expressed genes. Comparisons were made between ischemic tissues/cells and control tissues/cells. Data analysis and visualization, including PCA Plot and Volcano Plot, were performed using Phantasus (version: 1.7.3, build: master-709) [148].

2.9 *Ingenuity* Pathway Analysis

Bioinformatics analysis was performed using Ingenuity Pathway Analysis software (IPA; Qiagen Silicon Valley, Redwood City, California, USA, (http://www.ingenuity.com)). The set of differentially expressed genes (DEGs) was used to determine interactions among genes within gene networks, specifically for Rattus norvegicus. The specificity of the network connections for each DEG was calculated based on the percentage of its connections to other significant genes in the database. Canonical signaling pathway analysis was conducted based on the IPA's library of signaling pathways.

3 RESULTS AND DISCUSSION

3.1 Mechanisms of Activation of the Regenerative Potential in Cardiac Mesenchymal Cells

The objective of this section was to study the mechanisms of early activation of regenerative processes in post-infarct tissue. Given the accumulated data [149], suggesting that mechanisms of myocardial functional recovery are likely rooted in paracrine intercellular signaling, it's presumed that their activation occurs during the early response to injury. In this context, an analysis of early transcriptional events in cardiac tissue following infarction was conducted, along with a study of the cellular population extracted from post-infarct myocardial tissue.

3.1.1 Gene Expression Profile Significantly Alters in Myocardial Tissues 24 Hours Post-Infarction

To analyze early transcriptional events occurring in the heart because of hypoxia, acute myocardial infarction was induced in Wistar rats by ligating the left coronary artery. Then, a post-infarction section of the myocardium with a peri-infarction zone was isolated from the ischemic heart one day after the operation. Healthy myocardium obtained from rats with a “sham” operation was taken as a control. Using the RNA sequencing method, the genetic profile of post-infarction and healthy myocardial tissues was determined [23].

Principal component analysis (PCA) showed significant variability in the data (**Figure 6**). Transcriptional profiles of post-infarction and healthy tissues were separated and formed separate clusters [23].

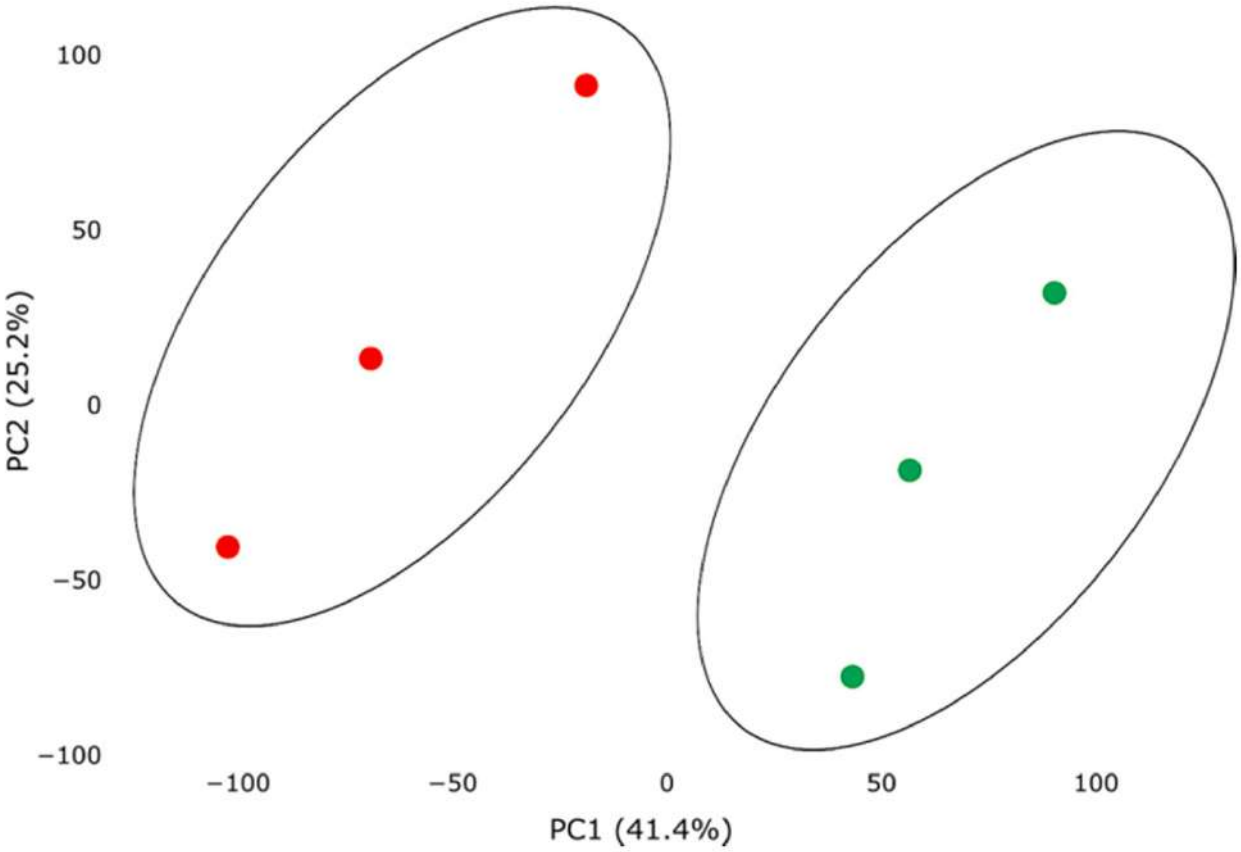

Figure 6. Principal Component Analysis (PCA) Demonstrates Variability of Gene Expression in Healthy (green dots, *n* = 3) and post-infarct (orange dots, *n* = 3) Myocardial Tissues Using the Web Tool Phantasus. Principal Component 1 (PC1) on the X-axis and PC2 on the Y-axis account for 41.4% and 25.2% of the total gene expression variability, respectively. PC1 captures a significant portion (41.4%) of the experimental variability and largely reflects the difference between the two states of the cardiac muscle. PC2 represents experimental variability (25.2%) related to differences in gene profiles between biological replicates (laboratory animals). Samples are visually divided into two main groups [23].

Analysis of differentially expressed genes (DEGs) revealed that in post-infarct tissues, 1241 genes were activated, and 1256 genes were suppressed (adj. p-value <0.05) (**Figure 7**).

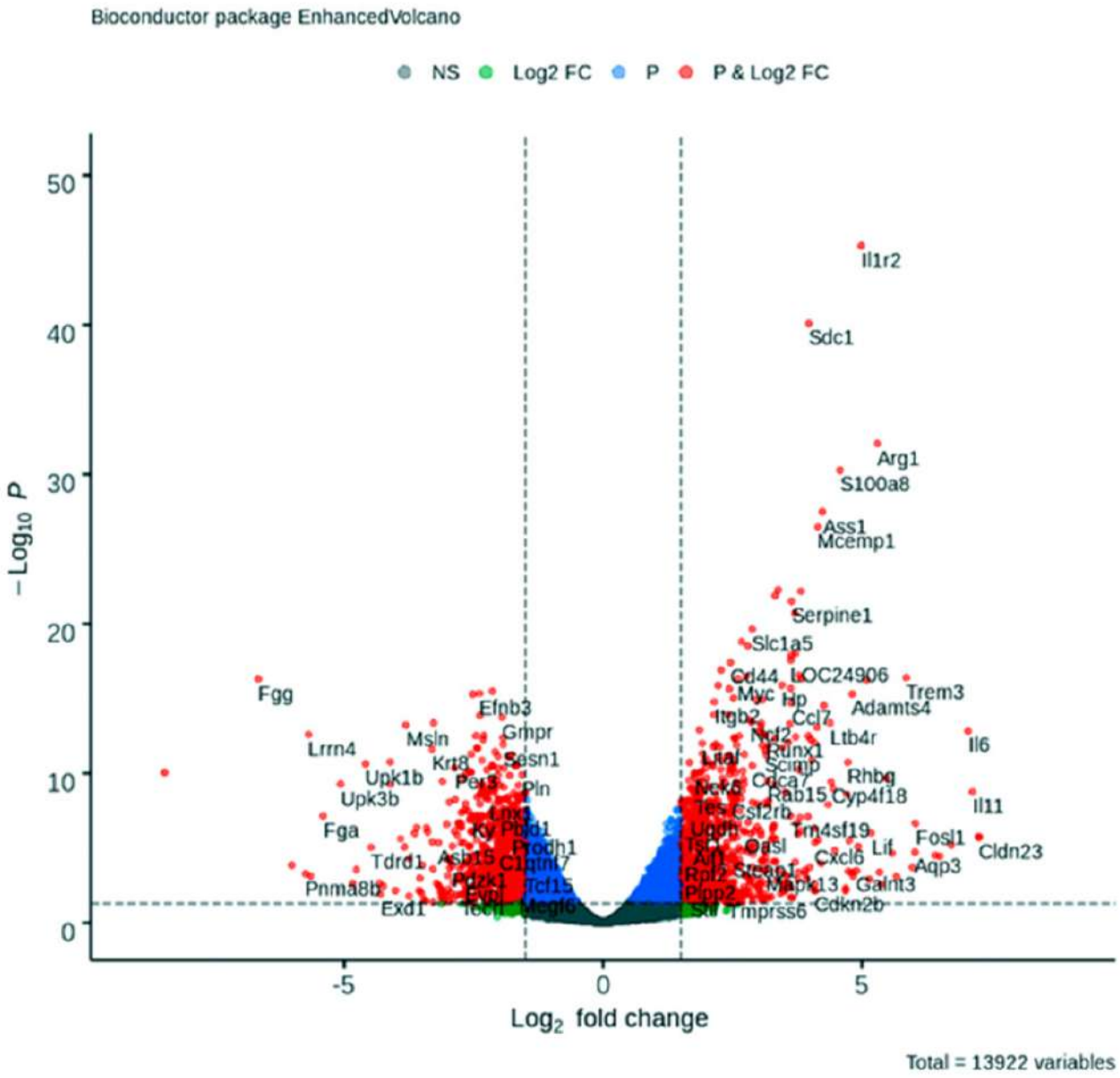

Figure 7. Volcano Plot Showing Differentially Expressed Genes (adj. p-value <0.05) in Post-Infarct Samples Compared to Control, Generated Using Bioconductor Software in R. The Y-axis corresponds to the mean expression value -log10 (p-value), and the X-axis displays the log2 (fold-change). Red dots represent differentially expressed genes [23].

The top 50 included DEGs associated with epithelial-mesenchymal transition, characteristic of both wound healing and fibrosis (*Cd44, Gpc1, Sdc1, Vcan, Plaur, Serpine1, Pmepa1, Pvr*); genes encoding proteins involved in glycolysis and gluconeogenesis (*Angptl4, Slc16a3*); genes activated by STAT5 in response to IL2 stimulation (*Myc, Slc1a5, Il1r2, Selp*). Also, genes regulated by NF-kB in response to TNF, responding to low oxygen levels (hypoxia) and defining the inflammatory response (**Table 3**).

Ensembl ID	Gene	FDR-adjusted p-value	Log2 fold-change
ENSRNOG00000014378	*Il1r2*	6,83E-42	4.9857
ENSRNOG00000059947	*Sdc1*	5,64E-37	3.9753
ENSRNOG00000013304	*Arg1*	3,94E-29	5.2988
ENSRNOG00000011557	*S100a8*	1,83E-27	4.5754
ENSRNOG00000008837	*Ass1*	8,86E-25	4.2348
ENSRNOG00000028259	*Mcemp1*	7,57E-24	4.1490
ENSRNOG00000019202	*Pvr*	1,07E-19	3.3820
ENSRNOG00000002794	*Selp*	1,11E-19	3.8235
ENSRNOG00000015514	*Bcat1*	1,95E-19	3.3250
ENSRNOG00000001414	*Serpine1*	4,23E-19	3.6392
ENSRNOG00000019433	*Rab3a*	6,84E-11	-2.3064
ENSRNOG00000032989	*Lrrn4*	6,26E-11	-5.6887
ENSRNOG00000019445	*Msln*	1,62E-11	-3.8116
ENSRNOG00000026217	*Armc2*	1,27E-11	-3.2730
ENSRNOG00000017250	*Gmpr*	5,64E-12	-1.9489
ENSRNOG00000027230	*Fhod3*	4,49E-12	-2.3839
ENSRNOG00000018997	*Myh7b*	2,10E-13	-2.5206
ENSRNOG00000010320	*Efnb3*	1,95E-13	-2.3865
ENSRNOG00000018233	*Gas6*	1,46E-13	-2.1429
ENSRNOG00000025074	*Fgg*	2,70E-14	-6.6579
ENSRNOG00000017897	*Adam8*	2,44E-18	3.7035
ENSRNOG00000015948	*Slc1a5*	2,64E-17	2.8822
ENSRNOG00000020465	*Ripk3*	1,67E-16	2.6771
ENSRNOG00000018371	*Tubb6*	3,04E-16	2.7982
ENSRNOG00000036677	*Slc16a3*	8,34E-16	3.7188
ENSRNOG00000037931	*Plaur*	1,08E-15	3.6347
ENSRNOG00000002820	*LOC24906*	2,20E-15	3.6261
ENSRNOG00000006094	*Cd44*	3,01E-15	2.4605
ENSRNOG00000015845	*Fam129b*	9,25E-15	2.2808
ENSRNOG00000019141	*Ch25h*	1,88E-14	3.7877
ENSRNOG00000057676	*Polr2m*	8,93E-10	-1.7560
ENSRNOG00000020244	*Perm1*	8,43E-10	-2.5532
ENSRNOG00000021128	*Kcnj11*	5,82E-10	-2.0874
ENSRNOG00000009779	*Krt8*	4,17E-10	-3.3038
ENSRNOG00000033722	*Rnf207*	3,48E-10	-2.4232

ENSRNOG00000042912	*Mycbpap*	3,48E-10	-2.4412
ENSRNOG00000000302	*Sesn1*	2,24E-10	-1.9286
ENSRNOG00000026493	*Cdnf*	1,13E-10	-2.3146
ENSRNOG00000049437	*Gpc1*	9,36E-11	-1.9317
ENSRNOG00000019278	*Fsd2*	7,06E-11	-2.4557
ENSRNOG00000029212	*Vcan*	2,15E-14	2.7637
ENSRNOG00000013748	*Trem3*	2,49E-14	5.8579
ENSRNOG00000004500	*Myc*	2,67E-14	2.5965
ENSRNOG00000022859	*Trem1*	2,67E-14	3.8338
ENSRNOG00000029768	*Ccl12*	2,97E-14	5.0897
ENSRNOG00000014964	*Hp*	6,41E-14	3.4569
ENSRNOG00000050404	*Pmepa1*	6,41E-14	2.2242
ENSRNOG00000007545	*Angptl4*	1,00E-13	3.6166
ENSRNOG00000020300	*Lsp1*	1,05E-13	2.4371
ENSRNOG00000003538	*Adamts4*	2,10E-13	4.8106

Table 3. Top 50 Differentially Expressed Genes (DEGs) in Post-Infarct Rat Myocardial Tissues, Sorted by Statistical Criterion Using DeSeq Analysis [23].

Consequently, we observed a significant change in gene expression patterns in the early response to myocardial infarction induction in myocardial tissue and identified a series of differentially expressed genes responsive to cardiac muscle damage.

3.1.2 Post-Infarct Myocardium Exhibits Enhanced Early Remodeling Processes Involving Components of NOTCH and BMP Signaling Pathways

To assess the impact of acute hypoxic stress on the disruption of canonical signaling pathways and biological functions in cardiac tissue 24 hours post-myocardial infarction induction, we performed an analysis of canonical signaling pathways and gene set enrichment (GSEA) using Qiagen software. Differentially expressed genes (DEGs) were uploaded to Qiagen Ingenuity Pathway Analysis (IPA) to identify enriched pathways in the dataset after filtering for significance (adj. p-value <0.05). A total of approximately 152 canonical signaling and metabolic pathways were identified, with significance levels above -log(P)>1.3, and only 82 signaling pathways had absolute z-score values greater than 1.0.

Following a myocardial infarction, massive cell death occurs in the affected area and a persistent inflammatory reaction is initiated, particularly aimed at facilitating reparative processes associated with early myocardial remodeling [150]. We observed a shift in gene expression characteristic towards early

myocardial remodeling 24 hours after inducing acute myocardial infarction. Accordingly, the following canonical signaling pathways were identified from the analyzed dataset: the "Apelin signaling pathway in cardiac fibroblasts" (ratio - 0.455, z-score - -2.333, p-value - 5.67E-04), associated with the activation of cardiac fibroblasts and their differentiation into myofibroblasts, subsequently leading to cardiac fibrosis and heart failure; "Remodeling of Epithelial Adhesion Contacts" (ratio - 0.382, z-score - 2.449, p-value - 1.71E-05); "Inhibition of Matrix Metalloproteinases" (ratio - 0.344, z-score -1.265, p-value - 4.57E-03); and "TGF-β Signaling Pathway" (ratio - 0.218, z-score - 1.5, p-value - 4.86E-02) (**Figure 8**).

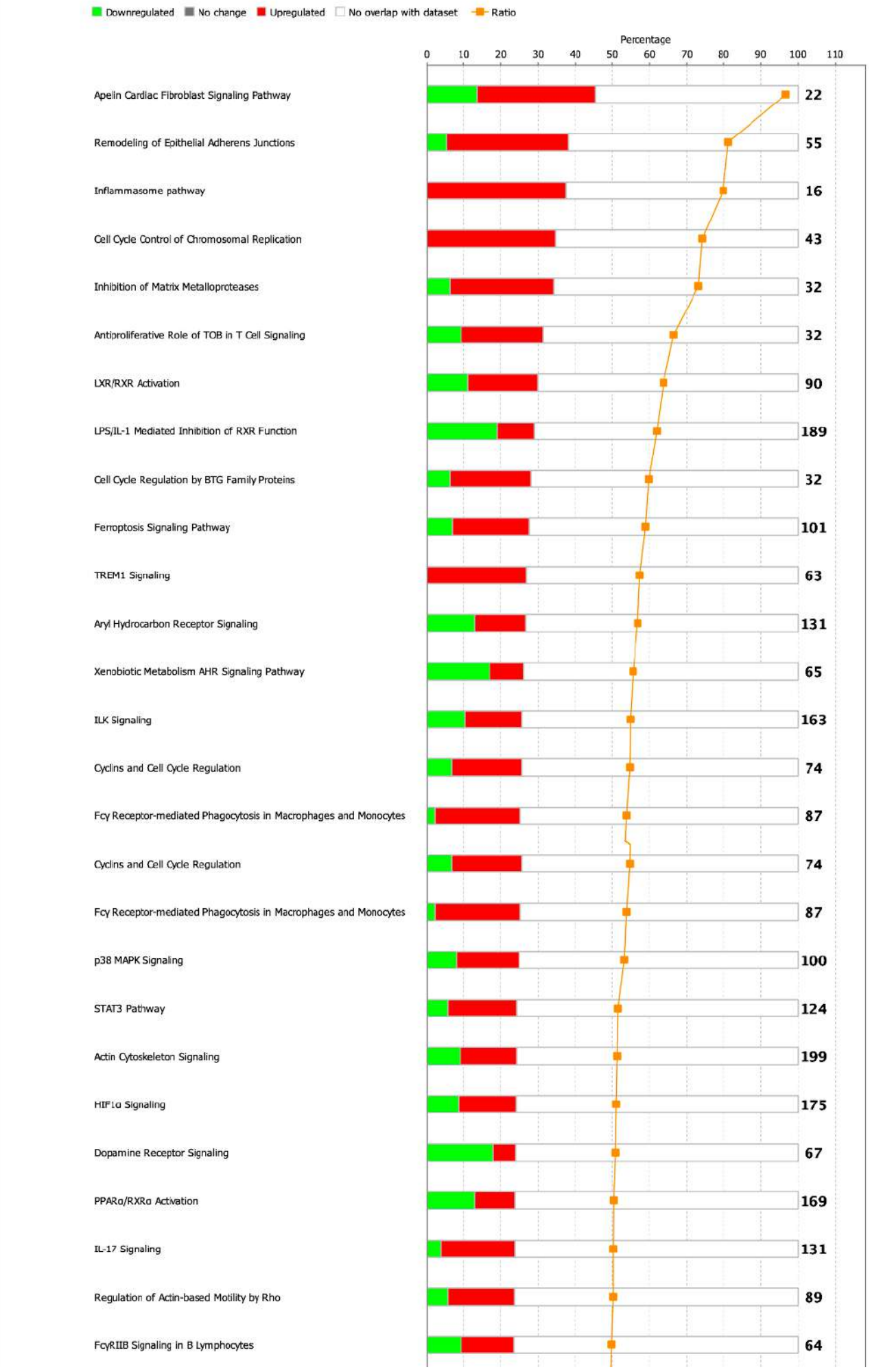
Downregulated
No change
Upregulated
No overlap with dataset
Ratio
Percentage
0
10
20
30
40
50
60
70
80
90
100
110
Apelin Cardiac Fibroblast Signaling Pathway
22
Remodeling of Epithelial Adherens Junctions
55
Inflammasome pathway
16
Cell Cycle Control of Chromosomal Replication
43
Inhibition of Matrix Metalloproteases
32
Antiproliferative Role of TOB in T Cell Signaling
32
LXR/RXR Activation
90
LPS/IL-1 Mediated Inhibition of RXR Function
189
Cell Cycle Regulation by BTG Family Proteins
32
Ferroptosis Signaling Pathway
101
TREM1 Signaling
63
Aryl Hydrocarbon Receptor Signaling
131
Xenobiotic Metabolism AHR Signaling Pathway
65
ILK Signaling
163
Cyclins and Cell Cycle Regulation
74
Fcγ Receptor-mediated Phagocytosis in Macrophages and Monocytes
87
Cyclins and Cell Cycle Regulation
74
Fcγ Receptor-mediated Phagocytosis in Macrophages and Monocytes
87
p38 MAPK Signaling
100
STAT3 Pathway
124
Actin Cytoskeleton Signaling
199
HIF1α Signaling
175
Dopamine Receptor Signaling
67
PPARα/RXRα Activation
169
IL-17 Signaling
131
Regulation of Actin-based Motility by Rho
89
FcγRIIB Signaling in B Lymphocytes
64

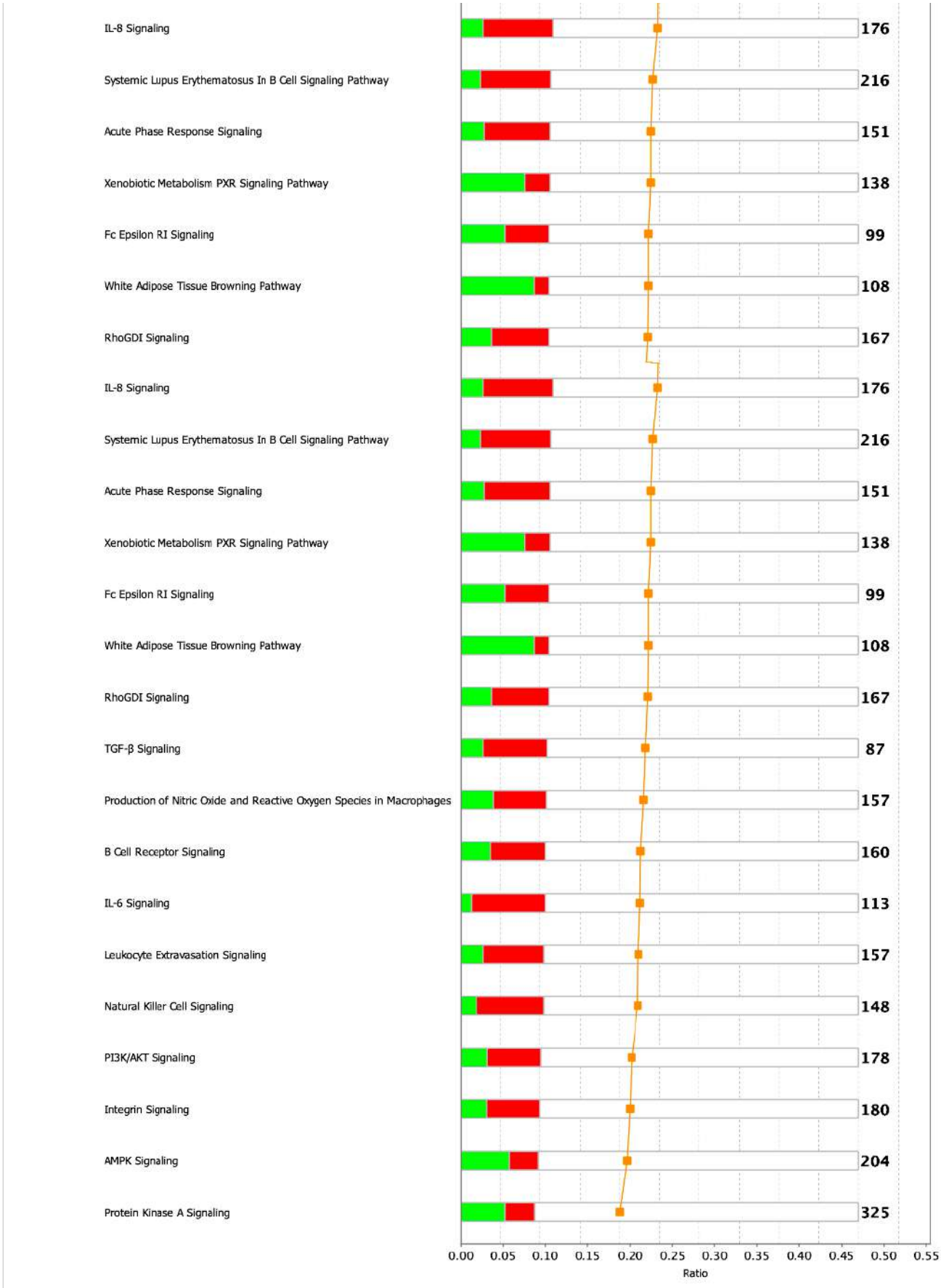

Figure 8. Deregulation of Biological Pathways (Excluding Metabolic Pathways) in Post-Infarct Tissue Samples Identified Using IPA Analysis. The figure represents deregulated canonical signaling pathways

as a histogram with accumulation based on the p-value obtained by Fisher's exact test (adj. p-value > 0.05, z-score > 1) [23].

In addition, signaling pathways involved in the regulation of the cell cycle and proliferative activity were noted, including "Chromosome Replication Control in Cell Cycle," "PI3K/AKT Signaling," "Aryl Hydrocarbon Receptor Signaling," "BTG Family Protein Cell Cycle Regulation," "STAT3 Pathway," "HIF-1α Signaling," and "Cyclins and Cell Cycle Regulation." Pathways related to migratory activity, such as "Actin-based Mobility Regulation by Rho" and "Actin Cytoskeleton Signaling," were also activated in post-infarct tissues.

Probabilistic gene networks generated using the IPA program reflect forms of non-canonical signaling that have been noted for various genes with increased and decreased expression, involved in tissue and cell growth and development (**Figure 9**).

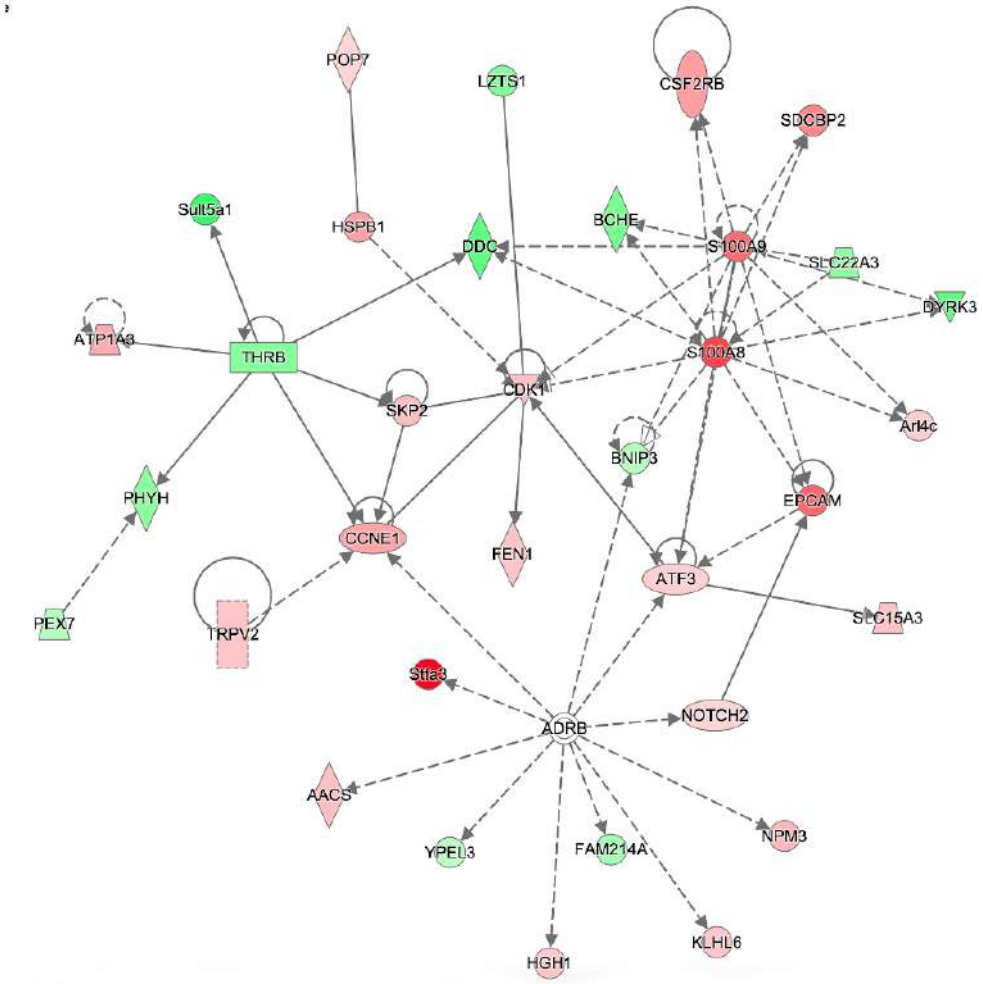
POP7
LZTS1
CSF2RB
SDCBP2
Sult5a1
HSPB1
DDC
BCHE
S100A9
SLC22A3
BYRK3
ATP1A3
THRB
S100A8
CDK1
SKP2
Arl4c
BNIP3
PHYH
EPCAM
CCNE1
FEN1
ATF3
SLC15A3
PEX7
TRPV2
Stfa3
ADRB
NOTCH2
AACS
NPM3
YPEL3
FAM214A
KLHL6
HGH1

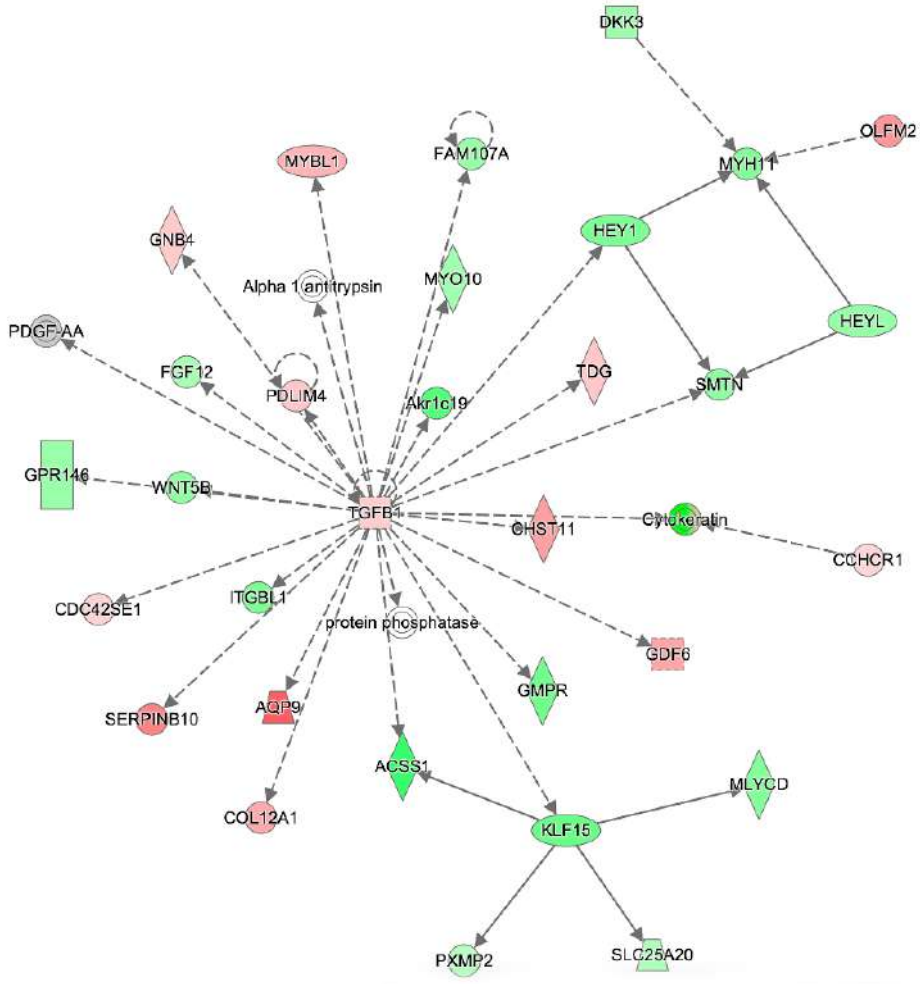
DKK3
OLFM2
MYBL1
FAM107A
MYH11
HEY1
GNB4
Alpha 1 antitrypsin
MYO10
HEYL
PDGF-AA
FGF12
TDG
SMTN
PDLIM4
Akr1c19
GPR146
WNT5B
TGFB1
CHST11
Cytokeratin
CCHCR1
CDC42SE1
ITGBL1
protein phosphatase
GDF6
GMPR
SERPINB10
AQP9
ACSS1
MLYCD
COL12A1
KLF15
PXMP2
SLC25A20

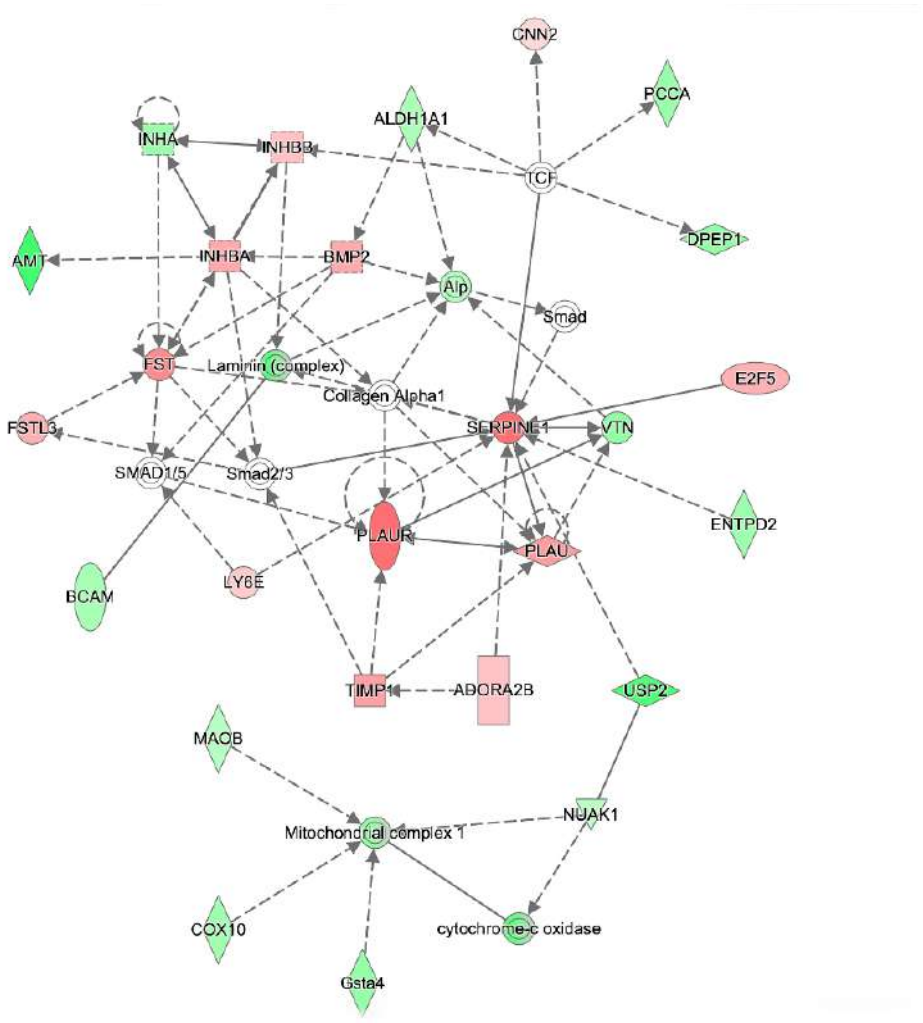

Figure 9. Deregulated Gene Networks Associated with Tissue and Cell Growth and Development, Generated Using IPA Software. Red indicates increased expression, while green represents decreased expression. The brightness of the color signifies the intensity of gene expression in the dataset [23].

Using Gene Set Enrichment Analysis (GSEA), over 100 molecules involved in the formation of immune responses, influencing the growth and development of the cardiovascular system, cell division processes, and changes in cell morphology were identified. The main deregulated biological functions and diseases associated with differentially expressed genes (DEGs) are reflected in **Table No.4**.

Name	**P-value Range**	**# Molecules**
Physiological System Development and Function		
Immune Cell Trafficking	1.45E-04–2.40E-23	341
Hematological System Development and Function	1.93E-04–6.17E-21	552
Organismal Development	1.88E-04–7.23E-16	505
Organismal Survival	1.44E-08–9.00E-16	638
Tissue Morphology	2.20E-04–4.63E-15	411

Molecular and Cellular Functions		
Cellular Movement	1.40E-04–3.50E-24	365
Cell Death and Survival	2.20E-04–2.80E-16	400
Cell-To-Cell Signaling and Interaction	2.32E-04–5.63E-16	329
Cellular Function and Maintenance	2.20E-04–1.46E-15	416
Protein Synthesis	2.26E-04–5.66E-14	228
Diseases and Disorders		
Inflammatory Response	1.88E-04–4.23E-19	498
Organismal Injury and Abnormalities	2.27E-04–1.84E-15	864
Metabolic Disease	1.89E-04–5.49E-14	280
Connective Tissue Disorders	9.94E-05–1.69E-13	178
Cardiotoxicity		
Cardiac Enlargement	6.17E-01–5.00E-13	149
Cardiac Dysfunction	3.43E-01–4.24E-09	74
Cardiac Infarction	5.90E-02–2.33E-07	34
Cardiac Fibrosis	3.81E-01–5.08E-07	74
Cardiac Dilatation	3.81E-01–9.55E-07	57

Table 4. Top Diseases and Biological Functions Affected in Post-Infarct Tissues, Identified Using IPA Software [23].

Among the deregulated processes, there is also the proliferation of smooth muscle cells, differentiation of connective tissue cells, and organization of sarcomeres in cardiomyocytes **(Figure 10)**. This suggests activity of these processes in the ischemic heart.

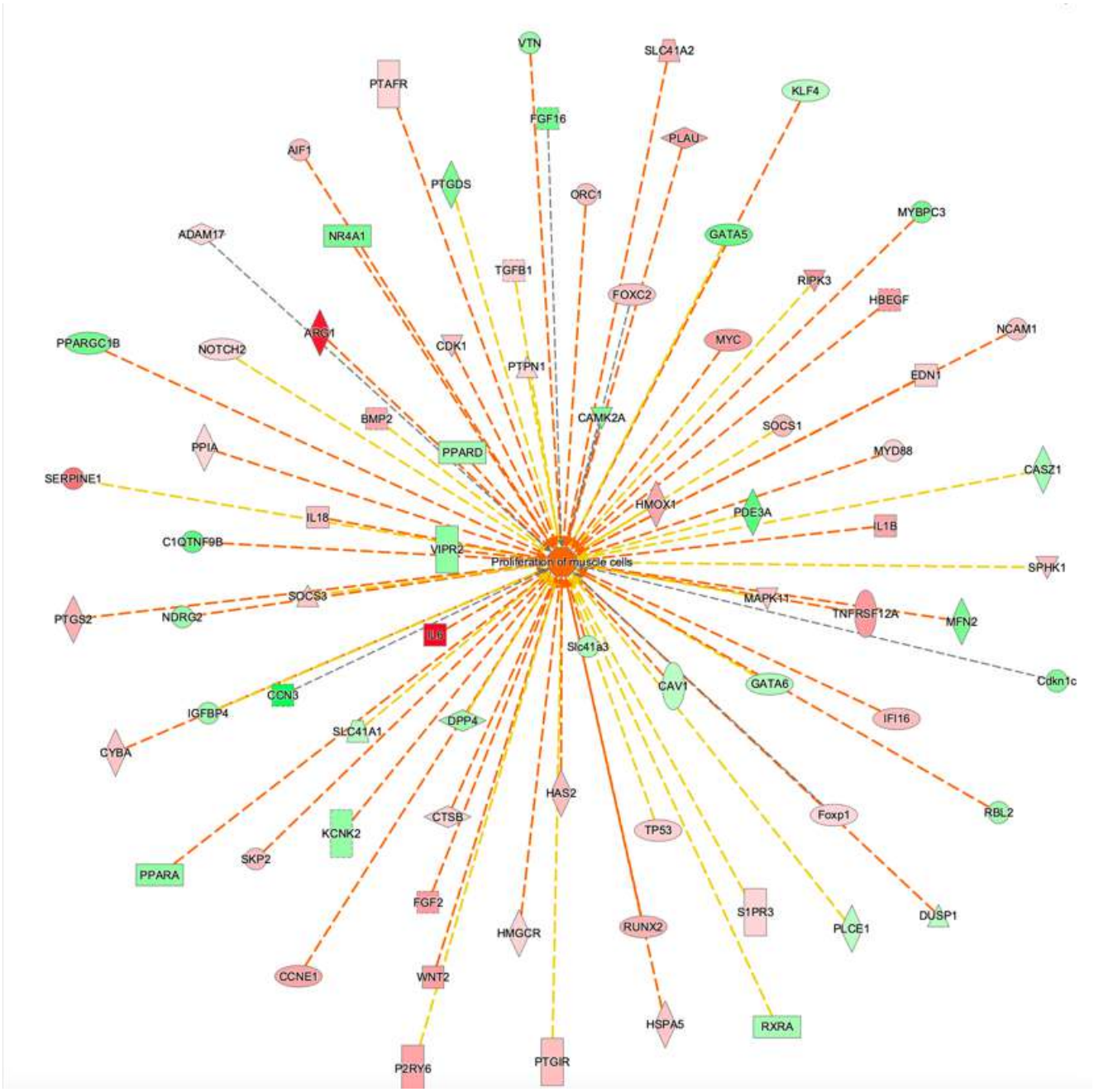
VTN
SLC41A2
PTAFR
KLF4
FGF16
PLAU
AIF1
PTGDS
ORC1
MYBPC3
ADAM17
NR4A1
GATA5
TGFB1
RIPK3
FOXC2
HBEGF
ARG1
MYC
NCAM1
PPARGC1B
NOTCH2
CDK1
PTPN1
EDN1
BMP2
CAMK2A
SOCS1
PPIA
PPARD
MYD88
CASZ1
SERPINE1
HMOX1
PDE3A
IL18
IL1B
C1QTNF9B
VIPR2
Proliferation of muscle cells
SPHK1
SOCS3
MAPK11
PTGS2
NDRG2
TNFRSF12A
MFN2
IL6
Slc41a3
Cdkn1c
CAV1
GATA6
CCN3
IGFBP4
IFI16
DPP4
SLC41A1
CYBA
HAS2
RBL2
CTSB
Foxp1
KCNK2
TP53
SKP2
PPARA
FGF2
S1PR3
DUSP1
HMGCR
RUNX2
PLCE1
CCNE1
WNT2
HSPA5
RXRA
P2RY6
PTGIR

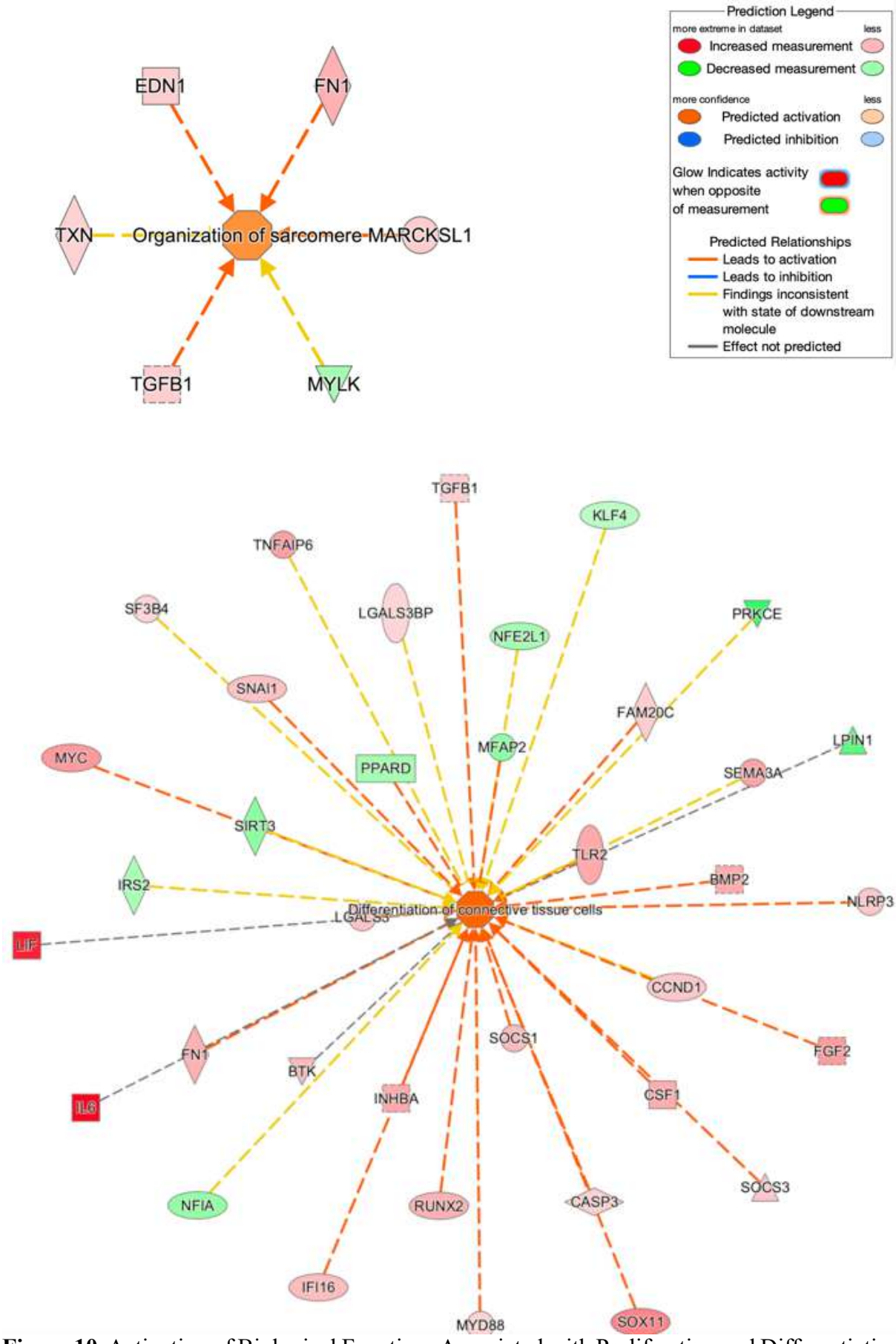

Figure 10. Activation of Biological Functions Associated with Proliferation and Differentiation of Heart Cells, Identified Using Gene Set Enrichment Analysis in IPA Software. Red indicates increased

expression, while green indicates decreased expression. The brightness of the color represents the intensity of gene expression in the dataset [23].

In the processes depicted above, activity of several components of the Notch signaling pathway was noted [151, 152], such as the *Notch2* receptor, target genes *Myc* and *Ccnd1*, and the transcription factor *Runx2*, which were activated, while the target gene *Hey1* was suppressed. In particular, among the key regulators, the *Bmp2* gene was activated, coding for the eponymous ligand from the TGF-β superfamily, involved in many developmental processes including cardiogenesis, neurogenesis, and osteogenesis [153-155]. A complete list of overexpressed components of the Notch signaling pathway is presented in the form of a table (**Table 5**).

Ensembl ID	**Gene**	***p-value***	**Log2 fold-change**
ENSRNOG00000004500	*Myc*	2,67E-14	2,5965
ENSRNOG00000059968	*Jak2*	9,13E-05	1,1905
ENSRNOG00000020918	*Ccnd1*	1,92E-04	1,4416
ENSRNOG00000020193	*Runx2*	8,87E-04	1,9919
ENSRNOG00000018835	*Notch2*	5,35E-03	1,0877
ENSRNOG00000013218	*Sap30*	8,97E-03	1,3621
ENSRNOG00000060694	*Adam17*	1,06E-02	1,0066
ENSRNOG00000006350	*Tle6*	7,26E-03	-1,6074
ENSRNOG00000050848	*Dtx1*	5,56E-03	-2,319
ENSRNOG00000005133	*Mapt*	2,12E-03	-1,5349
ENSRNOG00000008257	*Mfap2*	1,97E-03	-1,622
ENSRNOG00000015318	*Heyl*	5,74E-05	-1,5211
ENSRNOG00000008697	*Ccn3*	1,04E-05	-2,7564
ENSRNOG00000002272	*Lnx1*	3,22E-07	-2,2148
ENSRNOG00000018384	*Adam12*	3,12E-02	2,1
ENSRNOG00000059059	*Skp2*	3,68E-02	1,6709
ENSRNOG00000025100	*Ikbke*	4,20E-02	1,0854
ENSRNOG00000017259	*Tacc3*	4,94E-02	1,1216
ENSRNOG00000016640	*Dner*	3,28E-02	-1,755
ENSRNOG00000011593	*Hey1*	2,10E-02	-1,8048

Table 5. Notch Signaling Pathway Components Differentially Expressed in Post-Infarct Myocardial Tissues 24 Hours After Surgery [23].

Thus, it has been established that in post-infarct tissues, there is a reactivation of genes associated

with embryonic development processes. This includes the identified activation of Notch signaling pathway components and *Bmp2/Runx2* genes, which may be associated with the early remodeling of the myocardium.

3.1.3 Activation of Notch Pathway Components and *Bmp2/Runx2* in Post-Infarct Myocardial Tissues

To confirm RNA sequencing data indicating the activation of *Bmp2/Runx2* and Notch pathway components in post-infarct tissues, we analyzed them using quantitative PCR. Furthermore, we selected an even earlier time point after inducing myocardial infarction in rats – 8 hours – to assess the difference in gene expression between the two time points.

We found [23] that acute hypoxia in vivo activates the expression of Notch pathway components and *Bmp2/Runx2* in ischemic myocardium compared to healthy heart tissue. The quantitative PCR data fully corresponded with the RNA sequencing results for the 24-hour time point (**Figure 11**).

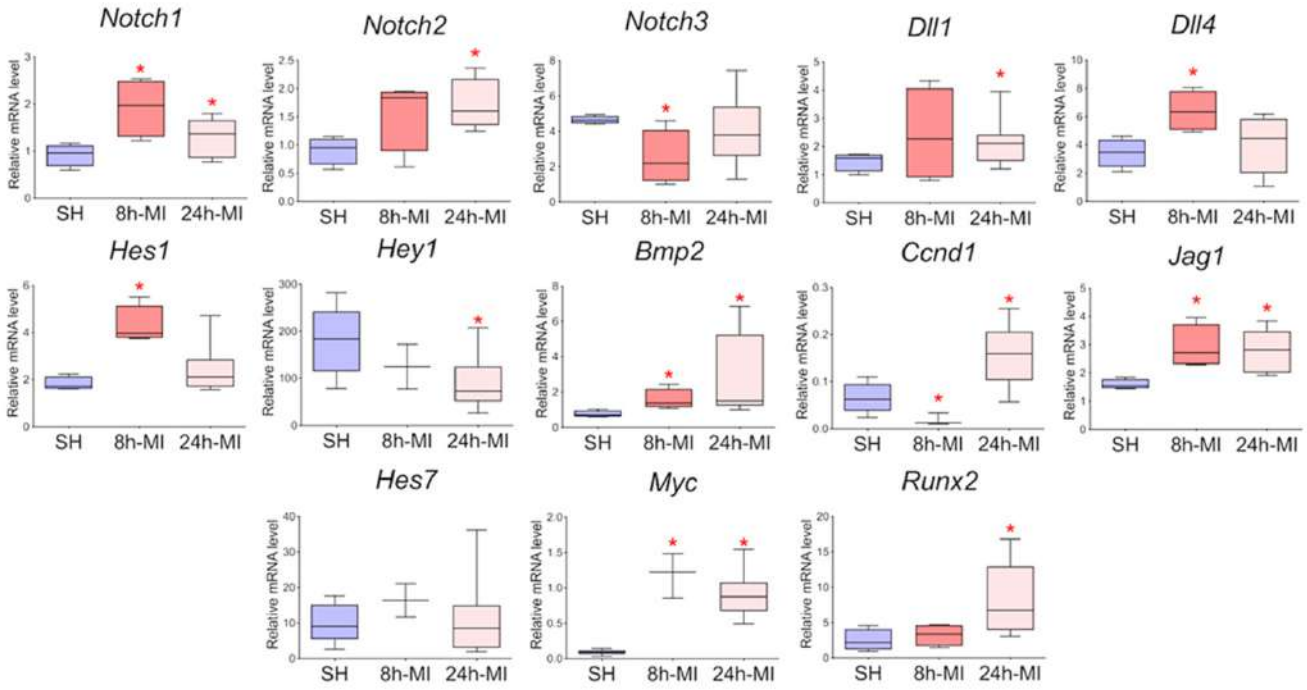

Figure 11. Dynamics of Notch Pathway Components and *Bmp2/Runx2* Gene Expression in Tissues According to Quantitative PCR Analysis. SH - samples from the healthy myocardium of sham-operated rats ($n = 3$), 8h-MI - samples from post-infarct myocardial tissues of rats 8 hours after induction ($n = 4$), 24h-MI - samples from post-infarct myocardial tissues of rats 24 hours after induction ($n = 9$). Vertically - relative mRNA quantity in each group measured by the $2^{-\Delta\Delta CT}$ method; presented are box plots with whiskers showing values from minimum to maximum. An asterisk indicates significant differences between SH and MI groups at $p < 0.05$ (Mann-Whitney U test) [23].

Thus, we noted that RNA sequencing and quantitative PCR results in post-infarct myocardial tissues are congruent, and we observed the activation of Notch pathway components and *Bmp2/Runx2*, including at an even earlier point – 8 hours. Whether this activation persists in primary cell cultures from post-infarct myocardium in vitro became the subject of our further study.

3.1.4 Post-Infarct Rat Cardiac Mesenchymal Cells Exhibit Properties of Mesenchymal Stem Cells and Have Pronounced Differentiation Potential

To study the properties of cells isolated from post-infarct myocardium in vitro, we induced myocardial infarction in Wistar rats to obtain primary cultures of cardiac mesenchymal cells from the post-infarct area (including the peri-infarct zone) of the myocardium at 8- and 24-hours post-operation. Cardiac mesenchymal cells from the myocardium of the ventricles of the healthy heart of sham-operated rats were used as a negative control (**Figure 12**).

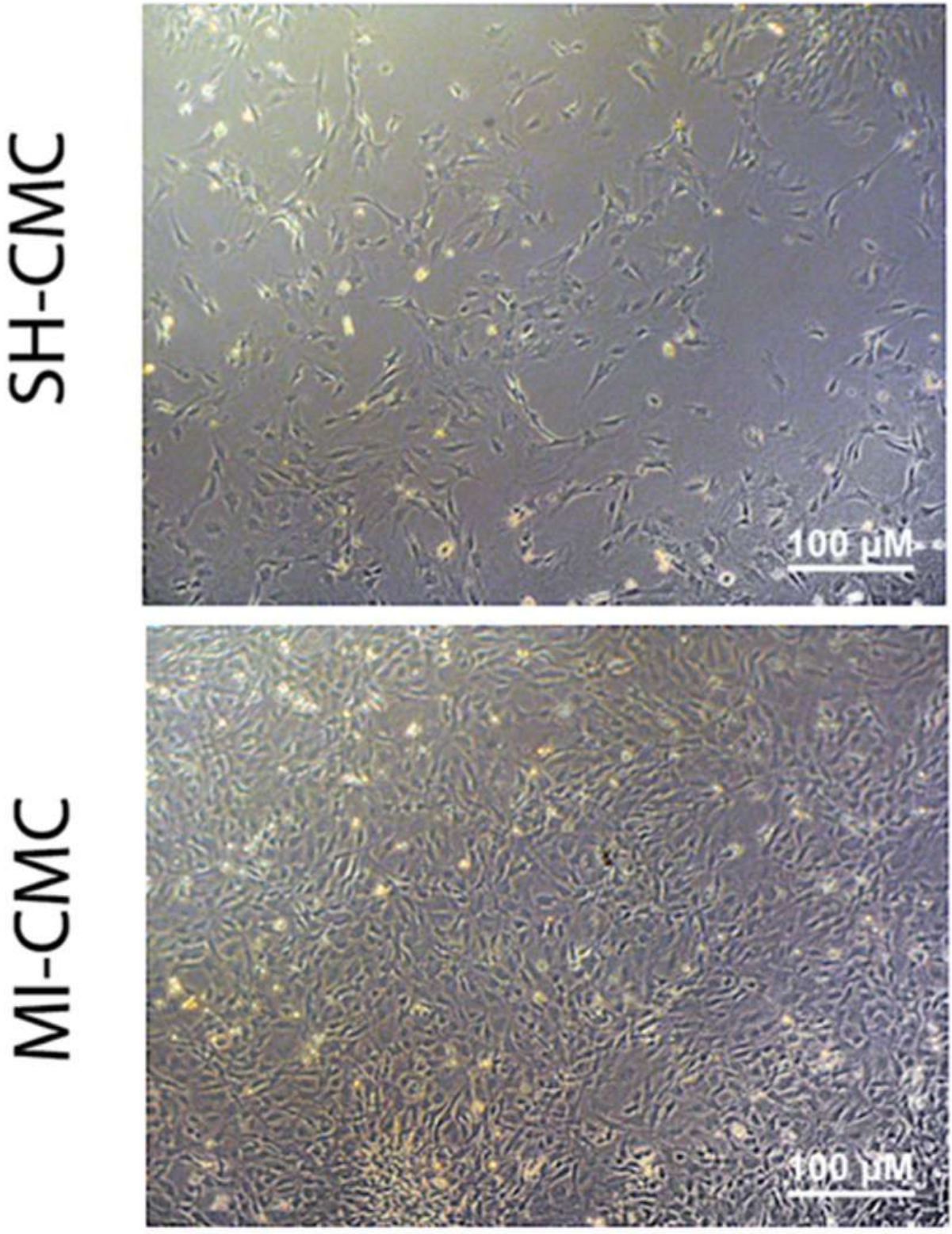

Figure 12. Cardiac mesenchymal cells (CMC) derived from healthy (SH-CMC) and post-infarct (MI-CMC) rat myocardium on the 5th day of cultivation. CMCr were isolated 24 hours post-myocardial infarction. SH-CMC were obtained from the hearts of rats following sham surgery. The primary culture of CMCr demonstrated the ability to form fibroblast colony-forming units (CFU-F) and adhered to the

culture plastic. These cells were capable of proliferating for up to 20 passages [23].

The phenotypic characterization of mesenchymal stem cells (MSCs) is complex, and the International Society for Cellular and Gene Therapies has established the following criteria for identifying MSCs: adhesion to plastic, expression of specific markers, the ability for adipogenic, chondrogenic, and osteogenic differentiation, as well as the formation of fibroblast colony-forming units (CFU-F) [156]. Here, we use the term cardiac mesenchymal cells (CMCr) due to some terminological differences related to the correct classification of these cells [157, 158].

The obtained primary cultures of CMCr expressed CD90 and were positive for CD166, which was previously described as a marker of resident cardiac mesenchymal cells and one of the populations of cardiac stem cells derived from cardiospheres [159]. They were also negative for endothelial and hematopoietic markers [156], namely CD45, CD31, and CD34 (**Figure 13**).

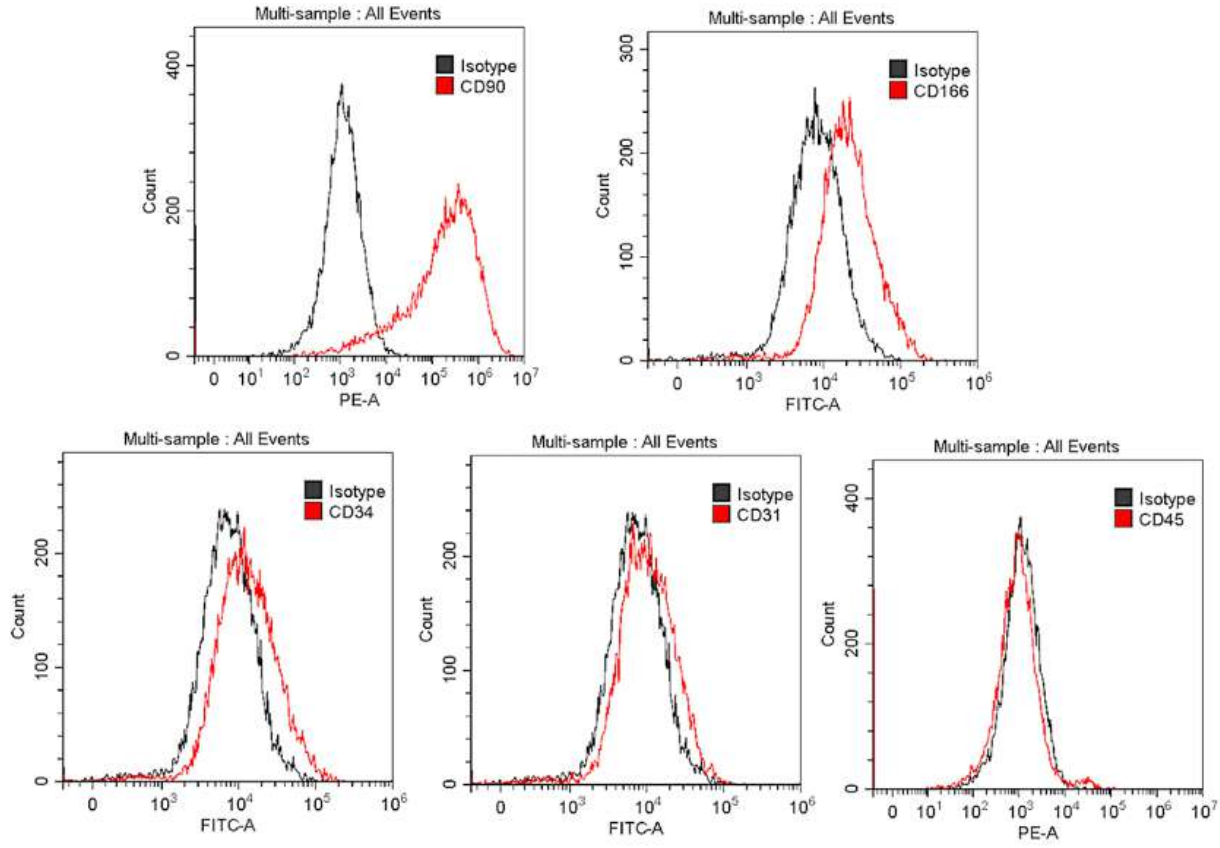

Figure 13. Immunophenotyping of primary cultures of cardiac mesenchymal cells (CMCr) using flow cytometry. Histograms display the expression levels of surface markers CD31, CD34, C45, CD90, and CD166 (red lines) relative to the isotype (gray lines) [23].

Mesenchymal stem cells can differentiate into different cell types depending on conditions and chemical inducers [160]. The potential of rat heart mesenchymal cells to differentiate in cardiogenic, osteogenic and adipogenic directions was assessed. It was demonstrated that CMCr are capable of forming α-actin filaments 24 days after the induction of cardiogenic differentiation. In the presence of adipogenic factors, they accumulated lipid droplets 14 days after the start of differentiation, and intense staining of CMCr on day 21 in the form of detection of alkaline phosphatase was recorded when cultivated with osteogenic inducers (**Figure 14**). Thus, the CMCr obtained from rat myocardium had the characteristic properties of mesenchymal stem cells in the form of the ability to differentiate in various directions [24].

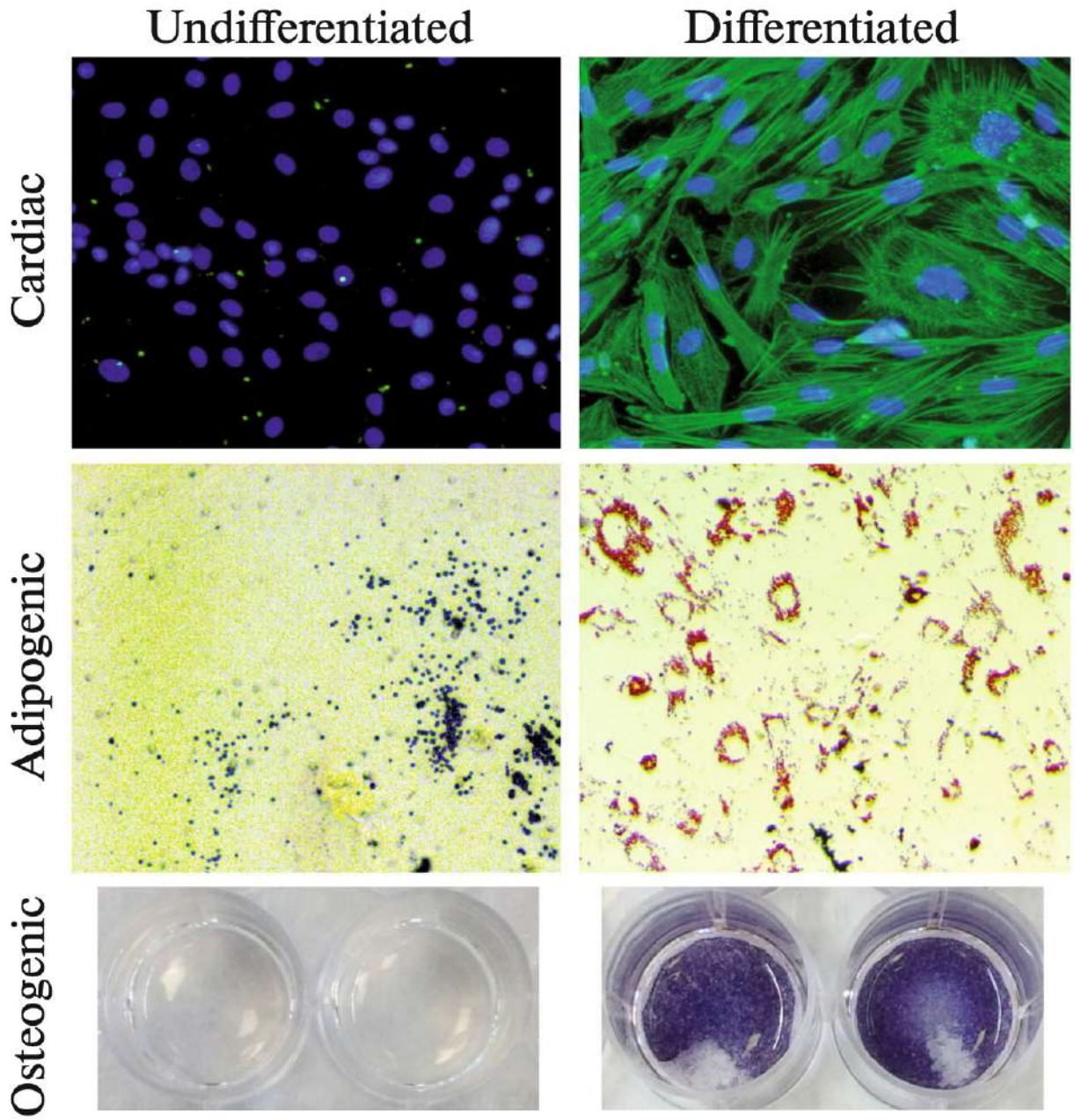

Figure 14. Cardiogenic (green), adipogenic (red), and osteogenic (blue) differentiation of rat cardiac mesenchymal cells (CMCr). Differentiation was induced by adding specific inducers to the culture medium. Immunocytochemical staining for α-actinin and DAPI, staining for fat accumulations (Sudan red), and alkaline phosphatase (NBT/BCIP stain) [161].

To assess specific differentiation, the expression of the genes troponin (*Tnnt2*), a marker of cardiomyocytes, and vimentin (*Vim*), a marker of fibroblasts, was measured (**Figure 15, a**). In the ischemic zone, 3 days after infarction, *Tnnt2* decreased and *Vim* increased, indicating the formation of a fibrotic state and replacement of dead cardiomyocytes [161].

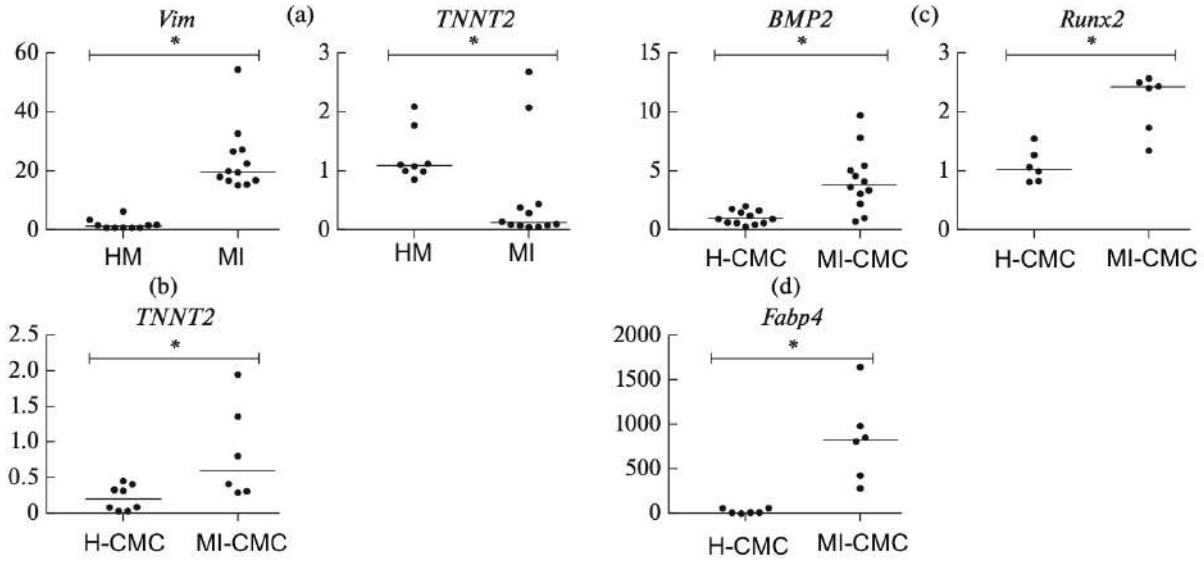

Figure 15. Expression of markers in tissues (*a*) and cells (*b, c, d*) according to quantitative PCR data. H-CMC - healthy cells from the myocardium, MI-CMC - post-infarction cells from ischemic myocardium. The graph shows the relative amount of mRNA for each gene using the $2^{-\Delta\Delta CT}$ method; an asterisk indicates statistically significant differences between H-CMC and MI-CMC at $P < 0.05$. a - expression of a mesodermal marker (*Vim*) and a cardiogenic marker (*Tnnt2*) in ischemic and healthy tissues. *b* - Expression of the troponin T2 gene, encoding the cardiomyocyte-specific isoform of troponin I, in cells from the ischemic zone and myocardium during cardiogenic differentiation. *c* - Expression of *Bmp2* and *Runx2* (markers of osteogenic differentiation) in CMCr differentiated in the osteogenic direction. *d* - Expression of the adipogenic marker *Fabp4* in CMCr differentiated in the adipogenic direction [161].

A comparison was made of the differentiation ability of CMCr obtained from the post-infarction area of the myocardium with CMCr from healthy myocardium. As a result of the induction of cardiogenic differentiation, an increase in the expression of the *Tnnt2* gene was found (**Figure 15, b**) in MI-CMCr compared to H-CMCr. With the induction of osteogenic differentiation, an increase in the expression of *Bmp2* and *Runx2* (markers of osteogenic differentiation) was observed in MI-CMCr compared to H-CMCr (**Figure 15, c**). Upon induction of adipogenic differentiation, an increase in the expression of *Fabp4* (a marker of adipogenic differentiation) was detected in MI-CMCr compared to the control **(Figure 15, d**). Thus, an increase in the expression of cardiogenic, osteogenic and adipogenic markers is characteristic of MI-CMCr, which indicates a more pronounced potential of these cells to differentiate in various directions.

3.1.5 Post-infarct rat cardiac mesenchymal cells exhibited the ability for active proliferation and migration

To evaluate and compare the proliferative activity of post-infarct and healthy cardiac mesenchymal cells obtained one day after surgical intervention from the ischemic heart, we conducted two functional tests: manual counting for growth curve construction and automatic calculation using the xCELLigence system for real-time cell proliferation monitoring.

The growth rate of post-infarct cardiac mesenchymal cells (MI-CMCr) was significantly higher than that of healthy cells (H-CMCr) obtained from the healthy myocardium of the ischemic heart, and this trend continued for 6 days after cell seeding ($P < 0.05$) (**Figure 15**).

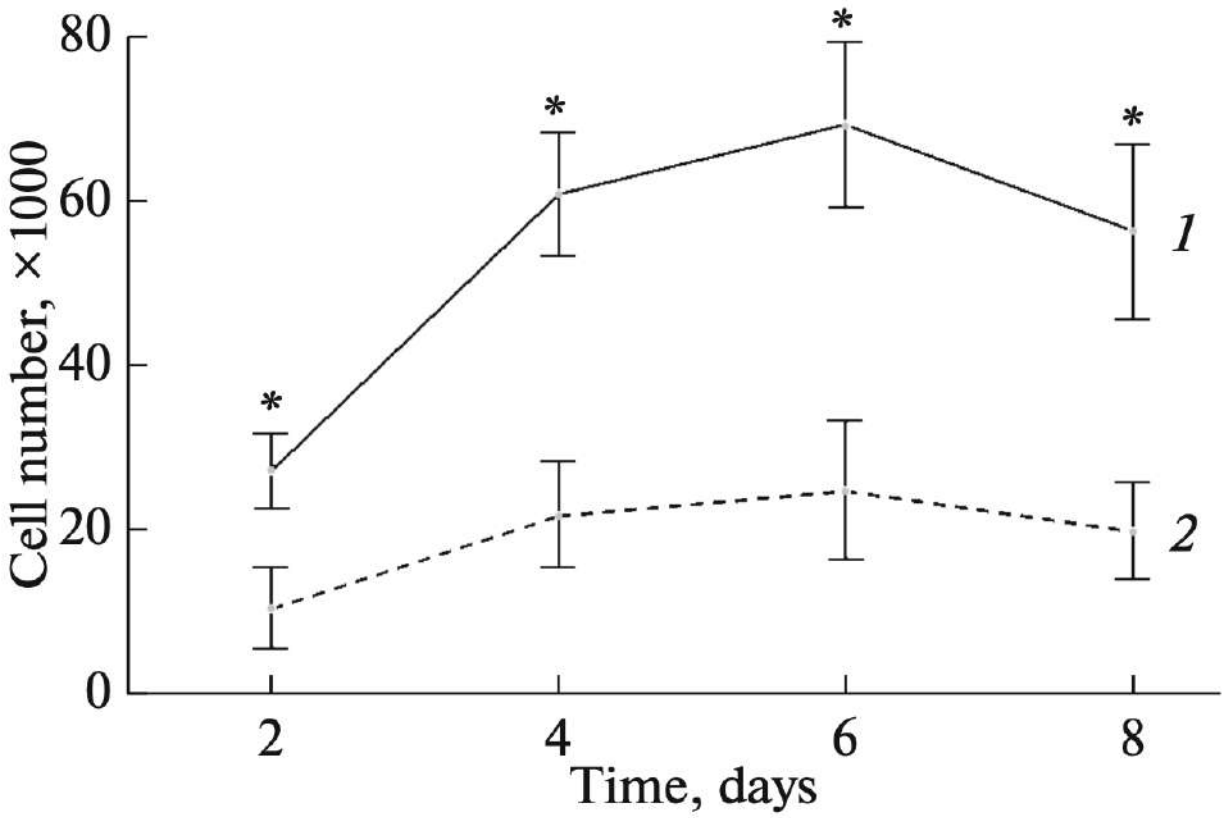

Figure 15. Proliferation rates of MI-CMCr (curve 1) and H-CMCr (curve 2). The cell seeding density was 10^3 cells/cm²; the figure shows the mean values and standard deviations (vertical segments). The significance of differences between the control group and post-infarct CMCr is indicated with an asterics [161].

These observations were also confirmed by automatic monitoring of cell proliferation in real-time. It was observed that MI-CMCr (orange curve) have a more pronounced proliferation potential and, accordingly, an activation stimulus in response to acute hypoxic stress compared to H-CMCr (blue curve), obtained from the healthy myocardium of sham-operated rats. The experiment lasted for 72 hours

with measurements taken every 15 minutes (**Figure 16**).

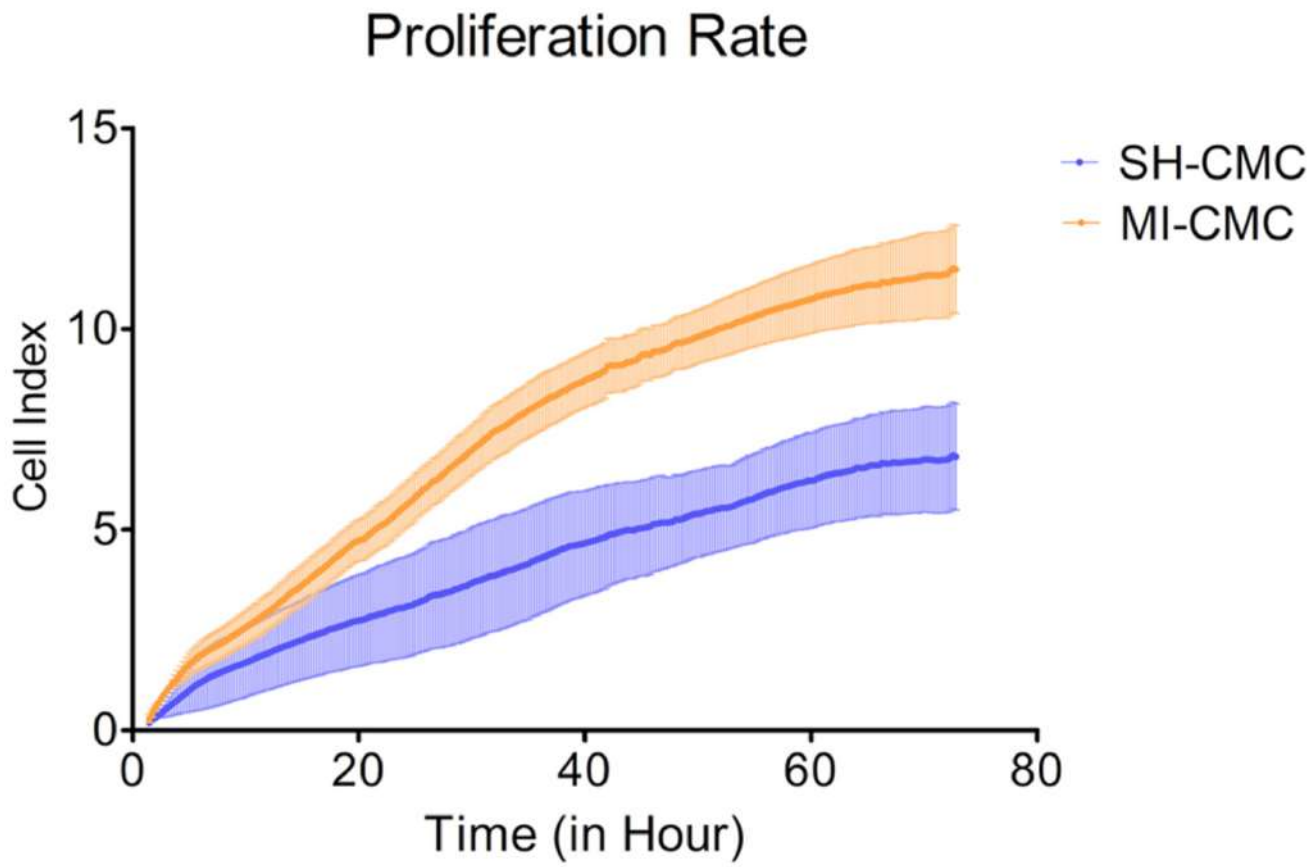

Figure 16. Proliferation rate of post-infarct cardiac mesenchymal cells (MI-CMCr, orange curve, $n = 9$) and healthy cardiac mesenchymal cells from sham-operated rats (SH-CMCr, blue curve, $n = 3$). Each curve represents the mean values across samples and the standard error of the mean (vertical lines). The horizontal axis indicates the time over which measurements of proliferative activity were taken every 15 minutes. The experiment lasted 72 hours. The vertical axis shows the cell index value, reflecting quantitative information about the biological status of the cells, including their quantity and viability. The seeding density was 5,000 cells per well. The significance of the differences between SH-CMCr and MI-CMCr was $p < 0.05$ using the D'Agostino & Pearson omnibus normality test [23].

Cell migration to the damage's zone is one of the regenerative mechanisms. A functional test for the migration ability of CMCs was carried out using the scratch test method with quantitative analysis [161]. MI-CMCr migrated to the scratch area more intensively than H-CMCr ($P < 0.05$) (**Figure 17 a, b**).

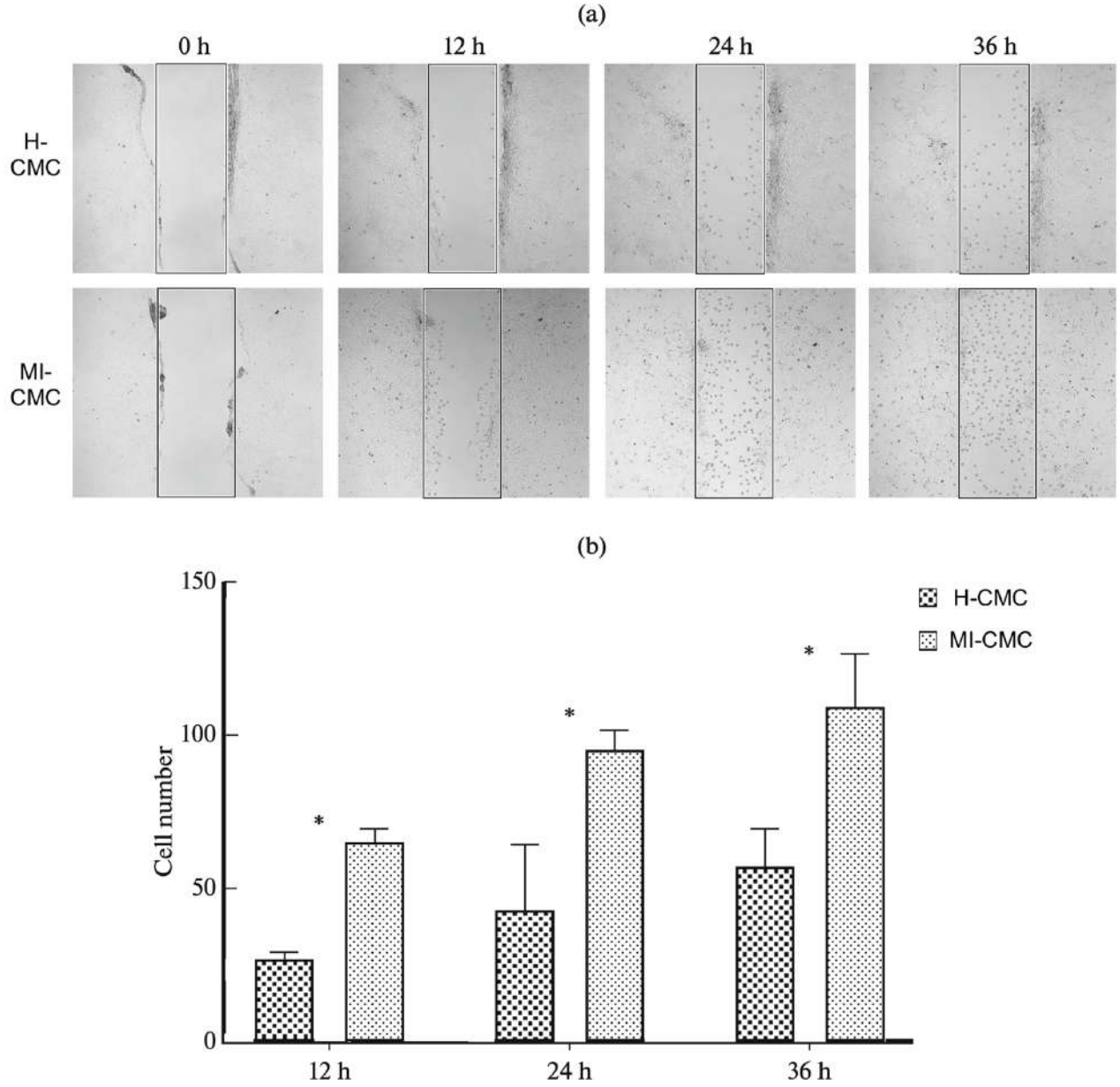

Figure 17. Migration (a) and quantitative analysis (b) of CMCr in the scratch test from post-infarct and healthy sections of ischemic myocardium. a - migrating cells into the scratch area (highlighted by a rectangle). H-CMCr - cells from the healthy myocardial section, MI-CMCr - post-infarct cells. Upon formation of a cell monolayer, a scratch was applied and the number of cells was counted after 12 hours, 24 hours, and 36 hours. b - migration rate of CMCr. The median with range (standard deviation) is shown; significant differences between H-CMCr and MI-CMCr groups at each time point are indicated with an asterisk, $P < 0.05$ [161].

Thus, it was established that MI-CMCr possess a more pronounced potential for proliferation and migration compared to the populations of healthy cells H-CMCr and SH-CMCr.

3.1.6 Altered Gene Expression Profile of Postinfarction Cardiac Mesenchymal Cells

To assess the activation of MI-CMCr, we analyzed their transcriptomic profile using RNA sequencing; SH-CMCr served as the control. Principal component analysis revealed major patterns in the dataset. Principal Component 4 (PC4) accounts for a minor portion of the experimental variability (14.5%, P <0.05), reflecting a relatively small difference between the two states of CMCr. This may indicate a gradual change in the expression profile when cultivating cells under normal conditions (**Figure 18**).

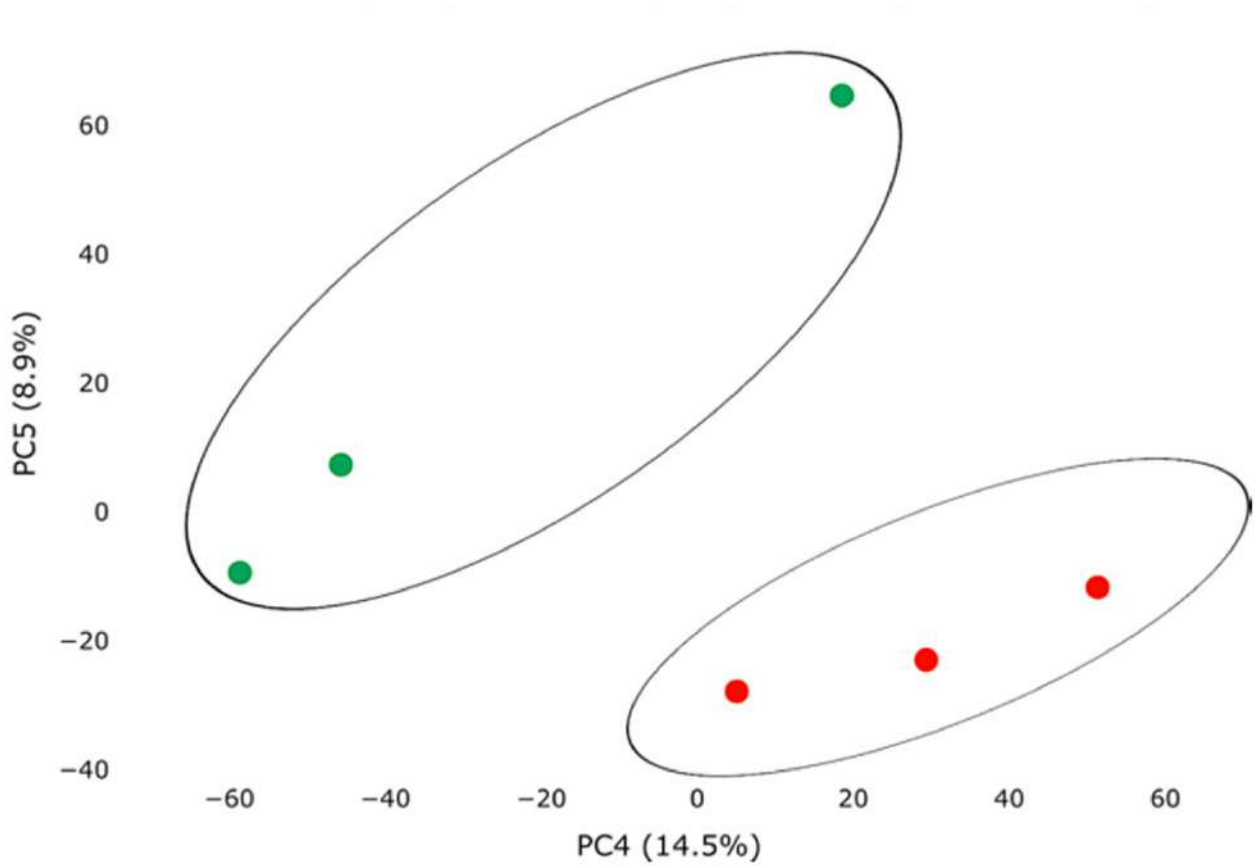

Figure 18. Principal Component Analysis (PCA) showing gene expression variability in healthy (green dots, *n* = 3) and post-infarct (orange dots, *n* = 3) CMCr using the Phantasus web tool. Principal Component 4 (PC4) on the X-axis and PC5 on the Y-axis account for 14.5% and 8.9% of the total gene expression variability, respectively. The samples are visually divided into two main groups [23].

RNA sequencing data analysis revealed 13 differentially expressed genes (adj. p-value <0.05) in the obtained post-infarct cell cultures. Among the activated genes, *Spp1, RGD1565131, Tagap, Myh1* expressions were notable, whereas expressions of *Bmp3, Fgl2, Sfrp4* were decreased in post-infarct

CMCr (log2(fold change) ≥ 1.9) (**Figure 19**).

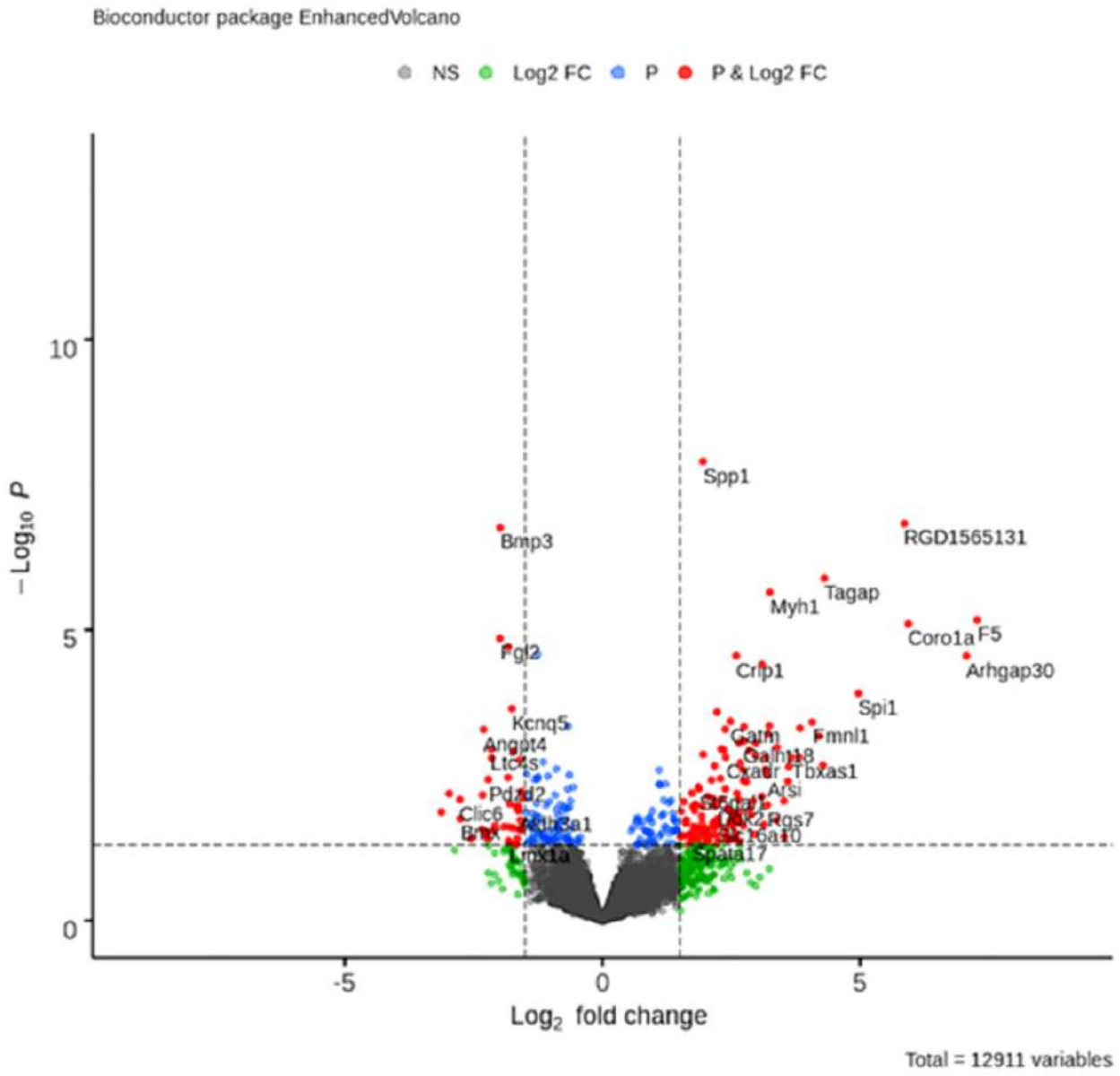

Figure 19. A volcano plot depicting differentially expressed genes (adj. p-value <0.05) in post-infarct samples compared to the control, generated using Bioconductor software in R. The Y-axis represents the mean expression value -log10 (p-value), while the X-axis displays the log2(fold-change) value. Red dots represent differentially expressed genes [23].

The complete list of differentially expressed genes (DEGs), sorted by adj. p-value, is provided in **Table #6**.

Ensembl ID	Gene	FDR-adjusted *p*-value	Log2 fold-change
ENSRNOG00000043451	*Spp1*	1.61 x 10^{-4}	1.9501
ENSRNOG00000002381	*Bmp3*	7.42 x 10^{-4}	-1.9863
ENSRNOG00000025212	*RGD1565131*	7.42 x 10^{-4}	5.8595
ENSRNOG00000018915	*Tagap*	4.12 x 10^{-3}	4.3067
ENSRNOG00000049695	*Myh1*	5.74 x 10^{-3}	3.2468
ENSRNOG00000057855	*F5*	1.42 x 10^{-2}	7.2708
ENSRNOG00000019430	*Coro1a*	1.44 x 10^{-2}	5.9357
ENSRNOG00000012881	*Fgl2*	2.23 x 10^{-2}	-1.9900
ENSRNOG00000054957	*Sfrp4*	2.79 x 10^{-2}	-1.8279
ENSRNOG00000004192	*Arhgap30*	2.99 x 10^{-2}	7.0626
ENSRNOG00000016267	*Chst15*	2.99 x 10^{-2}	-1.2591
ENSRNOG00000027990	*Crip1*	2.99 x 10^{-2}	2.5954
ENSRNOG00000030625	*Tf*	3.88 x 10^{-2}	3.0969

Table 6. Complete list of differentially expressed genes in post-infarct cardiac mesenchymal cells [23].

Additionally, we compiled the 50 most highly expressed genes, sorted by statistical criteria (**Table 7**).

Ensembl ID	Gene	p-value	Log2 fold-change
ENSRNOG00000043451	*Spp1*	1,26E-08	1.9501
ENSRNOG00000025212	*RGD1565131*	1,47E-07	5.8595
ENSRNOG00000018915	*Tagap*	1,29E-06	4.3067
ENSRNOG00000049695	*Myh1*	2,24E-06	3.2468
ENSRNOG00000057855	*F5*	6,67E-06	7.2708
ENSRNOG00000019430	*Coro1a*	7,87E-06	5.9357
ENSRNOG00000027990	*Crip1*	2,77E-05	2.5954
ENSRNOG00000004192	*Arhgap30*	2,80E-05	7.0626
ENSRNOG00000030625	*Tf*	3,94E-05	3.0969
ENSRNOG00000012172	*Spi1*	1,23E-04	4.9652
ENSRNOG00000009273	*LOC259244*	1,61E-03	-2.1494
ENSRNOG00000010529	*Thbs2*	1,23E-03	-1.7230
ENSRNOG00000003244	*Ltc4s*	1,12E-03	-2.1610
ENSRNOG00000005008	*Angpt4*	5,17E-04	-2.3083
ENSRNOG00000020918	*Ccnd1*	4,54E-04	-0.66557
ENSRNOG00000013781	*Kcnq5*	2,25E-04	-1.7575

ENSRNOG00000016267	*Chst15*	2,61E-05	-1.2591
ENSRNOG00000054957	*Sfrp4*	1,96E-05	-1.8279
ENSRNOG00000012881	*Fgl2*	1,39E-05	-1.9900
ENSRNOG00000002381	*Bmp3*	1,74E-07	-1.9863
ENSRNOG00000012956	*Tgm2*	2,58E-04	2.2209
ENSRNOG00000000168	*Gatm*	3,75E-04	2.4814
ENSRNOG00000003207	*Fmnl1*	3,86E-04	4.0698
ENSRNOG00000057880	*Myh11*	4,47E-04	3.2359
ENSRNOG00000014294	*Ptpn6*	4,64E-04	2.7474
ENSRNOG00000004067	*Nrcam*	4,91E-04	3.8321
ENSRNOG00000050123	*Gdf5*	5,11E-04	2.3823
ENSRNOG00000003365	*Cadm3*	6,10E-04	3.2075
ENSRNOG00000006324	*Trpc6*	6,68E-04	4.2013
ENSRNOG00000017021	*Galnt18*	8,10E-04	2.7438
ENSRNOG00000013140	*Pdzd2*	3,74E-03	-2.2145
ENSRNOG00000004110	*Trib2*	3,66E-03	-1.2600
ENSRNOG00000014137	*Fbln1*	3,46E-03	-1.8347
ENSRNOG00000053766	*Ramp3*	3,37E-03	-1.2514
ENSRNOG00000016687	*Ssc5d*	3,26E-03	-1.0617
ENSRNOG00000010789	*Dusp7*	3,14E-03	-0.64020
ENSRNOG00000043486	*Tnfrsf26*	3,02E-03	-1.4638
ENSRNOG00000019955	*Ogdhl*	2,47E-03	-0.89841
ENSRNOG00000046168	*Ppm1l*	1,87E-03	-1.1518
ENSRNOG00000007947	*Fam13a*	1,73E-03	-1.6005
ENSRNOG00000017020	*Inpp5d*	8,97E-04	2.9746
ENSRNOG00000006952	*Prex1*	1,05E-03	3.3868
ENSRNOG00000019662	*Tm6sf1*	1,12E-03	2.3036
ENSRNOG00000002273	*Naaa*	1,16E-03	2.3480
ENSRNOG00000032150	*Adcy2*	1,18E-03	2.8485
ENSRNOG00000007866	*Clec2dl1*	1,39E-03	1.9554
ENSRNOG00000009401	*Lmo2*	1,43E-03	2.9767
ENSRNOG00000001557	*Cxadr*	1,55E-03	2.3917
ENSRNOG00000055721	*Rnf128*	1,55E-03	3.8165
ENSRNOG00000026870	*Clic6*	8,29E-03	-2.7685

Table 7. Complete list of genes actively expressed in post-infarct cardiac mesenchymal cells, sorted by statistical criteria (P-value <0.05) [23].

We observed reduced expression of *Twist1* and Notch target genes *Hey2* and *Ccnd1* in post-infarct

cardiac mesenchymal cells. Additionally, the activity of the *Thbs2* gene, implicated in angiogenesis inhibition, and *Dnm1*, involved in vesicular transport, was decreased (p-value > 0.05) (**Table 8**).

Ensembl ID	**Gene**	***p*-value**	**Log2 fold-change**
ENSRNOG00000020918	*Ccnd1*	4,54E-04	-0,66557
ENSRNOG00000010529	*Thbs2*	1,23E-03	-1,723
ENSRNOG00000033835	*Dnm1*	1,23E-02	-0,89893
ENSRNOG00000013364	*Hey2*	2,32E-02	-2,0844
ENSRNOG00000011101	*Twist1*	5,74E-02	-0,555

Table 8. Components of the Notch signaling pathway whose expression was suppressed in post-infarct MSCs [23].

Thus, we discovered that the gene expression profile of MI-CMCr differs from the transcriptional profile of SH-CMCr. However, the activation potential of the cultures obtained from the post-infarct region was comparatively lower than in post-infarct tissues.

3.1.7 Analysis of Canonical Signaling Pathways and Upstream Regulators Reveals Partial Preservation of Gene Expression Patterns Characteristic of Ischemic Hearts in MI-CMCr

To identify enriched signaling pathways in the obtained dataset, genes were uploaded to Qiagen Ingenuity Pathway Analysis (IPA) after filtering for significance (p-value <0.05). In total, approximately 14 canonical signaling pathways were identified, including metabolic and signaling pathways with significance exceeding -log(P)>1.3. Only one signaling pathway, *STAT3*, had an absolute z-score exceeding 2.0 (**Figure 20**).

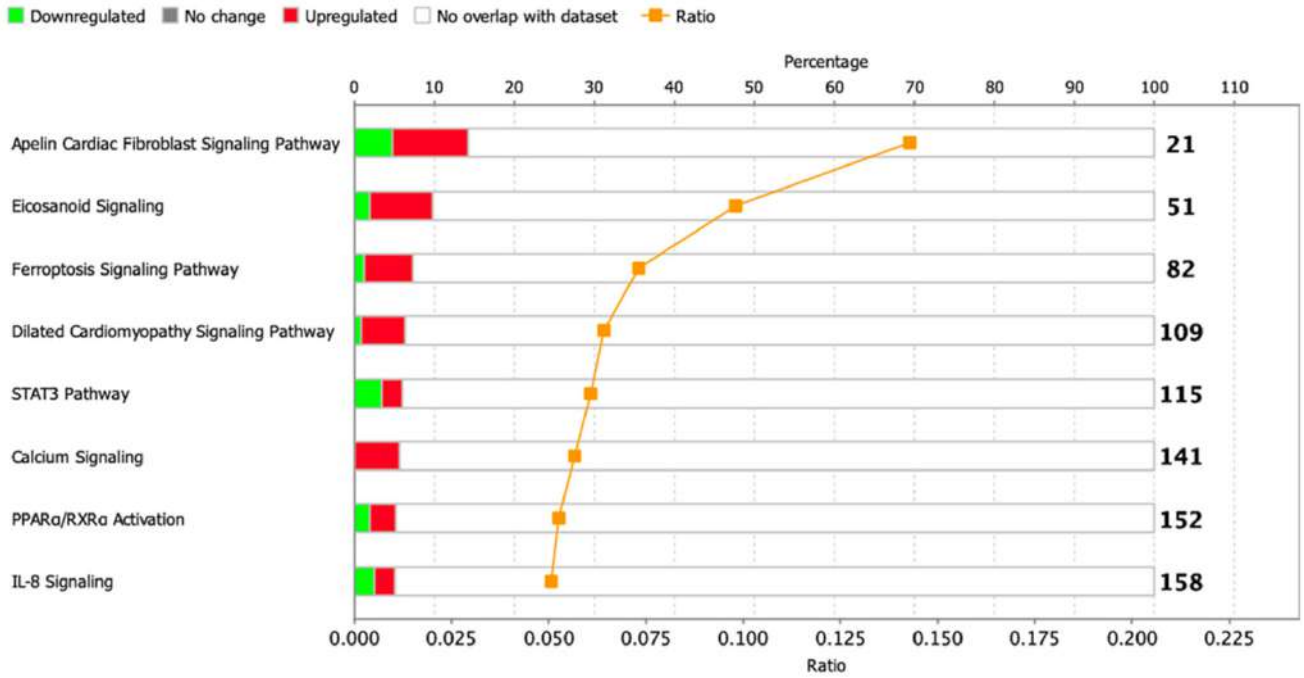

Figure 20. Dysregulation of Signaling Pathways in Post-Infarct MI-CMCr Revealed by IPA Analysis. The figure depicts dysregulated canonical signaling pathways in the form of a histogram with cumulative p-value values obtained using the Fisher's exact test method (p-value <0.05, z-score > 1). The ratio plot shows the count of significant genes expressed in the dataset compared to the total number of genes in that specific signaling pathway [23].

Among the dysregulated signaling pathways, it is noteworthy that MI-CMCr exhibits aberrant signal transduction characteristic of post-infarction processes in ischemic hearts, including disruptions in cellular metabolism, inflammation, and cell death. The complete list of significant signaling pathways is presented in **Table 9**.

Ingenuity Canonical Pathways	-log(p-value)	Ratio	z-score	Down regulated	No change	Upregulated	No overlap with dataset	Molecules
Putrescine Degradation III	1,6	0,2		1/10 (10%)	0/10 (0%)	1/10 (10%)	8/10 (80%)	*Aldh3a1,Maob*
Tryptophan Degradation X (Mammalian, via Tryptamine)	1,38	0,154		1/13 (8%)	0/13 (0%)	1/13 (8%)	11/13 (85%)	*Aldh3a1,Maob*
Ethanol Degradation IV	1,38	0,154		2/13 (15%)	0/13 (0%)	0/13 (0%)	11/13 (85%)	*Acss2,Aldh3a1*

Ethanol Degradation II	1,32	0,143		2/14 (14%)	0/14 (0%)	0/14 (0%)	12/14 (86%)	*Acss2,Aldh3a1*
Apelin Cardiac Fibroblast Signaling Pathway	1,81	0,143		1/21 (5%)	0/21 (0%)	2/21 (10%)	18/21 (86%)	*Apln,Prkaa2,Tgfb3*
Eicosanoid Signaling	2,04	0,098		1/51 (2%)	0/51 (0%)	4/51 (8%)	46/51 (90%)	*Alox15,Ltc4s,Pla2g12a, Pla2g7,Tbxas1*
Ferroptosis Signaling Pathway	1,75	0,0732	1,342	1/82 (1%)	0/82 (0%)	5/82 (6%)	76/82 (93%)	*Alox15,Fth1,Prkaa2,Rasd1,Slc38a1,Tf*
Atherosclerosis Signaling	1,53	0,0652		2/92 (2%)	0/92 (0%)	4/92 (4%)	86/92 (93%)	*Alox15,Apoe,Il1rn,Il33, Pla2g12a,Pla2g7*
Dilated Cardiomyopathy Signaling Pathway	1,68	0,0642	-1,633	1/109 (1%)	0/109 (0%)	6/109 (6%)	102/109 (94%)	*Abcc9,Actg2,Adcy2,Cnn1,Myh11,Myl9,Tnnt2*
STAT3 Pathway	1,57	0,0609	-2	4/115 (3%)	0/115 (0%)	3/115 (3%)	108/115 (94%)	*Flt4,Igf2r,Il1r2,Il1rl2,Ntrk2,Ptpn6,Rasd1*
Calcium Signaling	1,57	0,0567		0/141 (0%)	0/141 (0%)	8/141 (6%)	133/141 (94%)	*Atp2b4,Casq2,Hdac11, Myh11,Myl9,Tnnt2,Tpm1,Trpc6*
PPARα/RXRα Activation	1,4	0,0526	0	3/152 (2%)	0/152 (0%)	5/152 (3%)	144/152 (95%)	*Adcy2,Cyp2c9,Il1r2,Il1rl2,Plcd4,Prkaa2,Rasd1,Tgfb3*
IL-8 Signaling	1,32	0,0506	0	4/158 (3%)	0/158 (0%)	4/158 (3%)	150/158 (95%)	*Arrb2,Ccnd1,Flt4,Gnat2,Mmp2,Myl9,Rasd1,Rhov*

Table 9. Complete list of canonical and metabolic signaling pathways with expressed genes obtained using IPA software [23].

To identify dysregulated biological functions and diseases associated with the obtained gene set, we conducted an analysis in the IPA program and identified approximately 12 categories linked to the detected DEGs (p-value – 0.05), with a z-score greater than 2 observed in only 3 affected processes. It is interesting to note that the activity of some genes related to heart failure is retained in post-infarct cells ("heart failure," p-value = 8.25E-03, z-score = 2.177), along with the ongoing modulation of processes related to neovascularization and cell migration. At the same time, "cell growth" was suppressed (p-value = 6.09E-03, z-score = -2.219), which may result from cell cycle delay, as "DNA synthesis" was also reduced (p-value = 1.31E-02, z-score = 1.077). The remaining processes affected in MI-CMCr are reflected in **Table 10**.

© 2000–2021 QIAGEN. All rights reserved.		
Category	p-value	Molecules
Cardiovascular Disease	4.12E-06–2.54E-02	*ABCC9,ACE,ACSS2,ACTA2,ADRA2B,AGT,ALOX15,APLN,APOE,ARRB2,ATP2B4,BMX,C1QTNF1,CASQ2,CCND1,CES1,CFD,CX3CL1,CXADR,DCBLD2,F5,FABP4,FBLN1,FCGR2A,FGF10,FLI1,FLT3,FLT4,FMO3,GSN,HEY2,HSD11B1,IGF2R,IL1RN,IL33,INHA,INPP5D,let-7,LMO2,MMP2,MYH11,NOX1,OSMR,PLAU,PRKAA2,RGS2,SCG5,SEMA3A,SFRP4,SMTN,SNAI2,SPI1,SPP1,TAGLN,TF,TGFB3,TGM2,THBS2,TNNT2,TRIM72,TRPC6,UNC13D,USP18,VAV1,XIRP1*
Cell-To-Cell Signaling and Interaction	1.86E-05–2.54E-02	*AGT,APOE,CCND1,COLEC12,CX3CL1,ECM1,FCGR2A,FGF10,FGF9,FLT3,GJA4,GSN,IGF2R,IL33,INPP5D,MMP2,MRC2,MYH11,MYO7A,NEDD9,PCSK5,PLAU,PTPN6,SIGIRR,SPI1,SPP1,TGM2,THBS2,TNNT2,UNC13D,VAV1,WNT5B*
Cellular Movement	3.08E-05–2.54E-02	*AGT,APOE,ARRB2,ATP2B4,BMX,CCND1,CFD,CNTF,CORO1A,CX3CL1,ECM1,FABP4,FBLN5,FGF10,FGF9,FGL2,GDF5,GSN,IGF2R,IGFBP5,IL1RN,IL33,INPP5D,LGALS9B,LIMA1,LMX1A,LPAR1,LPXN,MMP2,MRC2,MYO7A,NEDD9,NOX1,NRCAM,NTRK2,PCSK5,PLA2G7,PLAU,PLXNA4,PRKAA2,PTPN6,RAMP3,SATB1,SEMA3A,SFRP4,SNAI2,SPI1,SPP1,SPRY4,ST6GAL1,TGM2,THBS2,Tpm1,TWIST1,VAV1*
Cell Signaling	4.31E-04–2.54E-02	*ADRA2B,AGT,APLN,APOE,ATP2B4,C1QTNF1,CASQ2,CNTF,CX3CL1,DOK2,ECM1,FABP4,FGF10,FGF9,FLT3,GDF5,GLI2,GPR39,GSN,INPP5D,LGALS9B,LPAR1,MYH11,NOX1,NTRK2,PLAU,PLCD4,PRKAA2,PTPN6,RASSF2,RGS2,SCG2,SFRP4,SIGIRR,SPP1,TGFB3,TGM2,Tpm1,TRPC6,VAV1*
Cell Morphology	6.43E-04–2.54E-02	*AGT,ALOX15,ARRB2,BMX,CASQ2,CCND1,CXADR,DUSP4,ECM1,FERMT3,GSN,HEXB,HEY2,IL33,INPP5D,LPAR1,NOX1,PLAU,PRKAA2,PRSS12,RGS2,SPP1,STC1,THBS2,TNNT2,Tpm1,TRIM72,TRPC6,USP18*
Cellular Assembly and Organization	8.25E-04–2.54E-02	*AGT,ALOX15,APOE,ARRB2,CCND1,CORO1A,FGF9,GPR39,GSN,HSD11B1,LIMA1,LPAR1,MMP2,MYL9,MYO7A,NEFH,PLAU,PRKAA2,SPI1,STC1,Tpm1,UNC13D,VAV1*
Cellular Function and Maintenance	8.25E-04–2.54E-02	*ABCC9,AGT,ALOX15,APLN,APOE,ARRB2,ATP1A3,ATP2B4,B4GALNT1,BCL11B,CASQ2,CCND1,COLEC12,CORO1A,DUSP4,FABP4,FCGR2A,FGF9,FLI1,FMO5,GNAT2,GPR39,GSN,HEXB,HEY2,HSD11B1,IGFBP5,IL1RN,IL33,INHA,INPP5D,MAFB,MRC2,MYH11,MYO7A,NFIL3,PLAU,PRKAA2,PTPN6,SATB1,SCG5,SFRP4,SPI1,SPP1,STC1,TBXAS1,TF,TGFB3,TGM2,TRPC6,UNC13D,VAV1,XIRP1*
Cell Death and Survival	8.92E-04–2.54E-02	*ABCC9,ACE,ACSS2,AGT,APOE,ARRB2,ATP2B4,B4GALNT1,BCL11B,BMX,C1QTNF1,CASQ2,CCDC88B,CCND1,CES1,CNTF,CRIP1,CXADR,DUSP4,EGR2,EPHX1,F5,FCGR2A,FGF10,FLI1,FLT3,FLT4,FTH1,GLI2,GSN,HEXB,HOXB4,IGF2R,IGFBP5,IL1RN,IL33,INPP5D,let-7,LPAR1,MMP2,NOG,NOX1,NTRK2,PLAU,PRKAA2,PTPN6,RASSF*

		2,SEMA3A,SNAI2,SPI1,SPP1,STC1,TGFB3,TGM2,THBS2,TNNT2,TWIST1,USP18,VAV1
Cellular Development	1.54E-03–2.54E-02	*AGT,BCL11B,BMX,CCND1,CFD,CNTF,ECM1,EGR2,FBLN5,FGF10,FLI1,FLT3,FTH1,GSN,HEY2,HOXB3,HOXB4,IL1RN,IL33,INHA,INPP5D,let-7,LIMA1,LMX1A,MMP2,NAB2,NFIL3,NOG,NRCAM,NTRK2,PTPN6,RASD1,SATB1,SEMA3A,SFRP4,SNAI2,SPARCL1,SPI1,SPP1,STC1,TGFB3,TGM2,USP18*
Cellular Growth and Proliferation	1.54E-03–2.54E-02	*ADCY2,B4GALNT1,BCL11B,BMX,CCND1,CNTF,DOK2,DUSP4,ECM1,EGR2,FBLN5,FLI1,FLT3,GSN,HOXB3,HOXB4,IL1RN,IL33,INHA,INPP5D,let-7,LIMA1,LYL1,MAFB,MMP2,NFIL3,NOG,NRCAM,NTRK2,PTPN6,RASD1,SATB1,SEMA3A,SFRP4,SPARCL1,SPI1,SPP1,STC1,TF,TGFB3,USP18*
Vitamin and Mineral Metabolism	3.6E-03–2.54E-02	*AGT,APLN,APOE,ATP2B4,CASQ2,FABP4,GSN,HSD11B1,INPP5D,MYH11,PLAU,PLCD4,PRKAA2,RGS2,SPP1,TGM2,TRPC6,VAV1*
Carbohydrate Metabolism	5.23E-03–2.54E-02	*ABCC9,APLN,APOE,CCND1,CES1,CNTF,DLGAP3,FABP4,FCGR2A,FMO3,FMO5,GPR39,HEXB,HSD11B1,IGFBP5,IL33,INPP5D,SCG5,SPP1*
DNA Replication, Recombination, and Repair	1.31E-02–1.31E-02	*ADCY2,AFAP1L2,AGT,ARRB2,CCND1,FBLN5,FGF9,INHA,MMP2,SPP1*

Table 10. Top biological functions and diseases in post-infarct cells identified using IPA Software [23].

We constructed probabilistic dysregulated gene networks using the IPA program based on the detected activated/suppressed genes and those that were statistically filtered but present in the dataset (**Table 11**).

№	Molecules in Network	Score	Focus Molecules	Top Diseases and Functions
1	**ACTA2**, **AFAP1L2**, Akt, **ALOX15,** **APLN, APOE, ARRB2, CNN1, CNTF,** **DUSP7,** **EGR2**, ERK, ERK1/2, **FABP4,** **Fam13a,** **FBLN5, GLI2**, Gsk3, **IGF2R**, Jnk, MIR143-145a, **MMP2**, NFkB (complex), **NOX1**, PI3K (complex), Pkc(s), **PLAU, PRKAA2,** **PTPN6,** **RGS2**, ROCK, **TAGLN,** **TGM2,** **THBS2,** **TWIST1**	32	25	Cardiovascular Disease, Cardiovascular System Development and Function, Skeletal and Muscular System Development and Function
2	ADGRG1, **BCL11B**, CSF3, **DAPP1**, DMD, ERG, ESR2, **FGF9**, **FLI1**, GATA1, GATA2, GFI1B, **HEY2**, HOXA3, ID2, IKZF4, IRF8, ITGAM, **LMO2,** **LMX1A, LYL1, MAOB**, Meis1, mir-8, MSX2, **MYH1**, PKM,	10	12	Cellular Development, Cellular Growth and Proliferation, Gene Expression

	PPP4R3A, ¯**Pri8a2, PROM1**, RUNX1, SCX, **SPI1**, TAL1, ZFPM1			
3	**ADCY2**, **AGT**, AKAP12, AMPK, ¯**ANXA8/ANXA8L1**, BAX, BDNF, **C2, CFD**, COL1A1, DNMT3B, EIF2AK2, EP300, ¯**EPHX1,** ¯**ESM1,** ¯**GSN**, HES1, IFNB1, IGF1, IGF2, MAPK1, MAPK3, Mek, mir-34, ¯**MMP2**, NFE2L2, NOTCH1, NRAS, ¯**NTRK2**, PRKCE, RYR2, SIRT1, **STC1**, TP53, **XIRP1**	10	12	Cancer, Cell Death and Survival, Organismal Injury and Abnormalities

Table 11. Probabilistic networks of dysregulated genes constructed using IPA software based on the detected activated/suppressed genes and those that were statistically filtered but present in the dataset [23].

Among the biological functions and diseases associated with significant DEGs from the filtered gene set, processes related to the development and pathologies of the cardiovascular system are identified. One of the key regulatory genes in the obtained dataset was *Hey2*, a target gene of Notch, and its expression was altered in MI-CMCr.

To confirm the RNA sequencing results and assess the expression levels of Notch signaling components using real-time reverse transcription PCR, CMCs from passages 1–3 obtained from rat tissues at 8 and 24 hours after myocardial infarction induction were used. Specifically, we evaluated the expression levels of *Bmp2* and *Runx2*, whose dysregulation was identified in the transcriptome. Since the BMP signaling pathway plays a crucial role in cardiogenesis, like the Notch signaling pathway, and Runx2 can be a target for both types of signaling, and is also associated with heart development, according to our hypothesis, *Bmp2* and *Runx2* may be early remodeling genes. We found (**Figure 21**) that in post-infarct cardiac mesenchymal cells, the activation potential is partially preserved, as evidenced by increased expression of *Bmp2* and *Runx2* genes, as well as *Jag1* and *Hes1* genes of the Notch signaling pathway, compared to cells obtained from the healthy myocardium of sham-operated rats.

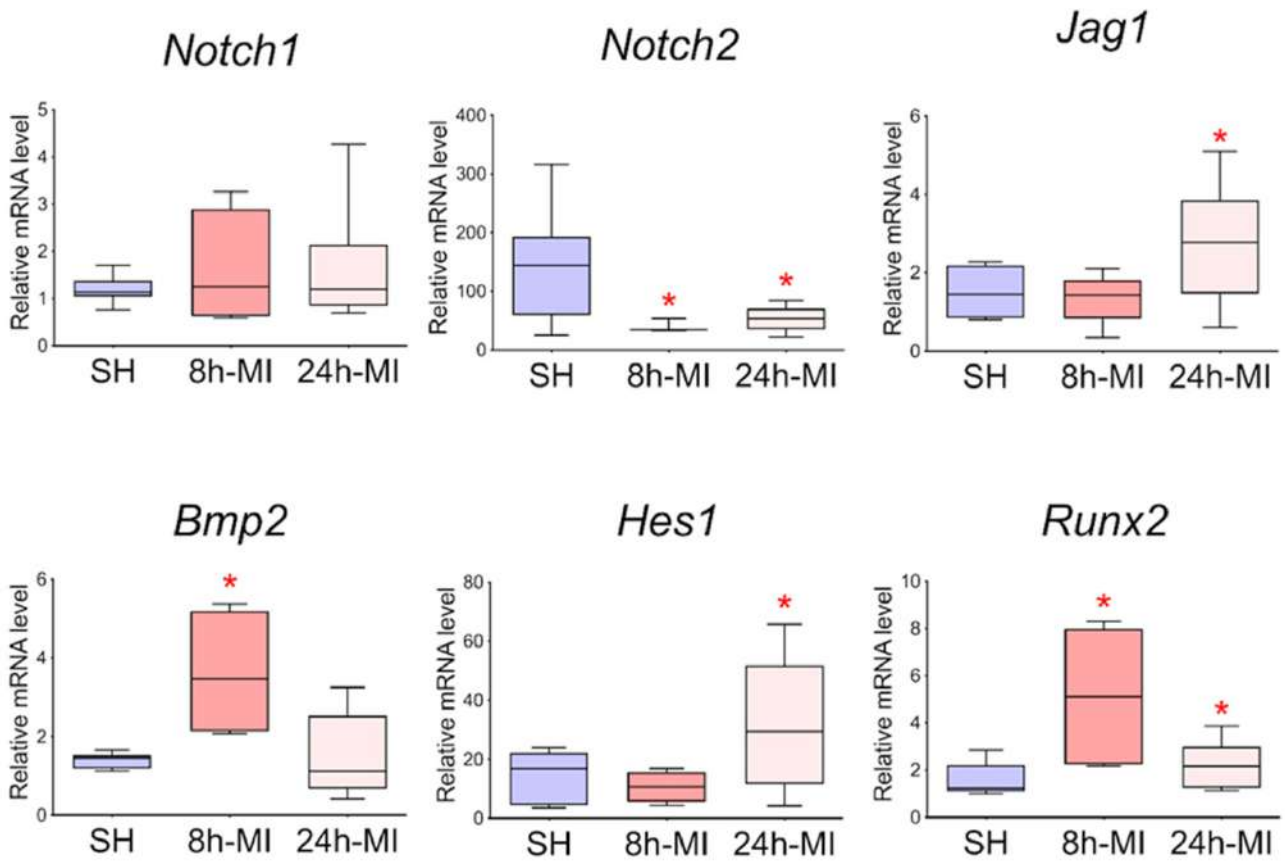

Figure 21. Dynamics of Notch signaling pathway components and *Bmp2/Runx2* genes expression in cardiac mesenchymal cells using quantitative PCR analysis. SH - healthy myocardial cells from sham-operated rats (n = 3), 8h-MI - post-infarct cells from rats at 8 hours after infarction induction (n = 4), 24h-MI - post-infarct cells from rats at 24 hours after infarction induction (n = 9). Vertically - relative mRNA levels in each group, measured by the $2^{-\Delta\Delta CT}$ method; Boxplots represent values from minimum to maximum. Asterisks indicate significant differences between SH-CMCr and MI-CMCr groups at $p < 0.05$ (Mann-Whitney non-parametric test) [23].

Thus, we demonstrated that MI-CMCr partially preserves the transcriptional activation profile characteristic of ischemic tissue, and the expression of Notch and *Bmp2/Runx2* components is also altered in post-infarct CMCr.

3.1.8 Activation of Notch Pathway Components and *Bmp2/Runx2* in Cardiac Mesenchymal Cells during *In Vitro* Hypoxia Induction

To determine whether hypoxia is a sufficient factor for activating the Notch pathway and *Bmp2/Runx2* in CMCs, we obtained cells from the healthy myocardium of sham-operated rats and induced in vitro hypoxia. SH-CMCs were subjected to hypoxic stress for 8 and 24 hours with oxygen concentrations of either 1% or 5%. We demonstrated (**Figure 22**) that under hypoxic conditions, Notch

and *Bmp2/Runx2* pathway components are activated in cells compared to SH-CMCs under normoxic conditions. *Hif-1α* and *Vegfa* were used as markers of hypoxia.

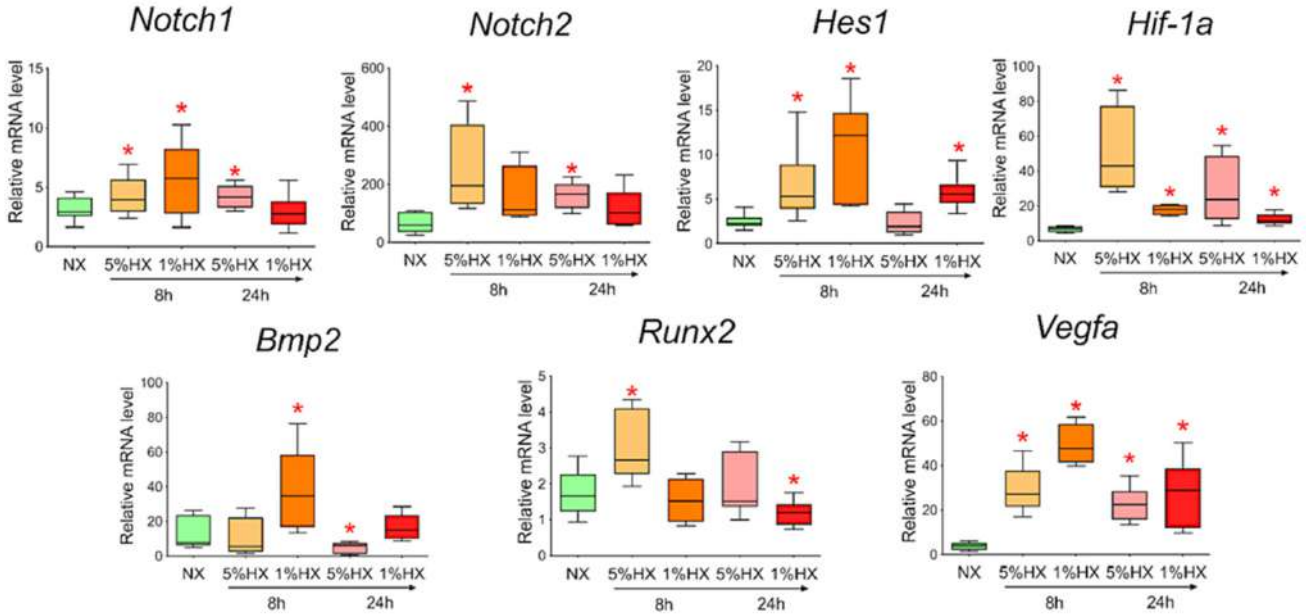

Figure 22. Dynamics of expression in cardiac mesenchymal cells obtained from the healthy myocardium of sham-operated rats, depicting the Notch pathway components, *Bmp2/Runx2* factors, and markers of hypoxic stress using quantitative PCR analysis. NX - healthy cells under normoxic conditions (n = 3), HX5% - healthy cells under hypoxia with 5% oxygen level (n = 3), HX1% - healthy cells under hypoxia with 1% oxygen level (n = 3). Horizontally – the duration of cells under hypoxic conditions. Vertically — relative mRNA quantity measured by the $2^{-\Delta\Delta CT}$ method; presented as box-and-whisker plots from minimum to maximum. The asterisk indicates significant differences between the control and HX5% and HX1% groups at $p < 0.05$ (Mann-Whitney U nonparametric test) [23].

Thus, we observed that hypoxia may be a factor in activating cardiac mesenchymal cells, leading to increased expression of Notch pathway components and *Bmp2/Runx2*.

3.1.9 Exogenous Activation of the Notch Signaling Pathway in Cardiac Mesenchymal Cells Dose-Dependently Activates *Runx2*

To elucidate the interplay between the Notch signaling pathway and the factors *Bmp2* and *Runx2*, we obtained cardiac mesenchymal cells (CMCr) from the healthy myocardium of sham-operated rats and transduced them with a lentiviral vector carrying the NICD insert to activate the Notch signaling pathway. Viral particles were added to the culture at two different concentrations: 3 µL and 15 µL. The cells were cultured with the virus for 24 hours. We demonstrated (**Figure 23**) that the activation of the

Notch signaling pathway leads to a dose-dependent activation of *Runx2*. Conversely, *Bmp2* did not respond to Notch activation.

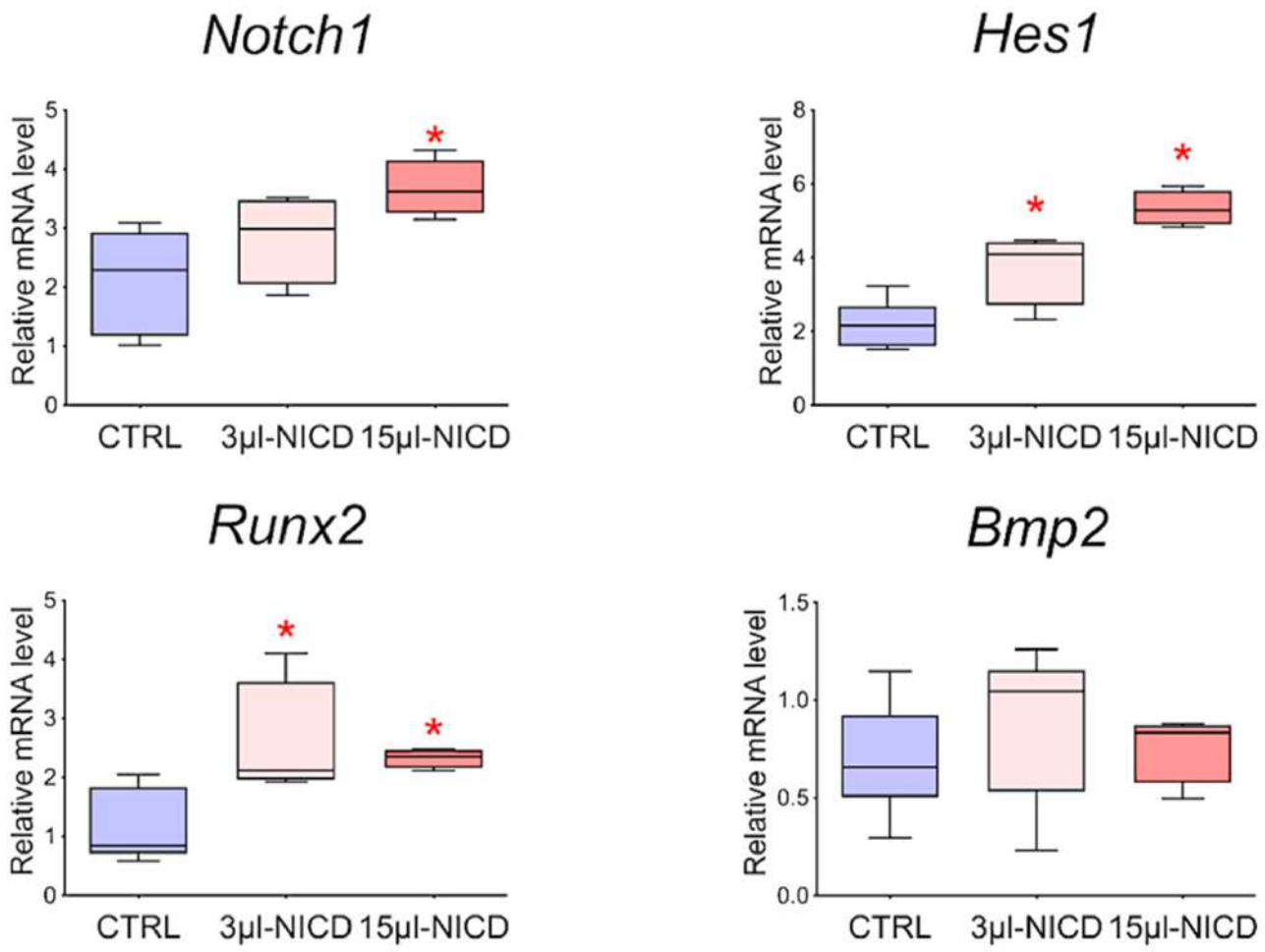

Figure 23. Dynamics of *Bmp2/Runx2* Factors and Notch Signaling Pathway Components in Cardiac Mesenchymal Cells Derived from the Healthy Myocardium of Sham-Operated Rats Using Quantitative PCR Analysis. Control – healthy cells as a negative control (n = 3), NICD 3 µL – healthy cells treated with 3 µL of NICD-containing virus (n = 3), NICD 15 µL – healthy cells treated with 15 µL of NICD-containing virus (n = 3). Vertical axis represents the relative mRNA quantity measured by the $2^{-\Delta\Delta CT}$ method; Boxplots depict the range from minimum to maximum. Asterisks indicate significant differences between the Control group and NICD (3 µL) and NICD (15 µL) groups at $p < 0.05$ (Mann-Whitney non-parametric test) [23].

3.1.10 Discussion of Results on Studying the Mechanisms of Activation of the Regenerative Potential of Cardiac Mesenchymal Cells

Myocardial infarction is a prevalent acute condition that disrupts heart function. The molecular and cellular mechanisms underlying early cardiac remodeling and recovery after post-infarction myocardium remain incompletely understood. Numerous studies have observed focal proliferative activity in the peri-infarct zone in response to damage [162, 163]. The impact of hypoxemia on

myocardial recovery following injury has also been noted *in vivo* experiments on mice [22]. This study aimed to investigate early transcriptional events in heart tissue after myocardial infarction and analyze the cellular population of cardiac mesenchymal cells (CMCr) that could be isolated from myocardial tissue to understand the molecular mechanisms of activating their regenerative potential.

To achieve this, we induced myocardial infarction in rats to study early transcriptional events occurring 8 and 24 hours after surgical procedures. RNA sequencing results revealed significant changes in the gene expression pattern in post-infarction tissue. Numerous signaling pathways and processes related to early heart remodeling, cell proliferation and migration, as well as the immune response, were affected. The immune response is currently a subject of active discussion, with researchers recognizing the importance of the immune response in the early stages of myocardial infarction development [164].

Several studies have demonstrated increased expression of certain components of the Notch signaling pathway in heart cells during myocardial infarction [165-168]. The Notch signaling pathway is a highly conserved pathway involved in the embryonic development of most multicellular organisms, as well as in tissue homeostasis regulation, cell differentiation, and maintenance of the stem cell population in the postnatal period [169, 170]. However, the role of Notch in myocardial recovery remains incompletely understood [171-173].

We observed the activation of components of the Notch signaling pathway in post-infarction tissue. Some of these components were identified as highly expressed target genes associated with non-canonical forms of the Notch signaling pathway, such as *Myc, Ccnd1,* and *Runx2* [151]. The transcription factor *Runx2* has previously been implicated in the development of the cardiovascular system [174]. Additionally, the BMP signaling pathway, known to participate in development [175], including its reactivation during myocardial infarction, particularly *Bmp2*, as indicated by our findings [23]. *Bmp2* is recognized for its critical role in heart development, inducing the differentiation of cardiac precursor cells into cardiomyocytes and stimulating their contraction [176, 177]. It may play a key role in regulating and modulating the Notch signaling pathway [178], and participate in early remodeling processes [179]. The expression of *Bmp2* has been observed in both cardiomyocytes and interstitial fibroblasts during myocardial infarction [180]; however, the activation mechanism remains unknown [129]. We hypothesize that the Notch signaling pathway, along with key factors Bmp2 and Runx2, may play a crucial role in early myocardial events in response to injury (**Figure 24**).

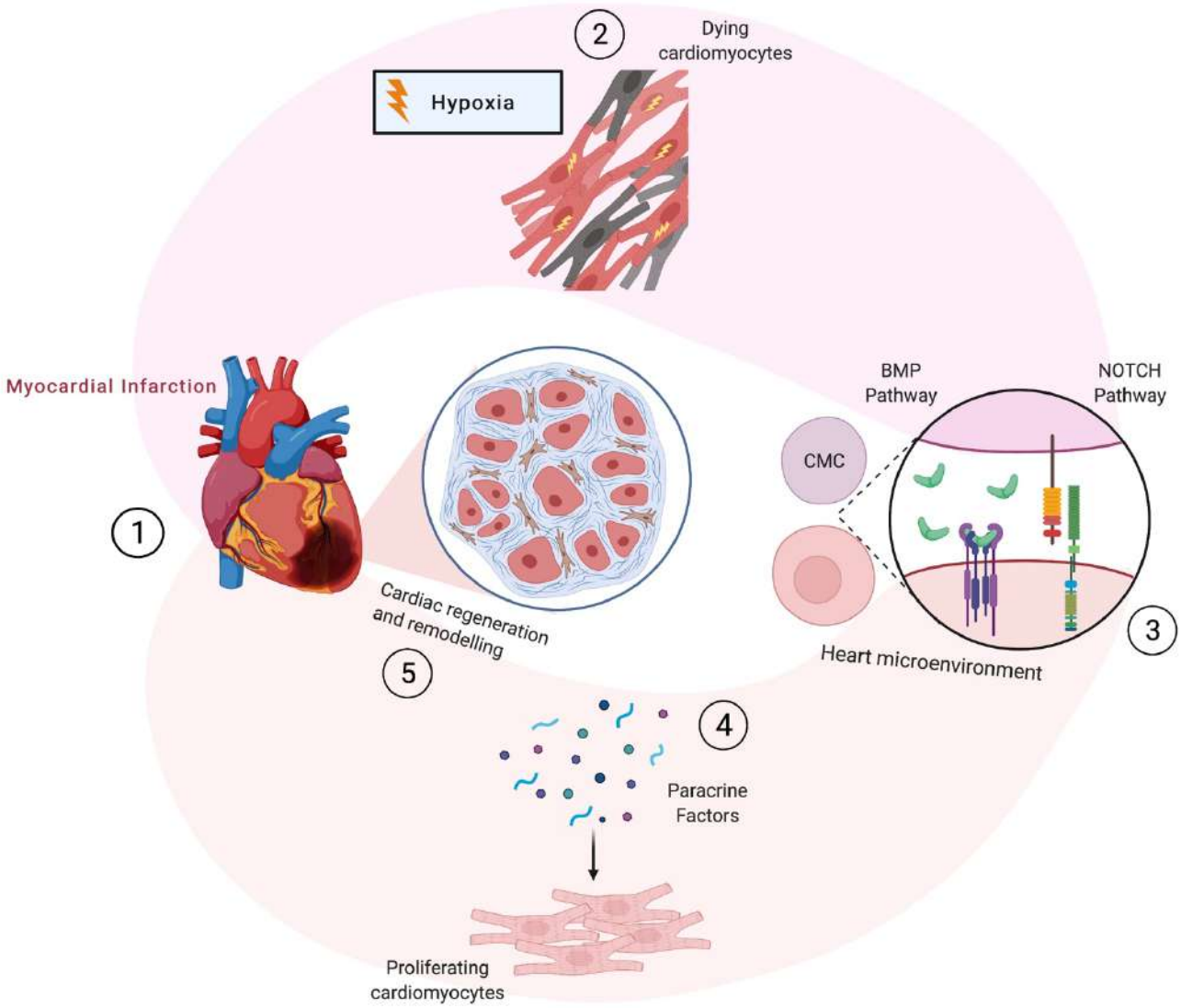

Figure 24. Graphic representation of the potential interaction between the Notch and Bmp signaling pathways in the processes of early myocardial remodeling after infarction [23].

To confirm this, we obtained a fraction of activated cardiac mesenchymal cells (CMCs) from the post-infarction area of the myocardium. Cells were isolated 24 hours after myocardial infarction induction, and during cultivation, they were passaged only three times to preserve their properties and conduct functional tests. We observed significant proliferative and migratory activity of post-infarction CMCs compared to the control population during cultivation and functional testing. CMCs are known to differentiate into cardiogenic, osteogenic, and adipogenic lineages [181, 182]. We also induced the differentiation of CMCs in three directions, as observed through immunocytochemical staining of cells. Assessing the expression of specific markers for cardiogenic, osteogenic, and adipogenic differentiation, we found a higher level of activation in cells originating from the post-infarction zone, in contrast to the control population from the healthy myocardial region.

Proliferative activity was assessed in real-time using the xCELLigence system. We discovered that post-infarction cardiac mesenchymal cells exhibit a more pronounced proliferative potential than CMCs obtained from the healthy hearts of sham-operated rats. This aligns with our findings in post-infarction tissues and is consistent with literature sources [183], demonstrating fibroblast activity in injury and their interaction with cardiomyocytes. Additionally, we conducted RNA sequencing of primary CMC cultures, revealing that post-infarction CMCs partially retain their transcriptional profile, reflecting early events in the affected myocardium.

For comparison, we obtained a fraction of activated cardiac mesenchymal cells (CMCs) eight hours after myocardial infarction induction. Subsequent analysis of the expression of Notch signaling pathway components and presumed early remodeling genes using real-time PCR revealed activation of the Notch target gene *Hes1* and factors *Bmp2/Runx2*. Importantly, the activation of the latter was specifically pronounced at an earlier time point.

Hypoxia has been described as a modulator of the Notch signaling pathway [184]. However, the impact of in vitro hypoxic stress on a similar activation of Notch signaling pathway components and early remodeling genes in healthy CMCs, obtained from sham-operated rats, remains unclear. *In vitro*, we induced hypoxia by placing cardiac mesenchymal cells in an incubator with controlled oxygen levels. CMCs experienced acute hypoxic stress at 1% or 5% oxygen levels for 24 hours. We isolated RNA and assessed gene expression, revealing that in vitro hypoxia also enhances the expression of Notch signaling pathway components and *Bmp2/Runx2* genes.

Intermolecular interactions between the Notch signaling pathway and Bmp2/Runx2 exist in embryonic development [56, 185]. However, whether Notch can act as an activator of presumed early remodeling factors in healthy CMCs remains unknown. We transduced healthy CMCs, obtained from sham-operated rats, with a lentiviral vector at low and high doses containing the intracellular domain of Notch 1 (*NICD1*). Activation of the Notch signaling pathway had a dose-dependent effect on *Runx2* expression. However, *Bmp2* did not respond to vector introduction, which may indicate its upstream role in the regulation of this gene network.

It is worth noting that the studies conducted had a number of limitations. Epicardium-derived cells may promote neovascularization and cardiomyogenesis through reactivation of fetal genes during myocardial infarction [186-188]. The epicardium was removed before RNA extraction and cell culture, but it is possible that its effect could still be exerted on the myocardium, so further studies will be required to clarify this effect. It should also be noted that culturing cells *in vitro* can change their properties, including proliferative and proangiogenic [189]. In the results of this study, post-infarction CMCr proliferated better than healthy CMCr, but how this will affect myocardial regeneration *in vivo* requires further study.

3.2 Dysregulation of the Notch Signaling Pathway in Cardiac Mesenchymal Cells from Tetralogy of Fallot Patients

Considering the significance of Notch signaling in heart development and the formation of a specific gene expression pattern, we hypothesized that the Notch pathway might be attenuated in cardiac tissue cells of Tetralogy of Fallot (TF) patients due to hypoxic stress [5]. This regulatory disruption could be associated with cardiac tissue remodeling in TF patients. Human cardiac progenitor cells or cardiac mesenchymal cells (CMCh) originating from the ventricular and atrial tissues are well-documented in both human and rodent hearts [190]. They serve as a convenient tool for unraveling mechanisms related to heart development and diseases [191, 192]. The aim of this section was to assess the activity of the Notch signaling pathway in CMCh derived from the ventricular myocardium of TF patients.

3.2.1 Cardiac mesenchymal cells from patients with tetralogy of Fallot have an alternative phenotype

CMCs were isolated from myocardial tissue obtained from patients with tetralogy of Fallot (TF-CMCh) and compared with CMCs from patients with isolated ventricular septal defect as a control (VSD-CMCh), since there was no effect of this pathology on the Notch signaling pathway [193]. CMCh were phenotyped using flow cytometry. Cells from passages 2–3 were used for analysis. It was demonstrated (**Figure 25**) that CMCh had a mesenchymal phenotype and moderately expressed CD117 (c-kit), characteristic of this lineage [194].

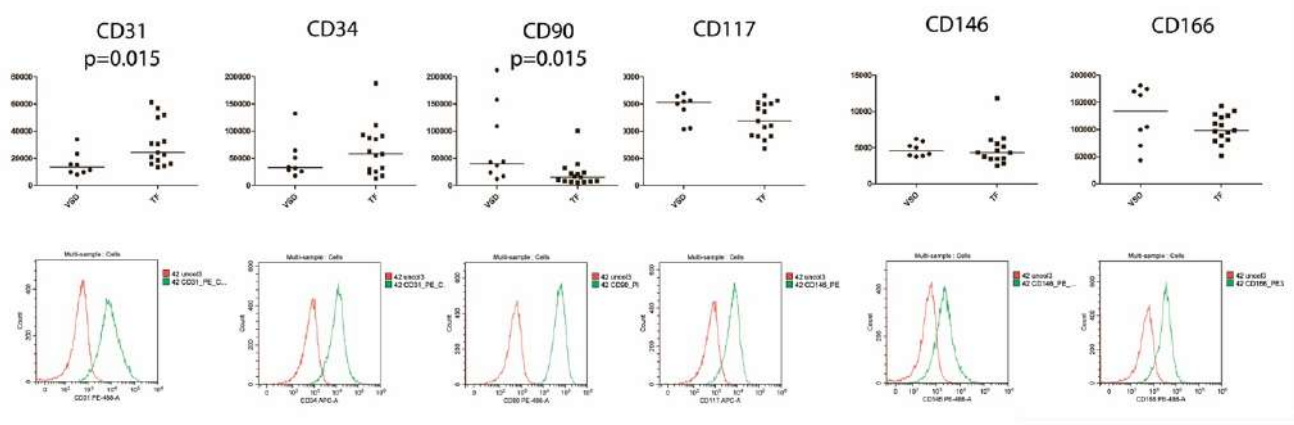

Figure 25. Expression levels of marker genes of mesenchymal stem cells in TF-CMCh and VSD-CMCh according to flow cytometry. Expression of markers in a typical CMCh population is indicated in the bottom panel. The top panel shows the scatter plots for TF-CMCh and VSD-CMCh. Isotypes (control) are marked with a red line, and CMCh - with a green line. The dot is the average fluorescence for the CMCh. Groups were compared using the nonparametric Mann-Whitney test; line - median; p >0.05 not specified. VSD-CMCh: *n* = 8; TF-CMCh: *n* = 15; the vertical axis is the fluorescence intensity [26].

TF-CMCh expressed more endothelial marker CD31 (*PECAM-1*) and less mesenchymal marker CD90 than VSD-CMCh [27]. Thus, the surface markers of TF-CMCh differed from VSD-CMCh.

3.2.2 Expression of Notch Signaling Pathway Components is Altered in TF-CMCh

To assess the expression of key genes in the Notch signaling pathway, we extracted total RNA from CMCh and performed RT-PCR using gene-specific primers (**Figure 26a**).

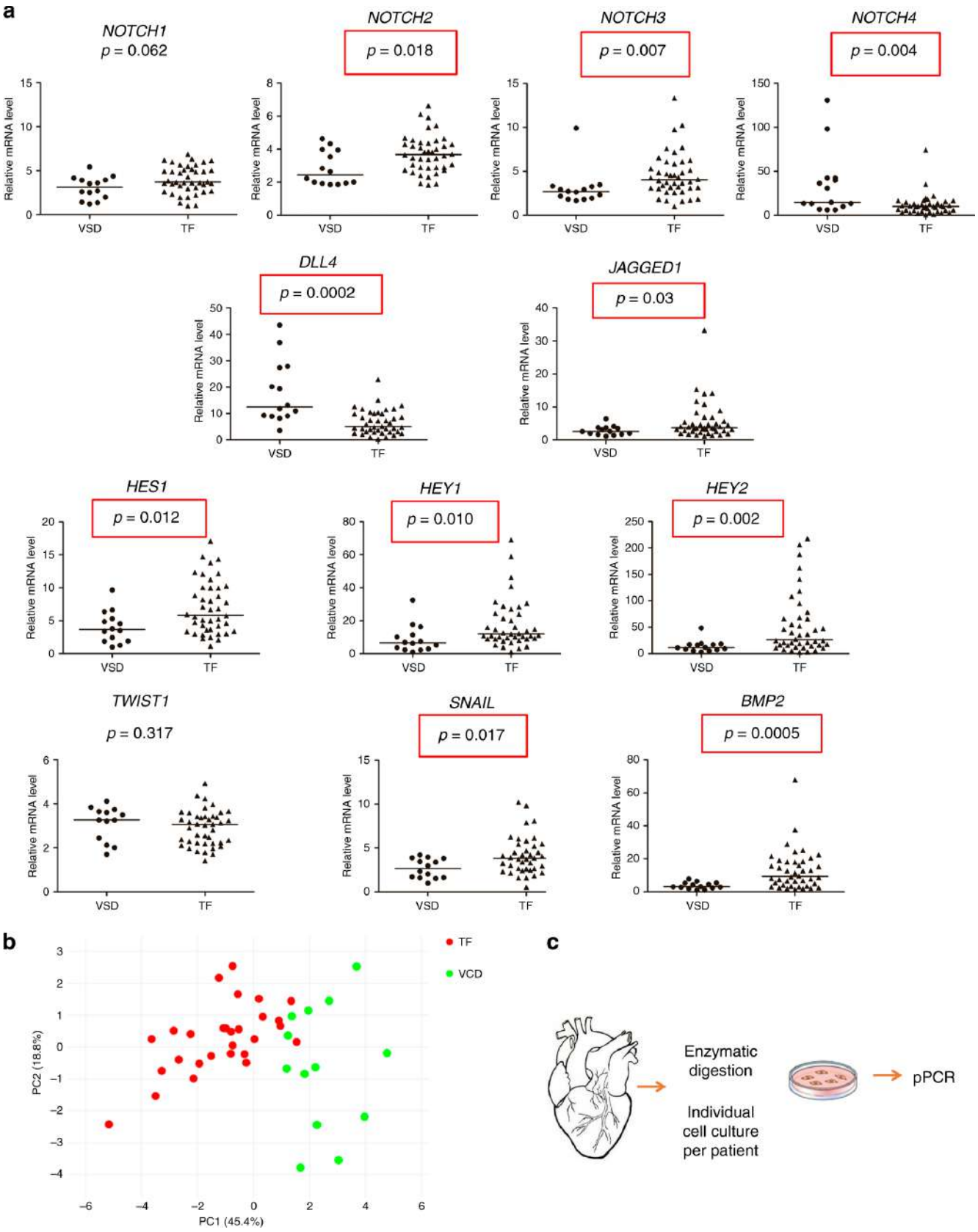

Figure 26. Evaluation of Notch Signaling Pathway Component Expression in Cardiac Mesenchymal Cells from Patients with Tetralogy of Fallot (TF-CMCh) and Ventricular Septal Defect (VSD-CMCh). **A.** Experimental scheme. **B.** mRNA levels were assessed using quantitative PCR and normalized to GAPDH. The vertical axis represents the relative mRNA content. Groups were compared

using the non-parametric Mann-Whitney test; the line represents the median; $p < 0.05$ was considered significant (highlighted by red squares). VSD: $n = 14$; TF: $n = 42$. The dot represents the mean from qPCR performed in duplicate for each individual CMCh culture. **C.** Principal component analysis showing differences in gene expression profiles between TF-CMCh and VSD-CMCh [26].

We evaluated the expression of Notch signaling pathway components, including *NOTCH1–4* receptors, ligands *JAG1, DLL4*, and target genes *HES1, HEY1, HEY2, TWIST*, and *SNAIL* (**Figure 26b**). As BMP2 was noted to cooperate with the Notch pathway in cardiac patterning [195], we also assessed *BMP2* gene expression. We found that *NOTCH4* and *DLL4* expression was decreased in TF-CMCh compared to VSD-CMCh, while *NOTCH2, NOTCH3, JAG1, HES1, HEY1*, and *HEY2* expressions were increased. *BMP2* expression was also elevated in TF-CMCh.

Principal component analysis revealed a difference in the expression pattern between TF-CMCh and VSD-CMCh, with TF-CMCh forming a distinct cluster of gene expression (**Figure 26c**). The variates included gene expression data obtained by RT-PCR and calculated using the $2^{-\Delta\Delta CT}$ method, specifically: *NOTCH1, NOTCH2, NOTCH3, NOTCH4, JAG1, DLL4, HEY1, HES1, HEY2, SNAIL*, *TWIST1*, and *BMP2*. Thus, our results indicate alterations in the baseline expression of Notch signaling pathway components in TF-CMCh.

Due to the high variability in the expression of Notch signaling pathway components in TF-CMCh, we assessed the correlation between target genes and Notch receptors (**Figure 27**).

.

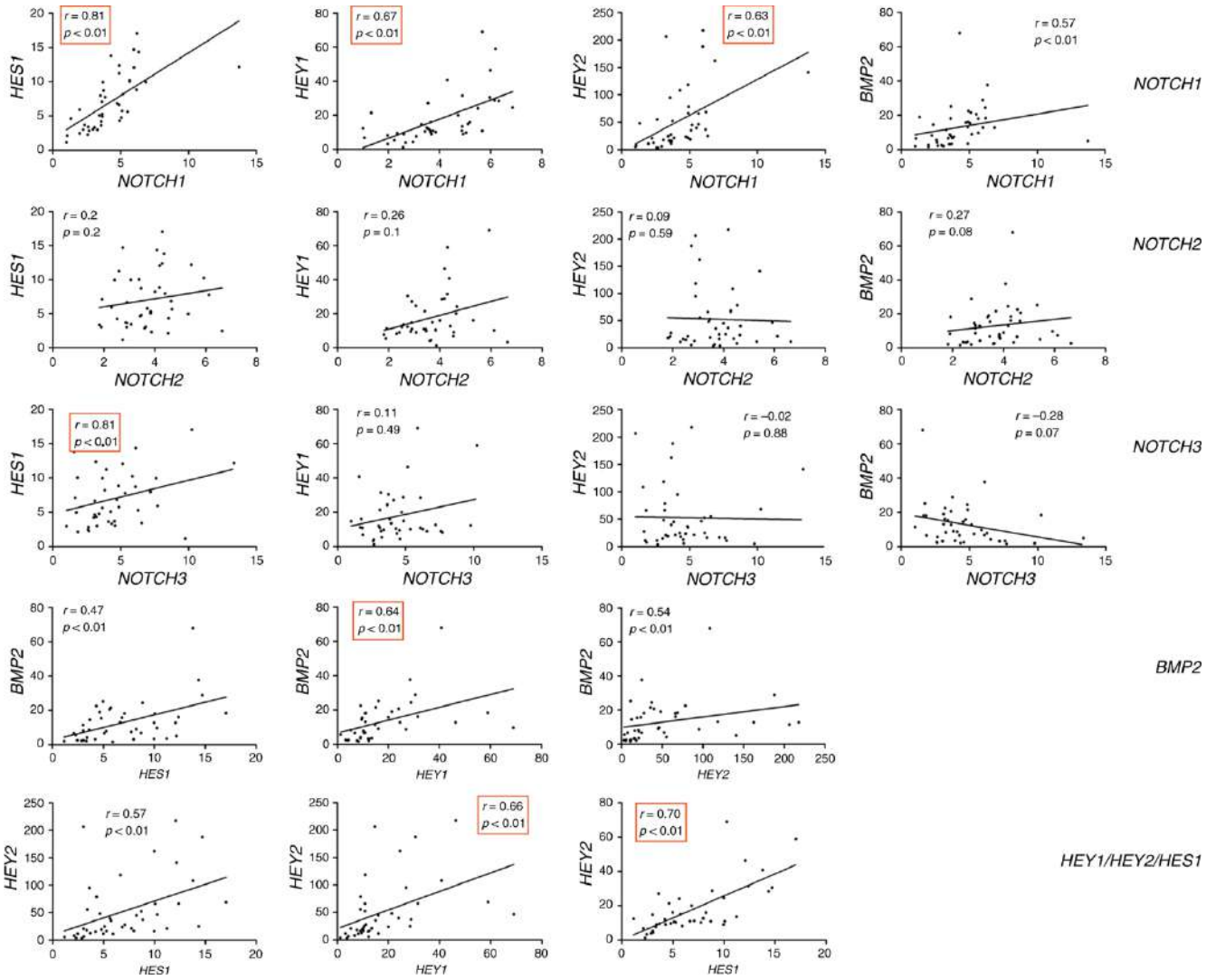

Figure 27. Scatter plots show correlations between Notch genes (*NOTCH1,2,3*), *BMP2*, and Notch targets (*HES1/HEY2/HES2*). r - Spearman's rank correlation coefficient; $p < 0.05$ is considered significant (highlighted by red squares); $n = 42$ [26].

We identified correlations between levels of *NOTCH1* and targets *HES1, HEY1, HEY2*; the level of *NOTCH3* correlated with *HES1*. This suggests that *NOTCH1* and *NOTCH3* likely contribute to the increased expression of the Notch signaling pathway observed through the activation of *HEY1, HEY2*, and *HES1* in TF-CMCh. We observed moderate correlation between *HEY1* and *BMP2*, indicating a potential interaction in determining the phenotype of TF-CMCh. We found no associations with high/low Notch signaling transduction with any clinical parameters or patient age (data not shown).

3.2.3 Differences in the Notch Gene Expression Pattern in TF-CMCh from the Right Atrium and Ventricle are Insignificant

To analyze the identified differences in gene expression in CMCh originating from different heart chambers, we isolated TF-CMCh from the right atrium (RA) and right ventricle (RV) of several TF patients and assessed gene expression using RT-PCR and qPCR analysis (**Figure 28**).

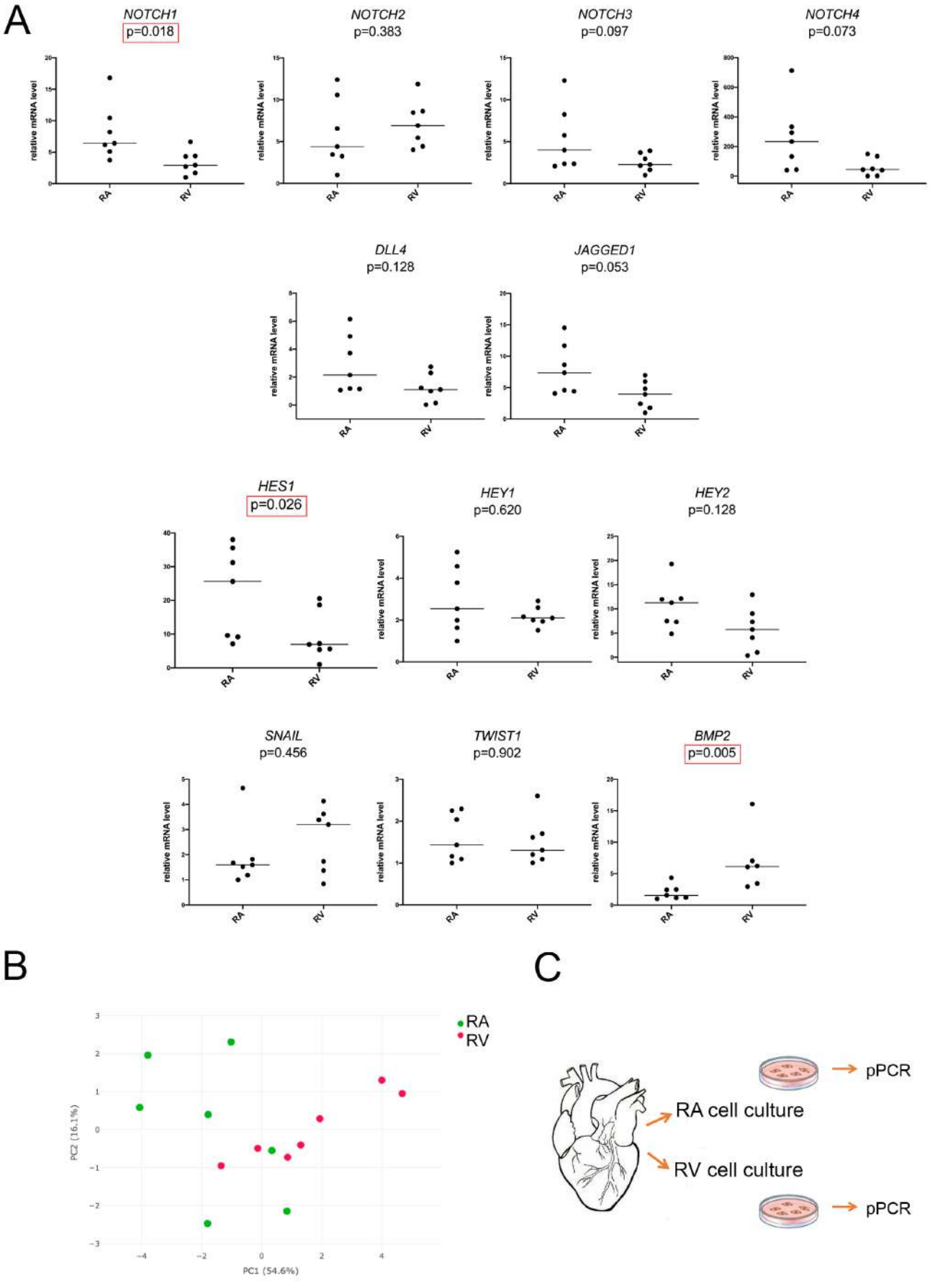
A
NOTCH1
p=0.018
NOTCH2
p=0.383
NOTCH3
p=0.097
NOTCH4
p=0.073
DLL4
p=0.128
JAGGED1
p=0.053
HES1
p=0.026
HEY1
p=0.620
HEY2
p=0.128
SNAIL
p=0.456
TWIST1
p=0.902
BMP2
p=0.005
relative mRNA level
RA
RV
B
RA
RV
PC2 (16.1%)
PC1 (54.6%)
C
pPCR
RA cell culture
RV cell culture
pPCR

Figure 28. Assessment of Notch Signaling Pathway Component Expression in Cardiac Mesenchymal Cells from TF Patients (TF-CMCh) from Two Sources: Right Atrium (RA) and Ventricle (RV). **A.** mRNA levels were assessed using quantitative PCR and normalized to GAPDH. The vertical axis represents the relative mRNA content. Groups were compared using the non-parametric Mann-Whitney test; the line represents the median; $p < 0.05$ was considered significant (highlighted by red squares). RA: $n = 7$; RV: $n = 7$. The point represents the mean value obtained from quantitative PCR, performed in duplicate for each individual TF-CMCh culture. **B.** Principal component analysis showing differences between TF-CMCh from RV and RA in gene expression profiles. **C.** Experimental design [26].

We did not find significant differences between TF-CMCh derived from RA and RV, especially in the key Notch signaling pathway target genes. However, differences in Notch expression are observed in the tissues between RV-TF and RA-TF (**Figure 29**), indicating a complex cellular composition of myocardial tissue.

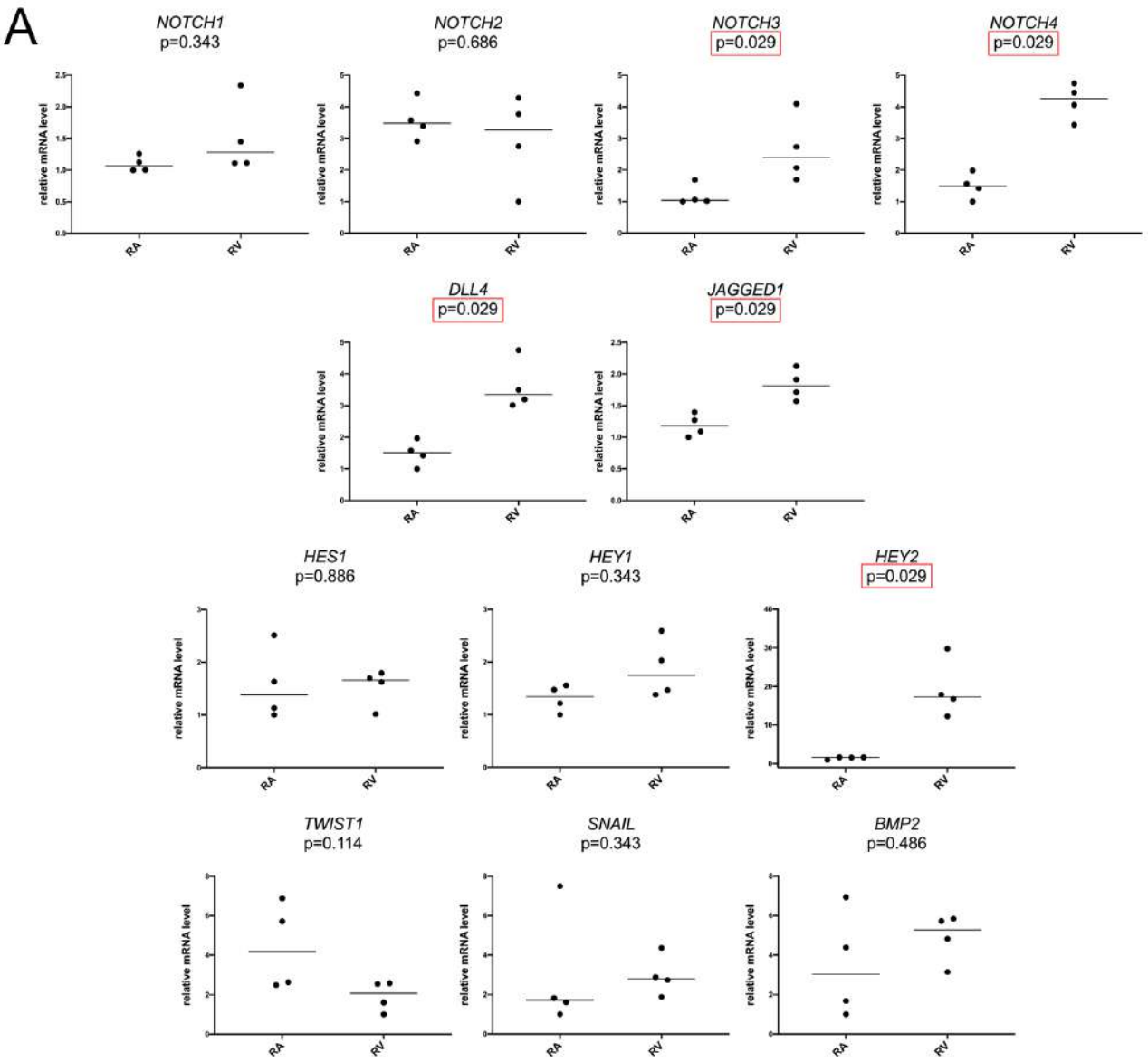
A
NOTCH1
p=0.343
NOTCH2
p=0.686
NOTCH3
p=0.029
NOTCH4
p=0.029
DLL4
p=0.029
JAGGED1
p=0.029
HES1
p=0.886
HEY1
p=0.343
HEY2
p=0.029
TWIST1
p=0.114
SNAIL
p=0.343
BMP2
p=0.486
relative mRNA level
RA
RV
B
RA
RV
PC2 (19.7%)
PC1 (48.7%)
C
RA tissue
RV tissue
qPCR
qPCR

Figure 29. Assessment of Notch Signaling Pathway Component Expression in Myocardial Tissues Obtained from the Right Ventricle (RV) and Right Atrium (RA) of TF Patients. **A.** mRNA levels were assessed using quantitative PCR and normalized to GAPDH. The vertical axis represents the relative mRNA content. Groups were compared using the non-parametric Mann-Whitney test; the line represents the median; $p < 0.05$ is considered significant and highlighted by red squares. RA: *n* using qua*n* uaing quantitative PCR and normalized to GAPDH. The vertical axis represents the relative mRNA content. Groups were comp**B.** Principal component analysis showing differences between RV and RA in gene expression profiles. **C.** Experimental design [26].

3.2.4 Notch Activation Level is Associated with Proliferative Activity of TF-CMCh

According to our hypothesis, the properties of TF-CMCh could depend not only on the age of the patients but also on the level of Notch activation, given the high variability in the expression of its components. To investigate this, we analyzed the correlation between patient age and low/high Notch levels, assessing the proliferation rate of TF-CMCh. Three age groups were established: neonates <14 days, 5–7 months, and >12 months. Proliferation of respective TF-CMCh lines was analyzed using the xCELLigence automated system [140], revealing no correlation between patient age and the proliferation rate of their cells (**Figure 30a**).

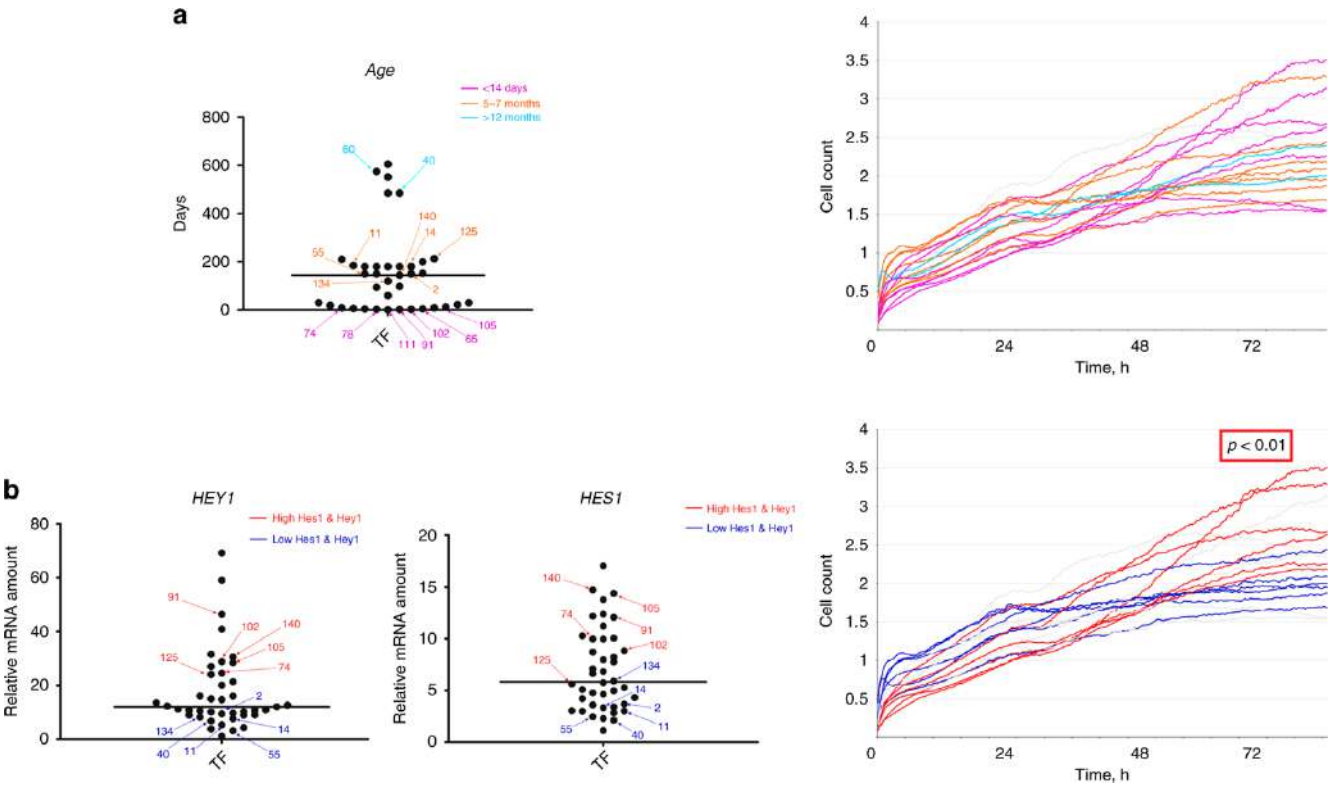

Figure 30. Cell Proliferation Assessment Using Real-Time Monitoring and Correlation Analyses a. Correlation between TF-CMCh Proliferation and Patient Age. Cell proliferation was assessed using

real-time xCELLigence cell division monitoring; *n* = 16. The dotted graph represents the age distribution of TF patients; *n* = 42. TF-CMCh from three age periods is color-coded, and their respective growth curves are presented on the right graph. b. Correlation between TF-CMCh Proliferation and Notch Activation. Dotted graphs depict the expression levels of *HES1* and *HEY1* in TF-CMCh based on qRT-PCR data. CMCh with "low" and "high" levels are denoted in blue and red, respectively. Growth curves are presented on the right graph. Patient identifiers are indicated with arrowed numbers. Horizontal lines indicate median values, *n* = 24 [26].

In contrast, when we categorized TF-CMCh lines based on their *HEY1/HES1* expression, we observed that higher expression of Notch pathway target genes was associated with increased proliferation rates, while low *HEY1/HES1* expression had the opposite effect (**Figure 30b**). Thus, we noted a correlation between the expression level of Notch pathway target genes and the proliferation rate of TF-CMCh.

3.2.5 Notch Activation Level Correlates with Enhanced Differentiation Capacity of TF-CMCh

The functional outcome of Notch signaling activation strongly depends on developmental context [196], and there are conflicting data regarding the activating and inactivating roles of Notch in various differentiation types, including cardiogenic differentiation [197]. The cardiogenic potential of CMCs has been previously described [194]. We investigated the impact of low/high Notch signaling levels on the differentiation capacity of TF-CMCh, demonstrating the cardiogenic properties of CMC lines through immunocytochemical staining and quantitative PCR for cardiogenic markers (**Figure 31, 32**).

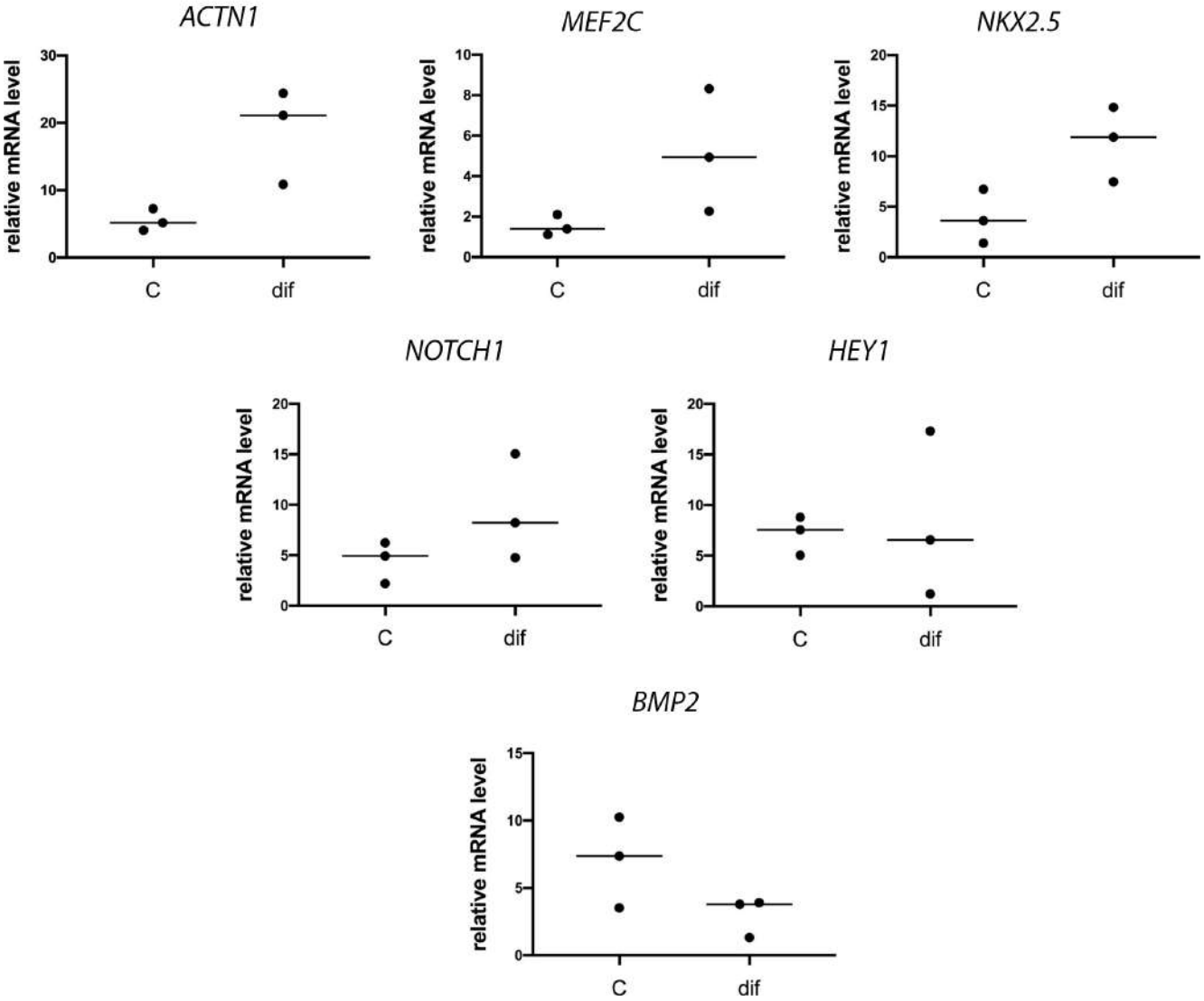

Figure 31. Dynamics of Cardiogenic Gene Markers and Notch Signaling Components Expression in TF-CMCh through Quantitative PCR Analysis. Differentiation – TF-CMCh subjected to directed cardiogenic differentiation; Control – control group without differentiation. On the vertical axis – relative mRNA levels for each gene, measured using the $2^{-\Delta\Delta CT}$ method [26].

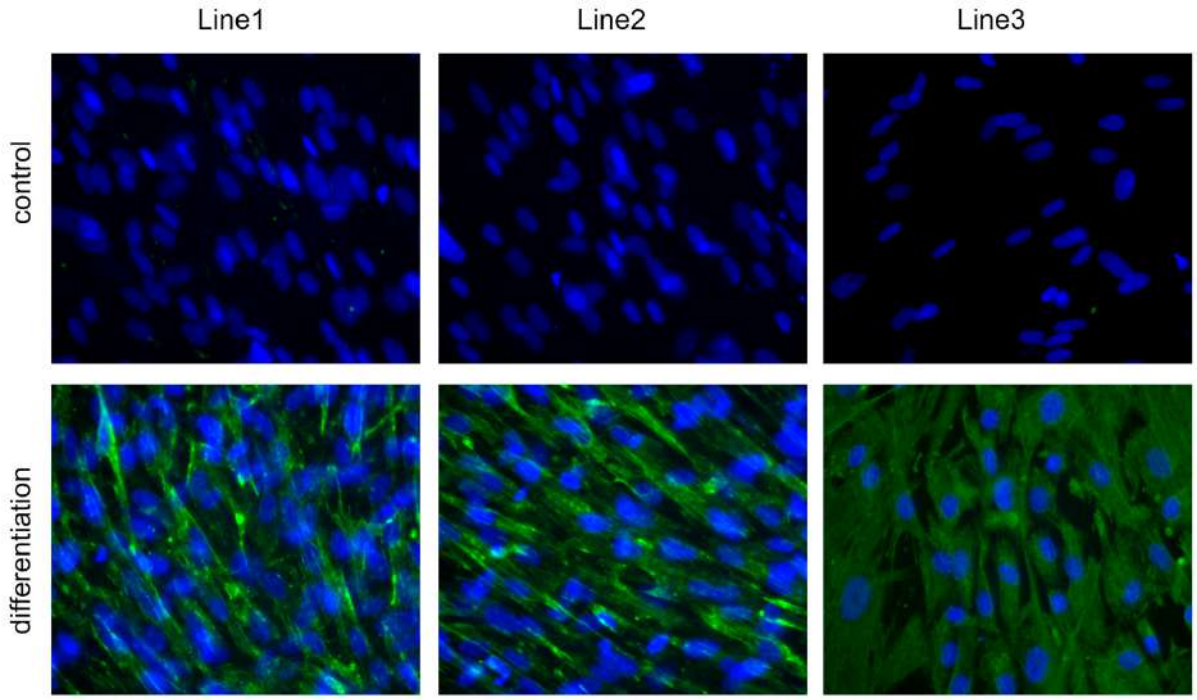

Figure 32. Cardiogenic (green color) Differentiation of TF-CMCh. Cells underwent differentiation by adding specific inductors to the culture medium. Immunocytochemical staining for α-actinin and DAPI [26].

We induced cardiogenic differentiation in TF-CMCh lines and categorized them into four groups based on Notch activation levels represented by the expression of *NOTCH1/HEY1* (**Figure 33**).

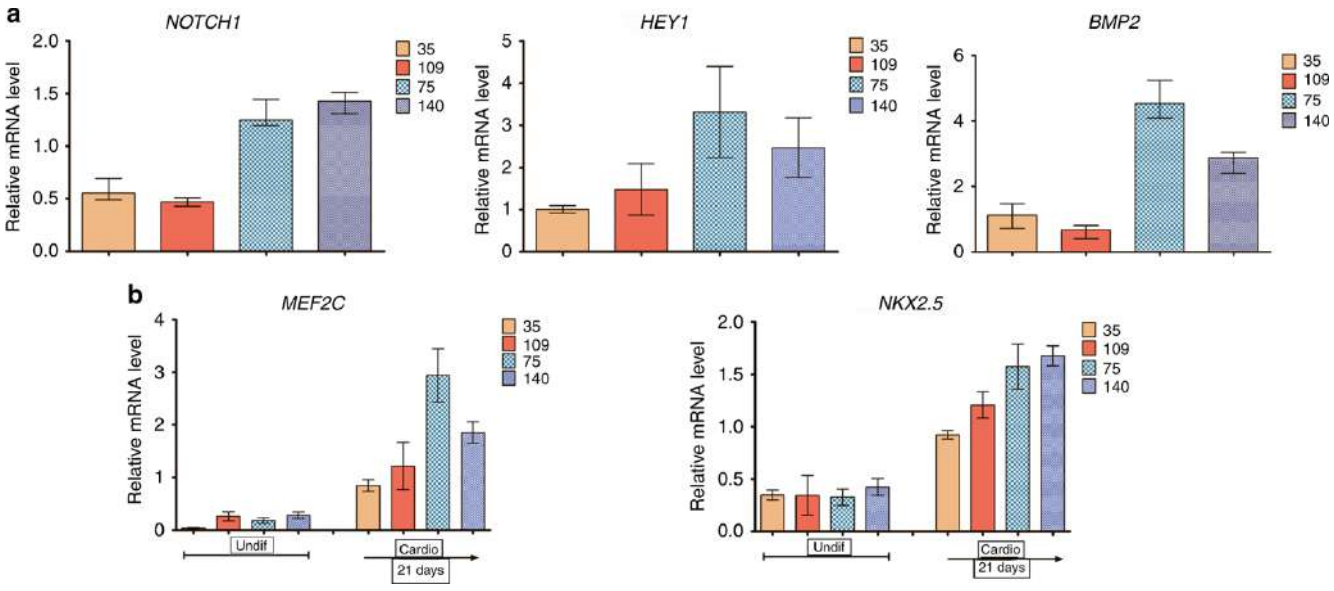

Figure 33. Analysis of Differentiation Capacity Depending on the Initial Notch Activation Level. **a** Four TF-CMCh lines were selected based on Notch activation levels. Evaluation of *NOTCH1, HEY1*, and *BMP2* expression was performed using quantitative PCR. **b** Cardiogenic differentiation was induced in the four CMCh lines. Levels of *MEF2C* and *NKX2-5* were also assessed via quantitative PCR 24 days

post-differentiation induction. Experiments were conducted in triplicate; error bars reflect the mean +/- SD for three replicates [26].

The expression level of BMP2 corresponded to the level of *HEY1/NOTCH1* (**Figure 33a**). After 24 days of cardiogenic differentiation induction, we observed an increase in the expression levels of the cardiogenic markers *MEF2C* and *NKX2-5* to a degree consistent with the initial Notch activation level (**Figure 33b**). Thus, elevated Notch signaling may contribute to increased plasticity of TF-CMCh.

3.2.6 Notch Dose-Dependently Promotes Differentiation

To confirm that high levels of Notch signaling activation can contribute to an increased differentiation potential of TF-CMCh, we activated Notch in cells by introducing lentiviruses carrying the intracellular domain of Notch1 – NICD [132] and induced cardiogenic differentiation. We demonstrated that transducing cells with NICD led to a dose-dependent increase in the expression of *NOTCH1* and *HEY1* in TF-CMCh (**Figure 34a**).

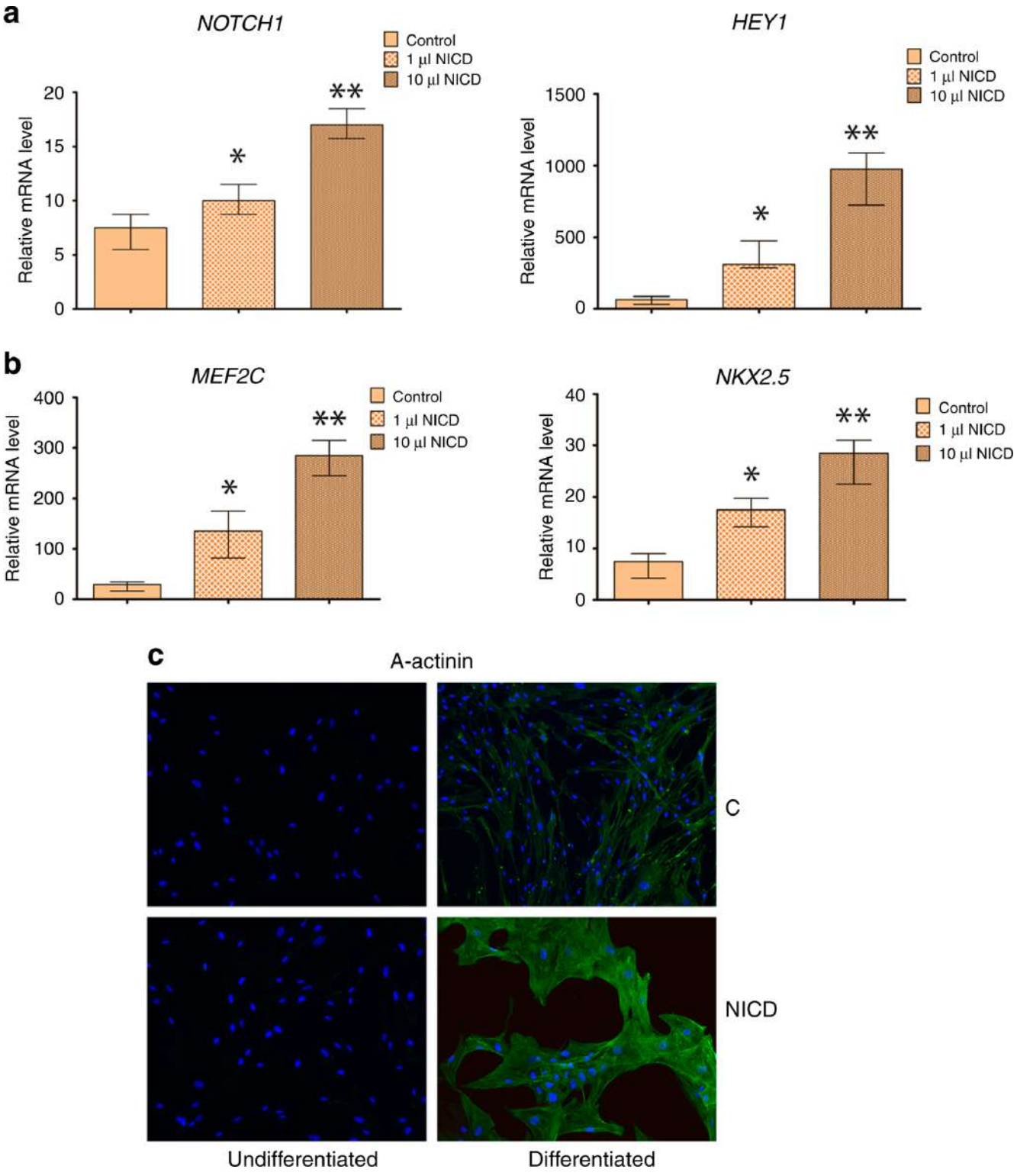

Figure 34. Notch Signaling Influences Cardiogenic Differentiation of TF-CMCh. **A.** Viruses carrying NICD were added to TF-CMCh (1 and 10 µL, respectively). Expression of *NOTCH1* and *HEY1* was confirmed using quantitative PCR. **B.** Cardiogenic differentiation was induced in five separate lines of TF-CMCh transduced with varying amounts of NICD-carrying viruses. Histograms represent the expression of *MEF2C* and *NKX2-5* using quantitative PCR on the 24th day after induction of cardiogenic differentiation. Error bars reflect the mean +/- SD for three replicates. *, ** $p < 0.05$ compared to control samples. **C.** Immunocytochemical staining of TF-CMCh for the cardiogenic marker α-actinin in the presence/absence of Notch activation using NICD (NICD and control, respectively) in undifferentiated

and differentiated cells. Experiments were conducted in triplicate [26].

Moreover, the introduction of NICD led to a dose-dependent increase in the expression levels of cardiogenic markers *MEF2C* and *NKX2-5* (**Figure 34b**), indicating the specific action of the intracellular domain of Notch. Transduced TF-CMCh exhibited more intense staining for the cardiac marker alpha-actinin after 24 days of cardiogenic differentiation (**Figure 34c**). The response of TF-CMCh from different patients to NICD vector introduction is presented in graphs (**Figure 35**).

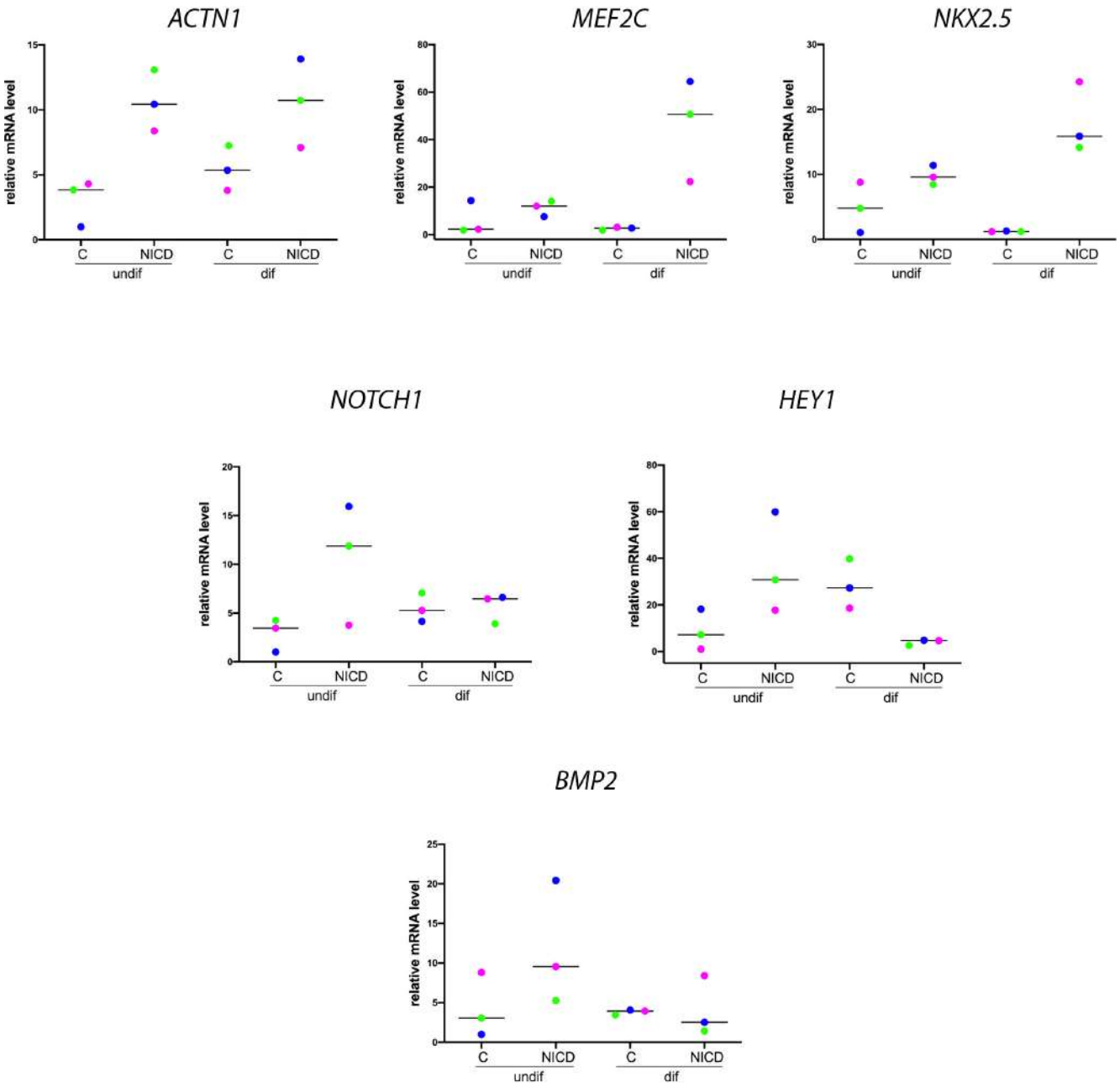

Figure 35. Notch Signaling Influences Cardiogenic Differentiation of TF-CMCh. Cells were treated with a vector carrying NICD. Gene expression was confirmed using quantitative PCR. Cardiogenic differentiation was induced in three lines of TF-CMCh. C - control, NICD – cells transduced with NICD virus. Each point represents the mean obtained by quantitative PCR and performed in duplicate for each

individual TF-CMCh line, indicated by a distinct color (blue, green, or purple). The horizontal line represents the median [26].

Thus, we established that Notch activation leads to an increase in the efficiency of TF-CMCh differentiation.

3.2.7 Hypoxic Stress Moderately Increases the Expression of Notch Signaling Components *in vitro*

Tetralogy of Fallot (TF) represents the most common cyanotic congenital heart defect. This pathology encompasses a broad spectrum of severity, ranging from pink TF without hypoxemia and nearly normal arterial saturation to highly cyanotic newborns with very low saturation levels. Over half of TF patients experience reduced saturation levels (hypoxemia). Hypoxia affects all tissues and organs in the body, including the brain and myocardial tissues. The role of Notch signaling in myocardial remodeling under hypoxic conditions remains unclear. We hypothesized that hypoxia itself could be a cause of increased expression of Notch signaling components in TF-derived cardiomyocyte-like cells (TF-CMCh). To confirm this, we cultured TF-CMCh from patients with Tetralogy of Fallot under hypoxic conditions using 1% and 5% O_2 levels, respectively, with culture under normoxic conditions (21% O_2) used as a control. Cultivating TF-CMCh under hypoxic conditions resulted in only a moderate increase in the transcription of *NOTCH1* and *HEY1*, as well as an elevation in *BMP2* transcription (**Figure 36a**).

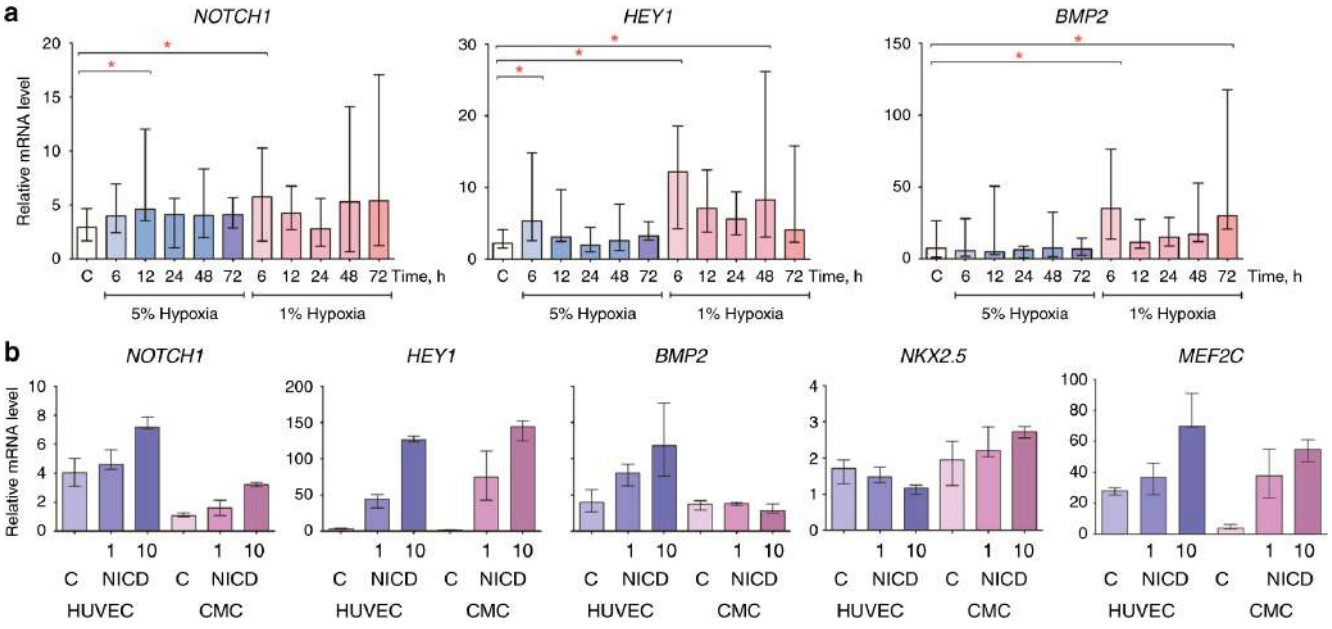

Figure 36. Hypoxic Stress Contributes to Increased Expression of Notch Signaling Pathway Components. **A.**VSD-CMCh were cultured under hypoxic conditions with 1% (1% Hypoxia) and 5% (5% Hypoxia) O_2 levels, respectively, and under normoxic conditions (21% O_2) as a control. Histograms represent the expression of *NOTCH1, HEY1*, and *BMP2* using quantitative PCR. Groups were compared using the Mann-Whitney non-parametric test; five VSD-CMCh lines were used in the experiment, repeated three times; *p <0.05. **B.** Analysis of Notch-activated genes in VSD-CMCh. Viruses carrying NICD (1 and 10 µl, respectively; Control C) were added to VSD-CMCh or HUVEC, used as a non-cardiogenic control. Histograms represent the corresponding gene expression 48 hours after viral transduction using quantitative PCR. Three separate VSD-CMCh lines were used in the experiment. Experiments were conducted in triplicate [26].

These data suggest that the hypoxic condition in TF patients may potentially contribute to the activation of the Notch signaling pathway in TF-CMCh. In our previous work [23] we reported a possible interaction between Notch and BMP2 in the context of MI-CMCr. To investigate whether the expression of BMP2, along with cardiac markers, depends on Notch activation in VSD-CMCh, we activated Notch in cells using lentiviruses carrying NICD. We observed a dose-dependent increase in *NOTCH1, HEY1, MEF2C*, and *NKX2.5*. HUVEC were used as a non-cardiogenic control. We also did not observe an increase in *BMP2* transcription with NICD in VSD-CMCh (**Figure 36**), suggesting that the activation mechanism of BMP2 in CMCs is independent of Notch activation.

3.2.8 Discussion of Notch Signaling Pathway Dysregulation in Cardiac Mesenchymal Cells from Tetralogy of Fallot Patients

Tetralogy of Fallot (TF) is the most common and severe cyanotic congenital cardiac defect, the cellular and molecular mechanisms of which are poorly understood. In this section of the work, the expression of Notch-dependent genes was assessed in cardiac mesenchymal cells of patients with TF (TF-CMCh). The gene expression pattern of TF-CMCh was compared with the genetic profile of CMCs obtained from patients with ventricular septal defect (VSD-CMCh). The expression of Notch genes varied significantly in TF-CMCh, but did not correlate with the age of the patients or with any clinical parameters. However, the study demonstrated that higher expression values of Notch signaling pathway genes contribute to the intensification of cell proliferation and differentiation.

Besides the 22q11 deletion, no other gene loci have been associated with TF [198]. Exome sequencing in sporadic nonsyndromic cases of TF has identified the *NOTCH1* gene locus as a frequent site for the emergence of genetic variants that predispose to the formation of this pathology. These studies frequently identified variants in *NOTCH1*, which occur in epidermal growth factor (EGF)-like functional repeats and are critical for ligand and receptor binding in Notch signaling [74, 199]. Gene variants associated with vascular endothelial growth factor signaling were found in patients with TF [74]. This

suggests that the pathogenesis of TF may be related to signaling pathways responsible for angiogenesis and endothelial function.

A study of cardiac tissue from patients with tetralogy of Fallot, both idiopathic and syndromic with 22q11.2 deletion, identified more than a thousand deregulated genes in right ventricular tissue [200]. Most of the genes associated with Wnt and Notch signaling had decreased expression. This pattern of gene expression, common to idiopathic and syndromic cases of TF, indicates that these episodes lead to the same pathological outcome despite different genetic origins. The findings indicate that the genetic profile of patients with TF tends to demonstrate an imbalance in the Notch signaling pathway rather than its complete suppression. This dysregulation may be responsible for the early abnormalities in cardiac patterning that characterize all cases of TF.

Heart formation is a complex process controlled by the precise spatiotemporal orchestration of multiple signaling pathways, among which Notch often interacts with other signaling such as Wnt and Bmp. Modern studies of the role of Notch signaling in cardiac development have confirmed its function as a signaling integrator in tissue patterning during outflow tract development, affecting cell proliferation, differentiation and apoptosis [56].

Studies using mice heterozygous for *Notch1* have found that such animals can appear phenotypically normal, without obvious cardiovascular problems [201]. However, when assessing the development of ascending aortic aneurysm in mice with the NOTCH1+/- genotype, especially on the 129S6 background, significant differences in aortic root dilatation were observed compared to mice with a mixed genetic background [202]. The results of the study demonstrate significant variability in the gene expression of Notch-dependent genes in TF-CMCh, which confirms the importance of the genetic background in the development of TF. However, the influence of a number of factors associated with the effects of *in vitro* cell culture, as well as the difference in the genotypes of patients with TF, may serve as a limitation of this study.

Hypoxia is one of the factors that manifests itself during the disease in patients with TF, affecting cardiac tissue, and may be involved in the modulation of the Notch signaling pathway [184]. Meanwhile, the results of a study on the induction of hypoxia *in vitro* showed only a slight increase in gene expression of signaling components Notch and Bmp2 pathways in CMCh. This indicates that changes in gene expression in cells from TF patients are likely due to their different genetic backgrounds rather than just the hypoxic condition.

Crosstalk between Notch and Bmp2 signaling has been demonstrated in early mouse heart development [195]. Under the influence of ectopic expression of the *Bmp2* gene in the cardiac muscle, the genetic profile of adjacent endocardial cells changes, ensuring the process of their epithelial-mesenchymal transition [195, 203]. This is of key importance for the formation of the correct cardiac

pattern and the development of the heart chambers. The results of the study showed altered expression levels of the Notch and Bmp2 signaling pathway components in TF-CMCh, which may reflect ongoing pathogenic processes that disrupt the cardiac pattern in patients with TF.

Some fractions of CMCh have been used in clinical trials aimed at improving single-ventricle heart function in patients with hypoplastic left heart syndrome [204]. These cells are considered as a potential source of multipotent cardiac cells [191, 192]. The results obtained demonstrated that higher expression levels of Notch signaling pathway components in TF-CMCh correspond to improved proliferation and differentiation abilities of these cells, which is consistent with literature data [197, 205, 206].

Recent studies emphasize the importance of the age factor when analyzing the stemness qualities of cardiac mesenchymal cells. At the same time, one of the latest studies found a decrease in the stemness of these cells in patients younger than one month and older than forty years. However, another study indicates that the differentiation potential of cells extracted from cardiospheres remains unchanged throughout the first year of life [191, 192]. In the context of TF, most patients undergo surgery at a very young age. This fact limited the ability of our study to fully examine how age influences the proliferative behavior of CMCh. Our analysis did not reveal any significant effect of age or clinical symptoms of TF on the proliferation of these cells.

A notable aspect of our study was the discrepancy between the gene expression profiles in the tissue samples and in the CMCh. This discrepancy creates problems when extrapolating results obtained from tissue samples to the subsets of cells that make up the mature heart. In doing so, our study is a pioneering study in which it is the first to directly compare the CMCh with heart tissue samples taken from the right atrium and right ventricle of the same patients. These comparisons have enriched our understanding of the biology of CMCh.

Despite significant advances in the surgical treatment of TF over the past four decades, which have led to improved survival rates (90% of patients now survive 30 years after surgery), these patients still face a lower life expectancy compared to the general population [207]. Postoperative complications such as pulmonary regurgitation, right ventricular dysfunction, recurrent right ventricular outflow obstruction, arrhythmias, sudden death and aortic dilatation remain common [208]. This raises critical questions about the long-term impact of genetic factors, including potential Notch gene dysregulation, in patients with TF even after surgical correction.

Our study of the transcriptional profiles of TF patients revealed specific dysregulation of Notch signaling rather than its general suppression (**Figure 37**). This pattern may play an important role in initiating early developmental processes in the heart, which is common in all cases of TF. We have previously reported similar dysregulation of the Notch gene in various cardiac diseases, such as thoracic aortic aneurysm, bicuspid aortic valve, and aortic valve calcification, independent of mutations in the

NOTCH1 gene [209-211]. These data suggest that such disorders are associated with a wide range of cardiac pathologies [170].

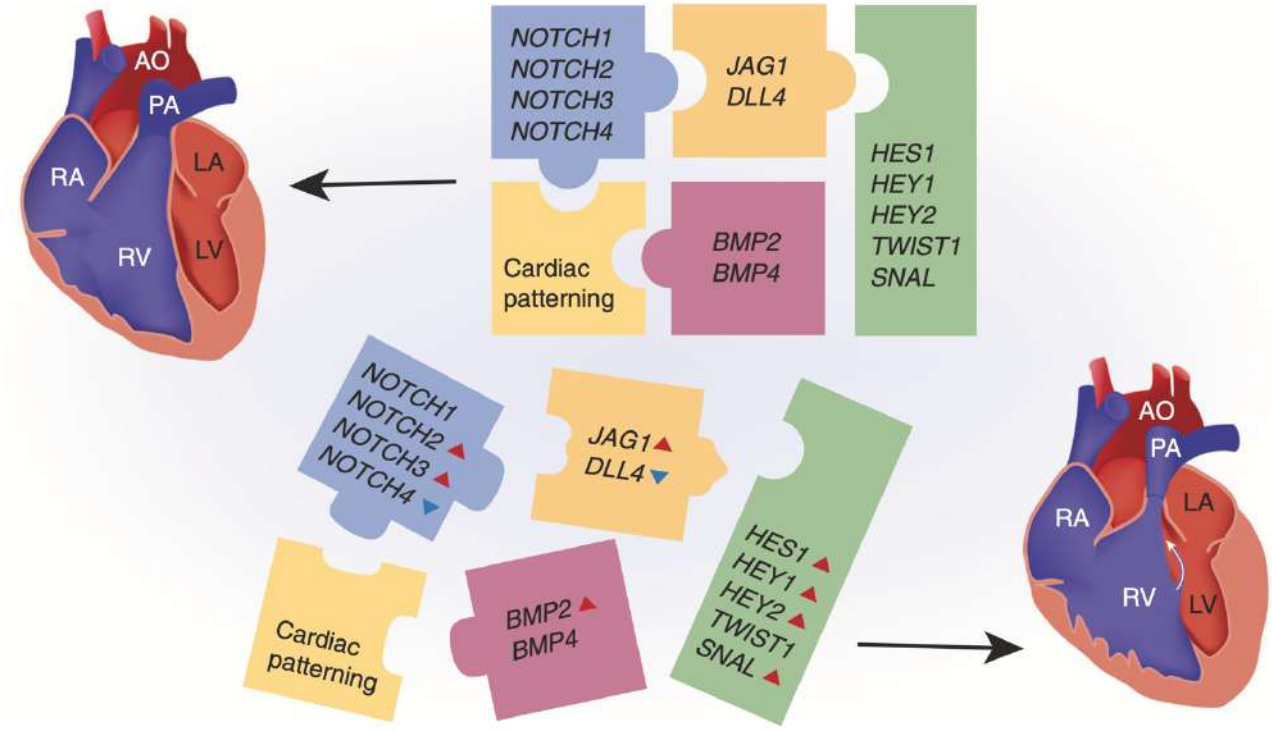

Figure 37. Notch signaling in the pathogenesis of the Tetralogy of Fallot represents a puzzle interacting with many components. If we put all its components together, the result will be a structurally and functionally normal heart, but if one or several details fall out, it will be impossible to get a complete picture. Coordinated action of Notch genes is a very important component of this puzzle [212].

One of the significant limitations of our study is the lack of data on cells obtained from normal myocardium in young patients. Obtaining age-appropriate control samples, especially in children after corrective surgery, poses a major challenge. In addition, our study lacks direct sequencing data for *NOTCH1*, leaving open the possibility of distinct genetic variants in our patient cohort. However, the main syndromic forms were excluded from the study. Therefore, further studies are needed to better understand the role of various factors involved in the pathogenesis of TF and the biology of CMCh. The results of this study may have vital implications for the development of future cell therapy strategies for heart disease.

3.3 Interaction between BMP2 and the Notch Signaling Pathway in Endothelial-Mesenchymal Transition in the Context of Myocardial Fibrosis

The group led by José Luis de la Pompa previously demonstrated [213, 214], that there is an interaction between the Notch signaling pathway and Bmp2 in the formation of heart valves in mice, with Snail1 acting as a common tissue-specific target of these pathways. In the developing heart, they were antagonistic to each other, and proper regulation of target gene expression ensured appropriate organ formation through a specific developmental pattern [215]. The Notch signaling pathway inhibits fibrosis during myocardial infarction in rats by preventing the transformation of cardiac fibroblasts into myofibroblasts through the suppression of TGF-β1/Smad3 signaling [216], a key regulator of endothelial-mesenchymal transition (EndoMT). The balance between Notch and Bmp2 signaling determines the fate of fibroblasts, and the progression of EndoMT and fibrosis in the heart.

We hypothesize that the specific contribution of cardiac mesenchymal cells (CMC) to the development of heart fibrosis in the context of EndoMT regulation is mediated by the interaction between the Notch and Bmp2 signaling pathways. Activation of these pathways in CMC leads to the regulation of common downstream targets, resulting in the modulation of EndoMT markers and subsequent fibrotic processes in the heart. In this section, evidence was obtained indicating a link between the Notch signaling pathway and Bmp2 in the regulation of EndoMT through a potential SLUG-dependent mechanism (*SNAI2*) in human CMC. Co-culturing CMC and human umbilical vein endothelial cells (HUVECs) in two different combinations led to opposite cellular responses regarding the expression of target genes and the synthesis of α-smooth muscle actin (α-SMA). Our results show that BMP2 and Notch activation is tissue-specific and highly dependent on the type of cells used.

3.3.1 Activation of BMP2 and Notch Signaling Pathways Modulates Target Gene Expression in CMCh and HUVECs

To assess the impact of activating Notch and BMP2 signaling on target gene expression, both CMCh and HUVECs were transduced with a lentiviral vector carrying either NICD (the active form of the NOTCH1 sequence) or BMP2. After 48 hours, total RNA was extracted for RT-PCR analysis. A 'blank' vector as a transduction control (TRC), lacking gene inserts, was used to evaluate the effect of cellular transduction. Additionally, cells without any induction served as a negative control.

It was noted that NICD activation led to increased expression of the Notch target gene *HEY1* and the *NOTCH1* receptor in both cell cultures (**Figure 38**), indicating successful cellular transduction with the NICD lentiviral vector. However, only HUVECs showed an increase in *BMP2* expression in response

to NICD vector introduction, while *BMP2* expression in CMCh remained unchanged. Furthermore, *RUNX2* was also suppressed in CMCh.

Upon the addition of the BMP2 lentiviral vector to the cell cultures, an increase in *BMP2* expression was observed in both cell types, thus confirming the effectiveness of this vector (**Figure 37**). Moreover, BMP2 induction led to the activation of *HEY1* in CMCh.

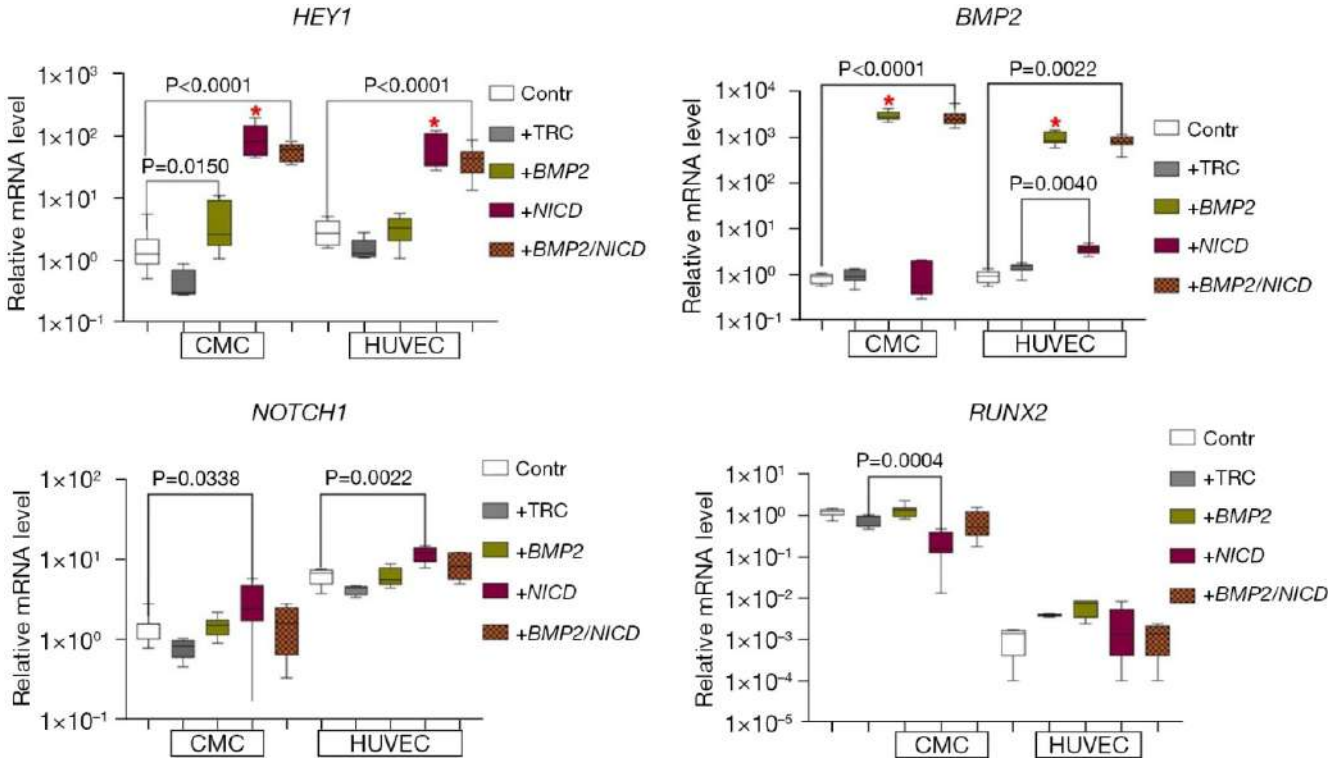

Figure 38. Exogenous activation of the Notch and Bmp2 signaling pathways using lentiviral constructs carrying NICD and/or BMP2 sequences led to an increase in the expression of components of these signaling pathways. Cells without induction were used as a negative control, and the lentivirus with TRC was the vector that did not carry any gene inserts. The y-axis represents the relative amount of mRNA in each group, measured using the $2^{-\Delta\Delta Ct}$ method; box plots with whiskers from minimum to maximum are presented. P-values and brackets indicate statistically significant differences between groups at $P<0.05$ (Mann-Whitney U non-parametric test). A red asterisk further denotes groups that have a statistically significant difference compared to the control and TRC. All comparisons are presented in **Figure 40**. The experiment was repeated three times. CMC, human cardiac mesenchymal cells; HUVEC, human umbilical vein endothelial cells; TRC, transduction control; BMP2, bone morphogenetic protein 2; NICD, intracellular domain of NOTCH1 [25].

To investigate the potential interaction between Notch and BMP2 signaling pathways, CMCh and HUVEC cultures were co-transduced with lentiviral vectors carrying NICD and BMP2 sequences, respectively. The BMP2 vector was introduced first, followed by NICD after 18 hours (+BMP2/NICD, **Figure 38**). The results showed that double transduction did not enhance the expression of the target gene compared to the induction of a single signaling pathway.

3.3.2 Activation of Notch and BMP2 Induces Elevated Synthesis of α-SMA in Cells, Except for HUVECs in Response to BMP2 Gene Induction

To assess the impact of the Notch and BMP2 signaling pathways on the expression of EndoMT markers, human cardiac mesenchymal cells (CMCh) and HUVECs were transduced with a lentiviral vector carrying either NICD or BMP2 sequences, respectively. Upon Notch induction (**Figure 39A**), active transcription of *SNAI2* (SLUG) was observed in both cell types, unlike *SNAI1*, which was overexpressed only in response to BMP2 induction in CMCh. Additionally, the expression of *SNAI2* in HUVECs increased to a level comparable to the baseline expression observed in control mesenchymal cells. However, double transduction of CMCh and HUVECs with BMP2 and NICD did not increase the expression level of EndoMT marker genes (+BMP2/NICD, **Figure 39A**).

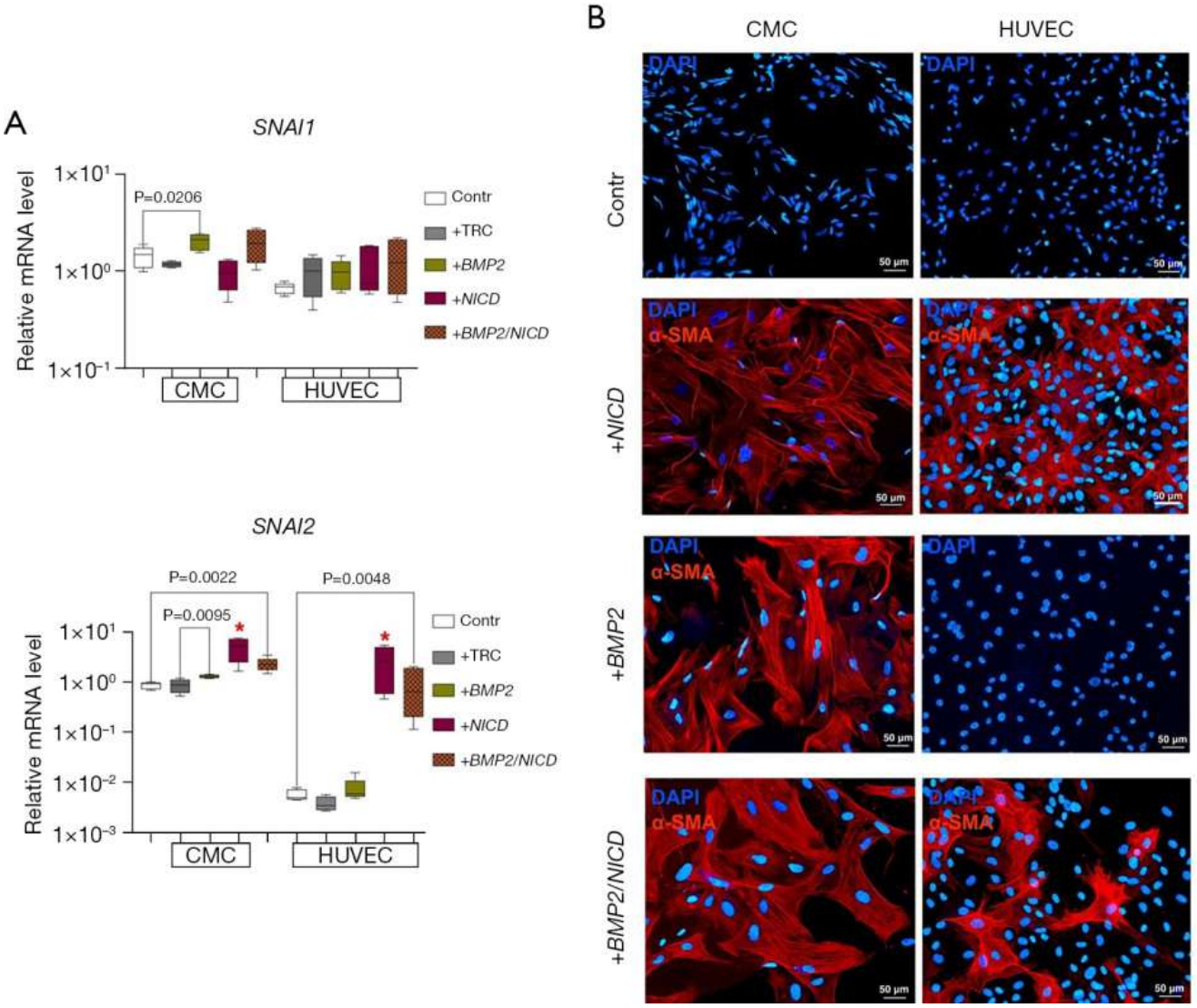

Figure 39. Activation of the Notch and BMP2 signaling pathways in response to the introduction of lentiviral constructs carrying NICD and/or BMP2 sequences facilitated increased synthesis of α-SMA in both cultures, except for HUVECs in response to BMP2 induction. **(A)** Dynamics of *SNAI1* and *SNAI2* expression (markers of endothelial-mesenchymal transition, EndoMT) in CMCh and HUVEC cultures

in response to transduction with lentiviral constructs carrying NICD and/or BMP2 sequences. Cells without induction were used as a negative control, and the TRC virus was a vector that did not carry any gene inserts. The y-axis represents the relative amount of mRNA in each group, measured using the $2^{-\Delta\Delta Ct}$ method; box plots with whiskers from minimum to maximum are presented. P-values and brackets indicate statistically significant differences between groups at $P<0.05$ (Mann-Whitney U non-parametric test). A red asterisk additionally denotes groups that have a statistically significant difference compared to the control and TRC. All comparisons are presented in **Figure 40**. **(B)** Immunophenotyping of CMCh and HUVECs for the EndoMT marker α-SMA in response to induction of the Notch and/or BMP2 signaling pathways. The experiment was repeated three times. CMCh, human cardiac mesenchymal cells; HUVECs, human umbilical vein endothelial cells; TRC, transduction control; BMP2, bone morphogenetic protein 2; NICD, intracellular domain of NOTCH1; α-SMA, α-smooth muscle actin; EndoMT, endothelial-mesenchymal transition; DAPI, 4',6-diamidino-2-phenylindole [25].

α-SMA is an important marker of EndoMT in both endothelial and mesenchymal cells, which are activated during development or injury [217-220]. To evaluate EndoMT activation in CMCh and HUVEC cultures in response to the induction of the Notch and BMP2 signaling pathways, immunostaining for α-SMA was conducted. Both CMCh and HUVECs did not synthesize α-SMA in the uninduced control (**Figure 39B**). Notch activation led to the accumulation of α-SMA in both CMCh and HUVECs (**Figure 39B**). Nevertheless, transduction of cell cultures with BMP2 lentivirus facilitated α-SMA synthesis only in CMCh, corresponding to the expression levels of *SNAI1* and *SNAI2* demonstrated by RT-PCR. As a result of adding both vectors, EndoMT activation was observed in both CMCh and HUVECs (**Figure 39B**). However, α-SMA synthesis was less pronounced in HUVECs compared to CMCh.

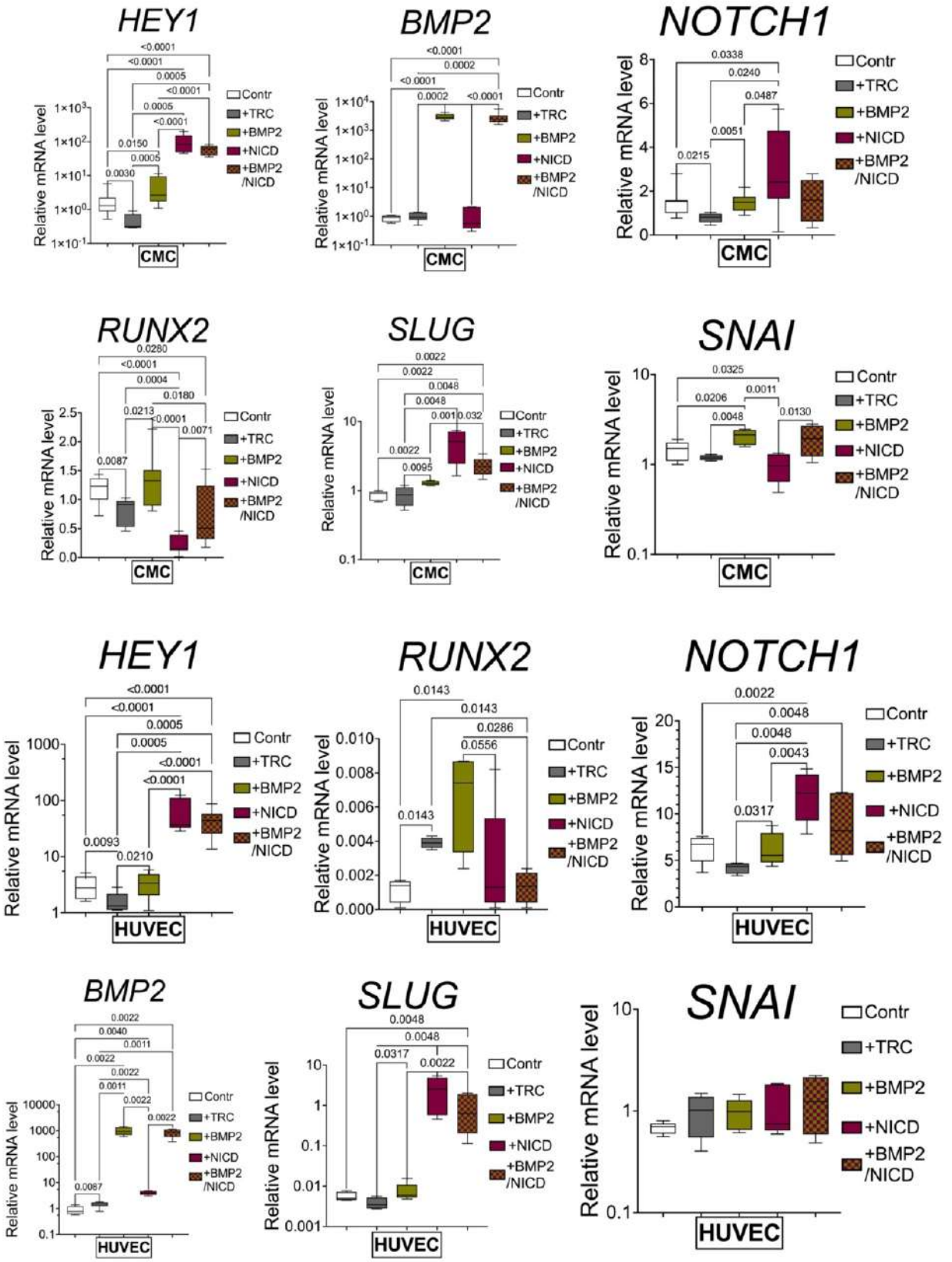

Figure 40. Exogenous activation of the Notch and Bmp2 signaling pathways by introducing lentiviral constructs carrying NICD and/or BMP2 sequences led to an increase in the expression of pathway components. Cells without induction were used as a negative control, and the TRC virus was a vector that did not carry any gene inserts. The Y-axis represents the relative amount of mRNA in each

group, measured using the $2^{-\Delta\Delta Ct}$ method; box plots with whiskers from minimum to maximum are presented. P-values (numbers) and brackets indicate significant differences between groups at $P<0.05$ (Mann-Whitney U non-parametric test). The experiment was repeated three times. CMCh, human cardiac mesenchymal cells; HUVECs, human umbilical vein endothelial cells; Contr, control; TRC, 'empty' vector; BMP2, bone morphogenetic protein 2; NICD, intracellular domain of NOTCH1 [25].

3.3.3 Co-Culturing CMCh and HUVECs Alters Target Gene Expression, Influencing the Activation of *HEY1* and *BMP2* Genes in Double Transduction of CMCh/HUVEC Cultures

Considering that the Notch signaling pathway is known to mediate intercellular communication, the influence of co-culturing mesenchymal and endothelial cells on the expression of the Notch and BMP2 signaling pathways was investigated. Upon the addition of the NICD lentiviral vector, increased expression of *HEY1* was observed in both types of co-cultures. Nevertheless, the expression of *NOTCH1* increased only in the HUVEC/CMCh co-culture. Similarly, transduction of cell cultures with the BMP2 vector led to the activation of *BMP2* in both co-cultures, confirming the effectiveness of the vectors in co-culturing conditions.

Our findings (**Figure 41**) demonstrate variability in the expression profile in cell cultures, which appears to be influenced by the order of cell seeding. Particularly, a decrease in target gene expression was observed compared to conditions of monoculture. However, a stimulating effect on the expression of *HEY1* and *BMP2* was noted in response to dual transduction, especially in the CMC/HUVEC combination (+BMP2/NICD, **Figure 41**).

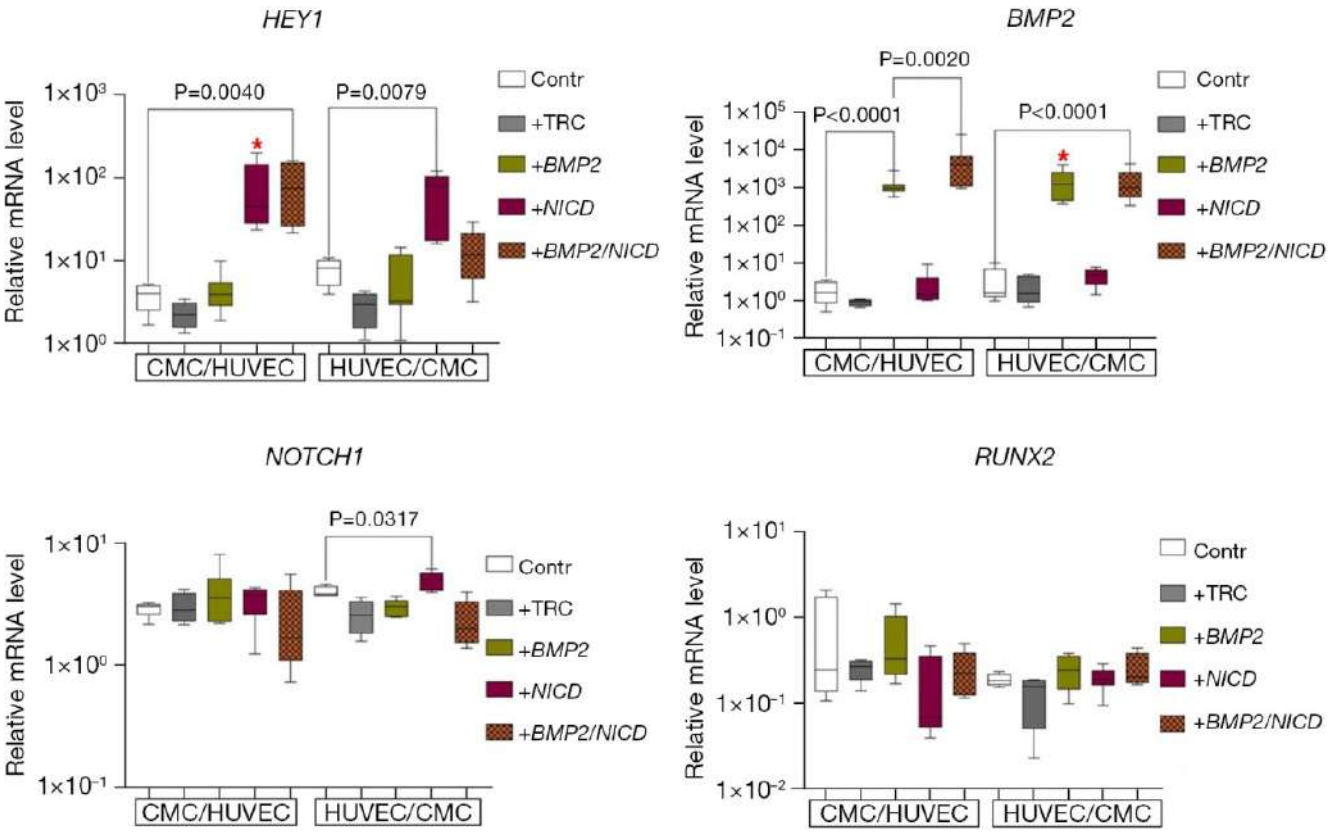

Figure 41. Activation of the Notch and BMP2 signaling pathways in co-cultured CMCh and HUVECs in response to the introduction of lentiviral constructs carrying NICD and/or BMP2 sequences led to a decrease in the expression of target genes compared to their activation in monocultures. Cells without induction were used as a negative control, and the TRC virus was a vector that did not carry any gene inserts. The y-axis represents the relative amount of mRNA in each group, measured using the $2^{-\Delta\Delta Ct}$ method; box plots with whiskers from minimum to maximum are presented. P-values and brackets indicate statistically significant differences between groups at $P<0.05$ (Mann-Whitney U non-parametric test). A red asterisk further denotes groups that have a statistically significant difference compared to the control and TRC. All comparisons are presented in **Figure 43**. The experiment was repeated three times. CMCh, human cardiac mesenchymal cells; HUVECs, human umbilical vein endothelial cells; TRC, transduction control; BMP2, bone morphogenetic protein 2; NICD, intracellular domain of NOTCH1 [25].

3.3.4 Induction of α-SMA Synthesis in CMCh is Modulated by BMP2 and BMP2/NICD Activation During Co-Culturing, Correlating with *SNAI2* Expression

To assess the influence of co-culturing CMCh and HUVECs on α-SMA synthesis in response to the induction of the Notch and BMP2 signaling pathways, immunophenotyping of cell co-cultures for α-SMA was conducted. The obtained results (**Figure 42**) show that activation of the Notch signaling pathway induces α-SMA synthesis in both CMC/HUVEC and HUVEC/CMC co-cultures, regardless of

the seeding order. Double transduction of the CMC/HUVEC co-culture led to an increase in *BMP2* expression (+BMP2/NICD, **Figure 41**) and, conversely, to the suppression of EndoMT markers (+BMP2/NICD, **Figure 42A**). This was also reflected in the suppression of α-SMA accumulation in the presence of a single BMP2 vector, or two vectors BMP2 and NICD (+BMP2/NICD, **Figure 42B**).

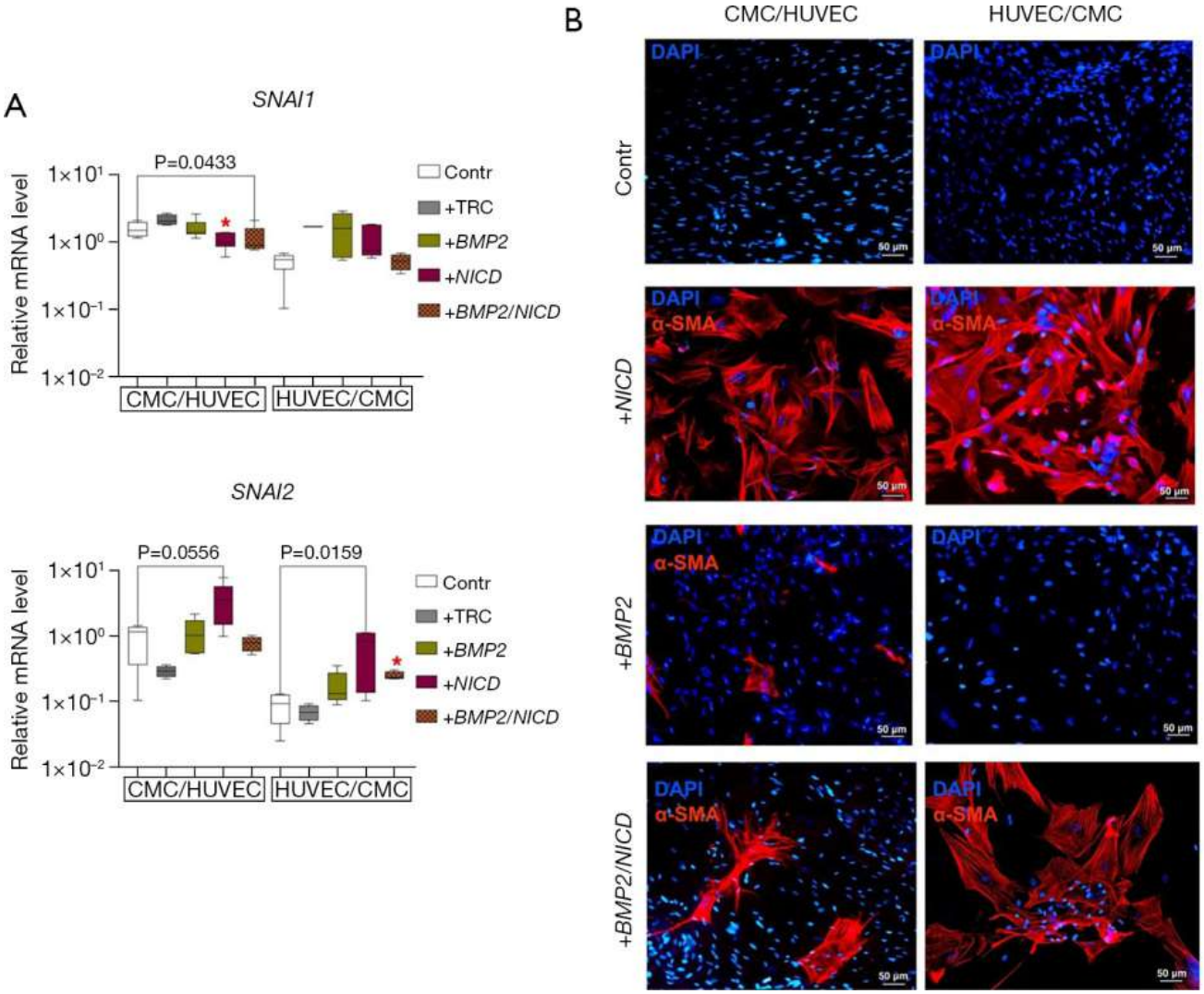

Figure 42. Synthesis of α-SMA in CMC Decreases in Response to BMP2 and BMP2/NICD Activation During Co-Culturing. (A) Dynamics of *SNAI1* and *SNAI2* expression (markers of endothelial-mesenchymal transition, EndoMT) in CMC and HUVEC cultures in response to transduction with lentiviral constructs carrying NICD and/or BMP2 sequences. Cells without induction were used as a negative control, and the TRC virus was a vector that did not carry any gene inserts. The y-axis represents the relative amount of mRNA in each group, measured using the $2^{-\Delta\Delta Ct}$ method; box plots with whiskers from minimum to maximum are presented. P-values and brackets indicate statistically significant differences between groups at $P<0.05$ (Mann-Whitney U non-parametric test). A red asterisk additionally denotes groups that have a statistically significant difference compared to the control and TRC. All comparisons are presented in **Figure 43**. **(B)** Immunophenotyping of CMC and HUVECs for the EndoMT marker α-SMA upon induction of Notch and/or BMP2 signaling pathways. The experiment was repeated three times. CMC, human cardiac mesenchymal cells; HUVECs, human umbilical vein endothelial cells; TRC, transduction control; BMP2, bone morphogenetic protein 2; NICD, intracellular domain of NOTCH1; α-SMA, α-smooth muscle actin; EndoMT, endothelial-mesenchymal transition; DAPI, 4',6-diamidino-2-phenylindole [25].

Transduction of cell cultures with BMP2 lentivirus had an inhibitory effect on α-SMA accumulation in mesenchymal cells and this was also accompanied by a decrease in *SNAI2* expression when co-cultured with endothelial cells. Activation of the Notch and BMP2 signaling pathways led to the induction of EndoMT in HUVEC/CMC co-cultures (+BMP2/NICD, **Figure 42B**), correlating with the accumulation of *SNAI2* (+BMP2/NICD, **Figure 42A**). Conversely, we observed that *SNAI1* expression was suppressed in response to Notch induction and double transduction in CMC/HUVEC co-culture.

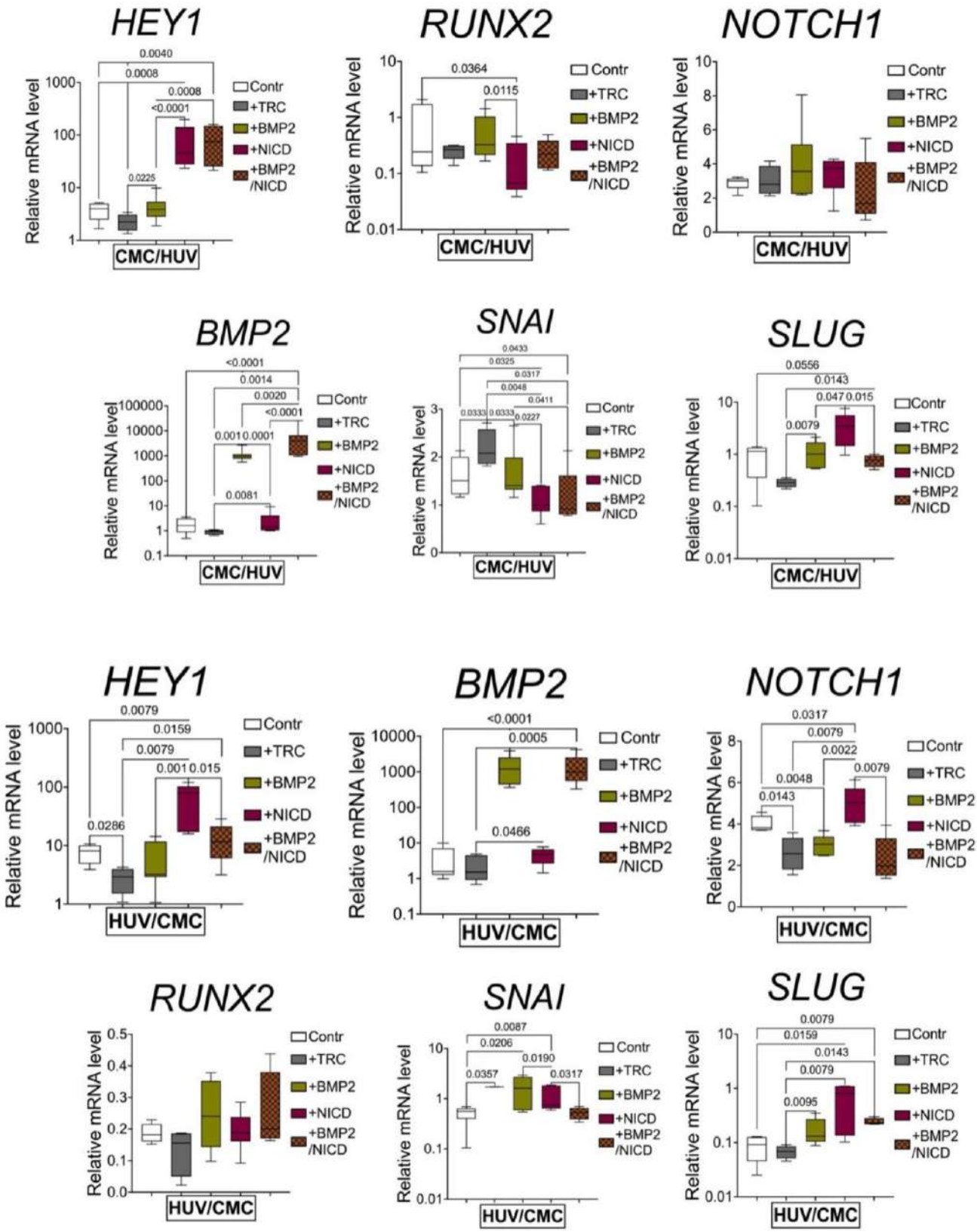

Figure 43. Activation of the Notch and BMP2 signaling pathways through co-culturing of CMC and HUVECs in response to the introduction of lentiviral constructs carrying NICD and/or BMP2 sequences led to a decrease in the expression of target genes compared to monocultures. Cells without induction were used as a negative control, and the TRC virus was a vector that did not carry any gene inserts. The y-axis represents the relative amount of mRNA in each group, measured using the $2^{-\Delta\Delta Ct}$ method; box

plots with whiskers from minimum to maximum are presented. P-values (numbers) and brackets indicate significant differences between groups at $P<0.05$ (Mann-Whitney U non-parametric test). The experiment was repeated three times. CMC, human cardiac mesenchymal cells; HUVECs, human umbilical vein endothelial cells; Contr, control; TRC, 'empty' vector; BMP2, bone morphogenetic protein 2; NICD, intracellular domain of NOTCH1 [25].

3.3.5 Discussion of Results on the Interaction between BMP2 and the Notch Signaling Pathway in Endothelial-Mesenchymal Transition

EndoMT is a critical process associated with the development and disorders of the cardiovascular system [221]. Although embryonic signaling pathways such as Notch and Bmp are known to regulate EndoMT, their interactions in this process are not yet fully understood. Consequently, determining how these pathways are regulated is a priority for treating cardiovascular pathologies in adulthood.

For this purpose, the Notch and Bmp pathways (specifically, BMP2) were induced in human cardiac mesenchymal cells (CMCh) and human umbilical vein endothelial cells (HUVECs) using various combinations. The cells were transduced with vectors carrying NICD and/or BMP2, and after 48 hours, RNA was extracted for RT-PCR to assess the expression of Notch and Bmp pathway components and the activation of EndoMT markers. Immunocytochemical staining for α-SMA was used to determine EndoMT 14 days post-induction.

The Notch signaling pathway involves receptors (e.g., NOTCH1), ligands, and target genes (e.g., HEY1). In the canonical Notch signaling pathway, the receptor and ligand of two adjacent cells interact, leading to the proteolytic cleavage of the intracellular part of the receptor and translocation of NICD to the nucleus to activate target gene expression. The Notch pathway was induced in CMC and HUVECs using a lentiviral vector carrying the NICD sequence. Upon activation, both cultures showed an increase in the expression of *HEY1* and *NOTCH1* receptors. Moreover, transduction of cell cultures with NICD led to the synthesis and subsequent accumulation of α-SMA in both CMCh and HUVECs 14 days post-induction. It was found that Notch pathway activation using NICD increases *BMP2* expression in HUVECs but does not affect CMCh. A decrease in the expression of *RUNX2*, one of the Bmp target genes [222, 223], was also observed in CMCh, indicating two opposing processes in endothelial and mesenchymal cells.

BMP2 is a growth factor and a component of the TGF-β superfamily, playing a role in many developmental processes, including cardiogenesis, neurogenesis, and osteogenesis [153-155]. BMP2 has also been noted in epithelial-mesenchymal transition (EMT) processes during development [224, 225]. It has been shown that the Notch signaling pathway regulates BMP2 during osteogenic differentiation [226]. However, its precise regulation in the context of EndoMT and its interaction with other embryonic

signaling pathways, including Notch, are still not fully understood. Transduction of cell cultures with a BMP2 vector successfully regulates *BMP2* expression in human cardiac mesenchymal cells (CMCh) and human umbilical vein endothelial cells (HUVECs). It was found that BMP2 induction in CMCh led to an increase in the expression of *HEY1* (a Notch target gene) and had no effect on the expression of *NOTCH1*, suggesting an interaction only with downstream targets. Meanwhile, *BMP2* activation in HUVECs did not affect the expression of Notch pathway components. Additionally, the addition of BMP2 had an inducing effect, particularly on CMCh, leading to the synthesis and accumulation of α-SMA. However, unlike CMCh, HUVECs did not respond to *BMP2* activation, indicating a potential tissue-specific effect of this signaling pathway.

During EMT in the heart, endocardial cells undergo significant changes in gene expression, including Notch-dependent induction of *ACTA2* (α-SMA), *SNAI1*, and *SNAI2* [132]. Despite differences in *BMP2* activation (**Figure 38**), an increase in *SNAI2* expression was observed in both cultures following the addition of NICD (**Figure 39A**). However, this did not affect the expression of *SNAI1* (**Figure 39A**).

Transduction with a BMP2 vector led to an increase in *BMP2* expression in both cultures, but the expression of EndoMT markers differed between CMCh and HUVECs. While *SNAI2* was activated in both cultures, only CMCh expressed *SNAI1*. Coordinated activity of the Notch and BMP2 signaling pathways has been previously noted in the developmental processes of the cardiovascular system [214]. Ectopic expression of one signaling pathway often led to suppression of another signaling system in the same tissue. However, coordinated signaling has been described, for example, between the myocardium and endocardium, and during heart valve formation with the activation of *SNAI1* influencing EMT processes [227].

Alternating activation of the Notch and Bmp pathways in CMCh and HUVECs was achieved by introducing a BMP2 vector, followed by the addition of NICD after 18 hours. It was noted that double transduction did not increase the expression of signaling pathway markers and EndoMT in both cultures compared to single induction and, most likely, reduces the effectiveness of their expression. Interestingly, in examining the impact of double transduction, no significant influence on α-SMA accumulation in CMCh was observed. α-SMA levels were comparable to those noted with single induction, indicating that double transduction also led to α-SMA synthesis. Nevertheless, the effect was less pronounced in HUVECs, suggesting that these signaling pathways may have opposite effects in this cell type.

According to the hypothesis, the interaction between the Notch signaling pathway and BMP2 may change during co-culturing of mesenchymal and endothelial cells. CMCh and HUVECs were seeded alternately, with a 24-hour difference, in two opposite combinations. An assessment of the expression of Notch, BMP2, and EndoMT genes in response to induction showed a decrease in target gene expression

compared to monocultures. Despite using the same cell cultures but seeded in different combinations, distinctly pronounced cellular responses were observed in the form of *HEY1* and *NOTCH1* expression in response to the introduction of NICD and BMP2. In the CMC/HUVEC combination, there was a consecutive increase in *HEY1* expression with the addition of NICD and BMP2/NICD. However, in the HUVEC/CMC combination, only the introduction of the NICD vector led to the activation of *HEY1*. The observed discrepancy implies a potential influence of seeding order on intercellular communication, potentially affected by the initial predominance of the HUVEC culture in the culture dish. Additionally, *NOTCH1* activation was noted in the HUVEC/CMC combination in response to NOTCH induction, reinforcing the notion of a tissue-specific response. These results suggest a potential influence of cell type interaction and seeding order on the modulation of marker expression and signaling pathways.

A reduction in the expression of EndoMT markers such as *SNAI1* and *SNAI2* in the CMC/HUVEC co-culture compared to the CMCh monoculture in response to BMP2 induction was noted, confirmed by the absence of α-SMA synthesis in immunocytochemical staining. This could mean that adding the HUVEC culture, which previously did not synthesize α-SMA in monoculture, hindered the marker's manifestation in the CMCh culture. At the same time, double transduction led to a significant increase in *BMP2* expression in the CMC/HUVEC co-culture compared to single induction, suggesting an additional effect when both factors are present in the co-culture. Conversely, in the HUVEC/CMC co-culture, double transduction positively influenced α-SMA accumulation and increased *SNAI2* expression. Throughout the experiment, it was repeatedly observed that *SNAI2* expression directly correlates with α-SMA synthesis in cultures in response to activation of Notch or BMP2.

BMP2, like Notch, plays a crucial role in altering the expression of EndoMT marker genes and components of Notch and Bmp signaling pathways and appears to contribute to Notch deregulation, possibly through a Slug-dependent mechanism (*SNAI2*). Nonetheless, the results obtained showed that in both CMCh and HUVECs, there is a relationship that changes during co-culturing, leading to the formation of antagonistic effects in gene expression, which are comparable when choosing cell fate between developing tissues.

The opposing cellular responses observed in co-cultured CMCh and HUVECs in various combinations can be attributed to complex interactions between cell types and the involved signaling mechanisms (**Figure 44**). In one study, where endothelial cells were co-cultured with mesenchymal stem cells (MSCs), it was found that endothelial cells induce the differentiation of smooth muscle cells (SMCs) in MSCs [228]. This induction of SMCs was mediated by the Notch signaling pathway and was independent of the growth factor signaling pathway. On the other hand, where endothelial cells were co-cultured with bone marrow stem cells (BMSCs), there was an induction of both osteogenesis and angiogenesis [229]. The co-cultured cells demonstrated increased expression of osteogenic genes,

indicating the supportive role of endothelial cells in facilitating both bone formation and blood vessel formation. These results suggest that the specific combination of cell types and their microenvironment can influence cellular response and fate determination, highlighting the importance of interactions between different types of cells depending on the context.

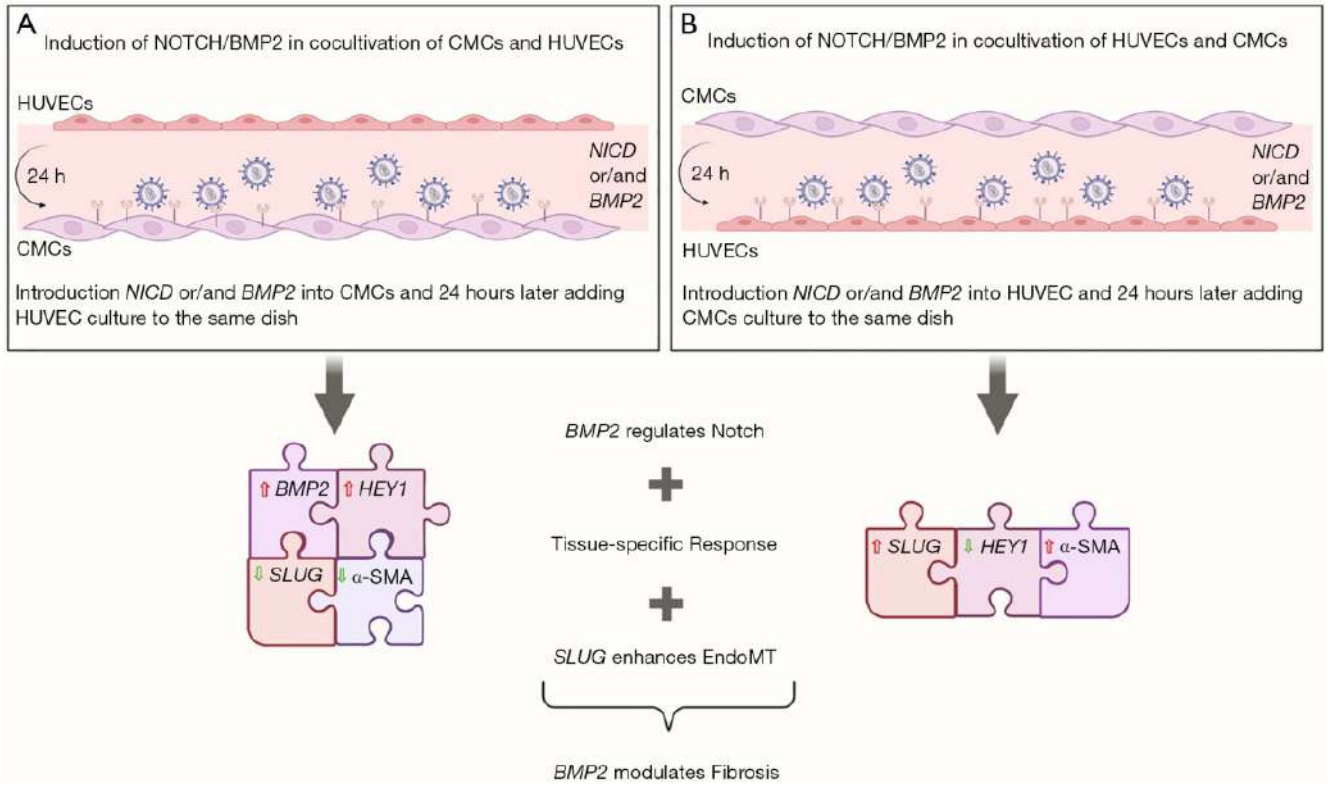

Figure 44. A schematic demonstrating the influence of activating Notch and BMP2 signaling pathways on altering cellular effects depending on the method of co-culturing CMCh and HUVECs. BMP2, bone morphogenetic protein 2; CMCh, human cardiac mesenchymal cells; HUVECs, human umbilical vein endothelial cells; NICD, intracellular domain of NOTCH1 [25].

Although markers of endothelial-mesenchymal transition (EndoMT) such as the expression of various genes and the accumulation of α-SMA were noted in the cell cultures, a broader spectrum of markers was not considered. This would allow for an expansion of the study, for example, by assessing endothelial markers like vascular endothelial cadherin, endothelial nitric oxide synthase (eNOS), and/or CD31; and mesenchymal-specific markers such as N-cadherin, FSP-1, vimentin, and/or fibronectin.

CONCLUSION

Restoring the contractile function of the heart and regenerating the myocardium after ischemic damage remain significant challenges in regenerative medicine and cellular biology. Traditional treatments, such as drug therapy and revascularization, only alleviate symptoms without contributing to full recovery from developing heart failure. The discovery and experimental use of human cardiac mesenchymal cells have marked a new phase in cardiovascular regenerative medicine, with clinical trials using these cells and their products raising hope for new heart failure therapies (**Figure 45**).

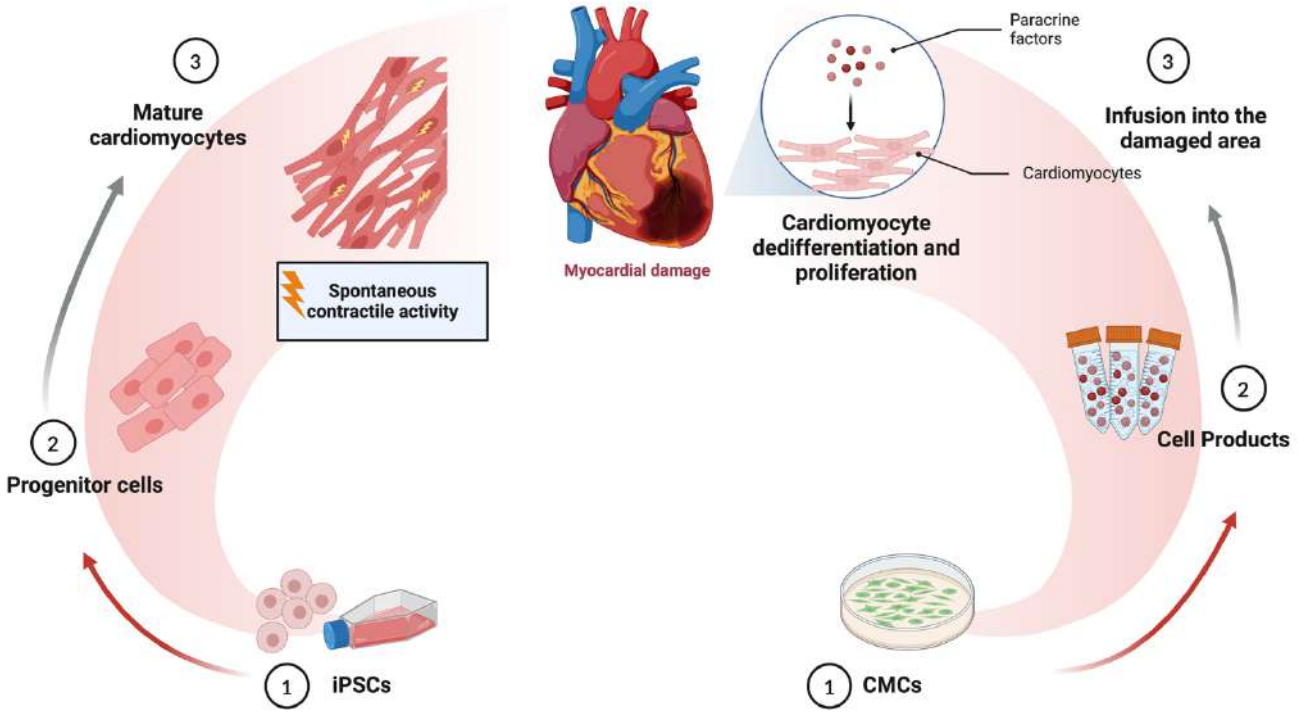

Figure 45. Possible approaches to myocardial regenerative therapy [29].

This study's results demonstrated that acute hypoxic stress could cause a temporary activation of embryonic signaling pathways Notch and Bmp in cardiac mesenchymal cells, and this interaction is closely related to early myocardial remodeling processes after a heart attack. The ability to accurately modulate and control the corresponding signals in the heart could enhance the regenerative capacity of the myocardium before the formation of fibrotic conditions.

Our research highlights the importance of the level of Notch activation in CMCh from patients diagnosed with Tetralogy of Fallot. The complex genetic background may be associated with Notch

signaling as a very sensitive and fine-tuned regulatory component of tissue integrity. Consequently, disruption in the regulation of gene expression related to Notch causes breakdown of the complex and balanced regulatory mechanism, potentially leading to developmental defects not necessarily related to mutations in Notch-associated genes.

Based on the objectives of our research, the following conclusions were made:

1. Myocardial infarction leads to significant changes in gene transcription patterns in post-infarct tissues 24 hours after acute infarction, promoting the activation of *Bmp2/Runx2* and Notch signaling components.
2. Myocardial infarction stimulates populations of resident cardiac mesenchymal cells in the injury zone, enhancing their *in vitro* capacity for proliferation, migration, and differentiation.
3. The transcriptional profile of post-infarct cardiac mesenchymal cells differs from healthy cells in the expression of Notch pathway components (*Jag1, Hes1*) and *Bmp2/Runx2*.
4. *In vitro* hypoxia activates Notch and BMP2 signaling pathways in human and rat cardiac mesenchymal cells.
5. Notch activation in rat and human cardiac mesenchymal cells leads to a dose-dependent change in the expression of Notch pathway components and does not affect *BMP2* expression.
6. The levels of Notch pathway activation influence the proliferation and differentiation processes in human cardiac mesenchymal cells, with dose-dependent Notch activation enhancing their cardiogenic differentiation capacity.
7. Alternating activation of Notch and *BMP2* affects the expression of endothelial-mesenchymal transition marker genes and the synthesis of alpha-actin, promoting the activation of human cardiac mesenchymal cells.

LIST OF ABBREVIATIONS

AVC - Atrioventricular Canal

Bmp2 - Bone Morphogenetic Protein 2

BSA - Bovine Serum Albumin

CI - Cell Index

CSL - CBF1-Suppressor of Hairless-LAG1 (Transcription Factor Responsible for Activating Notch Genes)

DAPI - 4',6-Diamidino-2-Phenylindole

DMEM - Dulbecco's Modified Eagle Medium

DNA - Deoxyribonucleic Acid

DMSO - Dimethyl Sulfoxide (Cryoprotector)

FBS - Fetal Bovine Serum

Fabp4 - Fatty Acid Binding Protein 4

H-CMCr – Rat Cardiac Mesenchymal Cells from the Healthy Part of Ischemic Heart

HS - Horse Serum

MAML1 - Mastermind-like Transcriptional Co-activator 1

MI-CMCr – Rat Cardiac Mesenchymal Cells from the Post-Infarction Area

NICD - Notch Intracellular Domain

PBS - Phosphate Buffered Saline

PEI - Polyethylenimine Hydrochloride

PFA - Paraformaldehyde

qRT-PCR - Quantitative Reverse Transcription Polymerase Chain Reaction

RNA - Ribonucleic Acid

Runx2 - Runt-Related Transcription Factor 2

SNAI2 - Snail Family Transcriptional Repressor 2

SH-CMCr – Rat Cardiac Mesenchymal Cells from the Healthy Myocardium of Sham-Operated Rats

TF-CMCh – Cardiac Mesenchymal Cells from Patients with Tetralogy of Fallot

Tnnt2 - Troponin T2 Gene

VSD-CMCh – Cardiac Mesenchymal Cells Obtained from Patients with Ventricular Septal Defect

BIBLIOGRAPHY

1. Li Z., Lin L., Wu H., Yan L., Wang H., Yang H., Li H. Global, Regional, and National Death, and Disability-Adjusted Life-Years (DALYs) for Cardiovascular Disease in 2017 and Trends and Risk Analysis From 1990 to 2017 Using the Global Burden of Disease Study and Implications for Prevention // Front Public Health. – 2021. – T. 9. – C. 559751.
2. Emmons-Bell S., Johnson C., Roth G. Prevalence, incidence and survival of heart failure: a systematic review // Heart. – 2022. – T. 108, № 17. – C. 1351-1360.
3. WHO. World health statistics 2023: monitoring health for the SDGs, Sustainable Development Goals. – 2023. – URL: https://www.who.int/publications/book-orders.
4. Blagova O. V., Nedostup A. V. Classification of Non-Coronary Heart Diseases. Point of View // Russian Journal of Cardiology. – 2017.10.15829/1560-4071-2017-2-7-21 № 2. – C. 7-21.
5. van der Ven J. P. G., van den Bosch E., Bogers A., Helbing W. A. Current outcomes and treatment of tetralogy of Fallot // F1000Res. – 2019. – T. 8.
6. Abumehdi M., Sasikumar D., Chaudhari M., Bhole V., Botha P., Mehta C., Stumper O. Stenting of the right ventricular outflow tract as an initial intervention in Tetralogy of Fallot with pulmonary stenosis and major aortopulmonary collateral arteries // Cardiol Young. – 2021. – T. 31, № 3. – C. 452-459.
7. Manshaei R., Merico D., Reuter M. S., Engchuan W., Mojarad B. A., Chaturvedi R., Heung T., Pellecchia G., Zarrei M., Nalpathamkalam T., Khan R., Okello J. B. A., Liston E., Curtis M., Yuen R. K. C., Marshall C. R., Jobling R. K., Oechslin E., Wald R. M., Silversides C. K., Scherer S. W., Kim R. H., Bassett A. S. Genes and Pathways Implicated in Tetralogy of Fallot Revealed by Ultra-Rare Variant Burden Analysis in 231 Genome Sequences // Front Genet. – 2020. – T. 11. – C. 957.
8. Reed G. W., Rossi J. E., Cannon C. P. Acute myocardial infarction // Lancet. – 2017. – T. 389, № 10065. – C. 197-210.
9. Vagnozzi R. J., Maillet M., Sargent M. A., Khalil H., Johansen A. K. Z., Schwanekamp J. A., York A. J., Huang V., Nahrendorf M., Sadayappan S., Molkentin J. D. An acute immune response underlies the benefit of cardiac stem cell therapy // Nature. – 2020. – T. 577, № 7790. – C. 405-409.
10. Du W. W., Xu J., Yang W., Wu N., Li F., Zhou L., Wang S., Li X., He A. T., Du K. Y., Zeng K., Ma J., Lyu J., Zhang C., Zhou C., Maksimovic K., Yang B. B. A Neuroligin Isoform Translated by circNlgn Contributes to Cardiac Remodeling // Circ Res. – 2021. – T. 129, № 5. – C. 568-582.
11. Groenewegen A., Rutten F. H., Mosterd A., Hoes A. W. Epidemiology of heart failure // Eur J Heart Fail. – 2020. – T. 22, № 8. – C. 1342-1356.
12. Stehlik J., Kobashigawa J., Hunt S. A., Reichenspurner H., Kirklin J. K. Honoring 50 Years of Clinical Heart Transplantation in Circulation: In-Depth State-of-the-Art Review // Circulation. – 2018. – T. 137, № 1. – C. 71-87.
13. Behfar A., Crespo-Diaz R., Terzic A., Gersh B. J. Cell therapy for cardiac repair--lessons from clinical trials // Nat Rev Cardiol. – 2014. – T. 11, № 4. – C. 232-46.
14. Beltrami A. P., Barlucchi L., Torella D., Baker M., Limana F., Chimenti S., Kasahara H., Rota M., Musso E., Urbanek K., Leri A., Kajstura J., Nadal-Ginard B., Anversa P. Adult cardiac stem cells are multipotent and support myocardial regeneration // Cell. – 2003. – T. 114, № 6. – C. 763-76.
15. Hsieh P. C., Segers V. F., Davis M. E., MacGillivray C., Gannon J., Molkentin J. D., Robbins J., Lee R. T. Evidence from a genetic fate-mapping study that stem cells refresh adult mammalian cardiomyocytes after injury // Nat Med. – 2007. – T. 13, № 8. – C. 970-4.
16. Mehanna R. A., Essawy M. M., Barkat M. A., Awaad A. K., Thabet E. H., Hamed H. A., Elkafrawy H., Khalil N. A., Sallam A., Kholief M. A., Ibrahim S. S., Mourad G. M. Cardiac stem cells: Current knowledge and future prospects // World J Stem Cells. – 2022. – T. 14, № 1. – C. 1-40.
17. Eschenhagen T., Bolli R., Braun T., Field L. J., Fleischmann B. K., Frisen J., Giacca M., Hare J. M., Houser S., Lee R. T., Marban E., Martin J. F., Molkentin J. D., Murry C. E., Riley P. R., Ruiz-

Lozano P., Sadek H. A., Sussman M. A., Hill J. A. Cardiomyocyte Regeneration: A Consensus Statement // Circulation. – 2017. – Т. 136, № 7. – С. 680-686.
18. Ghodrat S., Hoseini S. J., Asadpour S., Nazarnezhad S., Alizadeh Eghtedar F., Kargozar S. Stem cell-based therapies for cardiac diseases: The critical role of angiogenic exosomes // Biofactors. – 2021. – Т. 47, № 3. – С. 270-291.
19. Belien H., Evens L., Hendrikx M., Bito V., Bronckaers A. Combining stem cells in myocardial infarction: The road to superior repair? // Med Res Rev. – 2022. – Т. 42, № 1. – С. 343-373.
20. Nemir M., Kay M., Maison D., Berthonneche C., Sarre A., Plaisance I., Pedrazzini T. Inhibition of the NOTCH1 Pathway in the Stressed Heart Limits Fibrosis and Promotes Recruitment of Non-Myocyte Cells into the Cardiomyocyte Fate // J Cardiovasc Dev Dis. – 2022. – Т. 9, № 4.
21. Xiao C., Hou J., Wang F., Song Y., Zheng J., Luo L., Wang J., Ding W., Zhu X., Xiong J. W. Endothelial Brg1 fine-tunes Notch signaling during zebrafish heart regeneration // NPJ Regen Med. – 2023. – Т. 8, № 1. – С. 21.
22. Nakada Y., Canseco D. C., Thet S., Abdisalaam S., Asaithamby A., Santos C. X., Shah A. M., Zhang H., Faber J. E., Kinter M. T., Szweda L. I., Xing C., Hu Z., Deberardinis R. J., Schiattarella G., Hill J. A., Oz O., Lu Z., Zhang C. C., Kimura W., Sadek H. A. Hypoxia induces heart regeneration in adult mice // Nature. – 2017. – Т. 541, № 7636. – С. 222-227.
23. Docshin P. M., Karpov A. A., Mametov M. V., Ivkin D. Y., Kostareva A. A., Malashicheva A. B. Mechanisms of Regenerative Potential Activation in Cardiac Mesenchymal Cells // Biomedicines. – 2022. – Т. 10, № 6.
24. Docshin P. M., Karpov A. A., Eyvazova S. D., Puzanov M. V., Kostareva A. A., Galagudza M. M., Malashicheva A. B. Activation of Cardiac Stem Cells in Myocardial Infarction // Cell and Tissue Biology. – 2018. – Т. 12, № 3. – С. 175-182.
25. Docshin P., Bairqdar A., Malashicheva A. Interplay between BMP2 and Notch signaling in endothelial-mesenchymal transition: implications for cardiac fibrosis // Stem Cell Investig. – 2023. – Т. 10. – С. 18.
26. Kozyrev I., Dokshin P., Kostina A., Kiselev A., Ignatieva E., Golovkin A., Pervunina T., Grekhov E., Gordeev M., Kostareva A., Malashicheva A. Dysregulation of Notch signaling in cardiac mesenchymal cells of patients with tetralogy of Fallot // Pediatr Res. – 2020. – Т. 88, № 1. – С. 38-47.
27. Kozyrev I. A., Golovkin A. S., Ignatieva E. S., Dokshin P. M., Grekhov E. V., Gordeev M. L., Pervunina T. M., Kostareva A. A., Malashicheva A. B. Characterization of mesenchymal heart cells obtained from patients with tetralogy of Fallot and ventricular septal defect // Translational Medicine. – 2019. – Т. 6, № 5. – С. 16-23.
28. Docshin P. M., Bairqdar A., Malashicheva A. B. Current status, challenges and perspectives of mesenchymal stem cell-based therapy for cardiac regeneration // Complex Issues of Cardiovascular Diseases. – 2021. – Т. 10, № 3. – С. 72-78.
29. Dokshin P. M., Malashicheva A. B. Heart stem cells: hope or myth? // Russian Journal of Cardiology. – 2021. – Т. 26, № 10.
30. Developmental Biology. / Barresi M., Gilbert, S. – Thirteenth Edition изд., 2023.
31. Zhang Q., Carlin D., Zhu F., Cattaneo P., Ideker T., Evans S. M., Bloomekatz J., Chi N. C. Unveiling Complexity and Multipotentiality of Early Heart Fields // Circ Res. – 2021. – Т. 129, № 4. – С. 474-487.
32. Meilhac S. M., Buckingham M. E. The deployment of cell lineages that form the mammalian heart // Nat Rev Cardiol. – 2018. – Т. 15, № 11. – С. 705-724.
33. Pelullo M., Zema S., Nardozza F., Checquolo S., Screpanti I., Bellavia D. Wnt, Notch, and TGF-beta Pathways Impinge on Hedgehog Signaling Complexity: An Open Window on Cancer // Front Genet. – 2019. – Т. 10. – С. 711.
34. Li X., Yan X., Wang Y., Kaur B., Han H., Yu J. The Notch signaling pathway: a potential target for cancer immunotherapy // J Hematol Oncol. – 2023. – Т. 16, № 1. – С. 45.
35. Zhou B., Lin W., Long Y., Yang Y., Zhang H., Wu K., Chu Q. Notch signaling pathway: architecture, disease, and therapeutics // Signal Transduct Target Ther. – 2022. – Т. 7, № 1. – С. 95.

36. Oswald F., Kovall R. A. CSL-Associated Corepressor and Coactivator Complexes // Adv Exp Med Biol. – 2018. – T. 1066. – C. 279-295.
37. L Hernandez S., Cuervo H., J Kandel J., Flores-Guzman F., Garcia T., Hahn P., Kirschner R., M Defnet A., Bagrodia N., Nelson M., Biermann H., Shen S., L Wu L. The long and winding road: detecting and quantifying Notch activation in endothelial cells // Vascular Cell. – 2021. – T. 13, № 1.
38. Sjoqvist M., Andersson E. R. Do as I say, Not(ch) as I do: Lateral control of cell fate // Dev Biol. – 2019. – T. 447, № 1. – C. 58-70.
39. Binshtok U., Sprinzak D. Modeling the Notch Response // Adv Exp Med Biol. – 2018. – T. 1066. – C. 79-98.
40. Hirano K. I., Hosokawa H., Yahata T., Ando K., Tanaka M., Imai J., Yazawa M., Ohtsuka M., Negishi N., Habu S., Sato T., Hozumi K. Dll1 Can Function as a Ligand of Notch1 and Notch2 in the Thymic Epithelium // Front Immunol. – 2022. – T. 13. – C. 852427.
41. Wu X., Yao J., Wang L., Zhang D., Zhang L., Reynolds E. X., Yu T., Bostrom K. I., Yao Y. Crosstalk between BMP and Notch Induces Sox2 in Cerebral Endothelial Cells // Cells. – 2019. – T. 8, № 6.
42. Kiyokawa H., Morimoto M. Notch signaling in the mammalian respiratory system, specifically the trachea and lungs, in development, homeostasis, regeneration, and disease // Dev Growth Differ. – 2020. – T. 62, № 1. – C. 67-79.
43. Ho D. M., Artavanis-Tsakonas S., Louvi A. The Notch pathway in CNS homeostasis and neurodegeneration // Wiley Interdiscip Rev Dev Biol. – 2020. – T. 9, № 1. – C. e358.
44. Moore R., Alexandre P. Delta-Notch Signaling: The Long and The Short of a Neuron's Influence on Progenitor Fates // J Dev Biol. – 2020. – T. 8, № 2.
45. Mukherjee M., Fogarty E., Janga M., Surendran K. Notch Signaling in Kidney Development, Maintenance, and Disease // Biomolecules. – 2019. – T. 9, № 11.
46. Yu J., Canalis E. Notch and the regulation of osteoclast differentiation and function // Bone. – 2020. – T. 138. – C. 115474.
47. Yoshioka H., Yamada T., Hasegawa S., Miyachi K., Ishii Y., Hasebe Y., Inoue Y., Tanaka H., Iwata Y., Arima M., Sugiura K., Akamatsu H. Senescent cell removal via JAG1-NOTCH1 signalling in the epidermis // Exp Dermatol. – 2021. – T. 30, № 9. – C. 1268-1278.
48. Wang X., Liu Y., He J., Wang J., Chen X., Yang R. Regulation of signaling pathways in hair follicle stem cells // Burns Trauma. – 2022. – T. 10. – C. tkac022.
49. Brown R. M., 2nd, Nelson J. C., Zhang H., Kiernan A. E., Groves A. K. Notch-mediated lateral induction is necessary to maintain vestibular prosensory identity during inner ear development // Dev Biol. – 2020. – T. 462, № 1. – C. 74-84.
50. Misiorek J. O., Przybyszewska-Podstawka A., Kalafut J., Paziewska B., Rolle K., Rivero-Muller A., Nees M. Context Matters: NOTCH Signatures and Pathway in Cancer Progression and Metastasis // Cells. – 2021. – T. 10, № 1.
51. Luxan G., D'Amato G., de la Pompa J. L. Intercellular Signaling in Cardiac Development and Disease: The NOTCH pathway // Etiology and Morphogenesis of Congenital Heart Disease: From Gene Function and Cellular Interaction to Morphology / Nakanishi T. и др. – Tokyo: Springer, 2016. – C. 103-14.
52. Seya D., Ihara D., Shirai M., Kawamura T., Watanabe Y., Nakagawa O. A role of Hey2 transcription factor for right ventricle development through regulation of Tbx2-Mycn pathway during cardiac morphogenesis // Dev Growth Differ. – 2021. – T. 63, № 1. – C. 82-92.
53. Ihara D., Watanabe Y., Seya D., Arai Y., Isomoto Y., Nakano A., Kubo A., Ogura T., Kawamura T., Nakagawa O. Expression of Hey2 transcription factor in the early embryonic ventricles is controlled through a distal enhancer by Tbx20 and Gata transcription factors // Dev Biol. – 2020. – T. 461, № 2. – C. 124-131.
54. Luxan G., D'Amato G., MacGrogan D., de la Pompa J. L. Endocardial Notch Signaling in Cardiac Development and Disease // Circ Res. – 2016. – T. 118, № 1. – C. e1-e18.

55. Stankunas K., Ma G. K., Kuhnert F. J., Kuo C. J., Chang C. P. VEGF signaling has distinct spatiotemporal roles during heart valve development // Dev Biol. – 2010. – T. 347, № 2. – C. 325-36.
56. MacGrogan D., Munch J., de la Pompa J. L. Notch and interacting signalling pathways in cardiac development, disease, and regeneration // Nat Rev Cardiol. – 2018. – T. 15, № 11. – C. 685-704.
57. D'Amato G., Luxan G., de la Pompa J. L. Notch signalling in ventricular chamber development and cardiomyopathy // FEBS J. – 2016. – T. 283, № 23. – C. 4223-4237.
58. Samsa L. A., Givens C., Tzima E., Stainier D. Y., Qian L., Liu J. Cardiac contraction activates endocardial Notch signaling to modulate chamber maturation in zebrafish // Development. – 2015. – T. 142, № 23. – C. 4080-91.
59. Ribatti D. Role of notch and notch ligands // New Insights on the Development of the Vascular System, 2022. – C. 41-44.
60. James A. C., Szot J. O., Iyer K., Major J. A., Pursglove S. E., Chapman G., Dunwoodie S. L. Notch4 reveals a novel mechanism regulating Notch signal transduction // Biochim Biophys Acta. – 2014. – T. 1843, № 7. – C. 1272-84.
61. Breikaa R. M., Denman K., Ueyama Y., McCallinhart P. E., Khan A. Q., Agarwal G., Trask A. J., Garg V., Lilly B. Loss of Jagged1 in mature endothelial cells causes vascular dysfunction with alterations in smooth muscle phenotypes // Vascul Pharmacol. – 2022. – T. 145. – C. 107087.
62. Wolf K., Hu H., Isaji T., Dardik A. Molecular identity of arteries, veins, and lymphatics // J Vasc Surg. – 2019. – T. 69, № 1. – C. 253-262.
63. Lahm H., Schon P., Doppler S., Dressen M., Cleuziou J., Deutsch M. A., Ewert P., Lange R., Krane M. Tetralogy of Fallot and Hypoplastic Left Heart Syndrome - Complex Clinical Phenotypes Meet Complex Genetic Networks // Curr Genomics. – 2015. – T. 16, № 3. – C. 141-58.
64. Pradegan N., Vida V. L., Geva T., Stellin G., White M. T., Sanders S. P., Padera R. F. Myocardial histopathology in late-repaired and unrepaired adults with tetralogy of Fallot // Cardiovasc Pathol. – 2016. – T. 25, № 3. – C. 225-231.
65. Bailliard F., Anderson R. H. Tetralogy of fallot // Orphanet Journal of Rare Diseases. – 2009. – T. 4, № 1. – C. 2.
66. Mercer-Rosa L., Paridon S. M., Fogel M. A., Rychik J., Tanel R. E., Zhao H., Zhang X., Yang W., Shults J., Goldmuntz E. 22q11. 2 deletion status and disease burden in children and adolescents with tetralogy of Fallot // Circulation: Genomic and Precision Medicine. – 2015. – C. CIRCGENETICS. 114.000819.
67. Topf A., Griffin H. R., Glen E., Soemedi R., Brown D. L., Hall D., Rahman T. J., Eloranta J. J., Jungst C., Stuart A. G., O'Sullivan J., Keavney B. D., Goodship J. A. Functionally significant, rare transcription factor variants in tetralogy of Fallot // PLoS One. – 2014. – T. 9, № 8. – C. e95453.
68. Morgenthau A., Frishman W. H. Genetic Origins of Tetralogy of Fallot // Cardiol Rev. – 2018. – T. 26, № 2. – C. 86-92.
69. Diab N. S., Barish S., Dong W., Zhao S., Allington G., Yu X., Kahle K. T., Brueckner M., Jin S. C. Molecular Genetics and Complex Inheritance of Congenital Heart Disease // Genes (Basel). – 2021. – T. 12, № 7.
70. Shabana N. A., Shahid S. U., Irfan U. Genetic Contribution to Congenital Heart Disease (CHD) // Pediatr Cardiol. – 2020. – T. 41, № 1. – C. 12-23.
71. Greenway S. C., Pereira A. C., Lin J. C., DePalma S. R., Israel S. J., Mesquita S. M., Ergul E., Conta J. H., Korn J. M., McCarroll S. A., Gorham J. M., Gabriel S., Altshuler D. M., de Lourdes Quintanilla-Dieck M., Artunduaga M. A., Eavey R. D., Plenge R. M., Shadick N. A., Weinblatt M. E., De Jager P. L., Hafler D. A., Breitbart R. E., Seidman J. G., Seidman C. E. De novo copy number variants identify new genes and loci in isolated sporadic tetralogy of Fallot // Nature Genetics. – 2009. – T. 41. – C. 931.
72. Bittel D. C., Butler M. G., Kibiryeva N., Marshall J. A., Chen J., Lofland G. K., O'Brien J. E. Gene expression in cardiac tissues from infants with idiopathic conotruncal defects // BMC medical genomics. – 2011. – T. 4, № 1. – C. 1.

73. Monaghan R. M., Page D. J., Ostergaard P., Keavney B. D. The physiological and pathological functions of VEGFR3 in cardiac and lymphatic development and related diseases // Cardiovasc Res. – 2021. – Т. 117, № 8. – С. 1877-1890.
74. Page D. J., Miossec M. J., Williams S. G., Monaghan R. M., Fotiou E., Cordell H. J., Sutcliffe L., Topf A., Bourgey M., Bourque G., Eveleigh R., Dunwoodie S. L., Winlaw D. S., Bhattacharya S., Breckpot J., Devriendt K., Gewillig M., Brook J. D., Setchfield K. J., Bu'Lock F. A., O'Sullivan J., Stuart G., Bezzina C. R., Mulder B. J. M., Postma A. V., Bentham J. R., Baron M., Bhaskar S. S., Black G. C., Newman W. G., Hentges K. E., Lathrop G. M., Santibanez-Koref M., Keavney B. D. Whole Exome Sequencing Reveals the Major Genetic Contributors to Nonsyndromic Tetralogy of Fallot // Circ Res. – 2019. – Т. 124, № 4. – С. 553-563.
75. Nadal-Ginard B., Kajstura J., Leri A., Anversa P. Myocyte death, growth, and regeneration in cardiac hypertrophy and failure // Circ Res. – 2003. – Т. 92, № 2. – С. 139-50.
76. Uygur A., Lee R. T. Mechanisms of Cardiac Regeneration // Dev Cell. – 2016. – Т. 36, № 4. – С. 362-74.
77. Grwth Hyperplasia Card Muscle. / Rumyantsev P. P. – 1st Edition изд. – London, 2017.
78. Bergmann O. Clearing up the mist: cardiomyocyte renewal in human hearts // Eur Heart J. – 2019. – Т. 40, № 13. – С. 1037-1038.
79. Senyo S. E., Steinhauser M. L., Pizzimenti C. L., Yang V. K., Cai L., Wang M., Wu T. D., Guerquin-Kern J. L., Lechene C. P., Lee R. T. Mammalian heart renewal by pre-existing cardiomyocytes // Nature. – 2013. – Т. 493, № 7432. – С. 433-6.
80. Porrello E. R., Mahmoud A. I., Simpson E., Hill J. A., Richardson J. A., Olson E. N., Sadek H. A. Transient regenerative potential of the neonatal mouse heart // Science. – 2011. – Т. 331, № 6020. – С. 1078-80.
81. Mahmoud A. I., Porrello E. R., Kimura W., Olson E. N., Sadek H. A. Surgical models for cardiac regeneration in neonatal mice // Nat Protoc. – 2014. – Т. 9, № 2. – С. 305-11.
82. Aurora A. B., Porrello E. R., Tan W., Mahmoud A. I., Hill J. A., Bassel-Duby R., Sadek H. A., Olson E. N. Macrophages are required for neonatal heart regeneration // J Clin Invest. – 2014. – Т. 124, № 3. – С. 1382-92.
83. Haubner B. J., Schneider J., Schweigmann U., Schuetz T., Dichtl W., Velik-Salchner C., Stein J. I., Penninger J. M. Functional Recovery of a Human Neonatal Heart After Severe Myocardial Infarction // Circ Res. – 2016. – Т. 118, № 2. – С. 216-21.
84. Soonpaa M. H., Rubart M., Field L. J. Challenges measuring cardiomyocyte renewal // Biochim Biophys Acta. – 2013. – Т. 1833, № 4. – С. 799-803.
85. Leri A., Kajstura J., Anversa P. Cardiac stem cells and mechanisms of myocardial regeneration // Physiol Rev. – 2005. – Т. 85, № 4. – С. 1373-416.
86. Windmueller R., Leach J. P., Babu A., Zhou S., Morley M. P., Wakabayashi A., Petrenko N. B., Viatour P., Morrisey E. E. Direct Comparison of Mononucleated and Binucleated Cardiomyocytes Reveals Molecular Mechanisms Underlying Distinct Proliferative Competencies // Cell Rep. – 2020. – Т. 30, № 9. – С. 3105-3116 e4.
87. Galow A. M., Wolfien M., Muller P., Bartsch M., Brunner R. M., Hoeflich A., Wolkenhauer O., David R., Goldammer T. Integrative Cluster Analysis of Whole Hearts Reveals Proliferative Cardiomyocytes in Adult Mice // Cells. – 2020. – Т. 9, № 5.
88. Arjmand B., Abedi M., Arabi M., Alavi-Moghadam S., Rezaei-Tavirani M., Hadavandkhani M., Tayanloo-Beik A., Kordi R., Roudsari P. P., Larijani B. Regenerative Medicine for the Treatment of Ischemic Heart Disease; Status and Future Perspectives // Front Cell Dev Biol. – 2021. – Т. 9. – С. 704903.
89. Jarrige M., Frank E., Herardot E., Martineau S., Darle A., Benabides M., Domingues S., Chose O., Habeler W., Lorant J., Baldeschi C., Martinat C., Monville C., Morizur L., Ben M'Barek K. The Future of Regenerative Medicine: Cell Therapy Using Pluripotent Stem Cells and Acellular Therapies Based on Extracellular Vesicles // Cells. – 2021. – Т. 10, № 2.

90. Murry C. E., MacLellan W. R. Stem cells and the heart-the road ahead // Science. – 2020. – T. 367, № 6480. – C. 854-855.
91. Bhartiya D. Adult tissue-resident stem cells-fact or fiction? // Stem Cell Res Ther. – 2021. – T. 12, № 1. – C. 73.
92. Mannino G., Russo C., Maugeri G., Musumeci G., Vicario N., Tibullo D., Giuffrida R., Parenti R., Lo Furno D. Adult stem cell niches for tissue homeostasis // J Cell Physiol. – 2022. – T. 237, № 1. – C. 239-257.
93. Pinto A. R., Ilinykh A., Ivey M. J., Kuwabara J. T., D'Antoni M. L., Debuque R., Chandran A., Wang L., Arora K., Rosenthal N. A., Tallquist M. D. Revisiting Cardiac Cellular Composition // Circ Res. – 2016. – T. 118, № 3. – C. 400-9.
94. Orlic D., Kajstura J., Chimenti S., Jakoniuk I., Anderson S. M., Li B., Pickel J., McKay R., Nadal-Ginard B., Bodine D. M., Leri A., Anversa P. Bone marrow cells regenerate infarcted myocardium // Nature. – 2001. – T. 410, № 6829. – C. 701-5.
95. van Berlo J. H., Kanisicak O., Maillet M., Vagnozzi R. J., Karch J., Lin S. C., Middleton R. C., Marban E., Molkentin J. D. c-kit+ cells minimally contribute cardiomyocytes to the heart // Nature. – 2014. – T. 509, № 7500. – C. 337-41.
96. Bearzi C., Rota M., Hosoda T., Tillmanns J., Nascimbene A., De Angelis A., Yasuzawa-Amano S., Trofimova I., Siggins R. W., Lecapitaine N., Cascapera S., Beltrami A. P., D'Alessandro D. A., Zias E., Quaini F., Urbanek K., Michler R. E., Bolli R., Kajstura J., Leri A., Anversa P. Human cardiac stem cells // Proc Natl Acad Sci U S A. – 2007. – T. 104, № 35. – C. 14068-73.
97. Chong J. J., Yang X., Don C. W., Minami E., Liu Y. W., Weyers J. J., Mahoney W. M., Van Biber B., Cook S. M., Palpant N. J., Gantz J. A., Fugate J. A., Muskheli V., Gough G. M., Vogel K. W., Astley C. A., Hotchkiss C. E., Baldessari A., Pabon L., Reinecke H., Gill E. A., Nelson V., Kiem H. P., Laflamme M. A., Murry C. E. Human embryonic-stem-cell-derived cardiomyocytes regenerate non-human primate hearts // Nature. – 2014. – T. 510, № 7504. – C. 273-7.
98. Keith M. C., Bolli R. "String theory" of c-kit(pos) cardiac cells: a new paradigm regarding the nature of these cells that may reconcile apparently discrepant results // Circ Res. – 2015. – T. 116, № 7. – C. 1216-30.
99. Gude N. A., Sussman M. A. Cardiac regenerative therapy: Many paths to repair // Trends Cardiovasc Med. – 2020. – T. 30, № 6. – C. 338-343.
100. Le T., Chong J. Cardiac progenitor cells for heart repair // Cell Death Discov. – 2016. – T. 2. – C. 16052.
101. Santini M. P., Forte E., Harvey R. P., Kovacic J. C. Developmental origin and lineage plasticity of endogenous cardiac stem cells // Development. – 2016. – T. 143, № 8. – C. 1242-58.
102. Li M., Naqvi N., Yahiro E., Liu K., Powell P. C., Bradley W. E., Martin D. I., Graham R. M., Dell'Italia L. J., Husain A. c-kit is required for cardiomyocyte terminal differentiation // Circ Res. – 2008. – T. 102, № 6. – C. 677-85.
103. Zaruba M. M., Soonpaa M., Reuter S., Field L. J. Cardiomyogenic potential of C-kit(+)-expressing cells derived from neonatal and adult mouse hearts // Circulation. – 2010. – T. 121, № 18. – C. 1992-2000.
104. Dergilev K., Tsokolaeva Z., Makarevich P., Beloglazova I., Zubkova E., Boldyreva M., Ratner E., Dyikanov D., Menshikov M., Ovchinnikov A., Ageev F., Parfyonova Y. C-Kit Cardiac Progenitor Cell Based Cell Sheet Improves Vascularization and Attenuates Cardiac Remodeling following Myocardial Infarction in Rats // Biomed Res Int. – 2018. – T. 2018. – C. 3536854.
105. Zakharova L., Mastroeni D., Mutlu N., Molina M., Goldman S., Diethrich E., Gaballa M. A. Transplantation of cardiac progenitor cell sheet onto infarcted heart promotes cardiogenesis and improves function // Cardiovasc Res. – 2010. – T. 87, № 1. – C. 40-9.
106. Tang X. L., Li Q., Rokosh G., Sanganalmath S. K., Chen N., Ou Q., Stowers H., Hunt G., Bolli R. Long-Term Outcome of Administration of c-kit(POS) Cardiac Progenitor Cells After Acute Myocardial Infarction: Transplanted Cells Do not Become Cardiomyocytes, but Structural and

Functional Improvement and Proliferation of Endogenous Cells Persist for at Least One Year // Circ Res. – 2016. – T. 118, № 7. – C. 1091-105.
107. Bolli R., Mitrani R. D., Hare J. M., Pepine C. J., Perin E. C., Willerson J. T., Traverse J. H., Henry T. D., Yang P. C., Murphy M. P., March K. L., Schulman I. H., Ikram S., Lee D. P., O'Brien C., Lima J. A., Ostovaneh M. R., Ambale-Venkatesh B., Lewis G., Khan A., Bacallao K., Valasaki K., Longsomboon B., Gee A. P., Richman S., Taylor D. A., Lai D., Sayre S. L., Bettencourt J., Vojvodic R. W., Cohen M. L., Simpson L., Aguilar D., Loghin C., Moye L., Ebert R. F., Davis B. R., Simari R. D., Cardiovascular Cell Therapy Research N. A Phase II study of autologous mesenchymal stromal cells and c-kit positive cardiac cells, alone or in combination, in patients with ischaemic heart failure: the CCTRN CONCERT-HF trial // Eur J Heart Fail. – 2021. – T. 23, № 4. – C. 661-674.
108. Chong J. J., Chandrakanthan V., Xaymardan M., Asli N. S., Li J., Ahmed I., Heffernan C., Menon M. K., Scarlett C. J., Rashidianfar A., Biben C., Zoellner H., Colvin E. K., Pimanda J. E., Biankin A. V., Zhou B., Pu W. T., Prall O. W., Harvey R. P. Adult cardiac-resident MSC-like stem cells with a proepicardial origin // Cell Stem Cell. – 2011. – T. 9, № 6. – C. 527-40.
109. Ball S. G., Worthington J. J., Canfield A. E., Merry C. L., Kielty C. M. Mesenchymal stromal cells: inhibiting PDGF receptors or depleting fibronectin induces mesodermal progenitors with endothelial potential // Stem Cells. – 2014. – T. 32, № 3. – C. 694-705.
110. Noseda M., Harada M., McSweeney S., Leja T., Belian E., Stuckey D. J., Abreu Paiva M. S., Habib J., Macaulay I., de Smith A. J., al-Beidh F., Sampson R., Lumbers R. T., Rao P., Harding S. E., Blakemore A. I., Jacobsen S. E., Barahona M., Schneider M. D. PDGFRalpha demarcates the cardiogenic clonogenic Sca1+ stem/progenitor cell in adult murine myocardium // Nat Commun. – 2015. – T. 6. – C. 6930.
111. Cai C. L., Liang X., Shi Y., Chu P. H., Pfaff S. L., Chen J., Evans S. Isl1 identifies a cardiac progenitor population that proliferates prior to differentiation and contributes a majority of cells to the heart // Dev Cell. – 2003. – T. 5, № 6. – C. 877-89.
112. Laugwitz K. L., Moretti A., Caron L., Nakano A., Chien K. R. Islet1 cardiovascular progenitors: a single source for heart lineages? // Development. – 2008. – T. 135, № 2. – C. 193-205.
113. Menasche P., Vanneaux V., Hagege A., Bel A., Cholley B., Parouchev A., Cacciapuoti I., Al-Daccak R., Benhamouda N., Blons H., Agbulut O., Tosca L., Trouvin J. H., Fabreguettes J. R., Bellamy V., Charron D., Tartour E., Tachdjian G., Desnos M., Larghero J. Transplantation of Human Embryonic Stem Cell-Derived Cardiovascular Progenitors for Severe Ischemic Left Ventricular Dysfunction // J Am Coll Cardiol. – 2018. – T. 71, № 4. – C. 429-438.
114. Smith R. R., Barile L., Cho H. C., Leppo M. K., Hare J. M., Messina E., Giacomello A., Abraham M. R., Marban E. Regenerative potential of cardiosphere-derived cells expanded from percutaneous endomyocardial biopsy specimens // Circulation. – 2007. – T. 115, № 7. – C. 896-908.
115. Oh H., Bradfute S. B., Gallardo T. D., Nakamura T., Gaussin V., Mishina Y., Pocius J., Michael L. H., Behringer R. R., Garry D. J., Entman M. L., Schneider M. D. Cardiac progenitor cells from adult myocardium: homing, differentiation, and fusion after infarction // Proc Natl Acad Sci U S A. – 2003. – T. 100, № 21. – C. 12313-8.
116. Li T. S., Cheng K., Lee S. T., Matsushita S., Davis D., Malliaras K., Zhang Y., Matsushita N., Smith R. R., Marban E. Cardiospheres recapitulate a niche-like microenvironment rich in stemness and cell-matrix interactions, rationalizing their enhanced functional potency for myocardial repair // Stem Cells. – 2010. – T. 28, № 11. – C. 2088-98.
117. Ye J., Boyle A. J., Shih H., Sievers R. E., Wang Z. E., Gormley M., Yeghiazarians Y. CD45-positive cells are not an essential component in cardiosphere formation // Cell Tissue Res. – 2013. – T. 351, № 1. – C. 201-5.
118. Malliaras K., Makkar R. R., Smith R. R., Cheng K., Wu E., Bonow R. O., Marban L., Mendizabal A., Cingolani E., Johnston P. V., Gerstenblith G., Schuleri K. H., Lardo A. C., Marban E. Intracoronary cardiosphere-derived cells after myocardial infarction: evidence of therapeutic regeneration in the final 1-year results of the CADUCEUS trial (CArdiosphere-Derived aUtologous

stem CElls to reverse ventricUlar dySfunction) // J Am Coll Cardiol. – 2014. – T. 63, № 2. – C. 110-22.
119. Makkar R. R., Smith R. R., Cheng K., Malliaras K., Thomson L. E., Berman D., Czer L. S., Marban L., Mendizabal A., Johnston P. V., Russell S. D., Schuleri K. H., Lardo A. C., Gerstenblith G., Marban E. Intracoronary cardiosphere-derived cells for heart regeneration after myocardial infarction (CADUCEUS): a prospective, randomised phase 1 trial // Lancet. – 2012. – T. 379, № 9819. – C. 895-904.
120. Makkar R. R., Kereiakes D. J., Aguirre F., Kowalchuk G., Chakravarty T., Malliaras K., Francis G. S., Povsic T. J., Schatz R., Traverse J. H., Pogoda J. M., Smith R. R., Marban L., Ascheim D. D., Ostovaneh M. R., Lima J. A. C., DeMaria A., Marban E., Henry T. D. Intracoronary ALLogeneic heart STem cells to Achieve myocardial Regeneration (ALLSTAR): a randomized, placebo-controlled, double-blinded trial // Eur Heart J. – 2020. – T. 41, № 36. – C. 3451-3458.
121. Russell J. L., Goetsch S. C., Gaiano N. R., Hill J. A., Olson E. N., Schneider J. W. A dynamic notch injury response activates epicardium and contributes to fibrosis repair // Circ Res. – 2011. – T. 108, № 1. – C. 51-9.
122. Bartczak A., McGilvray I., Keating A. Mesenchymal stromal cell therapy to promote cardiac tissue regeneration and repair // Curr Opin Organ Transplant. – 2017. – T. 22, № 1. – C. 86-96.
123. Zhao L., Borikova A. L., Ben-Yair R., Guner-Ataman B., MacRae C. A., Lee R. T., Burns C. G., Burns C. E. Notch signaling regulates cardiomyocyte proliferation during zebrafish heart regeneration // Proc Natl Acad Sci U S A. – 2014. – T. 111, № 4. – C. 1403-8.
124. Pandey R., Yang, Y., Jackson, L., & Ahmed, R. . MicroRNAs regulating Meis1 expression and inducing cardiomyocyte proliferation // Cardiovascular Regenerative Medicine. – 2018. – T. 3.
125. Kovacic J. C., Mercader N., Torres M., Boehm M., Fuster V. Epithelial-to-mesenchymal and endothelial-to-mesenchymal transition: from cardiovascular development to disease // Circulation. – 2012. – T. 125, № 14. – C. 1795-808.
126. Bischoff J. Endothelial-to-Mesenchymal Transition // Circ Res. – 2019. – T. 124, № 8. – C. 1163-1165.
127. Zhang J., Ogbu S. C., Musich P. R., Thewke D. P., Yao Z., Jiang Y. The Contribution of Endothelial-Mesenchymal Transition to Atherosclerosis // International Journal of Translational Medicine. – 2021. – T. 1, № 1. – C. 39-54.
128. Cheng W., Li X., Liu D., Cui C., Wang X. Endothelial-to-Mesenchymal Transition: Role in Cardiac Fibrosis // J Cardiovasc Pharmacol Ther. – 2021. – T. 26, № 1. – C. 3-11.
129. Hanna A., Frangogiannis N. G. The Role of the TGF-beta Superfamily in Myocardial Infarction // Front Cardiovasc Med. – 2019. – T. 6. – C. 140.
130. Mocumbi A. O., Stothard J. R., Correia-de-Sa P., Yacoub M. Endomyocardial Fibrosis: an Update After 70 Years // Curr Cardiol Rep. – 2019. – T. 21, № 11. – C. 148.
131. Kachanova O., Lobov A., Malashicheva A. The Role of the Notch Signaling Pathway in Recovery of Cardiac Function after Myocardial Infarction // Int J Mol Sci. – 2022. – T. 23, № 20.
132. Kostina A. S., Uspensky Vcapital Ie C., Irtyuga O. B., Ignatieva E. V., Freylikhman O., Gavriliuk N. D., Moiseeva O. M., Zhuk S., Tomilin A., Kostareva capital A C. A. C., Malashicheva A. B. Notch-dependent EMT is attenuated in patients with aortic aneurysm and bicuspid aortic valve // Biochim Biophys Acta. – 2016. – T. 1862, № 4. – C. 733-740.
133. Mercado-Pimentel M. E., Runyan R. B. Multiple transforming growth factor-beta isoforms and receptors function during epithelial-mesenchymal cell transformation in the embryonic heart // Cells Tissues Organs. – 2007. – T. 185, № 1-3. – C. 146-56.
134. Guide for the Care and Use of Laboratory Animals. Committee for the Update of the Guide for the Care and Use of Laboratory Animals. / Edition E. – 8 изд. – Washington, D.C.: National Academies Press, 2011.
135. Karpov A. A., Ivkin, D. Yu., Dracheva, A. V., Pitukhina, N. N., Uspenskaya, Yu. K., Vaulina, D. D., et al. Rat model of post-infarct heart failure by left coronary artery occlusion: technical aspects, functional and morphological assessment // Biomedicine. – 2014. – T. 1. – C. 32-48.

136. World Medical A. World Medical Association Declaration of Helsinki: ethical principles for medical research involving human subjects // JAMA. – 2013. – Т. 310, № 20. – С. 2191-4.
137. Smits A. M., van Vliet P., Metz C. H., Korfage T., Sluijter J. P., Doevendans P. A., Goumans M. J. Human cardiomyocyte progenitor cells differentiate into functional mature cardiomyocytes: an in vitro model for studying human cardiac physiology and pathophysiology // Nat Protoc. – 2009. – Т. 4, № 2. – С. 232-43.
138. Smits A. M., Van Vliet P., Metz C. H., Korfage T., Sluijter J. P., Doevendans P. A., Goumans M.-J. Human cardiomyocyte progenitor cells differentiate into functional mature cardiomyocytes: an in vitro model for studying human cardiac physiology and pathophysiology // Nature protocols. – 2009. – Т. 4, № 2. – С. 232-243.
139. Худяков А. А. К., Д.И.; Костарева, А.А.; Малашичева, А.Б. Получение предшественников кардиомиоцитов человека из ткани миокарда // Бюллетень ФЦСКЭ им. В.А. Алмазова. – 2012. – Т. 18, № 1.
140. Dowling C. M., Herranz Ors C., Kiely P. A. Using real-time impedance-based assays to monitor the effects of fibroblast-derived media on the adhesion, proliferation, migration and invasion of colon cancer cells // Biosci Rep. – 2014. – Т. 34, № 4.
141. Костина Д. А. В. И. В., Смагина Л. В., Гаврилюк Н. Д., Моисеева О. М., Иртюга О. Б., Успенский В. Е., Костарева А. А., Малашичева А. Б. . Исследование функциональных свойств гладкомышечных клеток при аневризме аорты // Цитология. – 2013. – Т. 55, № 10. – С. 725-731.
142. Baudin B., Bruneel A., Bosselut N., Vaubourdolle M. A protocol for isolation and culture of human umbilical vein endothelial cells // Nat Protoc. – 2007. – Т. 2, № 3. – С. 481-5.
143. Kostina A., Shishkova A., Ignatieva E., Irtyuga O., Bogdanova M., Levchuk K., Golovkin A., Zhiduleva E., Uspenskiy V., Moiseeva O. Different Notch signaling in cells from calcified bicuspid and tricuspid aortic valves // Journal of Molecular and Cellular Cardiology. – 2018. – Т. 114. – С. 211-219.
144. Malashicheva A., Kanzler B., Tolkunova E., Trono D., Tomilin A. Lentivirus as a tool for lineage-specific gene manipulations // Genesis. – 2007. – Т. 45, № 7. – С. 456-9.
145. Malashicheva A., Bogdanova M., Zabirnyk A., Smolina N., Ignatieva E., Freilikhman O., Fedorov A., Dmitrieva R., Sjoberg G., Sejersen T., Kostareva A. Various lamin A/C mutations alter expression profile of mesenchymal stem cells in mutation specific manner // Mol Genet Metab. – 2015. – Т. 115, № 2-3. – С. 118-27.
146. Dobin A., Davis C. A., Schlesinger F., Drenkow J., Zaleski C., Jha S., Batut P., Chaisson M., Gingeras T. R. STAR: ultrafast universal RNA-seq aligner // Bioinformatics. – 2013. – Т. 29, № 1. – С. 15-21.
147. Love M. I., Huber W., Anders S. Moderated estimation of fold change and dispersion for RNA-seq data with DESeq2 // Genome Biol. – 2014. – Т. 15, № 12. – С. 550.
148. Zenkova D., Kamenev, V., Sablina, R., Artyomov, M., and Sergushichev, A. Phantasus: visual and interactive gene expression analysis //. – 2018.10.18129/B9.bioc.phantasus.
149. Mabotuwana N. S., Rech L., Lim J., Hardy S. A., Murtha L. A., Rainer P. P., Boyle A. J. Paracrine Factors Released by Stem Cells of Mesenchymal Origin and their Effects in Cardiovascular Disease: A Systematic Review of Pre-clinical Studies // Stem Cell Rev Rep. – 2022. – Т. 18, № 8. – С. 2606-2628.
150. Silvestre J. S., Mallat Z. Editorial: Inflammation and Reparative Process After Cardiac Injury // Front Cardiovasc Med. – 2019. – Т. 6. – С. 162.
151. Ivan C., Hu W., Bottsford-Miller J., Zand B., Dalton H. J., Liu T., Huang J., Nick A. M., Lopez-Berestein G., Coleman R. L., Baggerly K. A., Sood A. K. Epigenetic analysis of the Notch superfamily in high-grade serous ovarian cancer // Gynecol Oncol. – 2013. – Т. 128, № 3. – С. 506-11.
152. Garg V., Muth A. N., Ransom J. F., Schluterman M. K., Barnes R., King I. N., Grossfeld P. D., Srivastava D. Mutations in NOTCH1 cause aortic valve disease // Nature. – 2005. – Т. 437, № 7056. – С. 270-4.

153. Lavery K., Swain P., Falb D., Alaoui-Ismaili M. H. BMP-2/4 and BMP-6/7 differentially utilize cell surface receptors to induce osteoblastic differentiation of human bone marrow-derived mesenchymal stem cells // J Biol Chem. – 2008. – Т. 283, № 30. – С. 20948-58.
154. Seeherman H. J., Berasi S. P., Brown C. T., Martinez R. X., Juo Z. S., Jelinsky S., Cain M. J., Grode J., Tumelty K. E., Bohner M., Grinberg O., Orr N., Shoseyov O., Eyckmans J., Chen C., Morales P. R., Wilson C. G., Vanderploeg E. J., Wozney J. M. A BMP/activin A chimera is superior to native BMPs and induces bone repair in nonhuman primates when delivered in a composite matrix // Sci Transl Med. – 2019. – Т. 11, № 489.
155. Tanaka K., Kaji H., Yamaguchi T., Kanazawa I., Canaff L., Hendy G. N., Sugimoto T. Involvement of the osteoinductive factors, Tmem119 and BMP-2, and the ER stress response PERK-eIF2alpha-ATF4 pathway in the commitment of myoblastic into osteoblastic cells // Calcif Tissue Int. – 2014. – Т. 94, № 4. – С. 454-64.
156. Viswanathan S., Shi Y., Galipeau J., Krampera M., Leblanc K., Martin I., Nolta J., Phinney D. G., Sensebe L. Mesenchymal stem versus stromal cells: International Society for Cell & Gene Therapy (ISCT(R)) Mesenchymal Stromal Cell committee position statement on nomenclature // Cytotherapy. – 2019. – Т. 21, № 10. – С. 1019-1024.
157. Epstein J. A. A Time to Press Reset and Regenerate Cardiac Stem Cell Biology // JAMA Cardiol. – 2019. – Т. 4, № 2. – С. 95-96.
158. Sultana N., Zhang L., Yan J., Chen J., Cai W., Razzaque S., Jeong D., Sheng W., Bu L., Xu M., Huang G. Y., Hajjar R. J., Zhou B., Moon A., Cai C. L. Resident c-kit(+) cells in the heart are not cardiac stem cells // Nat Commun. – 2015. – Т. 6. – С. 8701.
159. Oldershaw R., Owens W. A., Sutherland R., Linney M., Liddle R., Magana L., Lash G. E., Gill J. H., Richardson G., Meeson A. Human Cardiac-Mesenchymal Stem Cell-Like Cells, a Novel Cell Population with Therapeutic Potential // Stem Cells Dev. – 2019. – Т. 28, № 9. – С. 593-607.
160. Golpanian S., Wolf A., Hatzistergos K. E., Hare J. M. Rebuilding the Damaged Heart: Mesenchymal Stem Cells, Cell-Based Therapy, and Engineered Heart Tissue // Physiol Rev. – 2016. – Т. 96, № 3. – С. 1127-68.
161. Docshin P. M., Karpov A. A., Eyvazova S. D., Puzanov M. V., Kostareva A. A., Galagudza M. M., Malashicheva A. B. Activation of Cardiac Stem Cells in Myocardial Infarction // Tsitologiya. – 2018. – Т. 60, № 2. – С. 81-88.
162. de Sena-Tomas C., Aleman A. G., Ford C., Varshney A., Yao D., Harrington J. K., Saude L., Ramialison M., Targoff K. L. Activation of Nkx2.5 transcriptional program is required for adult myocardial repair // Nat Commun. – 2022. – Т. 13, № 1. – С. 2970.
163. Siatra P., Vatsellas G., Chatzianastasiou A., Balafas E., Manolakou T., Papapetropoulos A., Agapaki A., Mouchtouri E. T., Ruchaya P. J., Korovesi A. G., Mavroidis M., Thanos D., Beis D., Kokkinopoulos I. Return of the Tbx5; lineage-tracing reveals ventricular cardiomyocyte-like precursors in the injured adult mammalian heart // NPJ Regen Med. – 2023. – Т. 8, № 1. – С. 13.
164. Sattler S., Campos Ramos G., Ludewig B., Rainer P. P. Cardioimmunology: the new frontier! // Eur Heart J. – 2023. – Т. 44, № 26. – С. 2355-2357.
165. Kore R. A., Jenkins S. V., Jamshidi-Parsian A., Tackett A. J., Griffin R. J., Ayyadevara S., Mehta J. L. Proteomic analysis of transcription factors involved in the alteration of ischemic mouse heart as modulated by MSC exosomes // Biochem Biophys Rep. – 2023. – Т. 34. – С. 101463.
166. Kumar S., Shih C. M., Tsai L. W., Dubey R., Gupta D., Chakraborty T., Sharma N., Singh A. V., Swarup V., Singh H. N. Transcriptomic Profiling Unravels Novel Deregulated Gene Signatures Associated with Acute Myocardial Infarction: A Bioinformatics Approach // Genes (Basel). – 2022. – Т. 13, № 12.
167. Martin-Bornez M., Falcon D., Morrugares R., Siegfried G., Khatib A. M., Rosado J. A., Galeano-Otero I., Smani T. New Insights into the Reparative Angiogenesis after Myocardial Infarction // Int J Mol Sci. – 2023. – Т. 24, № 15.

168. Zheng Y., Lin J., Liu D., Wan G., Gu X., Ma J. Nogo-B promotes angiogenesis and improves cardiac repair after myocardial infarction via activating Notch1 signaling // Cell Death Dis. – 2022. – Т. 13, № 4. – С. 306.
169. Gozlan O., Sprinzak D. Notch signaling in development and homeostasis // Development. – 2023. – Т. 150, № 4.
170. Aquila G., Kostina A., Vieceli Dalla Sega F., Shlyakhto E., Kostareva A., Marracino L., Ferrari R., Rizzo P., Malaschicheva A. The Notch pathway: a novel therapeutic target for cardiovascular diseases? // Expert Opin Ther Targets. – 2019. – Т. 23, № 8. – С. 695-710.
171. Santema B. T., Arita V. A., Sama I. E., Kloosterman M., van den Berg M. P., Nienhuis H. L. A., Van Gelder I. C., van der Meer P., Zannad F., Metra M., Ter Maaten J. M., Cleland J. G., Ng L. L., Anker S. D., Lang C. C., Samani N. J., Dickstein K., Filippatos G., van Veldhuisen D. J., Lam C. S. P., Rienstra M., Voors A. A. Pathophysiological pathways in patients with heart failure and atrial fibrillation // Cardiovasc Res. – 2022. – Т. 118, № 11. – С. 2478-2487.
172. Ferrari R., Rizzo P. The Notch pathway: a novel target for myocardial remodelling therapy? // Eur Heart J. – 2014. – Т. 35, № 32. – С. 2140-5.
173. Marracino L., Fortini F., Bouhamida E., Camponogara F., Severi P., Mazzoni E., Patergnani S., D'Aniello E., Campana R., Pinton P., Martini F., Tognon M., Campo G., Ferrari R., Vieceli Dalla Sega F., Rizzo P. Adding a "Notch" to Cardiovascular Disease Therapeutics: A MicroRNA-Based Approach // Front Cell Dev Biol. – 2021. – Т. 9. – С. 695114.
174. Tavares A. L. P., Brown J. A., Ulrich E. C., Dvorak K., Runyan R. B. Runx2-I is an Early Regulator of Epithelial-Mesenchymal Cell Transition in the Chick Embryo // Dev Dyn. – 2018. – Т. 247, № 3. – С. 542-554.
175. Bobos D., Soufla G., Angouras D. C., Lekakis I., Georgopoulos S., Melissari E. Investigation of the Role of BMP2 and -4 in ASD, VSD and Complex Congenital Heart Disease // Diagnostics (Basel). – 2023. – Т. 13, № 16.
176. Edwards W., Greco T. M., Miner G. E., Barker N. K., Herring L., Cohen S., Cristea I. M., Conlon F. L. Quantitative proteomic profiling identifies global protein network dynamics in murine embryonic heart development // Dev Cell. – 2023. – Т. 58, № 12. – С. 1087-1105 e4.
177. Ye D., Liu Y., Pan H., Feng Y., Lu X., Gan L., Wan J., Ye J. Insights into bone morphogenetic proteins in cardiovascular diseases // Front Pharmacol. – 2023. – Т. 14. – С. 1125642.
178. Prados B., Gomez-Apinaniz P., Papoutsi T., Luxan G., Zaffran S., Perez-Pomares J. M., de la Pompa J. L. Myocardial Bmp2 gain causes ectopic EMT and promotes cardiomyocyte proliferation and immaturity // Cell Death Dis. – 2018. – Т. 9, № 3. – С. 399.
179. Morrell N. W., Bloch D. B., ten Dijke P., Goumans M. J., Hata A., Smith J., Yu P. B., Bloch K. D. Targeting BMP signalling in cardiovascular disease and anaemia // Nat Rev Cardiol. – 2016. – Т. 13, № 2. – С. 106-20.
180. Rutkovskiy A., Sagave J., Czibik G., Baysa A., Zihlavnikova Enayati K., Hillestad V., Dahl C. P., Fiane A., Gullestad L., Gravning J., Ahmed S., Attramadal H., Valen G., Vaage J. Connective tissue growth factor and bone morphogenetic protein 2 are induced following myocardial ischemia in mice and humans // Scand J Clin Lab Invest. – 2017. – Т. 77, № 5. – С. 321-331.
181. Soliman H., Rossi F. M. V. Cardiac fibroblast diversity in health and disease // Matrix Biol. – 2020. – Т. 91-92. – С. 75-91.
182. Soltani L., Mahdavi A. H. Role of Signaling Pathways during Cardiomyocyte Differentiation of Mesenchymal Stem Cells // Cardiology. – 2022. – Т. 147, № 2. – С. 216-224.
183. Uscategui Calderon M., Gonzalez B. A., Yutzey K. E. Cardiomyocyte-fibroblast crosstalk in the postnatal heart // Front Cell Dev Biol. – 2023. – Т. 11. – С. 1163331.
184. Borggrefe T., Lauth M., Zwijsen A., Huylebroeck D., Oswald F., Giaimo B. D. The Notch intracellular domain integrates signals from Wnt, Hedgehog, TGFbeta/BMP and hypoxia pathways // Biochim Biophys Acta. – 2016. – Т. 1863, № 2. – С. 303-13.
185. Wang Y., Fang Y., Lu P., Wu B., Zhou B. NOTCH Signaling in Aortic Valve Development and Calcific Aortic Valve Disease // Front Cardiovasc Med. – 2021. – Т. 8. – С. 682298.

186. Bollini S., Vieira J. M., Howard S., Dube K. N., Balmer G. M., Smart N., Riley P. R. Re-activated adult epicardial progenitor cells are a heterogeneous population molecularly distinct from their embryonic counterparts // Stem Cells Dev. – 2014. – Т. 23, № 15. – С. 1719-30.
187. Vieira J. M., Howard S., Villa Del Campo C., Bollini S., Dube K. N., Masters M., Barnette D. N., Rohling M., Sun X., Hankins L. E., Gavriouchkina D., Williams R., Metzger D., Chambon P., Sauka-Spengler T., Davies B., Riley P. R. BRG1-SWI/SNF-dependent regulation of the Wt1 transcriptional landscape mediates epicardial activity during heart development and disease // Nat Commun. – 2017. – Т. 8. – С. 16034.
188. Wagner K. D., Wagner N., Bondke A., Nafz B., Flemming B., Theres H., Scholz H. The Wilms' tumor suppressor Wt1 is expressed in the coronary vasculature after myocardial infarction // FASEB J. – 2002. – Т. 16, № 9. – С. 1117-9.
189. Wagner K. D., Vukolic A., Baudouy D., Michiels J. F., Wagner N. Inducible Conditional Vascular-Specific Overexpression of Peroxisome Proliferator-Activated Receptor Beta/Delta Leads to Rapid Cardiac Hypertrophy // PPAR Res. – 2016. – Т. 2016. – С. 7631085.
190. Menasche P. Cell therapy trials for heart regeneration - lessons learned and future directions // Nat Rev Cardiol. – 2018. – Т. 15, № 11. – С. 659-671.
191. Sharma S., Mishra R., Bigham G. E., Wehman B., Khan M. M., Xu H., Saha P., Goo Y. A., Datla S. R., Chen L., Tulapurkar M. E., Taylor B. S., Yang P., Karathanasis S., Goodlett D. R., Kaushal S. A Deep Proteome Analysis Identifies the Complete Secretome as the Functional Unit of Human Cardiac Progenitor Cells // Circ Res. – 2017. – Т. 120, № 5. – С. 816-834.
192. Traister A., Patel R., Huang A., Patel S., Plakhotnik J., Lee J. E., Medina M. G., Welsh C., Ruparel P., Zhang L., Friedberg M., Maynes J., Coles J. Correction: Cardiac regenerative capacity is age- and disease-dependent in childhood heart disease // PLoS One. – 2021. – Т. 16, № 1. – С. e0245808.
193. Zaidi S., Brueckner M. Genetics and Genomics of Congenital Heart Disease // Circ Res. – 2017. – Т. 120, № 6. – С. 923-940.
194. Parameswaran S., Kumar S., Verma R. S., Sharma R. K. Cardiomyocyte culture - an update on the in vitro cardiovascular model and future challenges // Can J Physiol Pharmacol. – 2013. – Т. 91, № 12. – С. 985-98.
195. Papoutsi T., Luna-Zurita L., Prados B., Zaffran S., de la Pompa J. L. Bmp2 and Notch cooperate to pattern the embryonic endocardium // Development. – 2018. – Т. 145, № 13.
196. Bray S. J. Notch signalling in context // Nat Rev Mol Cell Biol. – 2016. – Т. 17, № 11. – С. 722-735.
197. Gude N., Joyo E., Toko H., Quijada P., Villanueva M., Hariharan N., Sacchi V., Truffa S., Joyo A., Voelkers M., Alvarez R., Sussman M. A. Notch activation enhances lineage commitment and protective signaling in cardiac progenitor cells // Basic Res Cardiol. – 2015. – Т. 110, № 3. – С. 29.
198. Mercer-Rosa L., Paridon S. M., Fogel M. A., Rychik J., Tanel R. E., Zhao H., Zhang X., Yang W., Shults J., Goldmuntz E. 22q11.2 deletion status and disease burden in children and adolescents with tetralogy of Fallot // Circ Cardiovasc Genet. – 2015. – Т. 8, № 1. – С. 74-81.
199. Kovall R. A., Gebelein B., Sprinzak D., Kopan R. The Canonical Notch Signaling Pathway: Structural and Biochemical Insights into Shape, Sugar, and Force // Dev Cell. – 2017. – Т. 41, № 3. – С. 228-241.
200. Bittel D. C., Butler M. G., Kibiryeva N., Marshall J. A., Chen J., Lofland G. K., O'Brien J. E., Jr. Gene expression in cardiac tissues from infants with idiopathic conotruncal defects // BMC Med Genomics. – 2011. – Т. 4. – С. 1.
201. Conlon R. A., Reaume A. G., Rossant J. Notch1 is required for the coordinate segmentation of somites // Development. – 1995. – Т. 121, № 5. – С. 1533-45.
202. Koenig S. N., LaHaye S., Feller J. D., Rowland P., Hor K. N., Trask A. J., Janssen P. M., Radtke F., Lilly B., Garg V. Notch1 haploinsufficiency causes ascending aortic aneurysms in mice // JCI Insight. – 2017. – Т. 2, № 21.

203. de la Pompa J. L., Epstein J. A. Coordinating tissue interactions: Notch signaling in cardiac development and disease // Dev Cell. – 2012. – T. 22, № 2. – C. 244-54.
204. Sano T., Ousaka D., Goto T., Ishigami S., Hirai K., Kasahara S., Ohtsuki S., Sano S., Oh H. Impact of Cardiac Progenitor Cells on Heart Failure and Survival in Single Ventricle Congenital Heart Disease // Circ Res. – 2018. – T. 122, № 7. – C. 994-1005.
205. Urbanek K., Cabral-da-Silva M. C., Ide-Iwata N., Maestroni S., Delucchi F., Zheng H., Ferreira-Martins J., Ogorek B., D'Amario D., Bauer M., Zerbini G., Rota M., Hosoda T., Liao R., Anversa P., Kajstura J., Leri A. Inhibition of notch1-dependent cardiomyogenesis leads to a dilated myopathy in the neonatal heart // Circ Res. – 2010. – T. 107, № 3. – C. 429-41.
206. Collesi C., Felician G., Secco I., Gutierrez M. I., Martelletti E., Ali H., Zentilin L., Myers M. P., Giacca M. Reversible Notch1 acetylation tunes proliferative signalling in cardiomyocytes // Cardiovasc Res. – 2018. – T. 114, № 1. – C. 103-122.
207. Geva T. Indications and timing of pulmonary valve replacement after tetralogy of Fallot repair // Semin Thorac Cardiovasc Surg Pediatr Card Surg Annu. – 2006.10.1053/j.pcsu.2006.02.009. – C. 11-22.
208. Dluzniewska N., Podolec P., Skubera M., Smas-Suska M., Pajak J., Urbanczyk-Zawadzka M., Plazak W., Olszowska M., Tomkiewicz-Pajak L. Long-term follow-up in adults after tetralogy of Fallot repair // Cardiovasc Ultrasound. – 2018. – T. 16, № 1. – C. 28.
209. Kostina A., Bjork H., Ignatieva E., Irtyuga O., Uspensky V., Semenova D., Maleki S., Tomilin A., Moiseeva O., Franco-Cereceda A., Gordeev M., Faggian G., Kostareva A., Eriksson P., Malashicheva A. Notch, BMP and WNT/beta-catenin network is impaired in endothelial cells of the patients with thoracic aortic aneurysm // Atheroscler Suppl. – 2018. – T. 35. – C. e6-e13.
210. Kostina A., Shishkova A., Ignatieva E., Irtyuga O., Bogdanova M., Levchuk K., Golovkin A., Zhiduleva E., Uspenskiy V., Moiseeva O., Faggian G., Vaage J., Kostareva A., Rutkovskiy A., Malashicheva A. Different Notch signaling in cells from calcified bicuspid and tricuspid aortic valves // J Mol Cell Cardiol. – 2018. – T. 114. – C. 211-219.
211. Ignatieva E., Kostina D., Irtyuga O., Uspensky V., Golovkin A., Gavriliuk N., Moiseeva O., Kostareva A., Malashicheva A. Mechanisms of Smooth Muscle Cell Differentiation Are Distinctly Altered in Thoracic Aortic Aneurysms Associated with Bicuspid or Tricuspid Aortic Valves // Front Physiol. – 2017. – T. 8. – C. 536.
212. Kozyrev I., Dokshin P., Kostina A., Kiselev A., Ignatieva E., Golovkin A., Pervunina T., Grekhov E., Gordeev M., Kostareva A., Malashicheva A. Insights Image for "Dysregulation of Notch signaling in cardiac mesenchymal cells of patients with Tetralogy of Fallot" // Pediatr Res. – 2020. – T. 88, № 1. – C. 139.
213. MacGrogan D., Luna-Zurita L., de la Pompa J. L. Notch signaling in cardiac valve development and disease // Birth Defects Res A Clin Mol Teratol. – 2011. – T. 91, № 6. – C. 449-59.
214. Luna-Zurita L., Prados B., Grego-Bessa J., Luxan G., del Monte G., Benguria A., Adams R. H., Perez-Pomares J. M., de la Pompa J. L. Integration of a Notch-dependent mesenchymal gene program and Bmp2-driven cell invasiveness regulates murine cardiac valve formation // J Clin Invest. – 2010. – T. 120, № 10. – C. 3493-507.
215. Rutenberg J. B., Fischer A., Jia H., Gessler M., Zhong T. P., Mercola M. Developmental patterning of the cardiac atrioventricular canal by Notch and Hairy-related transcription factors // Development. – 2006. – T. 133, № 21. – C. 4381-90.
216. Zhou X. L., Fang Y. H., Wan L., Xu Q. R., Huang H., Zhu R. R., Wu Q. C., Liu J. C. Notch signaling inhibits cardiac fibroblast to myofibroblast transformation by antagonizing TGF-beta1/Smad3 signaling // J Cell Physiol. – 2019. – T. 234, № 6. – C. 8834-8845.
217. Shinde A. V., Humeres C., Frangogiannis N. G. The role of alpha-smooth muscle actin in fibroblast-mediated matrix contraction and remodeling // Biochim Biophys Acta Mol Basis Dis. – 2017. – T. 1863, № 1. – C. 298-309.

218. Nakajima Y., Mironov V., Yamagishi T., Nakamura H., Markwald R. R. Expression of smooth muscle alpha-actin in mesenchymal cells during formation of avian endocardial cushion tissue: A role for transforming growth factor β3 // Developmental Dynamics. – 1997. – Т. 209, № 3. – С. 296-309.
219. Piera-Velazquez S., Li Z., Jimenez S. A. Role of endothelial-mesenchymal transition (EndoMT) in the pathogenesis of fibrotic disorders // Am J Pathol. – 2011. – Т. 179, № 3. – С. 1074-80.
220. Kovacic J. C., Dimmeler S., Harvey R. P., Finkel T., Aikawa E., Krenning G., Baker A. H. Endothelial to Mesenchymal Transition in Cardiovascular Disease: JACC State-of-the-Art Review // J Am Coll Cardiol. – 2019. – Т. 73, № 2. – С. 190-209.
221. Anbara T., Sharifi M., Aboutaleb N. Endothelial to Mesenchymal Transition in the Cardiogenesis and Cardiovascular Diseases // Curr Cardiol Rev. – 2020. – Т. 16, № 4. – С. 306-314.
222. Zamurovic N., Cappellen D., Rohner D., Susa M. Coordinated activation of notch, Wnt, and transforming growth factor-beta signaling pathways in bone morphogenic protein 2-induced osteogenesis. Notch target gene Hey1 inhibits mineralization and Runx2 transcriptional activity // J Biol Chem. – 2004. – Т. 279, № 36. – С. 37704-15.
223. Sharff K. A., Song W. X., Luo X., Tang N., Luo J., Chen J., Bi Y., He B. C., Huang J., Li X., Jiang W., Zhu G. H., Su Y., He Y., Shen J., Wang Y., Chen L., Zuo G. W., Liu B., Pan X., Reid R. R., Luu H. H., Haydon R. C., He T. C. Hey1 basic helix-loop-helix protein plays an important role in mediating BMP9-induced osteogenic differentiation of mesenchymal progenitor cells // J Biol Chem. – 2009. – Т. 284, № 1. – С. 649-659.
224. Gorelova A., Berman M., Al Ghouleh I. Endothelial-to-Mesenchymal Transition in Pulmonary Arterial Hypertension // Antioxid Redox Signal. – 2021. – Т. 34, № 12. – С. 891-914.
225. Ma L., Lu M. F., Schwartz R. J., Martin J. F. Bmp2 is essential for cardiac cushion epithelial-mesenchymal transition and myocardial patterning // Development. – 2005. – Т. 132, № 24. – С. 5601-11.
226. Shimizu T., Tanaka T., Iso T., Matsui H., Ooyama Y., Kawai-Kowase K., Arai M., Kurabayashi M. Notch signaling pathway enhances bone morphogenetic protein 2 (BMP2) responsiveness of Msx2 gene to induce osteogenic differentiation and mineralization of vascular smooth muscle cells // J Biol Chem. – 2011. – Т. 286, № 21. – С. 19138-48.
227. Andres-Delgado L., Galardi-Castilla M., Munch J., Peralta M., Ernst A., Gonzalez-Rosa J. M., Tessadori F., Santamaria L., Bakkers J., Vermot J., de la Pompa J. L., Mercader N. Notch and Bmp signaling pathways act coordinately during the formation of the proepicardium // Dev Dyn. – 2020. – Т. 249, № 12. – С. 1455-1469.
228. Lin C. H., Lilly B. Endothelial cells direct mesenchymal stem cells toward a smooth muscle cell fate // Stem Cells Dev. – 2014. – Т. 23, № 21. – С. 2581-90.
229. Gurel Pekozer G., Torun Kose G., Hasirci V. Influence of co-culture on osteogenesis and angiogenesis of bone marrow mesenchymal stem cells and aortic endothelial cells // Microvasc Res. – 2016. – Т. 108. – С. 1-9.